UNIVERSITÉ DE NANTES
UFR MEDECINE

ÉCOLE DOCTORALE BIOLOGIE-SANTE NANTES ANGERS – ED 502

Année 2014 N° 06

Development of rAAV-mediated gene addition therapies in canine models of severe inherited photoreceptor dystrophies

THÈSE DE DOCTORAT

Discipline: Biologie-Médecine-Santé

Spécialités: Biologie et Biochimie Moléculaire

Présentée
et soutenue publiquement par

Lolita MONNIER-PETIT

Le 23 janvier 2014, devant le jury ci-dessous

Président Pr. Marie Anne COLLE

Rapporteurs Pr. Alberto AURICCHIO
Dr. Stylianos MICHALAKIS

Directeur de thèse: Dr. Fabienne ROLLING

Acknowledgments

I would like to thank my PhD advisor Dr. Fabienne Rolling for introducing me into the field of retinal gene therapy. She has shared with me her scientific experience and she has given me the freedom to explore my own ideas and various projects. I acknowledge her for her interest and enthuasiasm. I also would like to sincerely acknowledge Pr. Philippe Moullier, the director of the laboratory. Philippe has been very helpful in providing scientific and professional advices. I am also thankful for the excellent example he has provided as a researcher and mentor.

I was lucky to work with an execellent research group, always very motivated. Many thanks to all of the colleagues and members of the laboratory that contributed in many ways to this work.
I especially thank Pr. Michel Weber and Dr. Guylène Le Meur, who performed the subretinal injections; Pr. Jack-Yves Deschamps, who conducted anesthesia (and I know that it has not always been easy in very young dogs); Lyse Libeau, who performed the ERG and OCT examinations, Alexandra Mendes Madeira for her invaluable technical assistance; Nathalie Provost for the hours and hours we shared during behavioral testing and for her technical help with RT-PCR; Caroline Guihal for introducing me to molecular biology, Elsa Lhériteau for her mentoring during my Master degree and her important contributions to this work, Brahim Belbeella for teaching me immunohistochemistry, Mireille Ledevin for retinal sections; Jean-Baptiste Dupont for his contribution during the amplification of the canine PDE6α cDNA and Marine, Virginie, Baptiste and Kizito for critical reading of the dissertation .
I am also particularly grateful for members of the Vector Core, who produced all the AAV vectors used in this study (I have not forgot that you have produced the first batch of AAV2/5-RK-c*Pde6β* in only 3 weeks to allow the injection of the first *Pde6β*$^{-/-}$ puppies). Thank you also to the staff of the Boisbonne Center for animal care. Your commitment and professionalism were keys to the success of this project. I am also grateful to our group's admistrative assistace Anita Champion who was always ready to help.
My work was also dependent on the contribution of the *Association Française contre les Myopathies* that funded the development and maintenance of the colonies of PDE6β- and RPGRIP1-deficient dogs.

For the dissertation, I would like to thank very much my reading committee members: Pr. Alberto Auricchio and Dr. Stylianos Michalakis for their time, interest and very helpful comments. I would also like to thank Pr. Marie-Anne Colle, the other member of my oral defense committee, for her time and advices.

Last, but no least, loving thanks are sincerely expressed to the following persons: my husband Thierry for his continuous love, sense of humor and support; ma family for their encouragement, Martine Pernodet for being my first mentor in science; Joséphine, Christine, Myriam, Simon, Léa, Estelle et Lucile for understanding that putting one specific sentence for each one of you would have been too long. Merci.

Abstract

Inherited retinal dystrophies are the leading cause of familial blindness in Europe and the United States. They are characterized by dysfunction and degeneration of retinal photoreceptors in response to genetic defects. In the majority of inherited retinal dystrophies, both cone and rod photoreceptors die, but the degree to which these cells are affected differs between the various disorders. Rod-cone dystrophies are characterized by a predominant initial loss of rods, followed by more progressive cone dysfunction. In contrast, cone-rod dystrophies are characterized by the primary involvement of cones, followed by rod dysfunction and degeneration. To date, no treatment exists for inherited retinopathies.

The eye is small, enclosed, and immuno-privileged. It is therefore an attractive target for gene therapy. These favorable characteristics, together with the significant progress in understanding the molecular basis of inherited retinal diseases, have make possible to realistically consider the use of gene addition therapy to treat these disorders.
A new area of retinal therapeutics has been started by recent studies showing that treatment of animal models with gene addition therapy successfully restored visual function. These results have been successfully translated to the clinic for an RPE disease caused by *RPE65* mutations. The next level of challenge is to initiate treatment of the majority of disorders in which the genetic defects are in the photoreceptors.

For the development of new therapies, proof-of-concept studies in large animal models that share clinical features with their human counterparts represent a pivotal step. It is particularly true for primary photoreceptor diseases because the distribution, density and proportion of rods and cones in large animals more closely match those of primates.
This thesis describes a body of work addressing the potential and efficacy of gene addition therapy in two large models of severe inherited photoreceptor dystrophies:

(i) the PDE6β-deficient dog, a model of one of the most common forms of recessive rod-cone dystrophies caused by a genetic defect in rods
(ii) the RPGRIP1-deficient dog, a model of a severe cone-rod dystrophy caused by a genetic defect in both rod and cone photoreceptors.

Using vectors derived from adeno-associated virus, we showed that it is possible to restore retinal function, preserve photoreceptor structure and visually guided behavior in the two canine models, for at least 24 months postinjection. These results were the first examples of photoreceptor-targeted gene therapy correcting both photoreceptor function and visual-guided behavior in large models of severe photoreceptor diseases. The efficacy of gene addition therapy in these large animal models provides great promise for human treatment.

Publications and international conference abstracts

Publications:

Petit L., Lhériteau E., Weber M., Le Meur G., Deschamps JY, Provost N., Mendes-Madeira A., Libeau L., Guihal C., Colle MA., Moullier P. and Rolling F. Restoration of vision in the pde6β-deficient dog, a large animal model of rod-cone dystrophy. Molecular Therapy. Nov 2012; Vol20: 2019-2030

Lhériteau E.*, **Petit L**.*, Weber M., Le Meur G., Deschamps JY, Libeau L., Mendes-Madeira A., Guihal C., François A., Guyon R., Provost N., Lemoine F., Papal S., El-Amraoui A., Colle MA., Moullier P. and Rolling F. Successful gene therapy in the RPGRIP1-deficient dog, a large model of cone-rod dystrophy. Molecular Therapy. Oct 2013. Epub ahead of print. (* **co-first authors, equal contribution**).

International conference abstracts:

Monnier L., Lhériteau E., Weber M., Le Meur G., Deschamps JY, Provost N., Mendes-Madeira A., Libeau L., Guihal C., Colle MA., Moullier P. and Rolling F. AAV-mediated gene therapy restores retinal function and vision in the pde6β-deficient dog. Gene Therapy and Delivery I session, **ARVO 2012**. Fort Lauderdale, USA (Poster 1901/D718).

Monnier L., Lhériteau E., Weber M., Le Meur G., Deschamps JY, Provost N., Mendes-Madeira A., Libeau L., Guihal C., Colle MA., Moullier P. and Rolling F. AAV-mediated gene therapy restores retinal function and vision in the pde6β-deficient dog. Institut des Biothérapies session, **ESGCT 2012**. Versailles, France (oral presentation).

Petit L., Lhériteau E., Weber M., Le Meur G., Deschamps JY, Libeau L., Mendes-Madeira A., Guihal C., François A., Guyon R., Provost N., Lemoine F., Papal S., El-Amraoui A., Colle MA., Moullier P. and Rolling F. AAV-mediated gene therapy restores retinal funtion and vision in the rpgrip1-deficient dog. Gene Therapy and Delivery session. **ARVO 2013**. Seattle, USA (oral presentation).

Petit L. Lhériteau E., Weber M., Le Meur G., Deschamps JY, Provost N., Mendes-Madeira A., Libeau L., Guihal C., Colle MA., Moullier P. and Rolling F. AAV-mediated gene therapies in canine models of inherited retinal dystrophies. Gene Therapy session. **EVER/SFO 2013**. Paris, France (oral presentation)

List of Abbreviations

AAV: Adeno-associated virus
AIPL1: Aryl hydrocarbon Interacting-Protein Line 1
ATP: Adenosine 5'-triphosphate
b: Bovine
bp: Base pair
CBA: Chicken beta-actin
cDNA: Coding/complementary DNA
cGMP: Cyclic GMP
CMV: Cytomegalovirus promoter
CNSB: Congenital stationary night blindness
CORD: Cone-rod dystrophies
CRALBP: Cellular retinaldehyde-binding protein
DHA: Docosahexaenoic acid
DNA: Deoxyribonucleic acid
EIAV: Equine infection anaemia virus
eGFP: Enhanced GFP
ER: Endoplasmic reticulum
ERG: Electroretinogram
GC1: Guanylate cyclase 1
GC2: Guanylate cyclase 2
GCAP: Guanylate cyclase activator protein
GCL: Ganglion cell layer
GDP: guanosine 5'-diphosphate
GFP: Green fluorescent protein
GMP: guanosine 5'-monophosphate
GTP: guanosine 5'-triphosphate
h: Human
HIV: Human immunodeficiency virus
ILM: Inner limiting membrane
INL: Inner nuclear layer
IPL: Inner plexiform layer
IRBP: Interstitial retinal binding protein
ITR: Inverted terminal repeat
IS: Inner segments
kb: Kilobase
kDa: Kilodalton
LCA: Leber congenital Amaurosis
LRAT: Lecithin retinol acyltransferase
m: Murine
MERTK: Mer-receptor tyrosine kinase
mRNA: Messenger RNA
miRNA: MicroRNA
mpi: Months postinjection
OCT: Optical coherence tomography
OLM: Outer limiting membrane
ONL: Outer nuclear layer
OS: Outer segments
P(X): Postnatal day X

PBS: phosphate buffered saline
PCR: polymerase chain reaction
PDE: Phosphodiesterase
PDE6: Rod Phosphodiesterase 6
PDE6*: Activated PDE6
PDE6α: α subunit of the rod PDE6
PDE6α': α' subunit of the cone PDE6γ
PDE6β: β subunit of the rod PDE6
PDE6γ: γ subunit of the rod PDE6
PDE6γ': γ' subunit of the cone PDE6
Prph2: Peripherin
rAAV: Recombinant AAV
rd: Retinal degeneration
RDH: Retinol dehydrogenase
Rho: Rhodopsin
RK: Rhodopsin kinase
RNA: Ribonucleic acid
RP: Retinitis pigmentosa or rod-cone dystrophy
RPE: Retinal pigment epithelium
RPE65: Retinal pigment epithelium 65-kDa
RPGR: Retinitis pigmentosa GTPase regulator
RPGRIP1: RPGR-interacting protein 1
RT-PCR: Reverse-transcriptase PCR
SD-OCT: Spectral-domain OCT
T: transducin
T*: activated T
TD-OCT: Time-domain OCT
SIV: Simian immunodeficiency virus
smCBA: Chimeric chicken beta-actin promoter fused to the early enhancer of CMV
vg: Vector genome
VSV-G: vesicular stomatitis virus G-protein
wpi: Weeks postinjection
XIAP: X-linked inhibitor of apoptosis protein

Table of contents

General introduction

CHAPTER **I**

THE PHOTORECEPTORS: CELLS UNDER CONTROLED STRESS

This first chapter provides a general view of the anatomy and physiology of the mammalian retina, before focusing to photoreceptor cells, the main subject of this chapter.

I chose to present photoreceptor cells using a dynamic approach. My hope is to shed light on the specific features of photoreceptor cells that make them one of the most vulnerable cells in the body. These features include their specialized function (and consequent structure), their high oxidative metabolism, as well as their functional relationship with the retinal pigment epithelium (RPE). I believe that an overview of the complex physiology of photoreceptor cells is an important starting point to understand the causes and clinical presentation of primary photoreceptor defects. The notions develop in this chapter will thus provide landmarks for **Chapters 2** and **3**, where I will discuss in more details the consequences of photoreceptor and/or RPE genetic defects on photoreceptor function and survival.

Contents

I.1. Anatomy and physiology of the mammalian retina

Vision, the process of detecting and perceiving light, is considered by many to be the most important of our five senses. It is a highly complex process that requires the coordinated activity of numerous components in the eye and brain. The initial steps are carried out in the retina, a light-sensitive nervous tissue in the back of the eye. The retina has three main functions: (i) to receive the light focused by the lens and to convert its energy into electrical impulses, (ii) to perform the first step of neural analysis by amplifying and processing these electrical signals [1], (iii) to encode the end result into action potentials and transmit them to subcortical visual centers along the optic nerve.

Three major subcortical centers receive retinal inputs: the prectectal nucleus, the suprachiasmatic nucleus and the lateral geniculate nucleus. Retinal information received by the prectectal nucleus and the suprachiasmatic nucleus is mainly processed for non-visual light perception (regulation of pupil light reflex and circadian rhythms). Only retinal inputs that terminate in the lateral geniculate nucleus of the thalamus are processed for visual perception and relayed to the visual cortex. There, visual features are further analyzed and interpreted in one visual picture.

The mammalian retina has two major anatomical and functional components: the inner (more internal) neurosensory retina and the outer (more external) retinal pigment epithelium (RPE) (**Figure 1**). Although morphologically highly different, these tissues are derived from the same layer of neuroepithelium and co-differentiate during the development of the eye. They form a close functionally unit and rely on each others to function and survive properly.

I.1.1. The neuroretina

The neurosensory retina is the neural entry of the visual system. This tissue as a remarkable anatomic and functional complexity adapted to light detection, pre-processing and transmission of information in higher brain centers [2].
It involves five major types of visual neurons, each playing a specific role in processing visual images. They are organized in three morphologically distinct nuclear layers, that are, from external to internal (**Figure 1**):

- the outer nuclear layer (ONL), composed of photoreceptor cell bodies,
- the inner nuclear layer (INL), composed of excitatory bipolar, inhibitory horizontal and amacrine cell bodies,
- and the ganglion cell layer (GCL), occupied by ganglion and amacrine cell bodies.

Two synaptic (plexiform) layers formed of synaptic processes separate these three layers of cell bodies: the outer plexiform layer (OPL), which separates the ONL and the INL and the inner plexiform layer [3], which separates the INL and the GCL.

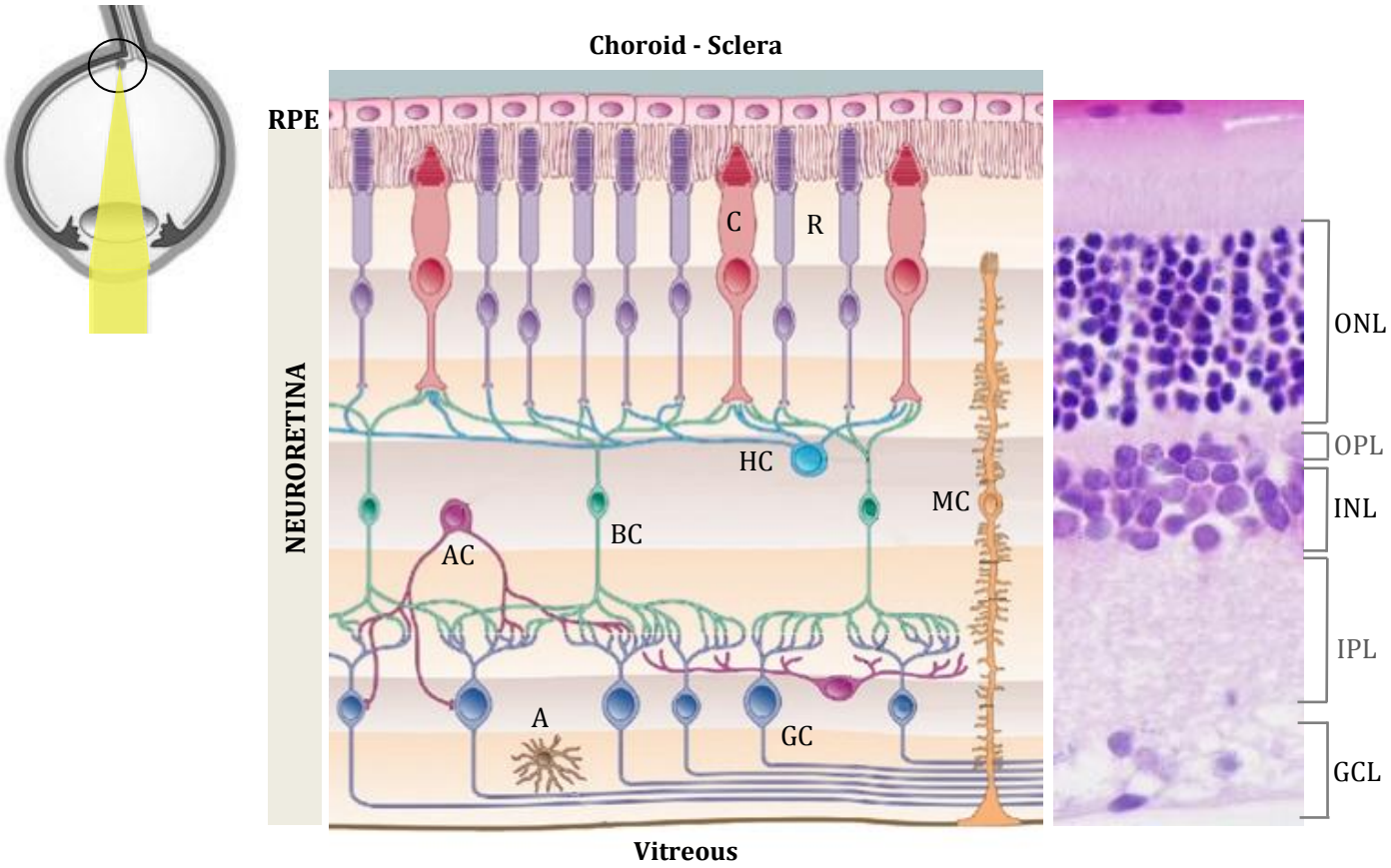

Figure 1. Schematic and histological cross-section of the mammalian retina. The neurosensory retina is structured in layers. The outer nuclear layer (ONL) contains the nuclei and cell bodies of the rod (R) and cone (C) photoreceptors. Rods confer peripheral and night vision, whereas cones are responsible for daylight and central vision. The inner nuclear layer (INL) contains the nuclei of the secondary neurons: the bipolar cells (BC), which provide the principal retinal circuit, and amacrine cells (AC) and horizontal cells (HC) that are involved in the processing of the signal from the photoreceptors. The ganglion cell layer (GCL) contains the ganglion cells that receive their signal from the bipolar and amacrine cells and project into the brain. Synaptic connexions between photoreceptors and bipolar and horizontal cells occur in the outer plexiform layer (OPL). Synaptic connexions between ganglion cells and bipolar and amacrine cells occur in the inner plexiform layer [3].

The photoreceptors are the cells that accomplished the conversion of light energy into electrical impulses. At the synaptic terminal of photoreceptors, in the OPL, these neural signals are sensed by bipolar and horizontal cells. Horizontal cells connect many photoreceptor synaptic terminations, providing lateral interactions that help integrate all the circuits. Bipolar cells transfer the light signals into the IPL, into the dendrites of amacrine and ganglion cells. Amacrine cells are inhibitory interneurons that extend laterally, connecting bipolar and ganglion cells. Ganglion cells are the final output neurons of the entire retina. They collect the signals of bipolar and amacrine cells and transmit, via their axons, these signals to the higher visual centers.

The retinal neurons are supported by Müller cells, the predominant glial cell type of the vertebrate retina. Müller cells traverse the retina from its inner to external border. Along their course, Müller cells extend processes that contact/interact every class of retinal neurons, at the level of soma, axons and/or dendrites. The adherens junctions between Müller cells and the inner segments of the photoreceptors form the outer limiting membrane.

I.1.2 The retinal pigment epithelium

The RPE is a monolayer of pigmented epithelial cells that separates the neural retina from its major blood supply, the choroid (**Figure 1**). The apical membrane of RPE cells faces the photoreceptors, containing long microvilli that surround and interacts with photoreceptor outer segments. The basal membrane of RPE cells contacts the Bruch's membrane, through which it communicates with the fenestrated endothelium of the choriocapillaris. The lateral membranes of RPE cells are sites of cell-cell communication and adhesion by gap, tight and adherens junctions, playing a role in maintaining RPE polarity. The basal membranes and the tight junctions form the RPE portion of the blood-retinal barrier (called outer blood-retinal barrier). Thus, passive and active transports of ions and selected molecules to the neural retina mainly occur across the RPE cells (transcellular transport), but also, to a lesser extent, across the tight junctions (paracellular transport).

The total number of pigmented epithelial cells in the human eye ranges from 4.2 to 6.1 millions. The density, the shape and the size of RPE cells vary across the retina, allowing a constant number of photoreceptors per RPE cells. In rhesus monkeys, each RPE cell interacts with 20 to 45 photoreceptors. In the human macula, it has been estimated that 23 photoreceptors interact with one RPE cell [4].

The RPE performs a variety of complex functions that are essential for proper visual function, through the maintenance of normal photoreceptor cell function and viability [5] [6]. This complex interaction between photoreceptor and RPE cells will be described further in this chapter.

I.2. The photoreceptors

I.2.1. Photoreceptor fundamentals

In the mammalian retina, two main classes of photoreceptors mediate light perception: the rods and the cones. Both share the same basic cellular organization (**Figure 2a**). They both contain four morphologically/functionally distinct compartments: an outer segment, an inner segment, a cell body and a synaptic terminal. The outer segment is a modified sensory cilium and the photosensitive organelle in which phototransduction occurs. It is formed of stack of discs containing photopigment molecules, formed from a light-absorbing 11-*cis* chromophore and a protein called opsin (**Figure 2b**). The inner segment is the site of metabolism and protein biosynthesis, and contains therefore numerous mitochondria. The cell body contains the genetic material and the machinery required for genetic expression functions. The synaptic termination holds synaptic vesicles, which distribute neurotransmitter, and thereby transmit light signal to second-order neurons of the retina. The synaptic neurotransmitter of the photoreceptors is glutamate, which is released in response to depolarization. The outer segment and the inner segment are physically linked through a narrow bridge called the connecting cilium (**Figure 2c**). This link maintains cytoplasmic and plasma membrane continuity from the soma to the outer segment. All soluble or membrane-bound materials synthetized in the inner segment and destined to the outer segment must pass through the connecting cilium.
Despite these similarities, rods and cones differ on many features as their density, proportion and location, morphology, synaptic connections, light properties and sensitivity. These differences determine the basic characteristics of our vision, but also, the unique and intrinsic vulnerability of rods and cones.

Rods: Rods are the predominant cell type in the mammalian retina accounting for 95% of all photoreceptors. The majority of rods is in the periphery of the retina and is thus responsible for peripheral vision. Most vertebrate retinas contain a single type of rods, which contains rhodopsin as visual pigment (maximum sensitivity to 496-500nm). Rods are able to recognize a single photon as a specific signal and mediate dim-light vision in humans.
This maximal degree of sensitivity and efficiency is the result of the unique structure of the rod pathway. Rods have slim cylindrically-shaped outer segments filled with around 1000 flattened, lamellar-shaped membrane discs that are perpendicularly ordered to the axis of the outer segment. These discs are physically separated from the plasma membrane, although filamentous structures bridge adjacent discs and disc rims to the nearby plasma membrane (**Figure 2b**). Rhodopsin comprises 95% of the total amount of disc protein and is densely packed within the disc lamellae around 25 000 molecules/μm^2 [7]. The high density of rhodopsin, as well as its ordered alignment to the light path, provides a high probability of capturing an incident photon. In addition, rods have low intrinsic noise and a powerful amplification cascade.

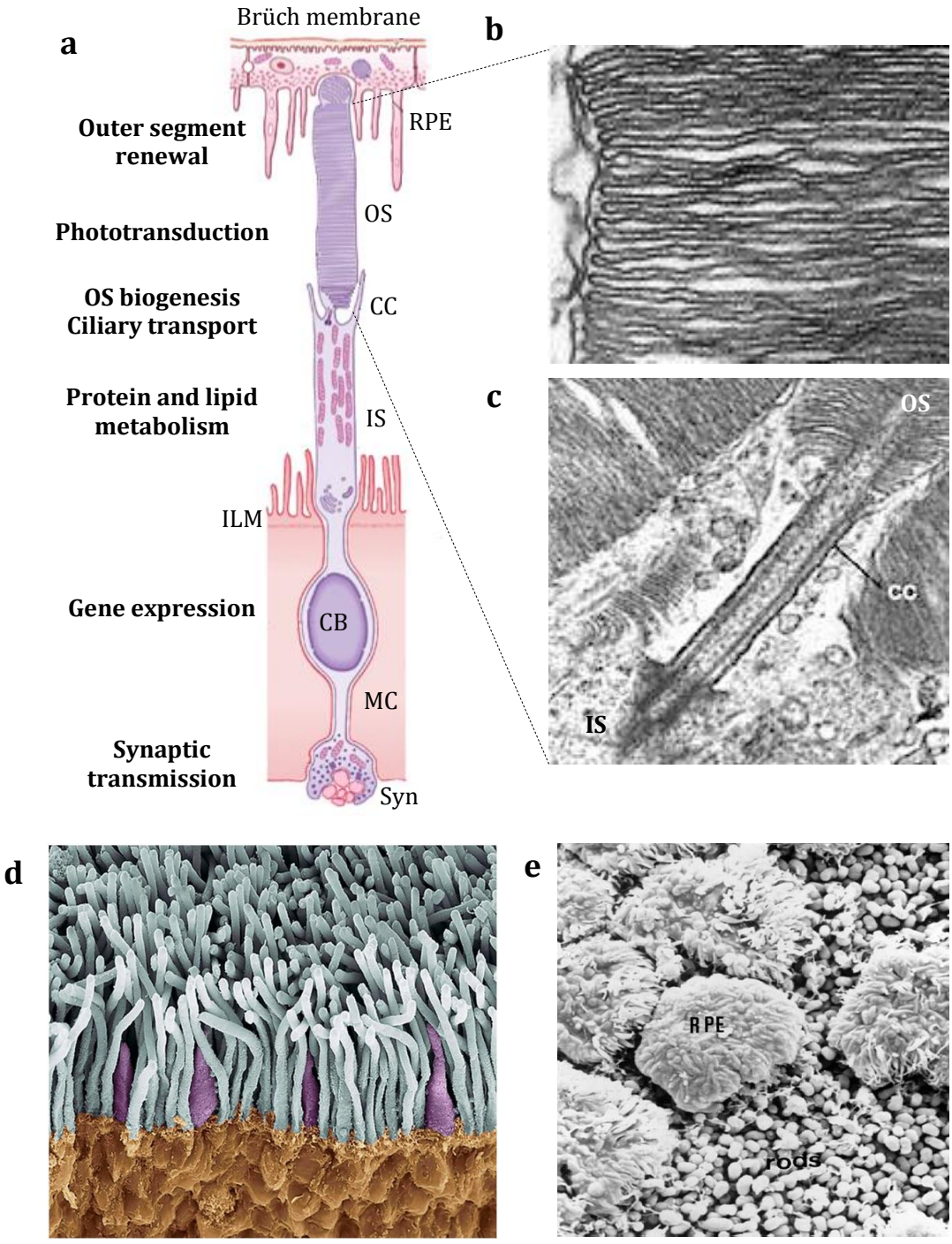

Figure 2. Structural organization of photoreceptor cells and the outer retina. (**a**) Schematic representation of vertebrate rod photoreceptor showing its functional parts. The cell is composed of an outer segment (OS), which contains stacks of photo-sensible discs, an inner segment (IS), which contains the biosynthetic machinery, a connecting cilium (CC) that connect the inner and outer segments, a cell body (CB) containing the nuclei and a synaptic terminal (Syn). (**b**) Electron micrography showing a longitudinal section of the rod outer segment, revealing stacks of discs surrounded by the plasma membrane [8]. (**c**) Electron micrograph showing the localization of the connecting cilium between the outer and inner segments of a vertebrate rod [8]. (**d**) Field emission scanning electron micrograph showing the differences between the morphology of cone (purple) and rod (grey) outer segments in the vertebrate retina. (e) Field emission scanning electron micrograph showing the association of the RPE cells with rod photoreceptor outer segment in the rat retina (http://starklab.slu.edu/lipofuscin1.htm).

Depending on the species, the signal from 20 to 100 rods converge onto a single rod bipolar cell, and many rod bipolar cells contact a given amacrine cell to generate a large response in ganglion cells. The convergence of the rod pathway provides a high sensitive vision, but with low spatial resolution.

Cones: Cones constitute only 5% of photoreceptors in the human retina and 3% in the murine retina. The human retina contains approximately 4-5 million cones. In human and other higher primates, cone cells are predominantly clustered in the central part of the retina, the macula, and comprised nearly 100% of the fovea, a 700μm diameter area in the center of the macula that enables the highest acuity vision due to structural and compositional specificities (**Figure 3**). Cone density rapidly declines radially toward the periphery (from 200 000 cones/mm^2 in the fovea to 2 000 cones/mm^2 at the edge of the fovea and 5 000 cones/mm^2 in the periphery) (**Figures 3**). The functional consequence of this extreme specialization of the fovea is that maximal central visual acuity can be generated in a very small area of the entire retina under photopic conditions.

In primates, cones contain one of three cone visual pigments with maximal absorption for a specific wavelength of light: the long (red), the middle (green) and the short (blue) wavelength sensitive opsins. Red cones contain the L sensitive opsin that has maximum sensitivity at 555-565nm. Green cones contain the M sensitive opsin that has maximum sensitivity at 530-537nm. Blue cones contain the S sensitive opsin, which best absorbs 415-430 nm. Our normal color vision is the result of the relative stimulation of these three types of cones. L cones (63% of cones) are as twice as many than M cones (32% of cones), whereas S cones constitute only 5% of all cones [9]. Most other mammals have di-chromatic vision, as they have only M- and S-sensitive cone pigments. In mice, M- and S-opsins have maximal spectral sensitivity at 508 and 360nm, respectively. In dogs, M- and S-opsins have maximal spectral sensitivity at 555 and 429nm, respectively

The cone system is relatively insensitive to light compared to the rod pathway, but it is optimized for good spatial and temporal resolution. Cones have faster response kinetics than rods and they can adapt to a wider range of light intensities. These physiological differences between rods and cones can be partially explained by the starkly contrast between cone and rod outer segments [10]. Cone outer segments are robust conical-shaped structures. They contain an orderly stack of membranous lamellas that are, contrary to rods, continuously connected to the plasma membrane. These open cone discs allow rapid exchange of substances between cell exterior and interior, such as chromophore transfer for pigment regeneration. The low sensitivity of the cone system can be explained by the fact that cone pathway is much less convergent than the rod system. In the macula, and particularly in the fovea, one cone will contact one bipolar cell that will contact one ganglion cell. Thus, more than 100 photons are required to produce a response in a cone comparable with a 1-photon response in a rod. This sacrifice is the cost for a high spatial resolution in the fovea.

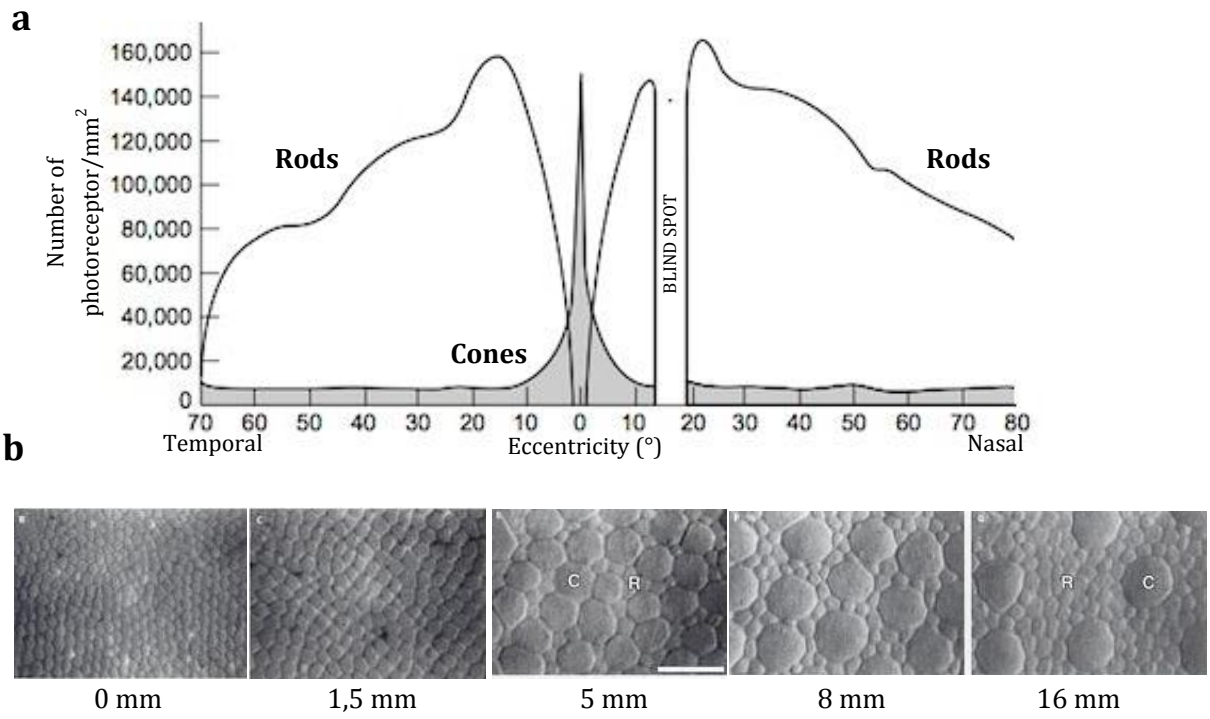

Figure 3. Rod and cone density in the human retina. (**a**) Graph showing rod and cone density along the horizontal meridian in the human retina. Cone density peaks in the center of the fovea and then rapidly declines toward the periphery. Rod density peaks in a ring of approximately 5mm from the center of the fovea (parafovea). Rods outnumbered cones from 2mm from the fovea to the far periphery. (**d**) Photoreceptor mosaic at 0; 1,5; 5; 8 and 16mm from the central fovea showing eccentricity dependent changes in rod (R) and cone (C) density and inner segment diameter.

I.2.2. Photoreceptor function

I.2.2.1. The phototransduction cascade

Both rods and cones express cyclic GMP (cGMP)-gated cation (Na^+/Ca^{2+}) channels in their outer segment, and a K^+-selective channel and Na^+/K^+ ATPase in their inner segment (**Figure 4a,b**). This distribution of channels allows the circulation of a current loop between the inner and outer segments, due to a constant influx of sodium and calcium into the outer segment and an outward gradient of K^+ in the inner segment. In darkness, this current (called dark current) is maximal, as most cGMP channels are maintained in an open-state. It keeps the photoreceptors partially depolarized. As a consequence, voltage-gated Ca^{2+} channels at the synapse are opened and Ca^{2+} influx promotes the fusion of synaptic vesicle membranes and the steady release of neurotransmitter glutamate from the photoreceptor terminal synapse (**Figure 4a**). In light condition, the dark current is suppressed by a rapid decrease in cGMP cytosolic levels and a concomitant closure of cGMP channels. There is a decrease in intracellular Ca^{2+} levels due to a continuous extrusion from the outer segment via Na^+/Ca^{2+}, K^+ exchangers. Photoreceptor membrane potential hyperpolarizes. At the synapse, voltage-sensitive Ca^{2+} channels close and there is a reduction of glutamate release (**Figure 4b**).

Light-dependent inhibition of the dark current is called phototransduction. This particular pathway is illustrated in **Figure 4c**. Phototransduction takes places in the photoreceptor outer segments. It begins with the activation of visual pigment molecules. Absorption of a photon by the 11-*cis*-retinal of the light sensitive opsin (R) isomerizes the chromophore from the 11-*cis* to the all-*trans* configuration. This *cis-trans* isomerization of retinal triggers a conformational change of the opsin protein and leads its transformation to its catalytic active form (R*).

The photoactivated pigment R* binds and activates the transducin (T), a G-protein, that comprises three subunits Tα, Tβ and Tγ, with GDP bound to its Tα subunit. The activation of G consists of a rapid GDP/GTP substitution on the Tα subunit and the subsequent dissociation of the GTP-Tα* activated transducin from Tβγ subunits. GTP-Tα* mediates activation of the cGMP phosphodiesterase (PDE6) by removal of the inhibitory PDE6γ subunits, allowing the catalytic PDE6αβ (PDE6*) core to hydrolyze the second messenger cGMP to GMP. As a result, the cytosolic concentration of cGMP falls, and the conductance of cGMP-gated channels decreases. There is a reduction of the circulating dark current and the membrane voltage becomes more and more negative relative to the outside. Hyperpolarization of the membrane potential results in (i) closure of the voltage-gated Ca^{2+} channels at the photoreceptor synaptic terminal, (ii) inhibition of neurotransmitter release at the synaptic terminal of the photoreceptor, and (iii) transmission of signals to adjacent horizontal and bipolar cells.

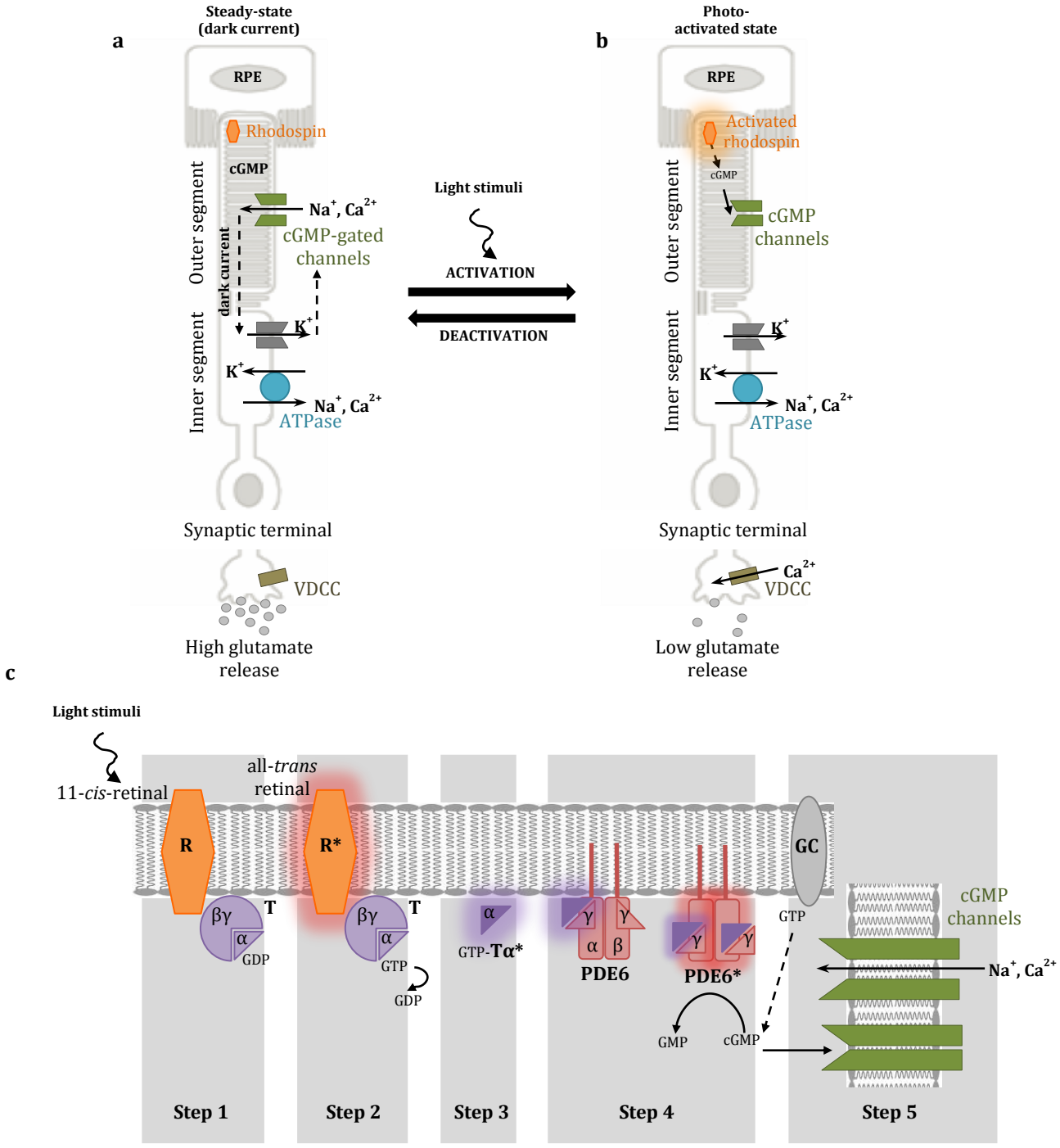

Figure 4. Photoreceptor phototransduction. (**a**) In the dark, cGMP is high and cGMP cation channels in the outer segment membrane are open, enabling entry of Na^+ and Ca^{2+}. A dark current circulates between the inner and outer segment, depolarizing the cell. (**b**) In light, phototransduction leads to the depletion of cGMP, which closes the cGMP-gated channels. This hyperpolarizes the photoreceptor membrane and inhibits the release of glutamate at the synaptic terminal. (**c**) Schematic representation of key steps of rod phototransduction cascade (modified from Lamb and Pugh, 2006). Step 1: upon absorption of a photon, 11-*cis*-retinal within rhodospin (R) is isomerized to all-*trans* retinal. This activates the rhodospin (R*) by conformational change. Steps 2 and 3: Activated rhodospin (R*) binds and activates the transducin (T) by accelerating guanine nucleotide exchange on its α subunit to form GTP-Tα*. Step 4: GTP-Tα* binds the inhibitory γ subunits of phosphodiesterase 6 (PDE6) and activates the PDE6αβ catalytic core. Activated PDE6 (PDE6*) hydrolyzes cGMP (synthetized by guanylyl cyclase, GC). Step 5: The rapid decline in cGMP cytosolic levels closes cGMP gated channels and reduces the Na^+ and Ca^{2+} influx.

I.2.2.2. Phototransduction shutdown and recovery

Following light activation, a recovery of the photoreceptor is essential so that it can respond to subsequent absorbed photons and signal rapid changes in illumination. This recovery from light is an active process. It requires efficient inactivation of each activated intermediates of the phototransduction cascade: R*, Tα* and PDE6*, as well as rapid restoration of the intracellular cGMP concentration. On the longer time scale, visual pigment has also to be regenerated (**Figure 5**).

The first step of the termination of the light response is the shutdown of the visual pigment R*. This process is initiated by phosphorylation of R* by rhodospin kinase (RK) and subsequent capping of partially inactivated R* by arrestin. Inactivation of activated GTP-Tα* is carried out by its endogenous GTPase activity, which hydrolyses bound GTP to GDP. The inactivation of GTP-Tα* and its separation to PDE6* ends the activation of the PDE6. The intracellular cGMP level returns to its original dark level by synthesis of cGMP by guanylate cyclase (GC), whose activity is increased when Ca^{2+} levels are reduced (via the activation of the Ca^{2+}-dependent gyanylate cyclase activating protein, GCAP). It re-opens cGMP-gated channels and the dark current is restored.

To restore the full dark-adapted sensitivity of photoreceptors, visual pigment must be continuously and efficiently regenerated from all-*trans*-retinal. Photoreceptors lack *cis*-*trans* isomerase function and are thus unable to regenerate themselves 11-*cis*-retinal after phototransduction. 11-*cis*-retinal is rather reformed in the RPE and exchanged to the photoreceptors through a process called the retinoid cycle (**Figure 5**). After signaling completion, the Schiff-base bond that attaches the all-*trans*-retinal to the opsin is hydrolyzed, permitting the dissociation of the retinoid from the binding pocket of the opsin. In photoreceptor outer segment, all-*trans*-retinal is reduced into all-*trans*-retinol by NADPH-dependent all-*trans*-retinol dehydrogenase. All-*trans*-retinol is then carried by interstitial retinal binding protein (IRBP) to the RPE. Lecithin retinol acyltransferase (LRAT) initiates the esterification of all-*trans*-retinol by adding an acyl group to retinol, forming all-*trans*-retinyl ester. Additionally, all-*trans* retinol from blood in the choroidal circulation can enter the visual cycle through the basal surface of RPE cells for esterification by LRAT. The retinal pigment epithelium-specific protein 65 kDa (RPE65) functions serve as the palmitoyl donor for LRAT. RPE65 hydrolyses and isomerizes all-*trans*-retinyl ester into 11-*cis*-retinol. Then, 11-*cis*-retinol is oxidized into 11-*cis*-retinal by NAD- and NADPH-dependent 11-*cis* retinol dehydrogenases (11-*cis* RDH). Finally, 11-*cis*-retinal is transported back to photoreceptors, either in IRBP-dependent or independent manner, where it reacts with opsin to regenerate the visual pigment.

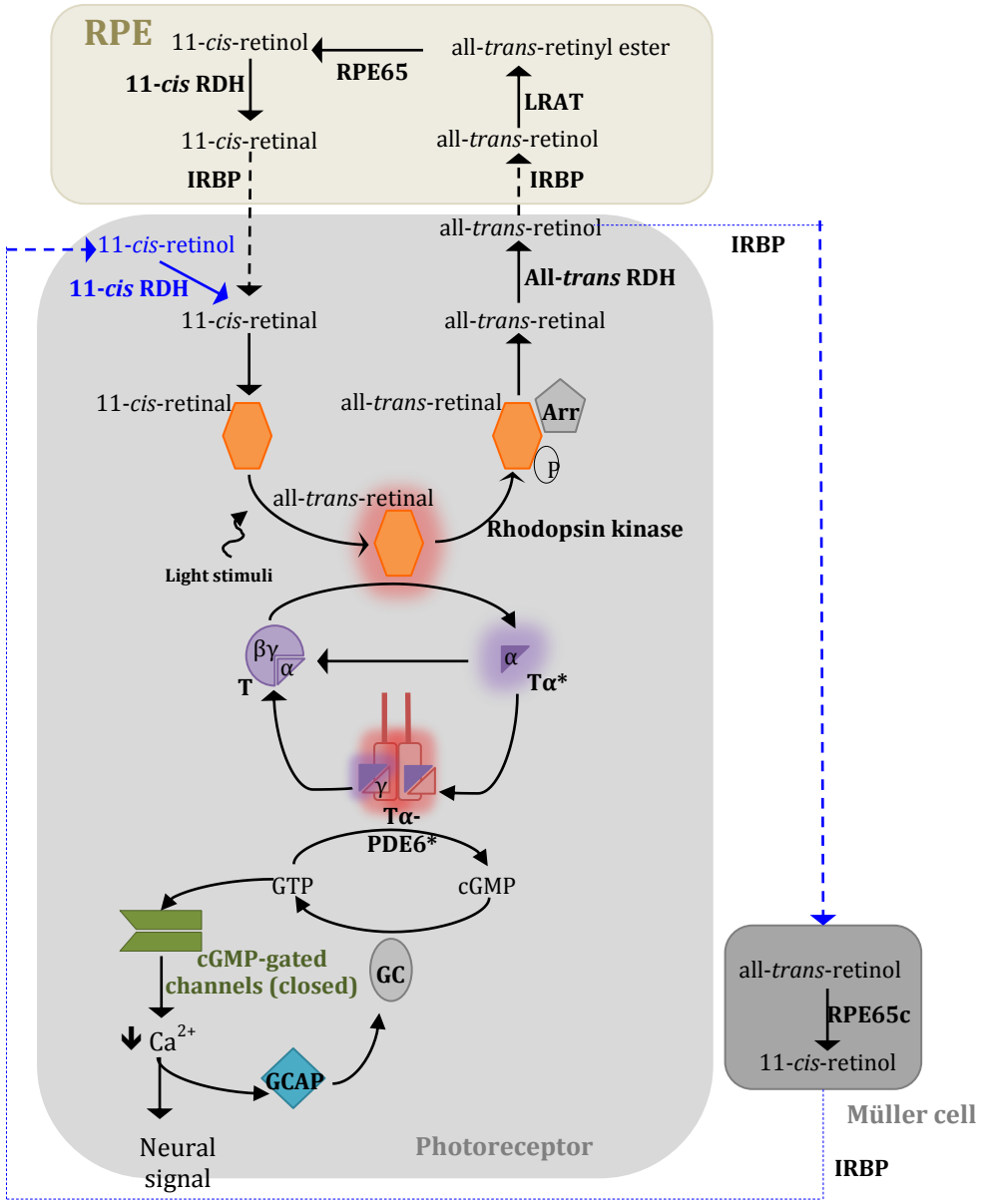

Figure 5. **Phototransduction shut-off and recovery in the vertebrate photoreceptor** (modified from McBee et *al*. Progress in Retinal and Eye Research, 2001).
Phototransduction shut-off: Following light-activation of rhodopsin (R*), the phototransduction cascade is activated, leading to the closure of cGMP-gated cation channels and hyperpolarization of the photoreceptor membrane. A consequence of channel closure is a rapid drop in internal free Ca^{2+}. This change in Ca^{2+} levels leads to activation of guanylate cyclase-activating proteins (GCAP), which can activate the guanylate cyclase to re-form cGMP (and thus re-open cGMP gated channels). For full recovery of photoreceptor cells, the intermediates of the phototransduction cascade, R*, T* and PDE6* need to be also deactivated. Inactivation of activated GTP-Tα* occurs by the mean of its endogenous GTPase activity, which hydrolyses bound GTP to GDP. This inactivation of GTP-Tα*and its separation toPDE6* ends the activation of Tα-PDE6*. R* is phosphorylated by rhodopsin kinase. Phosphorylated rhodopsin binds arrestin (Arr), quenching R* activity.

Retinoid cycle: All-*trans*-retinal is released from R* and reduced to all-*trans*-retinal by an all-*trans* retinal dehydrogenase (all-*trans* RDH). It is the first step of the retinoid cycle, which involves the transport of all-*trans*-retinol to the RPE, processing of this retinoid to 11-*cis*-retinal through a series of enzymatic reductions, and transport of the 11-*cis*-retinal back to the photoreceptor outer segment to recombine with opsin. Notably, a cone-specific retinoid cycle involving Müller glial cells was recently identified (in blue). In the proposed cone retinoid cycle, all-trans-retinol generated in photoreceptors is transported to Müller cells and is isomerized to 11-*cis*-retinal by RPE65c. At that time, 11-*cis*-retinol from Müller cells enters the inner segments of the cones and is oxidized to *11*-cis-retinal. RDH, retinol dehydrogenase; IRBP, interstitial retinal binding protein; LRAT, lecithin retinol acyltransferase; RPE65, retinal pigment epithelium-specific protein 65 kDa.

The retinoid cycle illustrates the importance of the intimate link between photoreceptors and RPE in the maintenance of retinal function. While rods depend completely on the output of 11-*cis*-retinal from adjacent RPE cells for rhodopsin regeneration, cones can regenerate a part of their 11-*cis* retinal in a second retinoid cycle, involving the Müller cells [11], [12], [13] (**Figure 3**). The existence of this cone-specific visual cycle can be explained by the continuous activation of cones in bright light and the need for rapid chromophore recycling and visual pigment regeneration [11]. The cone-specific visual cycle could be critical for extending the dynamic range of cones to bright light and their rapid and complete dark adaptation following exposure to light [14].

I.2.2.3. Cone and rod molecular specificities

From this rapid overview, it is quite evident that photoreceptor function is complex. Phototransduction activation, inactivation, regulation and recovery depend on numerous different proteins and important protein-protein interactions. This complexity contributes to explain why so many mutations in genes encoding phototransduction proteins are associated with a loss of photoreceptor function (**Chapter 2**).

Interestingly, although phototransduction activation and inactivation are broadly similar between rod and cone photoreceptors, most of the central components of rod and cone signaling pathways are distinct [15], [16]. It is still unclear how these differences between rod and cone phototransduction cascade contributes for the distinct ability of rods and cones to respond to light. Nevertheless, precise knowledge of rod- and cone-specific components is important to permit correlations between a specific phototransduction defect and the subtype of photoreceptor primarily affected (**Chapter 2**).

The most obvious distinction between rod and cone phototransduction proteins is the presence of cone- and rod-specific PDE6. Both rod and cone PDE6 complexes contain two catalytic subunits and a pair of two inhibitory/regulatory subunits. Rod PDE6 holoenzyme is composed of two homologous catalytic α- (PDE6α) and β-subunits (PDE6β) and two copies of inhibitory γ subunit (PDE6γ) [17] whereas cone PDE6 holoenzyme is composed of two identical α'-catalytic subunits (PDE6α') and two cone-specific inhibitory PDE6γ' subunits.
Interestingly, it was demonstrated that the ectopic rod PDE6 catalytic subunits functionally substitute for cone PDE6 to mediate light signaling in a mouse model lacking cone PDE6 catalytic subunit ($Nr^{l-/-}$ *cpfl1* mouse) [18]. In the same manner, the expression of PDE6α' has been recently shown to restore rod-mediated electroretinographic (ERG) responses and preserve retinal structure in a murine model of PDE6β-deficiency (retinal degeneration *rd10* mouse) [19]. This result has been attributed to the assembly of cone PDE6α' with rod PDE6γ subunits, indicating that cone PDE6α' can replace rod PDE6αβ and couple effectively to the rod visual signaling pathway in response to light. However, rods with cone PDE6α' are approximately two times more sensitive to light than wild-type rods and had a slower rate of

deactivation [19], likely because the affinity of rod PDE6γ for cone PDE6α' is lower than that for the rod PDE6αβ.
Other differences between rod and cone phototransduction components can be highlighted. For example, immunostaining of the murine retina with antibodies against guanylate cyclase have indicated that the isozyme GC1 is more abundant in cones, whereas the isozyme GC2 is rod-specific [20]. Rods and cone also have different isoforms of transducin, (Tα1 subunit in rods, Tα2 in cones), visual arrestin (cones express their own arrestin called cone arrestin), and cGMP-gated channels (CNGA1/CNGB1 in rods, CNGA3/CNGB3 in cones).

There are also species-specific differences in the expression of some proteins in rods and cones. For example, rodents express the same rhodopsin kinase 1 (RK1) in rods and cones, whereas in dogs, RK1 expression in limited to rods [21]. In dogs, desensitization of cones is rather modulated by a cone-specific isoform, the rhodopsin kinase 7 (RK7). In other species, including human and monkeys, both RK1 and RK7 are co-expressed in cones [21]. Interestingly, the exact function of RK7 is still unclear but it was shown to have considerably higher specific activity than RK1, partially explaining the faster shutoff of cones. All these observations should be taken into account when studying an animal model of retinal degeneration caused by a defect in rod and/or cone phototransduction.

I.2.2.4. The need of energy and oxidative stress

To fully understand the functional consequences of phototransduction, it is important to highlight that photoreceptor function is an energy demanding process.
A photoreceptor requires prodigious amount of ATP to maintain its membrane potential and transport Na^+ and K^+ against their concentration and electrical gradient by the Na^+/Ca^{2+}, K^+ ATPase. It was estimated in the rabbit retina that in darkness, about 50% of ATP generated is used to maintain the dark-current [22]. ATP is also used for (i) the GFP-GTP exchange in Tα, (ii) by Ca^{2+} ATPase to recycle Ca^{2+} out of the cell, (iii) for the phosphorylation of R* by RK and (iv) for the large turnover of cyclic nucleotides in the outer segment, including hydrolysis of GTP to cGMP. The reduction of all-*trans* retinal to all-*trans* retinol by the NADPH-retinol dehydrogenase is also highly energy-dependent.
Consequently, the photoreceptors are considered as one of the highest-energy consuming cells in the human body. This statement is particularly true for cones that consume even more energy than rods because they do not saturate in bright light. The rhodopsin activity of cones is much higher than those of rods and they use more ATP per seconds for light transduction and phosphorylation [23]. In addition, the reduction of 11-*trans* retinal to all-*trans* retinol is more than 30 times higher in cones than in rods [24].
The high-energy demand of photoreceptor function is an important source of fragility for the photoreceptors for two reasons:

(i) First, the outer retina is avascular, probably to optimize the capture of photons by photoreceptor outer segments. This particular anatomy creates "the paradox that the most energy-hungry region of the central nervous system is the only region that lack intrinsic vessels [25]". To generate ATP and maintain their function, photoreceptors mainly depend on the release of lactate by Müller glial cells and/or by the transfer of glucose from the choroid (via the RPE cells). This supply of energy fuels needs to be constant, because photoreceptors have limited glycogen reserves [26] and because only cones are capable of using endogenous glycogen stores in the primate retina [27].

(ii) Secondly, photoreceptors generate more than 80% of their ATP by oxidative (aerobic) metabolism in the mitochondria of their inner segments. Reactive oxygen species are formed as a natural by-product of mitochondrial metabolism. These reactive species can damage proteins, lipids and DNA. Consequently, the high metabolic activity of photoreceptors does not only imply a dependence of photoreceptors on RPE and Müller cells, but also represents a high risk of oxidative damage of photoreceptor inner segments (**Figure 6**). This risk appears particularly high regarding that in the rat retina, photoreceptors use 3 to 4 times more oxygen than other retinal neurons, being probably the cells of the body with the highest rate of oxidative metabolism [28].

Being non-dividing permanent cells, the photoreceptors are particularly vulnerable to the accumulation of peroxidation damage. Cone inner segments contain mitochondria that are much larger, more densely packed and, two fold more abundant than in rods in murine retinas (and 10 fold more in primate retinas). Therefore, the cone inner segments might be more vulnerable to oxidative stress than those of rods [29].

I.2.3. Building and maintenance of photoreceptor outer segments

Photoreceptor outer segments are also particularly prone to the generation of reactive oxygen species because of their high content in photosensitive molecules (as retinoids, lipids and docosahexaenoic acid), the elevated oxygen levels in the subretinal space and exposure to light. It creates the second paradox of healthy photoreceptors that the cellular compartment exquisitely suited for capturing photons is endangered by its own light-detector activity.

Contrary to inner segments, photoreceptor outer segments lack intrinsic antioxidants as NAPH-depend glutathione reductase, thioreduxin and thioredoxin reducatase. This is attributed to the fact that high amount of NADPH is required in outer segments for the conversion of all-*trans* retinol into all-*trans* retinal [30]. However, it raises the question how photoreceptor outer segments are not compromised by oxidative stress under normal conditions.

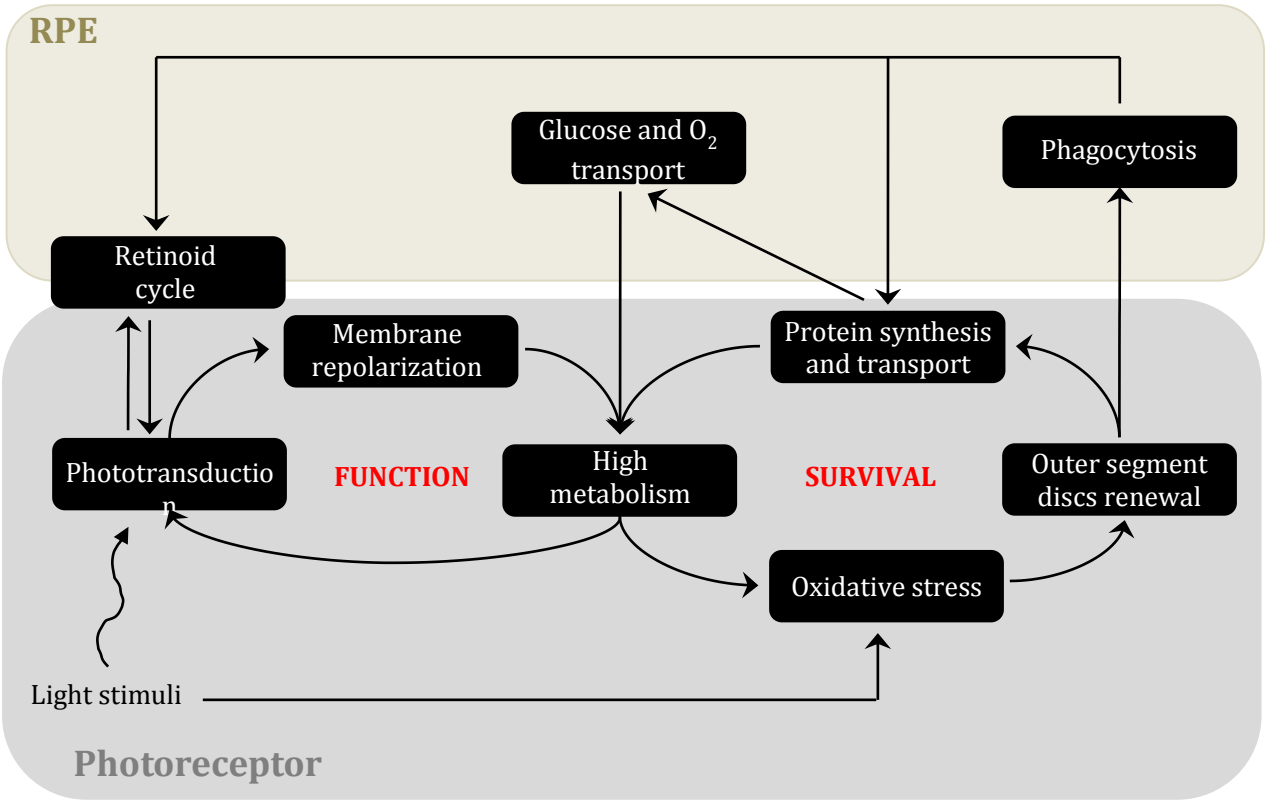

Figure 6. Physiology and biochemistry equilibrium in photoreceptor cells. The unique structural and functional organization of photoreceptor cells is finely adapted to the initial capture of photons and creation of visual signals, but this organization also makes them unusually vulnerable to metabolic and oxidative stress. In addition, the close interdependence among photoreceptors and the RPE cells represents an additional source of fragility. Thus, under normal conditions, function and/or survival of photoreceptor cells appear intimately linked and constantly on the razor's edge. This suggests that any imbalance can break this equilibrium, causing or predisposing photoreceptor to dysfunction and/or degeneration.

I.2.3.1. Outer segment phagocytosis

The response is likely in the acquisition from years of selective pressure by photoreceptors of an elaborate mechanism to minimize the damage potential of molecular constituents prone to oxidation: the daily renewal of their outer segments [30]. Aged membrane at the tip of outer segments (that contains the highest concentration of radicals and oxidized proteins) is discarded and replaced from its cilia end by incorporating proteins and lipids delivered from the inner segment. Thus, damaged molecules have a minimal residence time in photoreceptor outer segments.

This feature is unique to the photoreceptors and is mediated by the outer segment recognition, binding, engulfment, internalization and phagocytosis by the neighboring RPE cells. Each day, RPE cells phagocytize around 10% of photoreceptor cell volume (4000 discs) [31], [32]. In the monkey, it takes 9 days to replace the entire rod outer segment in the peripheral retina, and 13 days in the parafoveal retina. According to these data, deficits in RPE phagocytosis can be rapidly detrimental for photoreceptor function and survival.

I.2.3.2. *De novo* synthesis of outer segment lipids and proteins

Although outer segment turnover is essential to the survival of both photoreceptors and RPE cells, this process is not trivial for the photoreceptors. Indeed, to maintain constant outer segment length, shedding of old discs has to be compensated by constant *de novo* synthesis of outer segment lipids and proteins in the photoreceptor inner segment (**Figure 6**). It has been estimated, in the rodent retina, that up to 10^7 new rhodopsin/rod outer segment/day have to be synthetized. In addition, the membrane support must also be synthesized at the rate of 77 cm^2/day [33]. This corresponds to amounts of a cell division per day. Thus, biosynthesis of proteins in photoreceptor inner segments greatly increases the energy demand of photoreceptors, approaching the need of a proliferating cell [29].

Interestingly, cell anabolism (set of metabolic pathways that involves synthesis of molecules) is generally powered by glucose catabolism. Consequently, it has been recently proposed that most of the glucose taken up by photoreceptors never enter the Krebs cycle but is rather diverged into the pento-phosphate pathway to fuel membrane and protein biosynthesis [29]. Thus, photoreceptors may have a high glycolytic rate to generate enough glycolytic intermediates for the pento-phosphate pathway, and at the same time, compensate the shortfall of ATP that would have been produced in the Krebs cycle [34]. This observation has an high importance as it suggests that photoreceptor outer segments will be adversely shortened and/or disrupted by an energetic collapse, due to reduction of glycolytic flux [29].

Here again, the RPE cells play a key role in supporting photoreceptor outer segment renewal process. Indeed, they provide most of the glucose and oxygen required for membrane and protein biosynthesis. In addition, RPE cells digest photoreceptor outer segments, recycle and

return important molecules such as retinal and docosahexaeonic acid back to photoreceptor inner segments to ensure less costly rebuilding of the new photoreceptor outer segments [5]. Therefore, photoreceptor cells absolutely require an extremely metabolic and catabolic active RPE for their maintenance and survival. This statement is probably even truer around the fovea, where high levels of photoreceptors and high incidence of photons place a greater demand on the RPE cells. The specialization of the photoreceptor outer segment (required for the photoreceptor function) poses thus a major problem for maintenance of photoreceptor viability, and the answer that has evolved to solve this problem (discs shedding) is an important source of vulnerability for the photoreceptors (**Figure 6**).

I.2.3.3. Protein trafficking to the outer segment

The fragility of photoreceptors is further enhanced by the fact that the outer segment cannot synthesize the proteins and membranes required for the phototransduction and the renewal. These proteins and lipids, synthetized in the inner segment, must travel at high flow rates through the connecting cilium to reach the outer segment. It has been estimated that in human rods, about 4,500 rhodopsin molecules and 0.1 μm^2 of membrane have to pass through the connecting cilium every minute [35]. This continuous demand for proteins and lipids renewal emphasizes the photoreceptor requirement for a particularly efficient mechanism of its outer segment delivery. Rods and cones are thus highly dependent on their very thin and fragile connecting cilium for both morphogenesis and maintenance of their functional outer segments.

The connecting cilium of the photoreceptors mainly consists of a backbone, called the axoneme, which is comprised of nine microtubule doublets arranged in a circle. This cilium is anchored to the basal body that acts as microtubule organizing center of the photoreceptor cell. Among the multiple mechanisms involve in protein transport between the inner and the outer segments of photoreceptors (including diffusion), the intraflagellar transport (ITF), e.g., the bidirectional active transport of components along the microtubules of the axoneme plays a crucial role in the outer segment assembly and structure.

Microtubules of the axoneme are oriented by their minus-end toward the basal body and their plus-end toward the distal tip of the cilia. The transport of ITF components along the microtubules involves motor proteins that use energy from ATP to move along microtubules. These molecular motors move in a single direction, towards either the plus or the minus end of the microtubule. In photoreceptors, the motors are associated with at least two large multiproteins IFT complexes that are thought to facilitate the binding, trafficking and release of the cargo moieties at different steps of the protein transport pathways [36], [37].

Proteins destined to the outer segment (as rhodopsin, guanylate cyclase or cGMP-gated channels) are transported in vesicles from the Golgi network to the base of the cilium, where IFT proteins are concentrated. Proteins destined to the outer segment interact with IFT proteins, probably after fusion of the vesicles with the periciliary membrane, a particular

structure at the base of the cilia. They are transported to the outer segment by kinesin II. At the tip, cytoplasmic dynein 1B is activated to carry the ITF particles back to the cell body and replenished IFT components.

It appears more and more evident that hundred of different proteins are involved in the IFT transport in photoreceptors, as well as in its control and its tight regulation. Although IFT is a focus of current intense research, the precise nature, function, physiological relevance, spatial distribution and interactions of these proteins remained poorly understood.

Identification of IFT transport is further complicated by the fact that some protein assembly complexes present a strong degree of subcellular and physiological plasticity [38]. In addition, recent studies have shown that cone and rod photoreceptors possess distinct transport machinery and pathways for the trafficking of outer segment proteins, in particular for opsin, transducin, PDE6 and cation channels [39, 40], [41]. Due to the importance of the connecting cilium in photoreceptor development and physiology, the involvement of such numerous and complex protein interactions in ITF represents an important source of fragility for photoreceptors. It explains why the connecting cilium is considered as the Achilles heel of the photoreceptors [42].

I.3. Conclusion: photoreceptors are vulnerable cells under constant stress

Vertebrate photoreceptors provide the biological basis of light-perception and are critical for human vision. To obtain this high degree of sensitivity, photoreceptors have evolved from years of selective pressure as highly specialized cells. The functional and structural organization of photoreceptors is outstandingly adapted to the initial capture and processing of visual signals.

In the meantime, the specialization of photoreceptors represents the gateway of photoreceptor vulnerability. Indeed, photoreceptors require thousands of different proteins to develop and maintain their outer segments, representing innumerable possibilities of deregulation and dysfunction. Photoreceptors require considerable energy to recognize a single photon as a specific signal whereas they lack direct accessibility to glucose and oxygen. In addition, their extensive oxidative metabolism and high lipid composition represent an important risk of oxidative damage in a constant light-exposed environment. These sources of fragility are interrelated and have cumulative effects. Photoreceptors are thus damaged by their own (optimal) activity. Consequently, under normal conditions, function and/or survival of photoreceptor cells are constantly on the razor's edge.

This observation is fascinating when considering that, for most of us, photoreceptors live and remain functionally during our entire life. Thus, in healthy photoreceptors, a very efficient "physiology and biochemistry equilibrium" could be at work to control stresses before they reach detrimental levels. At the same time, it seems likely that any additional stress and/or imbalance of protective and toxic factors can break this equilibrium, tipping function and/or survival of photoreceptors under high risk.

CHAPTER **II**

GENETIC DEFECTS IN PHOTORECEPTOR OR RPE CELLS CAUSE PHOTORECEPTOR DYSTROPHIES

Inherited photoreceptor dystrophies are a group of retinal disorders characterized by dysfunction and degeneration of the photoreceptors in response to genetic defects. Inherited retinopathies are genetically and clinically variable. In the majority of inherited photoreceptor dystrophies, both cone and rod photoreceptor die, but the degree to which these cells are affected differs between the various disorders. In this chapter, an overall picture of inherited retinal disorders will be rapidly provided, including clinical, genetic and molecular information.

Then, we will summarize the literature on retinopathies caused by mutations in the *PDE6β* or *RPGRIP1* gene in human patients, as well as murine and canine models, with particular emphasis on the resulting photoreceptor dysfunction and degeneration. It is important to understand the etiology and subsequent natural history of these particular inherited photoreceptor dystrophies to define applicable therapeutic strategies to intervene them.

Contents

II.1. Inherited retinal dystrophies

The high specialization and vulnerability of photoreceptors make them particularly susceptible to additional environmental and/or genetic damages and stress. These stresses can lead to photoreceptor dysfunction and/or degeneration, and irreversible loss of vision. Primary or secondary loss of photoreceptors is the share feature of numerous retinal disorders and the leading cause of visual blindness worldwide.

II.1.1. Photoreceptor degenerations

Photoreceptor degenerations can be divided into two main classes: acquired photoreceptor degenerations and inherited photoreceptor dystrophies. Acquired photoreceptor degenerations comprise different disorders such as age-related macular degeneration (AMD), diabetic retinopathy and retinopathy of prematurity. They are caused by complex interactions of environmental and genetic contributors and are mainly characterized by retinal or choroidal neovascularization. They affect a very large number of people worldwide (30 millions individuals for AMD, 40 millions individuals for diabetic retinopathy and over 65 millions individuals worldwide for glaucoma).
Inherited photoreceptor dystrophies are usually defined as monogenic forms of photoreceptor degenerations. They represent the major cause of familial blindness in Europe, with an overall prevalence of 1/2000, and more than 2 million people affected worldwide. These genetic disorders will be the main focus of this chapter.

II.1.2. Phenotypes of inherited photoreceptor dystrophies

Classifying inherited photoreceptor degenerations can appear as a tremendous task because they are both clinically and genetically heterogeneous. Numerous disease classifications co-exist based on the main type of photoreceptor affected (cones, rods and/or RPE), the type of visual dysfunction, the typical age of onset, the rate of disease progression, the inheritance pattern or the underlying genetic defect [43]. This chapter focuses primarily on offering a phenotypic framework to categorize photoreceptor degenerations. A genetic/mechanistic classification will be provided thereafter [1].

[1] To facilitate the distinction between the genotype and the phenotype of inherited retinal dystrophies, I chose to use a particular nomenclature throughout this manuscript. The phenotype of inherited retinal degenerations will be expressed in **bold**. Genes will be expressed using the international guidelines, i.e. in *italic* with capital letter for human genes (ex: h*PDE6β*) and minuscule letters for murine, bovine or canine genes (ex: c*Pde6β*). Proteins will be indicated using capital letter (PDE6β).

II.1.2.1. Functional subtypes of inherited photoreceptor dystrophies

Inherited photoreceptor degenerations can be stationary or progressive, and affect primarily the function of cones and/or rods (and thus, predominantly affect the central and/or peripheral vision). This *functional* classification is established using ERG that demonstrates the overall functional status of photoreceptors by recording the electric responses of the retina to light stimulation. Five main groups of inherited photoreceptor degenerations can be defined:

- **Achromatopsia**: stationary cone dysfunction
- **Cone dystrophies**: progressive cone dysfunction
- **Cone-rod dystrophies**: progressive cone dysfunction followed by progressive rod dysfunction
- **Congenital stationary night blindness**: stationary rod dysfunction
- **Rod-cone dystrophies** or **retinitis pigmentosa**: progressive rod dysfunction followed by progressive cone dysfunction.

When the disorder is a more generalized photoreceptor disease, i.e., when both rod and cone responses are absent or severely impaired within the first years of life (**rod-cone** or **cone-rod dystrophies**) the term **Leber congenital Amaurosis** (**LCA**) is commonly used. Consequently, LCA refers to the most (functionally) severe form of inherited photoreceptor dystrophies.

II.1.2.2. Retinal dysfunction is not always associated with degeneration

In many cases, the visual symptoms of inherited retinal dystrophies reflect the progression of photoreceptor degeneration. However, it is not always the case. Indeed, in several inherited photoreceptor dystrophies, photoreceptor dysfunction precedes instead of accompanying the loss of photoreceptor cell bodies [44]. Loss of function is instead an indicator, or a cause of cellular deterioration. For instance, it has been elegantly showed that cone cell bodies are still present for years after the total loss of cone outer segments and related function in some patients or animal affected by **rod-cone dystrophies** [45].
The weak correlation between photoreceptor dysfunction and degeneration is particularly true for the pathologies characterized by absence of photoreceptor function from birth (congenital dysfunction). In these pathologies, the absence of retinal function at early ages (and thus the absence of apparent progressive dysfunction), has traditionally led them to be classified as stationary disorders (**achromatopsia or congenital stationary night blindness**). However, it is now clear that most of these stationary disorders are rather associated with early and slowly progressive photoreceptor degeneration [46], [47], [48].

Table 1. Summary prevalence and features of inherited retinal dystrophies

Summary prevalence and features of inherited retinal dystrophies		
Disease	**Prevalence**	**Characteristics**
Achromatopsia (ACH)	1: 33,000	➢ Poor vision and photophobia from birth ➢ Pendular nystagmus ➢ Poor or no color discrimination (complete or incomplete achromatopsia) ➢ Slow OCT changes with IS-OS junction disruption. Reduced foveal thickness at late stages ➢ Normal fundus at early stages. Subtle granularity or atrophy of the macula at late stages. ➢ Nearly nonrecordable or absent cone ERG responses – Normal scotopic ERG responses ➢ Slow OCT changes with IS-OS junction disruption
Cone dystrophy (CD)	1: 30,000 – 1: 40,000	➢ Usally symptomatic within childhood or early adult life ➢ Visual loss, decreased visual acuity over time, photophobia from early stages. ➢ Pendular nystagmus ➢ Abnormalities of color vision ➢ Absent or severely decreased photopic and 30Hz flicker ERG response. Normal rod responses ➢ Progressive change of fundus with macular atrophy and vessel attenuation. Normal retinal periphery
Cone-rod dystrophy (CD)	1: 40, 0000	➢ Usally present within childhood or early adult life ➢ Visual loss, decreased visual acuity, photophobia ➢ Pendular nystagmus ➢ Abnormalities of color vision ➢ Absent or severely decreased cone ERG responses. At later stages, rod system abnormalities leading to night-blindness ➢ Progressive change of fundus with macular atrophy and vessel attenuation. Peripheral RPE atrophy, retinal pigmentation, optic nerve disc pallor at late stages.
Congenital stationary night blindness (CSNB)	?	➢ Nonprogressive defects in scotopic vision with otherwise normal visual function ➢ Normal fundus ➢ Severely abnormal rod-mediated ERGs – Normal photopic and 30Hz flicker ERG response
Rod-cone dystrophy (RD)	1: 4,000	➢ Night blindness in early childhood ➢ Visual acuity preserved in early and mid stages. Photophobia at late stage. ➢ Progressive loss of peripheral visual field (tunnel vision). Central vision will remain good until most, if not all, the peripheral field is lost ➢ Dramatic reduction of rod-mediated ERG responses. Reduction of photopic responses ➢ Bone spicule intraretinal pigmentation, inially in the peripheral retina. Attenuated retinal vessels, motting and granularity of the RPE, optic disc head pallor. Various degrees of retinal atrophy. At late stages: atrophy of RPE and choriocapillaris

Therefore, a clinical classification scheme only based on functional features would be insufficient in the diagnosis of photoreceptor dystrophies. It would be preferable to define an inherited photoreceptor dystrophy considering together their dysfunction (= functional loss) and degeneration (= physical loss) components. This strategy also provides important opportunities to compare the human disease expression with that of animal models.

Both functional and structural symptoms of the main sub-groups of photoreceptor dystrophies are summarized in **Table 1**. As mentioned by Den Hollander *et al.*, the different forms of inherited retinal dystrophies can have significant overlapping symptoms (**Figure 8**). It is particularly true at early or late stages of the diseases [43]. At early stages, patients with complete **cone dystrophies**, **cone-rod dystrophies** or **LCA** present severe cone impairment and nystagmus [49]. Similarly, at late stages, when retinal function is almost or totally absent, **cone-rod dystrophies** do not differ from **rod-cone dystrophies** [50].

II.1.2.3. Inherited retinal diseases can be syndromic

Inherited retinal dystrophies are usually confined to the eye. However, 20-30% of retinal dystrophies can also be found with concomitant dysfunction of other organs (**syndromic retinal dystrophies**), falling within more than 30 different syndromes [51]. The most frequent syndromic retinal dystrophies are the **Usher** (10-20% of all cases; rod-cone dystrophy associated with hearing impairment or deafness)[52] and **Bardet-Bield** syndrome (5-6% of all cases; rod-cone dystrophy associated with obesity, polydactyly, hypogonadism, mental impairment and renal failure) [53, 54].

II.1.3. Genetic of inherited photoreceptor dystrophies

II.1.3.1. Genetic heterogeneity

As mentioned in **Chapter 1**, the complexity of the processes that allow photoreceptor survival and function, as well as acquisition of visual information, represents innumerable possibilities for gene mutations, and alterations in gene expression or regulation. This explains why human inherited retinopathies have so high genotypic heterogeneity, with over 202 genes and 242 loci implicated so far (https://sph.uth.edu/retnet/home.htm; last accessed September 20, 2013).

The high heterogeneity of photoreceptor degenerations makes complex the incorporation of genetic information with the phenotypic classification. Different genes may cause the same disease phenotype. In addition, there can be many different disease-causing mutations in each gene and different mutations in a same gene can cause different diseases. Furthermore, the same mutation in different patients may produce different phenotypes (in term of age of onset and progression of the disease), even among members of the same family.

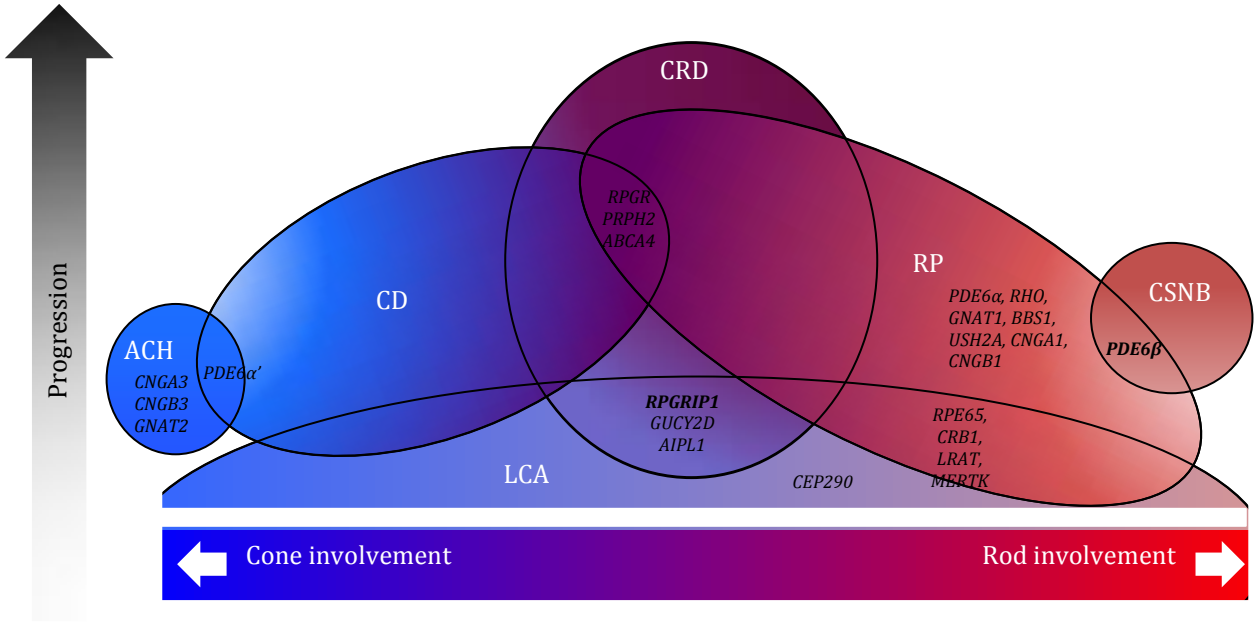

Figure 8. Schematic representation of phenotypic and genetic overlap among inherited retinal dystrophies (modified from Estrada-Cuzcano A. *et al*. Hum Mol Genet, 2012). The involvement of cone and rod photoreceptors and progression of diseases are shown in order to match the genetic overlap. At end stage, cone dystrophies (CD) can hardly be distinguished from cone-rod dystrophies (CRD). Patient with retinitis pigmentosa (RP) initially display night blindness due to rod defects, that progresses to complete blindness when the cones are also affected. In patients with LCA, both cones and rods are severely impacted. Thus, LCA, clinically and genetically overlap with CR, CRD and RP. Achromatopsia (ACH) and congenital stationary night blindness (CSNB) are pure cone or rod-functional defects, respectively. *PDE6β* is associated with both RP and CSNB. *RPGRIP1* is associated with LCA, CD and CRD.

II.1.3.2. Inheritance patterns

Determining the mode of transmission of inherited photoreceptor dystrophies has important diagnostic, prognostic and therapeutic implications, particularly for the development of appropriate gene-based therapies (**Chapter 4**).

There are four basic modes of transmission of inherited photoreceptor dystrophies: autosomal dominant, autosomal recessive, X-linked dominant and X-linked recessive. Other modes of inheritance exist, as in the cases of mitochondrial mutations or digenic pathologies.

The majority of heritable photoreceptor dystrophies are autosomal recessive. Among the 202 identified genes so far, 132 (65%) are associated with recessive disorders, 50 (25%) with dominant disorders, 13 (6%) with X-linked disorders and 7 (3%) with mitochondrial diseases (last access, October 17, 2013). Nevertheless, it is important to mention that these proportions for inheritance patterns assume that all *de novo* mutations are autosomal recessive and that 30 to 50% of the retinal dystrophies cases are sporadic.

II.1.3.3. Inherited photoreceptor dystrophies primarily arise from mutations in genes expressed in photoreceptors.

Another key question when studying inherited photoreceptor dystrophies is to identify the retinal cell type in which gene products are expressed. It allows (i) understanding the pathogenesis of photoreceptor degenerations; (ii) better distinguishing photoreceptor autonomous death (death of cells with primary damage) from photoreceptor non-autonomous death (death of cells without primary damage), and (iii) identifying the appropriate cell target for future therapies.

The great majority of inherited retinopathies arise primarily from mutations in genes expressed in photoreceptors (rods and/or cones). In addition, the RPE has been identified as the primary site of the etiology of several forms of inherited photoreceptor dystrophies. The outer retina is therefore the primary target for therapeutic strategies (**Table 2**).

Mutations altering the function and survival of cones cause pure cone disorders: Mutations in cone-specific genes generally only promote autonomous death of cones (**achromatopsia** or **cone dystrophies**), sparing the viability of rod photoreceptors. For example, mutations in the gene *PDE6C* that encodes the cone-specific PDE6α subunit of cone PDE6 holoenzyme lead to dysfunction/degeneration of cones only.

Mutations altering the function and survival of rods have secondary effects on cones: Contrary to cone-specific mutations, mutations in rod-specific genes that cause the death of rods are not confined to rods. They are also associated with the non-autonomous death of cone photoreceptors (rod-initiated **rod-cone dystrophies**). For example, *PDE6β* mutations affecting the rod PDE6 holoenzyme, lead not only to the degeneration of damaged rods, but also to that of healthy cones.

Nonsyndromic inherited retinal dystrophies				
Rod	Stationary	CSNB	Autosomal recessive	*GNAT1, GRK1(RK), NYX, RK*
			Autosomal dominant	*GNAT1, **PDE6β**, RHO (OPN2)*
	Progressive	RP	Autosomal recessive	*CNGA1, CNGB1, PDE6α, **PDE6β**, PDE6γ, NRL, RHO*
			Autosomal dominant	*NRL, RHO*
Cone	Stationary	ACHM	Autosomal recessive	*CNGA3 (ACHM2), CNGB3 (ACHM3), GNAT2 (ACHM4), PDE6C (PDE6α'), PDE6H (PDE6γ)*
			Autosomal dominant	*OPN1SW*
			X-linked	*OPN1LW/OPN1MW*
	Progressive	CD	Autosomal recessive	*CNGA3 (ACHM2), , CNGB3 (ACHM3), PDE6C (PDE6α'), PDE6H (PDE6γ)*
			Autosomal dominant	*GUCA1A (GCAP1)*
Rod and Cone	Stationary	CSNB	Autosomal recessive	*CABP4 (CSNB2B), SAG*
	Progressive	RP	Autosomal recessive	*ABCA4, AIPL1, ARL2BP, CLRN1, CRB1, CRX, DHDDS, EYS, FAM163A, GUCY2D, USH2A, NR2E3, RBP3, RDH12, RGR, RLBP1 (CRALBP),RGR, RP1, **RPGRIP1**, SAG, SPATA7, TULP1, USH2A*
			Autosomal dominant	*CRB1, CRX, FSCN2, GUCA1B (GCAP2), IMPDH1, KLHL7, NR2E3, PAP1, PRPF3, PRPF6, PRPF8, PRPF31, PRPH2, RDH12, ROM1, RGR, RP1, SNRNP200, TOPORS,*
			X-linked	*REP1, RP2, RPGR*
		CORD	Autosomal recessive	*ABCA4, ADAM9, CDHR1 (PCDH21), RLBP1 (CRALBP), RAB28, RAX2, **RPGRIP1***
			Autosomal dominant	*AIPL1, CRX, GUCY2D, HRG4, PHRP2, RIM1, UNC119*
			X-linked	*CACNA1F, RPGR*
		CD	Autosomal rcessive	*CACNARD4*
		LCA	Autosomal recessive	*AIPL1, CABP4, CEP290, CRB1, CRX, GUCY2D, IQCB1, LCA5, RD3, RDH12, **RPGRIP1**, SPATA7, TULP1*
			Autosomal dominant	*CRX, IMPDH1*
RPE	Stationary	CSNB	Autosomal recessive	*CABP4, RDH5*
	Progressive	RP	Autosomal recessive	*BEST1, LRAT, MERTK, RLBP1, RPE65*
			Autosomal dominant	*BEST1, RPE65*
		CORD	Autosomal recessive	*KCNV2, RPE65, RDH5*
		LCA	Autosomal recessive	*LRAT, MERTK, RPE65, KCNJ13*

Table 2. Identified genes associated with inherited retinal dystrophies

This secondary loss of cone function has the greatest impact on human vision, because cones mediate daylight and high acuity vision. A number of distinct models have been proposed to explain the secondary loss of cone photoreceptors in rod-initiated **rod-cone dystrophies**. They will be further discussed in paragraph III.5

Mutations altering the function and survival of rods and cones are associated with various phenotypes: When the causal mutations are in genes expressed in both photoreceptor subtypes, rod dysfunction/degeneration can slightly precede cone damage (**rod-cone dystrophies**) or inversely (**cone-rod dystrophies**) depending on the causal mutation, the gene, genetic modifiers and/or environmental factors. One example is the mutations in the *RPGRIP1* (encoding the Retinal Pigment GTPase Regulatory Protein 1, RPGRIP1) and the *GUCY2D* (encoding the retinal guanylate cyclase subunit 1, GC1) genes that are associated with **LCA**, **rod-cone dystrophies** and **cone-rod dystrophies**.
Similarly, mutations in genes expressed on RPE cells also hinder the function of the two subtypes of photoreceptors and are often associated with both **rod-cone** and **cone-rod dystrophies**. For instance, mutations in the *RPE65* gene cause **LCA** and/or **rod-cone dystrophies**.

The functions of the genes associated with photoreceptor dystrophies are varied. They encode proteins involve in almost all aspects of photoreceptor or RPE development, function and structure. Mutations affecting phototransduction or vitamin A metabolism are frequent. One third of non-syndromic retinal dystrophies is caused by a defect in a protein involved in the ciliary transport. This reflects the high level of specialization of photoreceptors and RPE. In addition, numerous mutations affect more general functions such as gene expression (transcription factors, splicing factors), protein folding, cytoskeleton, metabolism and cell-cell interactions. They reflect the vulnerability of photoreceptors and RPE cells.

The current study focuses on two recessive forms of inherited photoreceptor dystrophies caused by photoreceptor-specific defects in *PDE6β* (expressed in rods, involved the rod phototransduction cascade) and *RPGRIP1* (expressed in cones and rods, involved in the maintenance of photoreceptor outer segments).

II.2. Inherited photoreceptor dystrophies caused by mutations in *PDE6β*

II.2.1. *PDE6β* gene and transcripts

The *PDE6β* gene maps to chromosome 4p16.3 [55] and contains 22 exons [56]. The gene exhibits an alternative in-frame splice site at its 3' end. The alternative splice variants, *PDE6β-1* and *PDE6β-2,* encode either a 854 amino acid full-length protein (PDE6β-1) or a 853 amino acids protein with one missing amino acid near the C-terminus (PDE6β-2). A third variant *PDE6β-3* (NM-001145292.1) uses a downstream start codon compared to variants *PDE6β-1* and *-2*. The resulting isoform 3 lacks thus first 4 exons compared to variants PDE6β-1 and PDE6β-2.

The function and significance of the different human transcripts *PDE6β* is currently unknown. To date, no multiple *Pde6β* variants have been yet identified in other species, including the mouse, rat, bovine and dog (http://www.ncbi.nlm.nih.gov, last access September 26, 2013). In non-humans, the unique *Pde6β* transcript is closer to the human *PDE6β-1* transcript. Thus, I will focus on the *PDE6β-1/* PDE6β-1 variant.

II.2.2. PDE6β structure and biology

PDE6β encodes the PDE6β subunit of rod PDE6. Rod PDE6 is specifically expressed in rod photoreceptors and belongs to the vast superfamily of cyclic nucleotide PDE.

II.2.2.1. Rod PDE6 is the only PDE that contains two different catalytic subunits

In vertebrates, 11 different PDE families have been identified (PDE1 to PDE11). All PDE share a conserved catalytic domain but differ in their substrate specificity (cAMP and/or cGMP) and regulatory mechanisms [57]. As PDE5 and PDE9, PDE6 family strongly prefers cGMP as substrate. Rod PDE6 is the only heterotetrameric PDE [58]. As previously mentioned, rod PDE6 comprises two catalytic subunits PDE6α and PDE6β and two inhibitory subunits PDE6γ. Cone PDE6 catalytic dimer is instead composed of two identical PDE6α' subunits. Other PDE are thought to exist as homodimeric enzymes [57].

II.2.2.2. PDE6α and PDE6β catalytic subunits are highly homologous

PDE6α and PDE6β catalytic subunits are highly homologous, with 72% of identity at the protein level [59]. They have similar domain organization and both contain (**Figure 6a**):

- an N-terminal region of unknown function
- two regulatory GAF domains (cGMP phosphodiesterase, adenylyl cylases and the Escherichia coli protein Fh1A) : GAFa and GAFb [60]
- a catalytic domain
- and a C-terminal motif for post-translational modification

GAF domains: The GAF domains of PDE6α and PDE6β subunits are the primary dimerization domains between the two PDE6α and PDE6β subunits. The GAF domains contain non-catalytic cGMP-binding pockets. They are able to bind cGMP with high affinity and thus regulate the catalytic activity of PDE6. This regulation is also mediated by binding of PDE6γ by GAFa, in concert with cGMP [61].

Catalytic domain: Within the PDE6 structure, the catalytic domain is the most conserved and is enzymatically equivalent between the PDE6α and the PDE6β subunits [62], [63]. The structure-function relationship of this catalytic domain remains poorly understood due to difficulties in expressing functional PDE6 in heterologous systems [64], [65], [66], [67].

C-terminal domain: The C-terminal sequence of the PDE6α and the PDE6β catalytic subunits contains a CAAX motif for post-translational isoprenylation. This post-translational modification is a three-step process. First, a farnesyl or geranylgenerayl lipid is added to the C-terminal cysteine of the CAAX. Then, the last three –AAX amino acids are proteolyzed. Finally, the newly exposed isoprenyl-cysteine residue is esterified [68].
A unique feature of the rod PDE6 is the differential prenylation of its catalytic subunits: the PDE6α subunit is farnesylated whereas the PDE6β subunit is geranylgeranylated. These modifications serve as membrane anchors for attachment of PDE6α and PDE6β subunits to rod outer segment disc membranes. They are indispensable for the interactions between the rod PDE6 enzyme with its protein partners, such as Tα*.
The importance of PDE6 prenylation in retinal function has been illustrated by studies of the *rod-cone dysplasia type 1* (*rcd1*) dog, a canine model of *PDE6β* rod-initiated **rod-cone dystrophy**. This dog displays a nonsense mutation in the exon 21 of the *Pde6β* gene that truncates the PDE6β subunit by 49 amino acids and removes the C-terminal domain required for posttranslational modifications [69]. No rod PDE6 activity is detectable in affected dogs [69]. As a consequence, rod-mediated ERG responses are totally absent from birth, and rapid photoreceptor degeneration occurs [70], [71].

II.2.2.3. Both PDE6α and PDE6β are required for PDE6 activity

Dimerization of PDE6α and PDE6β catalytic subunits is indispensable for rod PDE6 holoenzyme expression/activity [72]. Thus, defects in any of the two catalytic PDE6α or PDE6β subunits are sufficient to severely affect rod PDE6 activity. The functional significance of rod PDE6β heterodimerization remains unclear.

II.2.3. *PDE6β* mutations are associated with different retinopathies

Mutations in the *PDE6β* gene lead to severe retinal dystrophies. *PDE6β* mutations have been found in 3-8% of patients with recessive **rod-cone dystrophy**, characterized by sequential degeneration of rod and cone photoreceptors [73, 74], [75] [76], [77], [78], [79], [80], [81], [82], [83]. In addition, *PDE6β* mutations have been detected in patients with dominant **stationary congenital night blindness** with rod dysfunction but mild photoreceptor degeneration and no cone deficits [84], [85]. **Figure 8** and **Table 3** depict all *PDE6β* mutations identified to date.

II.2.4. Rod-cone dystrophies resulting from *PDE6β* mutations: a short review

II.2.4.1. Human patients with PDE6β-linked rod-cone dystrophy

Allelic heterogeneity in patients with PDE6β rod-cone dystrophy

At least 24 different disease-causing *PDE6β* mutations have been identified in patients with autosomal recessive **rod-cone dystrophies.** Most of the identified gene defects in *PDE6β* are compound heterozygous recessive mutations, but some homozygous mutations have been identified in families showing consanguinity (**Table 3**). In addition, "double hits" have been reported within families with very high consanguinity, with patients carrying homozygous mutations in both *GPR98* and *PDE6β* genes [79] or in both *MYO7A* and *PDE6β* genes [86].

46% of the *PDE6β* mutations (n=11) are missense mutations. They include 8 mutations clustered in a limited region of the protein, which overlaps the catalytic domain of PDE6β (555-570): Leu527Pro, Ile535Asn, Arg552Gln, His557Tyr, Gly576Asp, Asp600Asn, Thr604Ile and Leu699Arg. The high frequency of pathogenic mutations in this domain may reflect the functionality and/or higher structural fragility of this region. In all cases, the importance of the mutated codons is further supported by their high conservation within mammals, including mice, bovines and dogs. These missense mutations are not expected to alter the reading frame but they may reduce PDE6 activity. However, *in sillico* analyses have suggested that these missense mutations can lead to structural instability of the PDE6β and thus produce *null* alleles.

Total absence of PDE6 activity is more easily predictable for all nonsense and frameshift mutations that would produce severely truncated PDE6β subunit (>33%, n>8) and removal of the C terminal domain. Alternatively, *PDE6β* mutations leading to premature stop codons may result in low levels of PDE6β due to nonsense-mediated decay of the mutant mRNA.

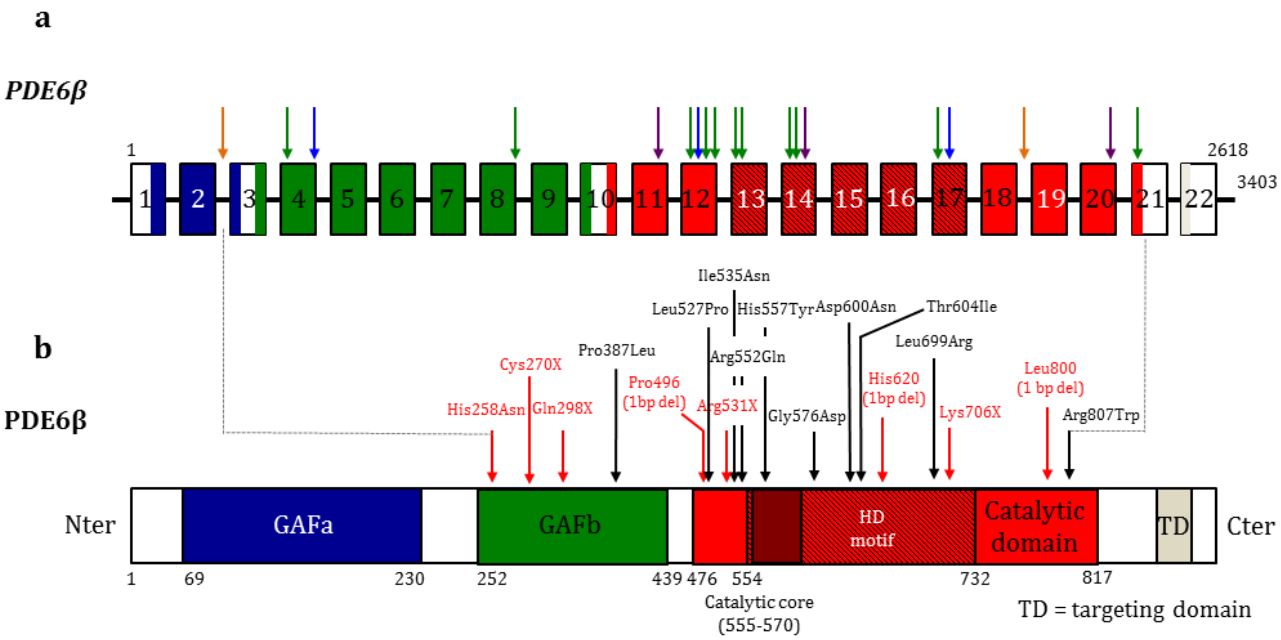

RP allele 1	RP allele 2
Cys270X	Cys270X
Gln298X	Lys706X
Gln288X	Arg513X
Pro387Leu	Arg552Gln
Pro496 (1 bp del)	His557Tyr
Leu527Pro	Intron 18
Ile535Asn	Ile535Asn
Arg552Gln	Arg552Gln
His557Tyr	His557Tyr
Gly576Asp	His620 (1 bp del)
Asp600Asn	Asp600Asn
Thr604Ile	?
Leu699Arg	Leu699Arg
Lys706X	Intron 2
Leu800 (1 bp del)	Leu800 (1 bp del)
Arg807Trp	?

CSNB allele 1	CSNB allele 2
His258Asn	/

Nonsense
Intronic
Missense
Expected *null* allele
Frameshift
Non-expected *null* allele

Figure 8. Schematic representation of the (a) human *PDE6β* gene and the (b) human PDE6β subunit showing functional protein domains and sequences variants that have been associated with rod-cone dystrophy or congenital stationary night blindness. The 22 exons of *PDE6β* are drawn to scale, introns are not. Protein domains are shown with colored boxes: GAFa in blue, GAFb in green, catalytic domain in red, targeting domain (TD) in beige. Sequence variants are depicted as arrow. They are then grouped per phenotype.
We can note than nearly all missense mutations are clustered in the catalytic domain of PDE6β. No pathogenic variants are observed in the GAFa domain, consistent with the important heterogeneity of this sequence between PDE6α and PDE6β and across different species (including the mouse, the rat, the bovine and the dog). RP, retintis pigmentosa; CSNB, congenital stationary night blindess.

Table 3. List of identified *PDE6β* mutations and genotype-phenotype correlations (1/4)

List of identified *PDE6β* mutations and genotype-phenotype correlations								
Exon	**Nucleotide change**	**Amino-acid change**	**Description**	**Expected PDE6 activity (if expressed)**	**Disease association**	**Age**	**Clinical findings**	**Refs**
Intron 2	/	Alteration slice acceptor site intron 12	? Heterozygous Predicted in-frame loss of exon 3	Decreased– Protein that will miss 30 amino acids from its non catalytic cGMP GAFA domain	arRP	24 y and < 24 y	• Night blindness since childhood • Slowly progressive visual field loss • Attenuated retinal vessels • Bone-spicule pigments in the mid-periphery • Visual field (V-4^e): full except some limitation in superior • Visual field (I-4^e): reduced to central island only • Dark-adapted threshold: reduced by 4 log units • No detectable rod and cone ERG	Danciger et al. 1995
17	c21887A>T	Lys706X	Nonsense Heterozygous Truncated protein	Decreased – protein truncated by 140 amino acids. Elimination of a portion of the catalytic domain	arRP	24 y and 21 y	/	McLaughlin et al. 1995
4	c11638C>T	Gln298X	Nonsense Heterozygous Truncated protein	Absent – total loss of the catalytic domain	arRP	44 y	• Night blindness since early childhood • Visual acuity: 20/40 • Visual field: 20° with peripheral islands • Dark-adapted threshold: reduced by more than 2 log units • No detectable rod ERG • Reduced cone ERG (amplitude/delay) • Attenuated retinal vessels • Bone-spicule pigments around the midperiphery	McLaughlin et al. 1993
12	c18086C>T	Arg531X	Nonsense Heterozygous Truncated protein	Absent – total loss of the catalytic domain				
12	c.1655G>A	Arg552Gln	Missense Homozygous	Reduced – substitution of a hydrophilic residue by a neutral residue close to the catalytic domain	arRP	/	/	Valverde et al. 1996

Table 3. List of identified *PDE6β* mutations and genotype-phenotype correlations (2/4)

List of identified *PDE6β* mutations and genotype-phenotype correlations								
Exon	**Nucleotide change**	**Amino-acid change**	**Description**	**Expected PDE6 activity (if expressed)**	**Disease association**	**Age**	**Clinical findings**	**Refs**
12	c.1728G>A	Arg552Gln	Missense Heterozygous	Reduced – substitution of a hydrophilic residue by a neutral residue close to the catalytic domain	arRP	28 y	• Night blindness since early childhood • Visual acuity: 6/24 (left and right) • No detectable rod and cone ERG • Attenuated retinal vessels • Waxy-palor optic nerve heads • Bone-spicule pigments in the peripheral and central retina	Ali et al. 2011
8	c.1160C>T	P387L	Missense Heterozygous	Reduced – substiution in the regulatory GAF domain + potential deleterious effect on the PDE6β structure		55 y	• Idem with visual acuity of 6/18 (left and right)	
11	1 bp del 17981	Pro496 (1bp del)	Nonsense Heterozygous Frameshift Mutant protein with premature stop at 574	Absent -catalytic domain with altered sequence and no Cter domain	arRP	41 y	• Night blindness since early childhood • Visual acuity: 20/40 • Visual field: 20° with peripheral islands • Dark-adapted threshold: reduced by more than 2 log units • No detectable rod ERG • Reduced cone ERG (amplitude/delay) • Attenuated retinal vessels • Bone-spicule pigments in midperiphery	McLaughlin et al. 1993
13	c19876C>T	His557Tyr	Missense Heterozygous	Decreased – elimination of a conserved positive residue within the catalytic domain				
13	c19876C>T	His557Tyr	Missense Homozygous	Decreased – elimination of a conserved positive residue within the catalytic domain	arRP			Kim et al. 2012
12	c18075T>C	Leu527Pro	Missense Heterozygous	Decreased – elimination of a conserved positive residue within catalytic domain/presence of an hydrophobic residue that can cause peptide chain bending	arRP	39 y and 35 y	• Night blindness since early childhood • Visual acuity: 20/40 • Visual field: 20° with peripheral islands • Dark-adapted threshold: reduced by more than 2 log units • No detectable rod ERG • Markedly reduced cone ERG (amplitude/delay) • Attenuated retinal vessels • Bone-spicule pigments in midperiphery	McLaughlin et al. 1995
Intron 18	G22624A	Alteration slice donor site intron 18	? Heterozygous Exon skipping? Inclusion of an intron?	Decreased or absent– probable alteration of protein sequence				

List of identified *PDE6β* mutations and genotype-phenotype correlations								
Exon	**Nucleotide change**	**Amino-acid change**	**Description**	**Expected PDE6 activity (if expressed)**	**Disease association**	**Age**	**Clinical findings**	**Refs**
13	c.1655G>A	Gly576Asp	Missense mutation Heterozygous	Altered - substitution of a conserved neutral residue by an acid residue within the catalytic domain	arRP	41 y and 49 y	• Early onset of night blindness • Progressive loss of visual field • Visual field : reduced to small central island of vision • Dark-adapted threshold: no • No detectable rod and cone ERG • Attenuated retinal vessels • Pigments in the mid and far-periphery • Waxy-appearing optic nerve heads	Danciger et al. 1995
14	/	His620 (1bp del)	Nonsense mutation Heterozygous Frameshift Mutant protein with premature stop at 642	Altered – protein truncated by more than 200 amino acids. No C ter domain				
17	/	Leu699Arg	Missense Homozygous	Decreased - substitution of a hydrophobic residue by a neutral residue in the catalytic domain	arRP	/	/	Valverde et al. 1996
12	/	Ile535Asn	Missense Homozygous	Decreased - substitution of a nonpolar residue by a polar residue close to the catalytic domain	arRP	40 y to 45 y	• First clinical exam at 40y for visual field disturbance • Poor night vision since childhood • Visual acuity: 8/10 (40y) then 10/10 (45y) • Visual field (V-4e): central field within 9° + arched temporal field in the left eye • No recordable rod and cone ERG • Moderate bone spicule pigmentation in all quadrants • No remarkable macular change	Saga et al. 1998
						46 y to 51 y	• Visual acuity: 6/10 (46y) then 5/10 (51y) • Visual field (V-4e): central field within 9° • No recordable rod and cone ERG • Moderate bone spicule pigmentation in all quadrants • No remarkable macular change	

Table 3. List of identified *PDE6β* mutations and genotype-phenotype correlations (3/4)

List of identified *PDE6β* mutations and genotype-phenotype correlations							
Exon	**Nucleotide change**	**Amino-acid change**	**Description**	**Expected PDE6 activity (if expressed)**	**Disease association**	**Age**	**Clinical findings**	**Refs**
14	c.1798G>A	Asp600Asn	Missense Homozygous	Decreased – The substitution is located in a conserved Zn^{2+} and Mg^{2+} binding site of the protein	arRP	81 y	• Visual acuity: 20/200 (right eye) and 20/30 (left eye) • Pale optic nerve heads • Intraretinal pigments in the mid-periphery • Atrophy of RPE in the macula and severe loss of RPE function in both eyes, except a central foveal island in the left eye	Tsang et al. 2006
21	c. 2419T>A	Arg807Trp	Missense Heterozygous	Decreased – Substitution of a conserved tryptophane with a polar residue.	arRP	/	/	Hmani-Aifa et al. 2009
20	c.2399 (1bp del)	Leu800Arg fsX17	? Homozygous	Altered or decreased -	arRP	16y to 47 y	• Visual acuity: 20/63 (47y) • Pale optic nerve heads • Attenuated retinal vessels • Atrophic maculopathy • Perimacular remnant ofnormal RPE • RPE atrophy in periphery with intraretinal bone-spicule pigments	Collin et al. 2012
14		Thr604Ile	Missense Heterozygous		arRP			Kim et al. 2012
4		His258Asn	Missense Heterozygous		adCNSB	/	/	

Table 3. List of identified *PDE6β* mutations and genotype-phenotype correlations (4/4)

Phenotypic homology in patients with PDE6β rod-cone dystrophy

Functional/visual deficits: Interestingly, although the patients carry different *PDE6β* mutations, those that received clinical analyses display a similar ocular phenotype, undistinguishable from other patients with different forms of **rod-cone dystrophies**. In these studies, the ages of patients at examination ranged from 16 to 81 years (mean 37,4 years, =15, see **Table 3**). Absent night vision appears since the early childhood, probably due to absence/loss of rod photoreceptor function. Rod-mediated ERG responses are undetectable in all patients (**Figure 9c** and **Table 3**). Dark-adapted kinetic responses are still detectable in some patients, but are reduced by more than 2 log units (**Figure 9b** and **Table 3**).

The visual field (a measure of the area of the retina that is still capable of responding to light) is generally restricted to a small central island, except some cases report of temporal and/or peripheral fields (**Figure 9a** and **Table 3**). Cone-mediated ERG responses are undetectable or severely reduced in amplitude (**Figure 9c** and **Table 3**). However, visual acuities are still relatively well preserved, ranging from 6/18 to 10/10 (mean 20/40, n=10, **Table 3**). Longitudinal evaluations of visual acuity are very limited. They have suggested that there is very mild or no progressive decline in visual acuity at late stages of the disease, usually over a 5 years follow-up (data not shown).

Fundus alterations: There is also a consensus in ophthalmoscopic fundus examinations (**Figure 10a-c and Table 3**). Fundi of all patients show marked attenuated retinal vessels and typical intraretinal bone-spicule pigmentation around the mid-periphery. In oldest patients, retinal pigmentation is also observed in the far-periphery and central retina (**Figure 10c**). In these patients, RPE are atrophic and optic nerve heads pale.

These findings mainly reflect the degeneration of rods. Indeed, vascular changes are thought to be secondary to decreased metabolic demand as the rods die and subsequent increase of oxygen concentration in the outer retina. Meanwhile, intraretinal pigment deposits are created when the RPE cells migrate into the neural retina in response to rod death.

Morphological alterations: The massive loss of rods is confirmed by analysis of retinal structure in three PDE6β-deficient patients by spectral-domain optical coherence tomography (SD-OCT) [87], [83] (**Figure 10d-e**). OCT is a non-invasive examination that provides morphological information of the retina, in particular of the outer/inner segments and the ONL. In all three patients (aged of 26, 34 and 51 years), the ONL is barely detectable in the central superior retina, and totally absent in the far-periphery (**Figure 10e**).

In addition, important loss of foveal cones is observed. Some foveal cone nuclei are still detectable in the 34-year old woman with Cys270X nonsense mutation (**Figure 10e**) and the 26-year old man with His557Tyr missense mutation [87], [83]. It was not the case in the 51-year old patient with His557Tyr missense mutation [83], a result that can be explained by age rather than inter-individual variations (data not shown).

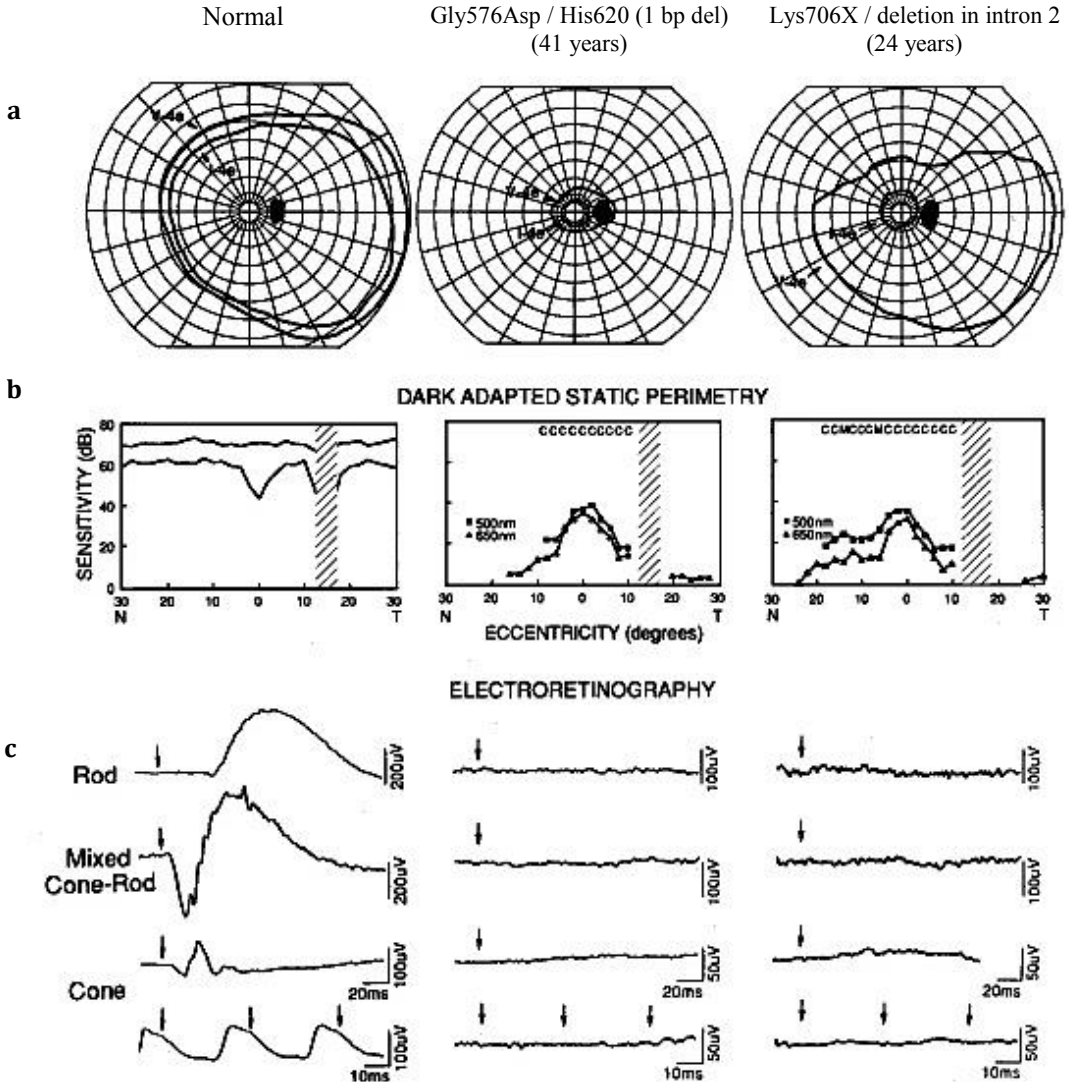

Figure 9. Representative visual field, dark adapted static perimetry and ERG profiles obtained in patients with PDE6β-linked rod-cone dystrophy. (**a**) Kinetic perimetry, (**b**) dark-adapted static perimetry and (**c**) ERG profiles obtained from one normal subject (left) and two patients with compound heterozygous mutations in *PDE6β* [75]. The kinetic fields are those of the right eye of each subject. For the normal dark-adapted perimetric profile, symbols connected by lines indicate the two different stimulus wavelengths used. Letters above the sensitivity measurements are the photoreceptor mediations for detection of the 500 and 650nm stimuli (M, mixed rod and cone detection), C (cone detection). For ERG profiles, arrows represent light stimuli.
In both patients, kinetic visual fields are reduced to a mall central island of vision, and dark-adapted perimetry indicated that there was only cone function remaining within the island. ERGs to all stimuli were not detectable. N, nasal; T, temporal.

Natural history of PDE6β photoreceptor degeneration remain unknown in patients with rod-cone dystrophies

The apparent homogeneity in clinical phenotypes of PDE6β-recessive **rod-cone dystrophies** is intriguing but difficult to interpret without significant genotype-phenotype analysis. Indeed, precautions need to be taken before proclaiming that all recessive *PDE6β* defects lead to a similar phenotype. We cannot rule out that **rod-cone dystrophy** is always associated with complete (or nearly complete) loss of function of PDE6β. In addition, the number of patients genotyped and clinically analyzed is very small, and all patients may have been examined/diagnosed at late-stages of retinal degeneration.

Very few or no longitudinal studies have evaluated the natural history of *PDE6β* photoreceptor degenerations. Systematic genotyping and phenotyping of a wider number of patients with autosomal recessive **rod-cone dystrophies** could reveal new phenotypic variations within patients, as it was the case for analogous PDE6α-linked **rod-cone dystrophy** (Zobor D. *et al*. ARVO 2011, Poster 4564/D1051). Studies of *Pde6β*-deficient animal models can also help understand genotype-phenotype correlations in PDE6β **rod-cone dystrophies**

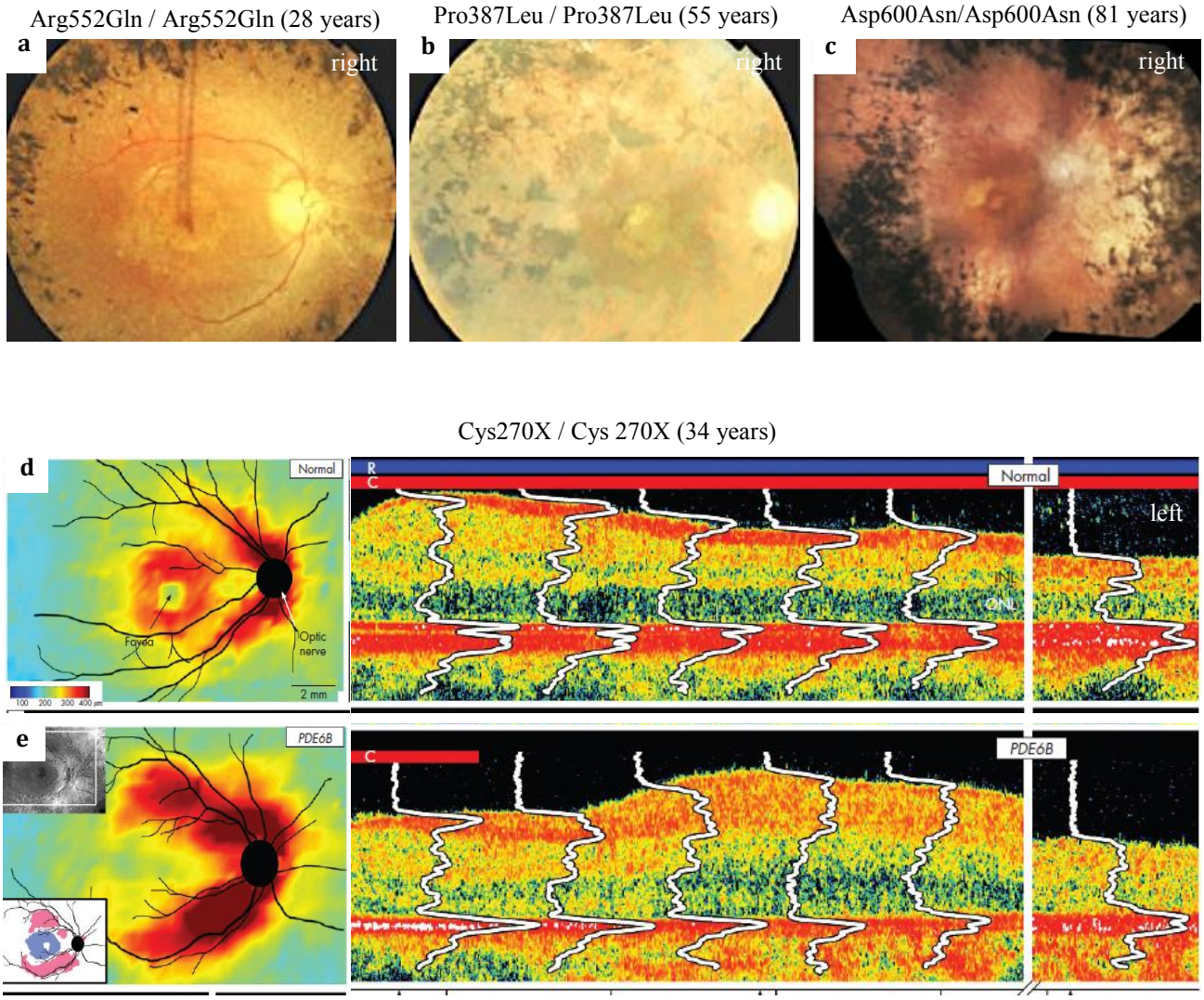

Figure 10. Representative fundus photographies, retinal topographies and spectral-domain ophthalmoscopy coherence tomography scans obtained from patients with PDE6β-linked rod-cone dystrophy. [88] Fundus photographs obtained from the right eye of three patients with homozygous missense *PDE6β* mutations [82], [89]. The peptidic sequence variants and the age of patients at time of examination are indicated above the photographs. All fundi display retinal abnormalities typical of those obtained in other patients with rod-cone dystrophies, as bone-spicule intraretinal pigments in the mid-periphery, severe RPE atrophy, attenuated retinal vessels and waxy pallor of the optic disc. Severe atrophy of the parafovea is observed [90] Retinal topography and spectral-domain ophthalmoscopy coherence tomography scans obtained in (**d**) a normal subject and (**e**) a patient with homozygous nonsense *PDE6β* mutation [87]. Bars above the cross-sections indicate presence or absence of rod (R) and cone (C) function, measured by dark-adapted perimetry. The patient has no rod function and detectable cone function in the central field only. ONL layer is totally absent in the periphery and severely reduced in the fovea. Signs of abnormal laminar architecture of the inner retina are also observed.

II.2.4.2. Animal models of PDE6β-linked rod-cone dystrophy

Small and large animals exist for *PDE6β*-associated **rod-cone dystrophy**. Causal mutations in these different models are depicted in **Figure 11**, whereas retinal dysfunction and photoreceptor degeneration resulting from these different models is summarized below.

Murine models of PDE6β-deficiency

***Rd1*, a natural *null* model:** In 1924, the *rd1* mouse was the first published mouse model of retinal degeneration [91]. This natural murine model carries an intronic viral insertion and a second nonsense mutation in exon 7 of the *Pde6β* gene [92], [93] (**Figure 11a**).
Rod PDE6 is normally synthetized in the *rd1* retina during retinal development, but the concentration of the enzyme is already very low at postnatal day (P) 6, before any sign of photoreceptor degeneration. Only minimal PDE6 activity is detected in the *rd1* mice [94], [95]. This residual PDE6 activity is likely to be that of cone PDE6.
The *rd1* mouse develops an early-onset severe **rod-cone dystrophy** (**Figure 11c**). Morphological differences in the *rd1* retina are first seen at P8-10, with delayed elongation of the inner and the outer segments [96], [97, 98]. By P18-21, the ONL (that represents mainly rods) is reduced to 10% of normal thickness [99]. This rod degeneration begins in the central and the inferior half of the retina, before reaching the periphery and the dorsal hemisphere [100].
Unlike rods, cones show a slow rate of degeneration. Massive degeneration of mouse cones is observed by 35 weeks of age [101]. At 78 weeks of age, around 3% of initial cones remain and these cells lack outer segments [99], [100], [45].

A criticism of the use of the *rd1* mouse as a model of human autosomal recessive **rod-cone dystrophy** is the fact that the disease overlays with the normal developmental process. In *rd1* mice, the dendrites of ON bipolar cells do not form proper invaginations within photoreceptor terminals. Moreover, photoreceptors fail to develop normal outer segments and several rows of ONL nuclei are lost before the retinal circuitry has reached full maturation.

***Rd10*, a natural hypomorphic model:** The *rd10* mouse represents a second naturally occurring mouse model with a later-onset phenotype [102] (**Figure 11c**). The *rd10* mouse carries a missense mutation in exon 13 of the *Pde6β* gene (Arg560Cys)[103] (**Figure 11a**). This mutation is located in the catalytic domain of PDE6β subunit (**Figure 11b**) and is thus though to reduce PDE6 holoenzyme activity and/or expression. PDE6β immunostaining is detectable at reduced levels of P10.

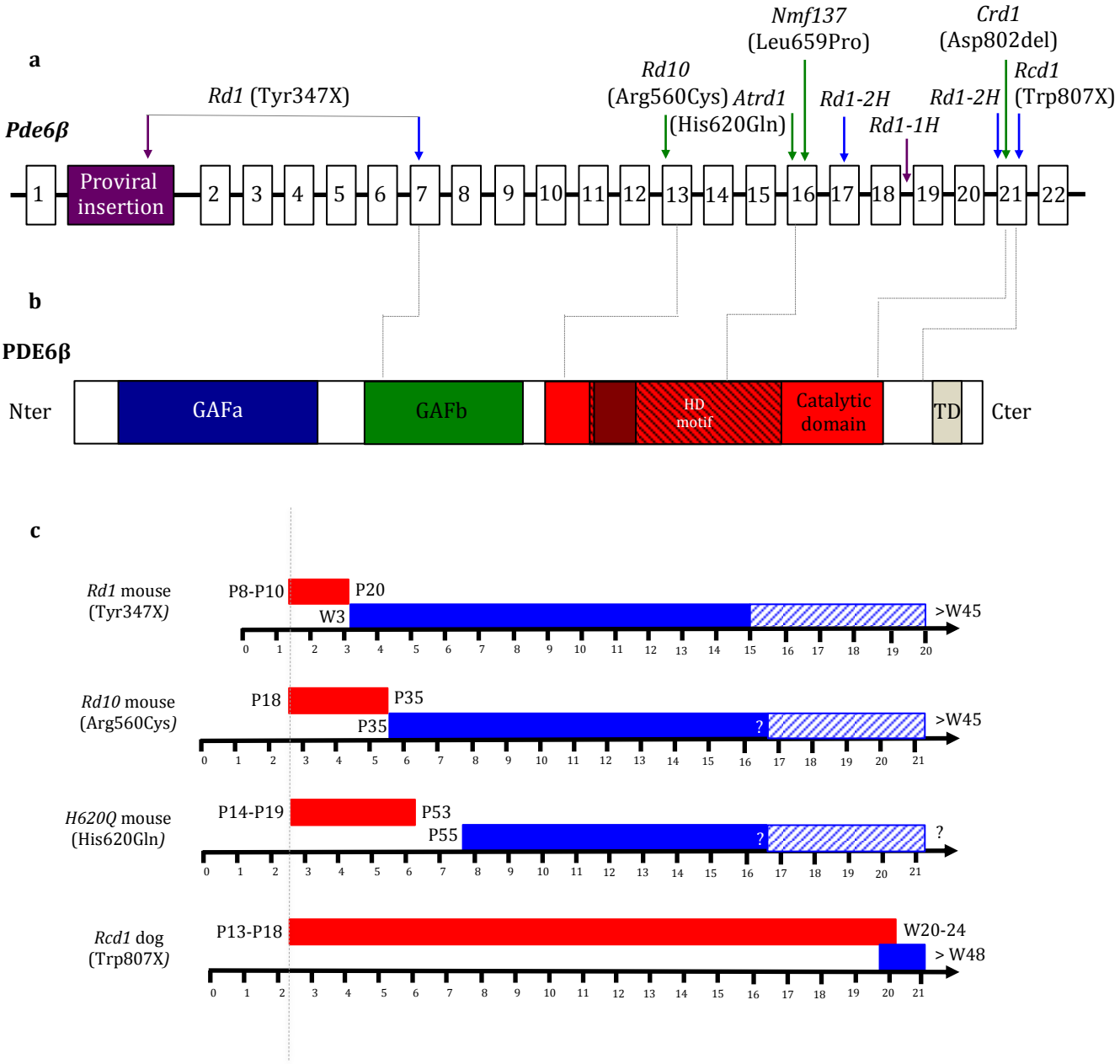

Figure 11. Schematic representation of the sequences variants and kinetics of photoreceptor degeneration that have been associated with animal models of PDE6β-linked rod-cone dystrophy. (**a**) Schematic representation of the murine or canine Pde6β gene. The 22 exons are drawn to scale, introns are not. (**b**) Schematic representation of the murine or canine PDE6β subunit. Protein domains are shown with colored boxes: GAFa in blue, GAFb in green, catalytic domain in red, targeting domain (TD) in beige. Sequence variants are depicted as arrow. (**c**) Schematic representation of the rod (red) and cone (blue) death kinetics found in the different animal models of PDE6β-linked rod-cone dystrophy. The rapid phase of photoreceptor degeneration are shown in full-colored boxes. The slow phase of photoreceptor degeneration are shown in hatched boxes. The onset of rod death is aligned. The corresponding time windows on the x axis are given in weeks post-birth. All animal models display similar kinetics of rod-cone degeneration.

Although the pathological mechanism of the *rd10* mutation has yet to be determined, the phenotype of the *rd10* mouse is characteristic of a hypomorphic allele [103]. Retinal degeneration in the *rd10* mice is evident by ERG at 3 weeks of age, after complete differentiation of the retina.

However, despite this delayed onset, the rate of photoreceptor loss in *rd10* mouse does not appear to be substantially different than the *rd1* mouse (**Figure 11c**) although a direct comparison has no been performed. Loss of rods in the *rd10* mouse begins around P18, with peak photoreceptor death occurring at P25 [104]. Degeneration of photoreceptors follows a center-to-periphery gradient, as seen in the *rd1* mouse. Most rods are lost at P35, with only a single row of cones without outer segments remaining. Several cone cell bodies are detectable as late as 9 months of age. The cone cell death occurs in a characteristic spatio-temporal pattern starting in the mid-peripheral retina and spreading peripherally and centrally toward the optic nerve [105].

The rate of degeneration in the *rd10* mouse depends on environmental factors. Dark-rearing delays degeneration for at least 4 weeks [103]. This result is counterintuitive because lack of PDE6-mediated photoresponses is thought to cause photoreceptor death in PDE6β-deficiency (**Chapter 3**). One hypothesis is that secondary cues for cell death may be accelerated by light and delayed by dark-rearing [106].

Engineered murine models: Eight engineered murine models of PDE6β-deficiencies have been generated, providing additional models to understand genotype-phenotype correlations in PDE6β-associated **rod-cone dystrophy**. Retinal morphology of engineered mice was compared to *rd1* mice at the ages of 3 and 6 weeks [107].

Five engineered models show retinal degeneration kinetics similar to that observed in the *rd1* mice: (i) the *nmf137* strain (missense mutation in exon 16, Leu659Pro), (ii) the *rd1*-1H mice (mutation in the splice donor site of intron 18), (iii) the *rd1-2H* mice (nonsense mutation in exon 21, Arg799X), (iv) the *rd1-3H* mice (nonsense mutation in exon 9, Trp378X) and (v) the *rd1-4H* mice (nonsense mutation in exon 17, Tyr689X). Except for Leu659Pro (*nmf137*), all these mutations are predicted to cause loss-of-function [107].

In contrast, *atrd1* (missense mutation in exon 15, His620Gln), *atrd2* (mutation in splice acceptor site of intron 11) and *atrd3* mice (missense mutation in exon 14, Asn606Ser) have a slightly less severe phenotype [107]. The *atrd1* mouse (thereafter named *H620Q*) harbors a substitution of a highly conserved residue in the catalytic domain of PDE6β [107]. Mutant PDE6β is expressed at 22-fold lower levels than in wild-type mice and specific mutant PDE6 activity is at 13% of wild-type PDE6. Due to this combined effect, the level of the total PDE6 activity in mutant *H260Q* retinas is only 0,6% of that present in normal retinas [108].

In the *H620Q* mouse, the photoreceptor differentiation is normal and retinal function is recordable by ERG before degeneration onset. ONL thickness is normal until P14 (**Figure 11c**). By 3 weeks of age, the ONL is reduced to 70% of wild-type retina (compared to 10%

for age-matched *rd1*). Nevertheless, retinal degeneration progresses rapidly over the next 3 weeks and from P53, the *H620Q* retina is indistinguishable from the *rd1* mice with only one row of remaining cone nuclei. Thus, residual PDE6 activity in the *H620Q* mouse is sufficient to slightly delay photoreceptor death but not to long-term preserve rods [108].

Canine models of PDE6β-deficiency

***Rdc1*, a natural null model:** The Irish Setter breed had been known to be affected with a recessively inherited retinopathy characterized by blindness under dim-light conditions and with various degrees of visual impairment under bright light ranging from near-normal to complete blindness (**rod-cone dysplasia** type 1, *rcd1*). Molecular genetic studies demonstrated that the disease is caused by a nonsense mutation in C-terminus of the PDE6β subunit (W807X) (**Figure 11a**), leading to truncation of the geranylgeranylated C-terminus that mediates PDE6 membrane targeting [69], [109] (**Figure 11c**).

Mutant *Pde6β* mRNA is detected at P21 in the *rcd1* dog, but it is not known if the mutant PDE6β subunit is expressed in rods. Interestingly, rod-mediated ERG responses are undetectable in the *rcd1* canine model from the earliest age measured (1 month of age) [110], and at this age, rod PDE6 function is absent [69]. This suggests that the *rcd1* dog carries a *null* mutation in *Pde6β*. In this manner, the *rcd1* dog is similar to the *rd1* mouse in which, PDE6 function is also completely lacking, but differs from the *rd10* and *H620Q* mice in which, photoreceptors develop and function almost normally before their degeneration.

As observed in the *rd1* mouse, retinal degeneration in the *rcd1* dog begins during postnatal retinal differentiation [70] (**Figure 11c**). At P13, rod outer segment elongation is arrested. Degeneration becomes histologically apparent at P25. Rod photoreceptor loss occurs gradually over 6 months. It starts in the posterior pole and equator regions, with preservation of normal peripheral structure. Subsequently, rod degeneration occurs in a quadrant-specific sequence, with a most rapid degeneration in the inferior retina [70] (Petit L. *et al*., in preparation).

Following nearly complete rod death, cone dysfunction occurs within 1 to 2 years. This loss of cone function is associated with the loss of cone outer segments. It is followed by progressive loss of cone cell bodies. Cone degeneration occurs through a periphery-central gradient that begins in the nasal inferior retina by 12-18 months of age (Petit L. *et al*., in preparation). Greater preservation of cones in observed in the superior retina, as observed in human patients. Interestingly, numerous intact cones are still detectable by PNA staining in the cone-rich visual streak and area centralis of *rcd1* dogs for at least 8 years Consistently, despite total loss of (recordable) cone ERG function, *rcd1* dog show no sign of visual impairment in dim-light for at least 8 years (Petit L *et al.*, in preparation).

***Crd1*, a natural hypomorphic model:** The *crd1* (**cone-rod dystrophy** *1*) American Staffordshire terrier was recently identified as a new canine model of PDE6β deficiency

[111]. It carries an in-frame 3-bp deletion in the exon 21 of the *Pde6β* gene (**Figure 11a**). This mutation would result in the deletion of the highly conserved amino acid Asp802 at the end of the catalytic domain of the PDE6β protein (Asp802del) (**Figure 11b**). PDE6 expression was not assessed in this model but a total loss of PDE6 enzymatic activity is not expected. Thus, the *crd1* dog can be analogous to the *rd10* mouse and could represent an interesting large model of human **rod-cone dystrophies** caused by missense PDE6β mutations.

As observed in *rd10* and *rd1* mice, retinal degeneration of the *crd1* dog is slightly delayed compared to that of the *rcd1* dog [111]. The ONL of the *crd1* dog is reduced to 50% at 11 weeks of age (versus 60-70% in the *rcd1* dog). By 20 months of age, 2 or 3 rows of photoreceptor nuclei remained in the *crd1* retina.

II.2.4.3. Summary

Murine, canine and human versions of PDE6β-linked **rod-cone dystrophies** are associated with a severe rate of rod photoreceptor degeneration, followed by more progressive loss of cones. Species comparisons of rate of photoreceptor degeneration can be made by use of allometric scaling with maximum lifespan [112]. If we compared the maximum lifespan of these different species, the age range of P10-P35 in the mouse would approximately correspond to 2-7 months in the dog and 1-3,5 years for the human, respectively. In the *rd1* and *rd10* models of *Pde6β*-**rod cone dystrophy**, ONL is reduced to one row of cone nuclei between P20 and P35. The kinetics of rod degeneration in the *rcd1* dog is comparable to murine diseases with a nearly total loss of rods at 6-8 months of age. It would suggest that most rods are lost during the first years of life in humans.

Delayed (but no significantly slowed) rod loss was observed in *H620Q* mice compared to *rd1* mice and in *Crd1* dogs compared to *rcd1* dogs. Similar inter-individual variations in rod degeneration are conceivable in young PDE6β-deficient patients, but additional data on the natural history of the human disease are needed to draw a definitive conclusion.

Regarding the cones, they are mainly lost within 8-9 months in *rd1* and *rd10* mice. It is comparable to the loss of cones in the peripheral and mid-peripheral retina of the *rcd1* dog between 1 and 1.5 year. However, there is a substantially greater retention of central cones in the *rcd1* dog, with intact cones still detectable in the cone-rich area centralis for at least 8 years. The long-term preservation of central cones in the *rcd1* dog mimics the long-term preservation of foveal cones and/or central visual field observed in patients with PDE6β-**rod cone dystrophy** after 30-40 years.

II.2.5. Congenital stationary night blindness resulting from *PDE6β* mutations

Signs of clinical variations among PDE6β deficiencies were obtained in a Danish family with compound heterozygous dominant His258Asn mutation [113]. His258Asn is located near the PDE6γ-binding domain of the PDE6β subunit and impedes the complete inactivation of PDE6 in dark-adapted photoreceptors [114]. In His258Asn patients, absence of rod-mediated ERG responses was not associated with cone function impairments and fundus modifications over time. Therefore, the pathology was classified as **congenital stationary night blindness** [113].

A similar "pure functional defect" was recently characterized in a murine model of His258Asn mutation [115], indicating a possible phenotype-genotype correlation. This point will be further discussed in **Chapter 3**.

II.3. Inherited photoreceptor dystrophies caused by mutations in RPGRIP1

II.3.1. *RPGRIP1* gene

The gene encoding for Retinitis Pigmentosa GTPase Regulatory (RPGR) Interacting Protein 1 (RPGRIP1) was mapped to chromosome 14q11. It encompasses 25 exons, within 24 coding exons encoding a 1287 amino acid protein [116, 117] (**Figure 12a**).

II.3.2. *RPGRIP1* biology

The RPGRIP1 protein has been first identified as an *in vitro* [118, 119] and *in vivo* [120] molecular partner of RPGR, a cause of X-linked **cone-rod** [121], [122] and **rod-cone dystrophies** [123], [124].

RPGRIP1 interacts with RPGR via its C-terminal RPGR interacting domain (RID) and a central coiled-coil (CC) domain, which is homologous to the domain of proteins involved in the vesicular trafficking [118] (**Figure 11b**). RPGRIP1 and RPGR proteins are expressed in both rods and cones, where they are essential for the function and survival of photoreceptors. However, functional relationships between RPGR and RPGRIP1 and their roles remain poorly understood.

II.3.2.1. Challenges to understand the specific function(s) of RPGRIP1

Investigations are complicated as *Rpgrip1* undergoes multiple slicing, leading to multiple RPGRIP1 isoforms with distinct cellular localizations and biochemical properties in the retina [125], [126]. In addition, RPGRIP1 isoforms undergo limited proteolysis, which influences the subcellular localization of the proteolytic products (because some functional domains, including the RID, are necessary for the relocation of the N-terminal domain of RPGRIP1 to the nucleus) [127].

In the bovine and the human retinas, the longest RPGRIP1 isoform and RPGR co-localize to the outer segment of photoreceptors [125]. It is not the case in the mouse, where the two proteins co-localize to the connecting cilium [125]. In mice, it has been suggested that one of the main roles of RPGRIP1 could be to anchor RPGR at the connecting cilium, because the absence of RPGRIP1 suppresses the cilium localization of RPGR [120], [38]. However, patients with mutations in RPGRIP1 have a much more severe phenotype compared to RPGR-patients, suggesting that RPGRIP1 performs additional functions in photoreceptors than anchoring RPGR.

In addition to RPGR, RPGRIP1 also interacts with nephrocystin-4/nephroretininin (NPHP4) in murine photoreceptors [38]. NPHP4 share a similar ciliary localization in the connecting cilium, and is an important cause of end-stage kidney disease (sometimes associated with retinal dystrophies). In the absence of RPGRIP1, NPHP4 ciliary targeting is suppressed and NPHP4 accumulates in the reticulum endoplasmic (RE) membrane [38]. Therefore, RPGRIP1 determines the ciliary targeting of at least two critical photoreceptor disease-related proteins in the mouse [128], [129].

Surprisingly, in the bovine and human retinas, other RPGRIP1 isoforms are also expressed in a subset of amacrine cells, located at the proximal edge of the INL [130]. In amacrine cells, these RPGRIP1 isoforms are expressed in the nuclear rims and axonal processes. They co-localize with RanBP2, a component of the nuclear pore complex, which has been implicated in nuclear-cytoplasmic trafficking. Thus, specific RPGRIP1 isoforms may participate in nuclear-cytoplasmic trafficking in a subset of amacrine cells [130]. From these data, it is conceivable that different RPGRIP1 isoforms perform different cell-specific functions [125],[130].

II.3.2.2. Role of the *Rpgrip1*$^{-/-}$ mouse to understand the function of RPGRIP1

To better understand the function of RPGRIP1, an *Rpgrip1* knockout mouse was generated [131]. The *Rpgrip1*$^{-/-}$ mouse carries targeted disruptions in the *Rpgrip1* gene and is thought to produce no RPGRIP1. Retinal degeneration in this model is relatively slow, with an almost total loss of photoreceptors by 3 months of age [131].

RPGRIP1 is not essential for photoreceptor development. In *the Rpgrip1*$^{-/-}$ mouse, normal retinal and photoreceptor development were observed at birth, indicating that RPGRIP1 is not essential for retinal proliferation, commitment to photoreceptor cell fate and/or initial correct development of cones and rods [131].

RPGRIP1 is essential for normal photoreceptor outer segments. Despite normal photoreceptor development, histological analysis of the *Rpgrip1*$^{-/-}$ mouse showed that photoreceptor outer segments became rapidly disorganized, with oversized discs observed at P15 [131].

It was associated with a mislocalization of abundant rod and cone opsins to the photoreceptor cell bodies, whereas arrestin, transducin and PDE6 remain correctly expressed in the outer segments [132]. The mislocalization of opsins in *Rpgrip1*$^{-/-}$ mice was first interpreted as a direct or indirect role of RPGRIP1 in the transport or restriction of proteins across the connecting cilium [132]. However, a recent study of the *Rpgrip1*$^{-/-}$ mice clearly demonstrated that loss of RPGRIP1 does not affect the apical targeting or cause the misrouting of opsins. Mislocalization of opsins was rather identified as a secondary effect of outer segment degeneration [133], as observed in other mouse models of photoreceptor degenerations [134].

Outer segment abnormalities are not associated with abnormal connecting cilium structure. None of the studies performed in the *Rpgrip1*$^{-/-}$ mice have found any abnormal ciliary microtubule structures caused by the lack of RPGRIP1, or RPGRIP1-dependent ciliary localization of RPGR or NPHP4 [133]. Thus, RPGRIP1 has neither been thought to play a primary role in the connecting cilium structure.

RPGRIP1 determines the ciliary targeting of critical proteins pivotal for the maintenance of outer segments. Instead, it was hypothesized that RPGRIP1 is a component of the connecting cilium axoneme required for disc morphogenesis of outer segments by regulating cytoskeleton dynamics [131]. Consistently, RPGRIP1 is predominantly localized to the detergent-insoluble cytoskeleton fraction of outer segments of bovine and murine photoreceptors [133]. Loss of ciliary localization of the RPGRIP1 interactome (RPGR or NPHP4) promotes the ruffling of the ciliary membrane likely through weakening of the sub-membrane cytoskeletal matrix of the connecting cilium [133]. Further investigations are required to completely define the role of RPGRIP1.

II.3.3. *RPGRIP1* mutations are associated with different retinopathies

Mutations in the *RPGRIP1* gene have been associated with a heterogeneous set of progressive human retinal diseases, including early onset and progressive **LCA** (3,3 to 7,5% of cases) [116], [117], [135], [136], [137], [138], [139] and juvenile **cone-rod dystrophy** [140], [141]. In addition, heterozygous variants of *RPGRIP1* were recently found to be associated with **glaucoma,** a form of retinal degeneration associated with the loss of ganglion cells [142].
The exact causes of the broad phenotypic heterogeneity of RPGRIP1-deficiencies remain unclear, but phenotypic heterogeneity is the hallmark of other pathologies linked to causal mutations expressed in both rods and cones (*RPGR, AIPL1, GUCY2D*...)[143], [144], [145]. It is possible that phenotype heterogeneity of RPGRIP1-deficiencies come from the differential function of distinct RPGRIP1 isoforms among retinal neurons [133], and the nature of the alleles. **Figure 12** and **Table 4** depict all *RPGRIP1* mutations identified to date.

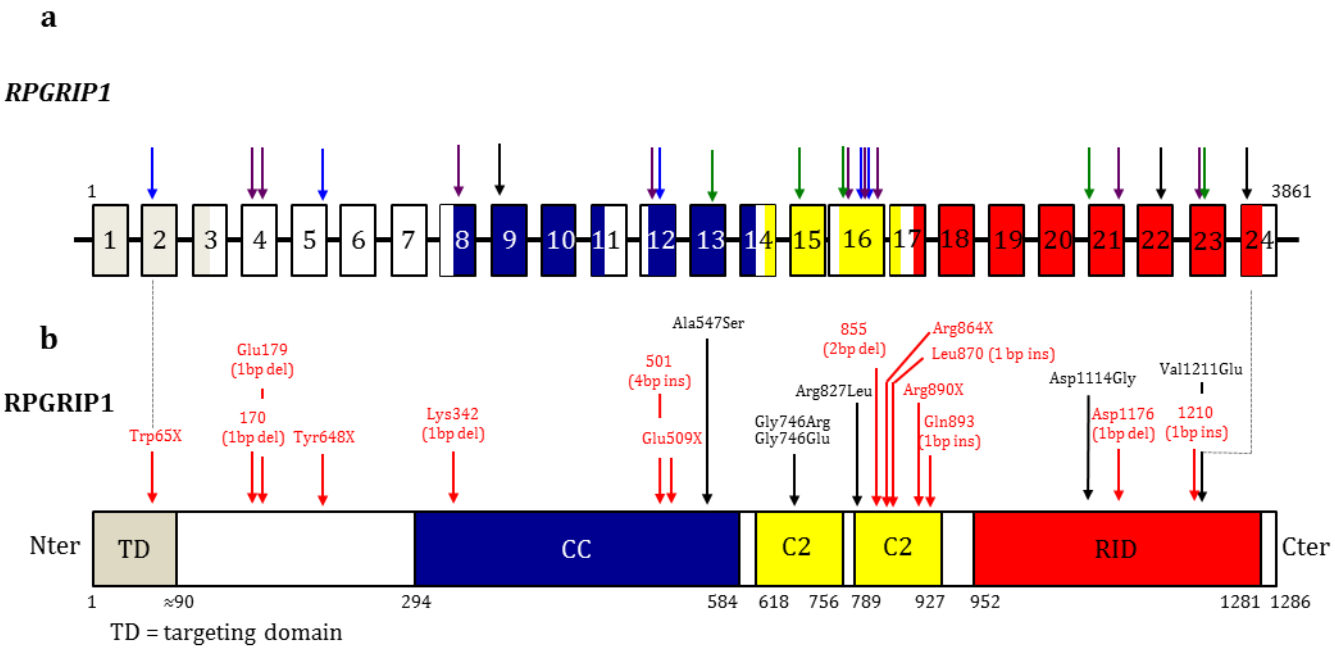

LCA allele 1	LCA allele 2
Trp65X	Asp1176 (1 bp del)
170 (1 bp del)	170 (1 bp del)
Glu179 (1 bp del)	Glu179 (1 bp del)
Tyr648X	Arg864X
Lys342 (1 bp del)	Lys342 (1 bp del)
501 (4 bp ins)	?
Glu509X	?
Gly746Arg	Gly746Arg
855 (2 bp ins)	1210 (1 bp ins)
Leu870 (1 bp ins)	Leu870 (1 bp ins)
Arg890X	Asp1114Gly
Gln893 (1 bp ins)	Gln893 (1 bp ins)
Asp1114Gly	Asp1114Gly
Val1211Glu	Val1211Glu

CORD allele 1	CORD allele 2
Ala547Ser	Ala547Ser
Tyr658X	Arg864X
Arg827Leu	Arg827Leu

Nonsense — Expected *null* allele
Missense — Non-expected *null* allele
Frameshift

Figure 12. Schematic representation of the (a) human *RPGRIP1* gene and the human (b) RPGRIP1 subunit showing functional protein domains and sequences variants that have been associated with Leber congenital Amaurosis and cone-rod dystrophy. The 24 coding exons of *RPGRIP1* are drawn to scale, introns are not. Protein domains are shown with colored boxes: targeting domain (TD) in beige, coiled-coiled (CC) domain in blue, proteinase K C2 (C2) domain in yellow and RID domain (for interacting with RPGR) in red. Sequence variants are depicted as arrow. They are then grouped per phenotype. We can note than nearly the vast majority of the mutations are nonsense or frameshift mutations expected to lead to *null* alleles (loss of RID).
LCA, Leber congenital Amaurosis; CORD, cone-rod dystrophy.

II.3.3.1. RPGRIP1-linked LCA

Clinical findings of patients with *RPGRIP1*-linked **LCA** are summarized in **Table 4**. Age at examination ranged from 6 months to 26 years (mean: 11 years).

Functional/visual deficits: An abnormal ERG is implied by the **LCA** diagnosis. Therefore, it is not surprising that all patients with RPGRIP1-**LCA** have severely impaired rod and cone ERG. Night blindness is present in almost all patients since early childhood, but for some of them, a decrease of central vision and photophobia is also observed at early stages of the diseases. At time of examination, best-corrected visual acuity is generally decreased to light perception, although one patient maintains a visual acuity of 0,3 at the age of 8 [137]. The youngest patient (mutation Glu179, 1 bp deletion), aged of 6 months, is not able to pursuit an object, a clinical feature diagnosed at 4 months of age [146].

Fundus abnormalities: Interestingly, RPGRIP1-**LCA** patients have uniformly profound loss of visual function, but fundus appearance can vary substantially (**Figure 13**). For example, the youngest patient aged of 6 months shows signs of retinal degenerations such as attenuated retinal vessels (data not shown)[146], whereas a 2 years-old patient has no fundus modifications [116] (**Figure 13a**). Likewise, in older patients, some have typical vascular attenuation and bone-spicule pigmentation in the mid-periphery (**Figure 13b,** white arrows) [116], whereas others have only moderate vascular attenuation and no intraretinal bone-spicule pigment (**Figure 13c,d**)[138], [137].

Morphological abnormalities: Variability in the rate of photoreceptor degeneration among patients with RPGRIP1-related LCA was confirmed by SD-OCT imaging (3 patients examined, aged of 19, 10 and 8 years) (**Figure 13e,g**)[135], [137]. In both 19- and 10-year old patients, retinal thickness remained subnormal in the fovea and in the periphery, whereas severe thinning was observed in the parafovea (**Figure 13e,g**)[135]. In contrast, the 8-year old patient retains a normal retinal thickness [137]. Thus, there is no simple relationship of age and retinal thickness. Potential contributions of remnant RPGRIP1 activity, genetic background or environment on the natural history of RPGRIP1 disease remain unexplored.

II.3.3.2. RPGRIP1-linked cone-rod dystrophy

Recently, mutations in *RPGRIP1* have been associated with **cone-rod dystrophies** (**Table 4**). All patients had an early onset severe form of retinal dystrophy with predominant cone involvement. They reported severe deterioration in central vision and color blindness from early childhood due to dysfunction of cones. Rod function was then affected in the second or third decade of life, leading to progressive visual field constriction and night blindness.
Funduscopy showed a variable degree of fundus granularity and macular degeneration. Attenuated retinal vessels were rare.

Table 4. List of identified *RPGRIP1* mutations and genotype-phenotype correlations

List of identified *RPGRIP1* mutations and genotype-phenotype correlations								
Exon	**Nucleotide change**	**Amino-acid change**	**Description**	**Expected RPGRIP1 expression/function**	**Disease association**	**Age**	**Clinical findings**	**Refs**
23	c.3633T>A	Val1211Glu	Homozygous Missense	?	LCA	19 y	• Night blindess from childhood • Peripheral vision loss from childhood • Reduced visual acuity from childhood • Nystagmus • Visual acuity: 20/100 • Visual field: limited to a central island No detectable rod and cone ERG • Attenuated retinal vessels • Waxy optic nerve heads • Pigmentation disturbance in periphery without bone-spicule like changes • Normal thickness in the fovea and periphery – thinning in the parafoveal and perifoveal areas • ONL thickness in the central retina normal to unmeasurable • Identifiable lamination in the central retina – loss in the periphery • Dark-adapted threshold: reduced by 3 log units • Light-adapted threshold: subnormal in the fovea, markedyl reduced outside.	Jacobson SG. et al. 2007
4	c.535 (1 bp del)	Glu179 (1 bp del)	Homozygous Frameshift	Expected *null* allele? Mutant protein with premature codon stop	LCA	0,5 y	• Poor visual responses and until 4 months of age • No poursuit of objects • No detectable cone and rod ERG • Attenuated retinal vessels • Carpet-like retinal degeneration	Cheng et al. 2013
15	c.2236G>A	Glu746Arg	Homozygous	?	LCA	7,5 y	• Poor vision • Nystagmus • Perception of hand movements • Attenuated retinal vessels • Carpet-like retinal degeneration	Cheng et al. 2013

Table 4. List of identified *RPGRIP1* mutations and genotype-phenotype correlations

List of identified *RPGRIP1* mutations and genotype-phenotype correlations								
Exon	**Nucleotide change**	**Amino-acid change**	**Description**	**Expected RPGRIP1 expression/function**	**Disease association**	**Age**	**Clinical findings**	**Refs**
21		Asp1176 (1 bp del)	Heterozygous Nonsense - Mutant protein with stop at 1189	Truncation of the last 100 amino acids, including the expected C-terminal RID	arLCA	26 y	• Nystagmus and light perception since early childhood • Light perception vision since early childhood • Moderate vascular attenuation • No intraretinal bone-spicule pigmentation	Dryja et al. 2001
2		Trp65X	Heterozygous Nonsense	Expected *null* allele				
16		Gln893 (1 bp ins)	Homozygous Nonsense - Frameshift Mutant protein with premature stop at 906	N*ull* allele? Truncation of one third of the protein, including the C-terminal RID	arLCA	15 y	• Nystagmus • Poor vision since early childhood • Hyperoptic • Vascular attenuation • Bone-spicule pigmentation in the mid-periphery • No detectable ERG max -Reduced cone flicker ERG responses	Dryja et al. 2001
						2 y	• Nystagmus • Hyperoptic • Follow objects only in a well-illuminated environment • No fundus modifications	
16	c.2608 (1 bp ins)	Leu870Tyrf sX7	Homozygous Frameshift Mutant protein with premature stop at residue 870		LCA	10 y	• Little visual responses, nystagmus and photophobia at 6 months of age • Nystagmus • No detectable rod and cone ERG • Fundus abnormalities at the level of RPE, spearing the macula • Mild pallor of the optic nerve head • Mild attenuation of retinal vessels • Normal retinal thickness in the fovea and periphery – thinned parafovea	Fakhratova 2013
					LCA	8 y	• Severe photophobia • Nystagmus • Visual acuity: 3/10 (right), 2/10 (left) • No detectable rod and cone ERG • Mild pigment disturbance • Mild pallor of the optic nerve head • Normal retinal thickness	

Table 4. List of identified *RPGRIP1* mutations and genotype-phenotype correlations

List of identified *RPGRIP1* mutations and genotype-phenotype correlations								
Exon	**Nucleotide change**	**Amino-acid change**	**Description**	**Expected RPGRIP1 expression/function**	**Disease association**	**Age**	**Clinical findings**	**Refs**
16	c.2566 (2 bp ins)	855 (2 bp ins)	Heterozygous Premature stop three residues downstream	Expected *null* allele? Truncation of of one third of the protein, including the C-terminal RID	arLCA	/	/	Gerber S. et al. 2001
23	c.3629 (1 bp ins)	1210 (1 bp ins)	Heterozygous Premature stop five residues downstream	Modification of 5 amino acids and loss of the 77 last amino acid corresponding to the RID				
12	c.1501 (4 bp ins)	501 (4 bp ins)	Heterozygous Nonsense Premature stop 8 residues downstream	Expected *null* allele Truncation of more than one half of the protein, including the C-terminal RID	arLCA	/	/	Gerber S. et al. 2001
12	c.1525C>T	Glu509X	Heterozygous Nonsense	Expected *null* allele Truncation of more than one half of the protein, including the C-terminal RID	arLCA	/	/	Gerber S. et al. 2001
15	c.2237G>A	Gly746Glu	Homozygous Missense	Substitution of a conserved uncharged residue by a charged residue	arLCA	/	/	Gerber S. et al. 2001
4	c.511 (1 bp del)	170 (1 bp del)	Homozygous Mutant protein with premature stop 19 residues downstream	Expected n*ull* allele Truncation of more than 2/3 of the protein	arLCA	/	/	Gerber S. et al. 2001
16	c.2668C>T	Arg890X	Heterozygous Nonsense	N*ull* allele? Truncation of of one third of the protein, including the C-terminal RID	arLCA	/	/	Gerber S. et al. 2001
21	c.3341G>A	Asp1114Gly	Heterozygous Missense	Substitution of a highly conserved charged residue by a non polar, uncharged residue closed to the predicted RID				
21	c.3341G>A	Asp1114Gly	Homozygous Missense	Substitution of a highly conserved charged residue by a non polar, uncharged residue closedto the predicted RID	arLCA	/	/	Gerber S. et al. 2001

List of identified *RPGRIP1* mutations and genotype-phenotype correlations							
Exon	**Nucleotide change**	**Amino-acid change**	**Description**	**Expected RPGRIP1 expression/function**	**Disease association**	**Age**	**Clinical findings**	**Refs**
16	c.2480G>T	Arg827Leu	Homozygous Missense	Decreased – Substitution of a positive residue by a nonpolar residue in a domain involved in the major Ca2+ dependent membrane binding module. No change of 3D predicted	arCORD	?	• Deterioration in central vision and colour blindness from early age • Severe photophobia since childhood • Rapid loss of vision between the ages of 14 and 16 years • Visual acuity: 1/60 • Variable degree of fundus abnormalities and macular degeneration • Macular bull's eye lesions	Hameed. et al. 2003
13	c.1639G>T	Ala547Ser	Homozygous Missense	Decreased – Substitution of one nonpolar amino acid by a polar residue in a domain involved in interaction with RPGR.		?	• Reduced cone and rod ERG responses (14y) but in young patients cone response reduced more than rod response	Hameed. et al. 2003
5	c.799C>T	Tyr648X	Heterozygous Nonsense	Expected *null* allele? Truncation of one third of the protein, including the C-terminal RID	arCORD	/	/	Huang et al. 2013
16	c.2592T>G	Arg2864X	Heterozygous Nonsense	Expected *null* allele? Truncation of one more than 2/3 of the protein, including the C-terminal RID				

Table 4. List of identified *RPGRIP1* mutations and genotype-phenotype correlations

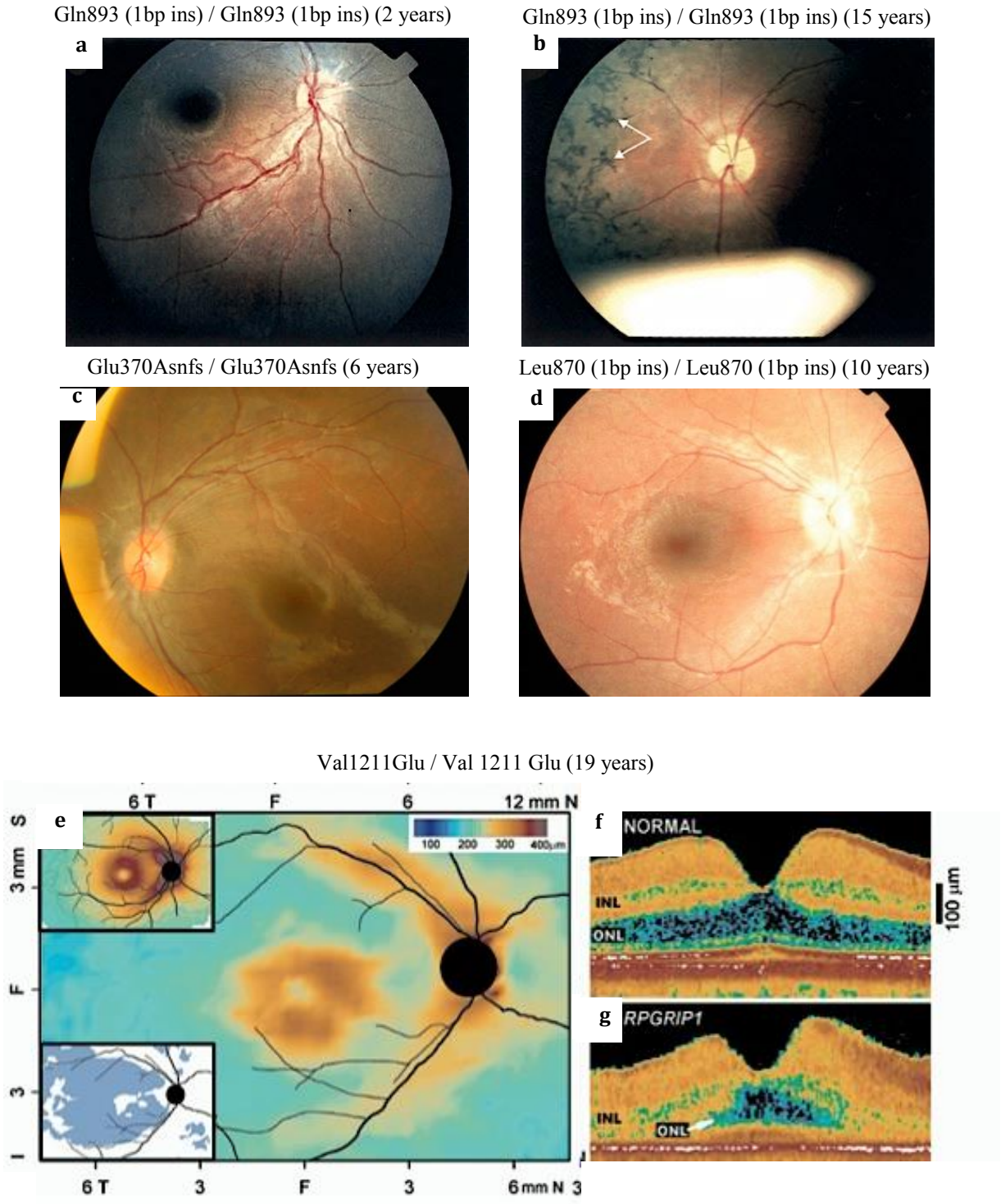

Figure 13. Representative fundus photographs, retinal topographies and spectral-domain ophthalmoscopy coherence tomography scans obtained from patients with RPGRIP1-LCA. (**a-d**) Fundus photographs obtained from the right eye of four patients with homozygous frameshift *RPGRIP1* mutations). The sequence variants and the age of patients at time of examination are indicated above the photographs. (**a**) The youngest patient shows no retinal abnormalities, whereas his older brother (**b**) displays bone-spicule intraretinal pigments in the mid-periphery [116]. (**c-d**) Both patients show signs of macular degeneration and attenuated retinal vessels, but no bone-spicule intraretinal pigments [138] [137].
(**e-g**) Retinal topography and spectral-domain ophthalmoscopy coherence tomography scans obtained in a patient with homozygous missense *RPGRIP1* mutation. ONL layer is totally absent in the periphery and reduced in the fovea [135].

II.3.3.2 Genotype-phenotype correlations for *RPGRIP1* mutations

It was hypothesized that **LCA** may be associated with complete loss of function of RPGRIP1, while patients with **cone-rod dystrophies** may have residual RPGRIP1 function [147]. This hypothesis is supported by the observation that among the 15 **LCA**-associated *RPGRIP1* mutations, 10 (67%) were nonsense or frameshift mutations predicting a severe truncation of the RPGRIP1 protein (and a loss of the RID domain necessary for RPGRIP1 and RPGR interactions). In addition, Lu *et al*. recently determined that the missense Asp1114Gly mutation (which is located in the RID domain of RPGRIP1 and was identified in 10 unrelated patients with **LCA**) completely abolishes the interaction with RPGR [127]. In contrast, homozygous Arg827Leu and Ala547Ser missense mutations associated with **cone-rod dystrophies** are not predicted to change the structure of the expected protein [140].

However, whether Arg827Leu and Ala547Ser missense mutations abolished or not the interaction of RPGRIP1 and RPGR remain to be determined. In addition, the Ala547Ser mutation was recently shown to be a very common polymorphism in the general population (Koenekoop, Poster 4727-B51, ARVO 2004), putting into question the contribution of this mutation in the retinal phenotype.

Furthermore, a recent study identified two nonsense Tyr864X and Arg267X mutations in Chinese families with **cone-rod dystrophies** that are expected to lead to the truncation of more than half of the protein [141]. These mutations do not appear very different from the nonsense mutations Arg890X associated with **LCA**. Nevertheless, as these mutations were only found in a heterozygous manner, we cannot exclude that a second non-*null RPGRIP1* allele contributes to the relative milder phenotype observed in these patients. Similar single heterozygous Arg267X was recently identified in **LCA** patients [148].

II.3.4. Animal models of *RPGRIP1*-linked retinopathies

Small and large animals exist for *RPGRIP1*-associated retinopathies. Causal mutations in these different models are depicted in **Figure 14**.

The Rpgrip1 knockout mouse: The *Rpgrip1* knockout mouse was degenerated by targeted disruption of the *Rpgrip1* gene (insertion of the neomycin resistance gene flanked by the exons 5-6 and the exons 14-15 within the exon 14 of *Rpgrip1* gene) [40] (**Figure 14a**). A premature stop codon was created before exon 15, leading to a predicted truncated RPGRIP1 polypeptide (500 amino acids out of the 1 331 amino acids full length protein, loss of the RID domain) (**Figure 14b**). Ablation of full-length RPGRIP1 was confirmed by Western-blot using antibodies raised against the N- (residues 2-222) and C-terminus (residues 991-1331) of mouse RPGRIP1 [40]. Thus, the *Rpgrip1*$^{-/-}$ mouse may carry a *null* allele for the longest variant form of RPGRIP1 [40].

The *Rpgrip1*$^{-/-}$ mice normally develop photoreceptors but their outer segments are disorganized with oversized discs that stack vertically. This morphological defect is more evident in rods than in cones. It is not associated with a loss of retinal function, as both sustained scotopic and photopic ERGs are detectable before the onset of photoreceptor degeneration.
Exponential loss of cone and rod responses is observed from P15 to 5 months (**Figure 14c**).
At 3 months of age, rod outer segments are severely shortened and rhodopsin is severely mislocalized. As well, cone outer segments are severely reduced and cone cell number is reduced. Over 50-70% of ONL nuclei are lost (3-4 rows of nuclei compared to 9-11 in the wild-type mouse). At 5 months of age, between 0 and 2 rows of photoreceptors remained [149]. Photoreceptor degeneration in the *Rpgrip1*$^{-/-}$ mouse is more pronounced in the superior retina compared to the inferior retina [149].

The nmf242 mouse: The *nmf242* mouse carries a nonsense mutation in the splice acceptor site of exon 6 [132] (**Figure 14a**). This mutation is expected to lead to the frameshift loss of the exon 7, and early termination [132]. If expressed, the RPGRIP1 polypeptide will be more severely truncated than that of *Rpgrip1*$^{-/-}$ mice (**Figure 14b**). Consistently, the *nmf242* mouse has a more severe phenotype than the *Rpgrip1*$^{-/-}$ mouse (**Figure 14c**). Rod outer segments never form, despite normal-appearing connecting cilium. In contrast, cone outer segments are initially formed but degenerate rapidly (from P12-P14). It was suggests that this discrepancy between rods and cones reflects a different function of RPGRIP1 in rods and cones [132]. However, it is possible that is reflects the earliest postnatal development of cones in the murine retina [150]. In the *nmf242* mouse, photoreceptor degeneration is nearly complete by P28 [132].

The MLHD-Cord1 dog: A close research colony of miniature longhaired dachshund (MLHD) breed has been known to be affected with a recessive retinopathy characterized by blindness under bright-light conditions and important degrees of visual impairment under dim light (**cone-rod dysplasia** type 1, *Cord1*). Molecular genetic studies have linked the disease with the *Cord1* locus (0,51 Mb in chromosome 15) that contains the canine *Rpgrip1* gene [151] and 17 other genes.
Sequence analysis of the canine *Rpgrip1* gene has revealed a frameshift 44bp insertion (polyA tract insertion of 29 nucleotides flanked by a 15-bp duplication, Ins44) in exon 2 (**Figure 14a**). If unaffected by nonsense-mediated decay, this mutated sequence is predicted to give rise to markedly truncated protein lacking the RID domain [151] (**Figure 14b**).

Rod function of MLHD-*Cord1* dog is almost normal at 1 month of age but rapidly declines thereafter. Cone-mediated scotopic and 30Hz flicker responses are undetectable from the earliest measured age (1 month of age) [152], [153]. Despite this lack of cone function, peanut agglutinin (PNA) staining of cone outer segments has been detected in 6-weeks old *Cord1* retinas, indicating that the MLHD-*Cord1* dog forms cone outer segments.

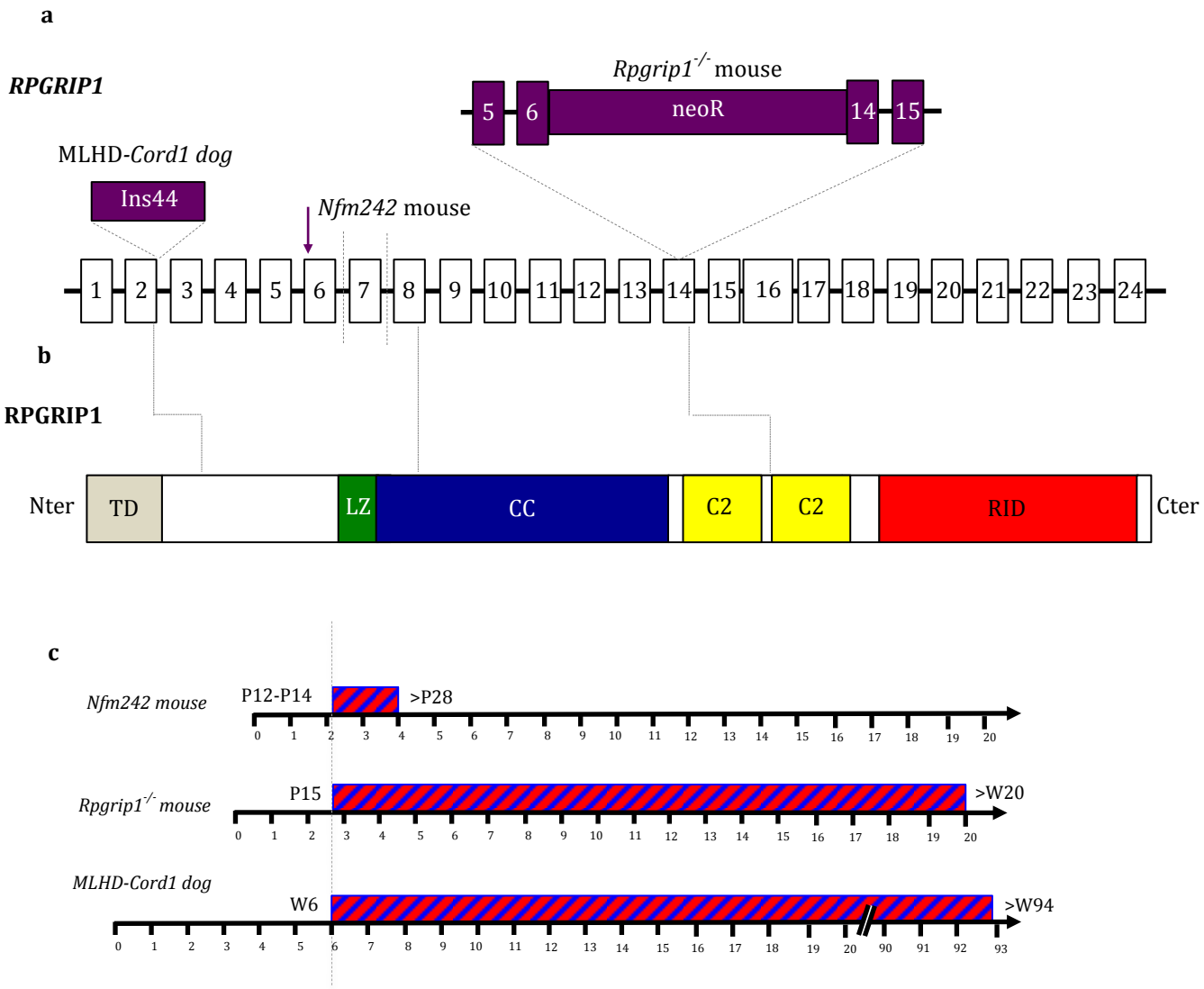

Figure 14. Schematic representation of the sequences variants and the kinetics of photoreceptor degeneration that have been associated with animal models of RPGRIP1-deficiencies. (**a**) Schematic representation of the murine or canine Rpgrip1 gene. The 24 exons are drawn to scale, introns are not. (**b**) Schematic representation of the murine or canine RPGRIP1 protein. Protein domains are shown with colored boxes: targeting domain (TD) in beige, coiled-coiled (CC) domain in blue, proteinase K C2 (C2) domain in yellow and RID domain (for interacting with RPGR) in red. (**c**) Schematic representation of the rod (red) and cone (blue) death kinetics found in the different animal models of RPGRIP1-deficiencies. The onset of photoreceptor death is aligned. The corresponding time windows on the x axis are given in weeks post-birth. All animal models display similar kinetics of rod-cone degeneration.

Photoreceptor degeneration progresses relatively rapidly in the MLHD-*Cord1* dog, with a loss of almost 70% of ONL nuclei at 12 months of age, and no remaining photoreceptors at 24 months [153], except in the cone-rich visual streak where 1-2 rows of nuclei are preserved at this late timepoint (Petit L., unpublished data) (**Figure 14c**). However, kinetics of rod and cone loss has not been defined to date. As well, it is not known if the pattern of cone loss is uniform and affects both M- and S- cones equally.

Of note, the MLHD-*Cord1* phenotype differs from those observed in other *Rpgrip1*$^{-/-}$ dogs in the outbred pet population [154], [155], [156] or in a crossbred research colony [157], that have the same genetic *Rpgrip1* mutation but display (i) no obvious clinical signs or (ii) a variable cone function, with no morphological changes. Variations of the phenotype have been observed in *Rpgrip1*$^{-/-}$ dogs within the same extended MLHD family with a shared environment, indicating that the cause of phenotypic variation is genetic and involved limited loci [154].

Consistently, a second independent 1,49 Mb locus in chromosome 15 (at around 35 Mb apart on *Rpgrip1*) was recently shown to recessively segregate in 90% of *Rpgrip1*$^{-/-}$ dogs with early-onset retinal degeneration or in MLHD-*Cord1* dogs. This second locus was present in 13% of *Rpgrip1*$^{-/-}$ dogs with late-onset retinal degeneration and 3% of *Rpgrip1*$^{-/-}$ dogs with no clinical signs of retinal disease [158]. The 1,49 Mb locus contained two known (*Gucy1a3* and *Gucyb3*), seven predicted (*Lrat, Rbm46, Nny2r, Map9, Accn5, Tdo2* and *Ctso*) and two hypothetical genes. Sequencing of these candidate genes showed polymorphisms but did not reveal any mutation segregating with early-onset retinal degeneration [158]. Nevertheless, the causative mutation of the 1,49Mb could be in microRNAs and alter gene regulation. Mutations in *Rpgrip1* and one of the genetic modifiers could have cumulative effects require for the phenotype.

Indeed, the Ins44 *Rpgrip1* mutation is leaky [159]. In the normal dog (as in human, murine and bovine retinas), *Rpgrip1* is subject to both alternative splicing and the use of internal promoter [160], [159]. Several *Rpgrip1* transcript variants contain the mutated exon 2, while other not, as they have 5' end downstream of exon 2. Thus, in *Rpgrip1*$^{-/-}$ dogs, retinal *Rpgrip1* mRNA includes functional transcripts that bypass the insertion mutation through the use of alternative transcription start sites. In addition, alternative slicing leads to the skipping of the mutated exon 2. In this case, the protein product is nearly identical to the full-length RPGRIP1 variant, but with a truncated N terminal-region and a putative start codon encoded by exon 5 [157]. Luciferase reporter gene assays in COS-7 cells have demonstrated that out-of-frame Ins44 insert still allowed downstream reporter gene expression at 40% of the efficiency of in-frame inserts [159].

A critical threshold of RPGRIP1 expression could determine the phenotype of *Rpgrip1*$^{-/-}$ dogs. If the modifier gene is acting as a miRNA that represses the translation of functional *Rpgrip1* mRNA or degrades functional *Rpgrip1* mRNA, it could reduce RPGRIP1 expression below the critical level.

II.3.5. Summary

In human, mice and dog, mutations in the photoreceptor-specific *RPGRIP1* gene severely affect both cones and rods function and survival.

In *Rpgrip1*$^{-/-}$ and *nmf247* mice, early morphological defects are more evident in rods. In the *Rpgrip1*$^{-/-}$ mouse, loss cone and rod ERG are concomitant, and seem to reflect the degeneration of photoreceptors cells. This phenotype does not faithfully replicates the human pathology as several RPGRIP1-deficient patients retain photoreceptor cells despite severe visual impairments (**Figure 13**). A more pronounced bi-phasic retinopathy is observed in the MLHD-*Cord1* dog. Cone function is totally absent from birth. Rod ERG function is progressively lost from 1 to 9-12 months of age, whereas most photoreceptor cells degenerate over 2 years of age. In addition, long-term preservation of the cone-rich visual streak was observed in MLHD-*Cord1* dogs for at least 30 months of age (Petit L. unpublished data).

II.4. Conclusion: mutations in *PDE6β* and *RPGRIP1* cause severe photoreceptor diseases

Inherited photoreceptor dystrophies are a major cause of blindness worldwide. The majority is due to mutations in genes expressed in the retinal photoreceptors.

Missense and nonsense mutations in the rod-specific *PDE6β* gene are associated with severe **rod-cone dystrophy** in humans, mice and dogs. In all these species, rod dysfunction and degeneration occur within the first tenth of their respective lifetime. Consequently, although PDE6 play a key role in photoreceptor function, small deviations from PDE6 physiological defects also have dramatic effects on rod cell survival. In addition, rod degeneration is associated with a dramatic loss of genetically healthy cones, leading to a highly debilitating disease.

Mutations in the photoreceptor-specific *RPGRIP1* gene also severely impact cones and rods physiology in mice, dogs and humans. Both photoreceptor subtypes are affected from early stages of the disease, with retinal dysfunction preceding retinal degeneration.

Consequently, both PDE6β- and RPGRIP1-linked retinopathies are complex retinopathies involving two components: photoreceptor dysfunction and photoreceptor degeneration. This finely reflects the intimate link between photoreceptor function and survival (**Chapter 1**). Having this into consideration, ideal treatments of inherited photoreceptor dystrophies should result in amelioration of both the dysfunction and the degeneration components of the diseases. With regard to this complexity, it is critical to better understand the nature of disease processes that lead to photoreceptor death. In particular, it is important to understand how photoreceptor degeneration uncouples from the primary genetic etiology at some point in the disease progression.

CHAPTER **III**

PHOTORECEPTOR DEATH IN INHERITED RETINOPATHIES IS CAUSED BY PROLONGED DISEQUILIBRIUM

The binary hallmark of inherited photoreceptor dystrophies is a combined dysfunction and degeneration of photoreceptor cells (**Chapter 2**). Having this into consideration, ideal treatments of inherited photoreceptor dystrophies should result in amelioration of both the dysfunction and the degeneration components of the diseases. However, there is still a large gap in the knowledge of the mechanisms that links genetic mutations to the death of mutant photoreceptors, a process that occurs sometimes years to decades after genetic defect expression. Why some mutations in a gene cause rapid photoreceptor degeneration although other mutations cause loss of photoreceptor function without apparent degeneration? Why some genetically affected photoreceptor cells survive for extended periods of time? These questions need to be explored to define the factors that would be required to stably prevent or delay photoreceptor loss.

Consequently, this third chapter represents an attempt to summarize the mechanisms of photoreceptor death in inherited retinal dystrophies, with an emphasis in those involved in retinopathies caused by mutations in *PDE6β* and *RPGRIP1*. My hope is to highlight that the common pathogenic factor behind the diversity of mutant genes associated inherited photoreceptor dystrophies may be the shared ability to stress the photoreceptors and subsequently disrupt photoreceptor homeostasis. In this scenario, photoreceptor death can be viewed as a consequence of prolonged disequilibrium and restoration of the photoreceptor "physiological equilibrium" would be required to stop disease progression.

Contents

III.1. Animal models for understanding inherited photoreceptor dystrophies

Many advances in understanding the molecular and cellular mechanisms of inherited photoreceptor dystrophies would not have been possible without the use of spontaneous and engineered animal models of human diseases. Indeed, information about the mechanisms of photoreceptor death in human retinas is still very limited due to a paucity of autopsy specimens with defined genetic defects. Moreover, cell lines of RPE or photoreceptors often show different gene expression patterns than their *in vivo* homologues. The animal model chosen to investigate the pathway of photoreceptor death should reflect the human disease as closely as possible (in terms of mutations that cause the disease and of pathologic and phenotypic features that follow). Advantages and disadvantages of rodent and large models to study mechanism of photoreceptor death will be rapidly reviewed.

III.1.1. Rodent models of inherited photoreceptor dystrophies

III.1.1.1. Rodents are useful to investigate the link between a genetic defect and photoreceptor death

Mice and rats are extensively used to investigate the role of genes/mutations in the process of photoreceptor degeneration. One main reason is their short gestation time and their relatively low cost. Mice and rats are thus available for relatively short experiments with large number of animals. Mouse orthologs are known for almost all retinal dystrophy identified genes. Numerous natural rodent models of photoreceptor degenerations have been identified and thousands transgenic or knockout rodent models of photoreceptor degeneration have been generated by genetic engineering.

III.1.1.2. Rodents are good models to understand diseases affecting the peripheral retina, but are sub-optimal for diseases affecting central cones.

However, the primary disadvantage of rodent models of photoreceptor dystrophies is that their retinas differ substantially from those of humans, especially regarding cone content. Rodents have only S and M cones, whereas human have S, M and L cones. In addition, in rodent, most of the cones co-expressed both S and M opsins [161, 162].

Rodents are mostly nocturnal animals, and thus have a very low proportion (3%) and density of cones (**Table 5**). Rodent eyes lack a macula-fovea region (**Figure 15a-b**). Consequently, although rodents serve as excellent models for diseases affecting the peripheral retina, they may be less suitable for questions regarding **cone dystrophies** or late stages of **rod-cone dystrophies**. Of note, some diurnal cone-rich laboratory rodents have been recently characterized [163, 164]. They can become potentially interesting experimental animal models for human vision research.

Density of rod and cone photoreceptors in various vertebrate species				
Species	**Mean rod density (cells/mm²)**	**Mean cone density (cells/mm²)**	**Rod/cone ratio**	**References**
Mouse	Dorsal: 450 000 Venral: 305 000	Dorsal: 12 000 Ventral: 12 000 – 13 000	30-40/1	Jeon et al. (1998)
Rat	nd	2000-7000	100/1	Hughes et al. (1979) Ortin-Martinez et al. (2013)
Rabbit	Dorsal rod peak: 300 000	Visual streak: 18 000 Periphery: 7 000-12 000	Central: 15/1	Famiglietti et al. (1995)
Cat	Area centralis: 275 000 Central annulus: 463 000 Periphery: 250 000	Area centralis: 27 000 Periphery: 4 000	Central: 10/1 Periphery:	Steinberg et al. (1973)
Dog	Area centralis: 250 000 Central annulus: 501 000 Periphery: 305 000	Area centralis: 26 000-32 000 Periphery: 7 000-10 000	Central: 3/1-10/1 Periphery: 41/1	Mowat et al. (2008) Petit et al. (in preparation)
Pig	Area centralis: 105 000 Central annulus: 162 000 Periphery: 86 000	Area centralis: 24 000-35 000 Periphery: 8 500-11 000	Central: 3/1-5/1 Periphery: 10-16/1	Chandler et al. (1999) Gerke GC et al. (1995)
NPH	Fovea: nd Parafovea: 184 000 Periphery: 23000-30 000	Fovea: 141 000 Periphery: 2000-4 000	Central: nd Periphery: 15-30/1	Wikler et al. (1990)
Human	Fovea: nd Parafovea: 176 000 Periphery: 30 000- 40 000	Fovea: 199 000- 300 000 Parafovea: 6 000 Periphery: 2 500-4 000	Central: 1/4 Periphery: 20-30/1	Curcio et al. (1990) Jonas et al. (1992) Aknet et al. (1998)

Table 5. Density of rod and cone photoreceptors in various vertebrate species.

nd, not determined

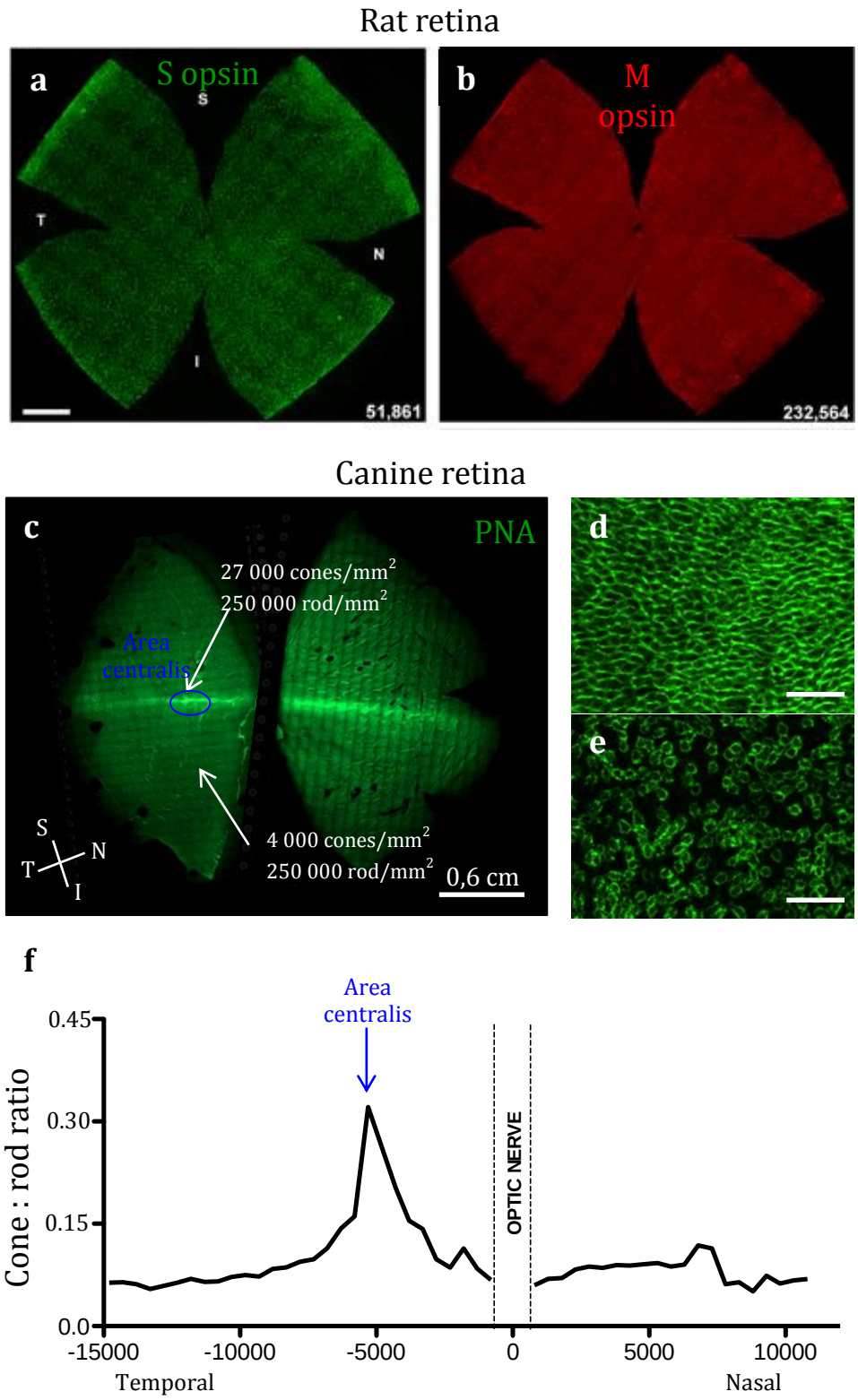

Figure 15. Comparison of cone topography between the rat and the canine retinas. (**a, b**) Rat retinal flatmounts immunostained with an antibody rose against (**a**) S opsin or (**b**) M opsin. The number of cones counted in that retinas are indicated in the bottom right of each map [165]. (c) Canine retina flatmount stained with peanut agglutinin (PNA). We identified a clear cone-rich visual streak superior to the optic nerve. Orientation is depicted: nasal (N), temporal (T), superior (S) and inferior (I). (**d,e**) Representative magnified imaged from the (**d**) cone-rich visual streak and (**e**) a comparable area in the mid-peripheral inferior retina. (**f**) Ratio between cones and rods across the cone-rich visual streak. The ratio was higher in the area centralis (Petit L *et al*. in preparation).

III.1.2. Large animal models of inherited photoreceptor dystrophies

III.1.2.1. Dogs, cats or pigs models are good models to understand cone disorders and spatio-temporal patterns of photoreceptor degeneration

Retinas of large animals such as dogs, cats or pigs are anatomically more similar to the human eye [166]. As rodent models, large mammals are rod-dominated; they have two discrete M and S cone subtypes and lack a foveal region. However, large mammals have a higher cone:rod ratio than rodents (**Table 5**) and they have a well-defined cone-rich region called the visual streak that extends from the nasal to temporal retina, just above the optic nerve (**Figure 15c-e**). More importantly, within the visual streak, there is a temporal area of peak photoreceptor density that shares great similarities with the human macula and is responsible for high visual acuity [167], [168] (**Figure 15c-f**). This region is defined as the *area centralis*. In beagle dogs, the *area centralis* contains a higher density of both rods and cones [168]. In contrast, in Irish setter dogs, the *area centralis* is cone-enriched, but also rod-depleted, moving closer to the human *fovea* (Petit L. *et al*. in preparation). L/M cones significantly outnumber S cones in the *area centralis* [168], similar to the primate parafoveal area [169].

Thus, in the virtual near absence of non-human primate models of inherited photoreceptor dystrophies, except [170], other large mammals are anatomically very attractive models, in particular regarding photoreceptor density, proportion and distribution. Studying the detailed cellular changes that occur in such animal models is critical to understand the spatio-temporal patterns of photoreceptor degenerations in humans.

II.1.2.2. Dogs and cats models have a *tapetum fundus*

Nevertheless, we can note that anatomic differences exist in the retinal structure of some large mammals compared to the humans. Cats and dogs (but no pigs and primates) have a *tapetum fundus*, a reflecting area enhancing light captivity and improving vision when there are low light levels by reflecting incoming light back to the outer segments [171] (**Figure 16a**). The *tapetum fundus* is located in the superior half retina (containing the cone-rich *area centralis*), where it forms a triangular area just above the optic nerve (**Figure 16b-c**).

The *tapetum fundus* is anatomically composed of a choroidal *tapetum lucidium*, and an absence of pigment in the overlying RPE cells (**Figure 16d**). The tapetal cells do not contain any pigmentation, but resorb and reflect different wavelengths of light (in particular short wavelengths), resulting in a particular color ranging from yellow-orange to green-blue (**Figure 16b**). The rest of the cat and dog retina is comprises the nontapetal fundus (*tapetum nigrum*), which is non-reflective. It is composed of pigmented RPE cells without *tapetum lucidium* (**Figure 16e**).

RPE pigmentation absorbs the scattered light and protects the photoreceptor cells against photo-oxidation.

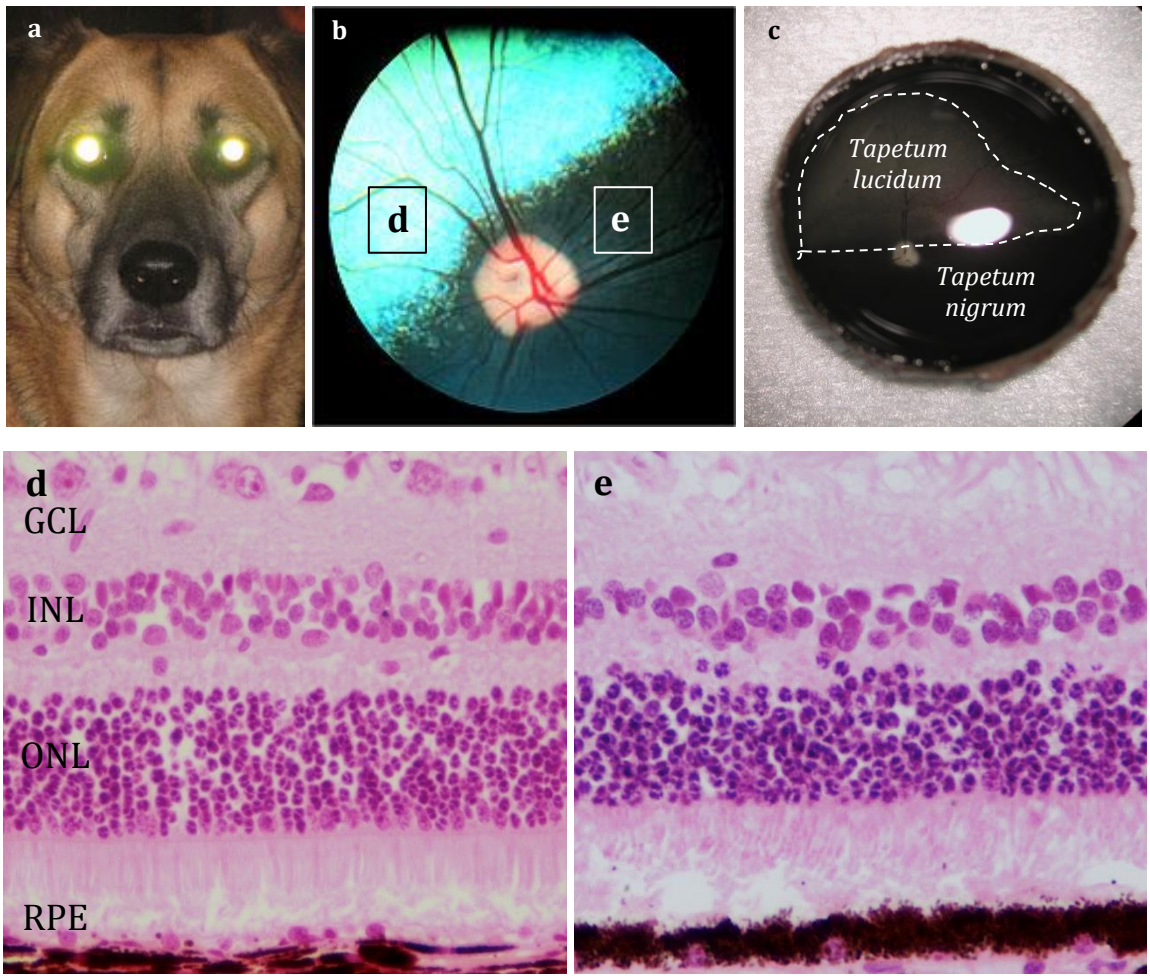

Figure 16. Pigmentation of RPE cells in the dog with tapetum lucidum. (**a**) Photograph of a dog showing reflection of camera flash from *tapetum lucidum* (**b**) Fundus photography of a dog showing the superior tapetal retina and the inferior non-tapetal retina (http://www.animaleyecare.com). (**c**) Eye cup dissected from a canine eye showing black *tapetum nigrum* and clear *tapetum lucidium* (Petit L, unpublished data). [90] Photomicrographs of canine retinal sections stained with hematoxylin-eosin. (d) Normal retina in superior tapetal zone (**e**) Normal retina in the inferior non-tapetal zone (Petit L, unpublished data).

III.1.2.3. Canine models of inherited photoreceptor dystrophies: the value of large natural models

With the exception of transgenic pigs [172], [173], [174] and a recently reported engineered sheep model [175], large animal models of retinal dystrophies mainly occur in the cat [176], [177] and the dog, and are naturally occurring disorders.

In dogs, numerous forms of retinal degeneration have been identified (**Table 6**) [178]. They are called progressive retinal atrophies and can be divided into two main groups depending on their onset:

- **retinal dysplasia**, when the retinal degeneration manifests during the retinal development
- **retinal degenerations**, when the pathological changes become evident after the normal development and the maturation of the retina.

Dogs born with an undeveloped retina that reaches maturity at around 6 postnatal weeks; whereas humans born with a retina that is further developed and undergoes milder postnatal differentiation (particularly concentrated in the fovea and macula).

To date, over 100 breeds of dogs are affected with progressive retinal atrophies and more than 10 genes have been associated with the etiology of progressive retinal atrophies (**Table 6**)[178]. Interestingly, they mimic the diversity of retinal phenotypes observed in humans. The vast majority of progressive retinal atrophies in the dog are progressive **rod-cone dystrophies**. Several forms of retinal dystrophies in the dog also resemble human **progressive cone-rod dystrophies** and stationary disorders [178].
Interestingly, variable ages of onset and disease severity of canine retinal dystrophies can arise from the same gene/mutation in different breeds, as observed among human patients with photoreceptor dystrophies. Thus, canine models of retinal dystrophies are excellent models for understanding the molecular mechanisms of this variability [178].

III.2. How photoreceptors die in inherited retinopathies?

III.2.1. Photoreceptor death in inherited retinopathies is programmed

Basically, two distinct cellular pathways can lead to cell death: (i) necrosis and (ii) programmed-cell death. Necrosis is traditionally thought to be a poorly controlled process, mainly independent on metabolic pathways. Hallmarks of necrosis include loss of cell membrane integrity, osmotic swelling of cellular organelles and the uncontrolled release of cell death products into the extracellular space. It results in an inflammatory reaction and damage to surrounding cells/tissue. This is not a feature commonly observed in inherited photoreceptor dystrophies, where inflammation is very limited. Photoreceptor death in response to genetic defect follows a more controlled process.

Examples of canine models of inherited retinal dystrophies				
Animal model	**Disease name**	**Affected Breeds**	**Gene**	**References**
rcd1	Rod-cone dysplasia 1	Irish Setter	*Pde6β*	Aguirre et al. (1978) Clements et al. (1993) Parry (1953) Suber et al. (1993)
rcd1a	Rod-cone dysplasia 1a	Sloughi	*Pde6β*	Dekomien et al. (2000)
rcd2	Rod-cone dysplasia 2	Collies	*Rd3*	Acland et al. (1989) Kukekova et al. (2006, 2009)
rcd3	Rod-cone dysplasia 3	Cardigan Welsh corgi	*Pde6α*	Petersen-Jones et al. (1999) Tuntivanich et al. (2009)
rcd4	Rod-cone dysplasia 4	Gordon/Irish Setter	*C2orf71*	Downs et al. (2013)
prcd	Progressive rod-cone degeneration	22 breeds	*Prcd*	Acland et al. (1998) Aguirre et al. (1988) Golstein et al. (2006)
Pra	Progressive retinal atrophy	Papillon, Phalène	*Cngb1*	Ahonen et al. (2013) Winkler et al. (2013)
XPRA1	X-linked progressive retinal atrophy 1	Samoyed, Siberian Husky	*Rpgr*	Acland et al. (1994) Zeiss et al. (1999) Zhang et al. (2002)
XPRA2	X-linked progressive retinal atrophy 2	Mongrel-derived	*Rpgr*	Zhang et al. (2002)
ADRPA	Autosomal dominant progressive retinal atrophy	Bullmastiff, English mastiff	*Rho*	Kijas et al. (2002, 2003)
cord1	Cone-rod dysplasia 1	Miniature longhaired dachshund	*Rpgrip1*	Mellersh et al. (2006) Turney et al. (2007) Lhériteau et al. (2009) Miyadera et al. (2010)
crd1	Cone-rod dystrophy 1	American Staffordshire terrier	*Pde6β*	Kijas et al. (2004) Golstein et al. (2013)
crd2	Cone-rod dystrophy 2	American pit bull terrier	*ND*	Kijas et al. (2004)
crd3	Cone-rod dystrophy 3	Glen of Imaal	*Adam9*	Goldstein et al. (2010)
Cngb3-/-	Achromatopsia /Cone degeneration	3 breeds	*Cngb3*	Sidjanin et al. (2002)
Rpe65-/-	Congenital stationary night blindness	Briard, Alaskan Malamute	*Rpe65*	Aguirre et al. (1998) Narfström et al. (1989)
cmr1-3	Canine multifocal retinopathy 1-3	11 breeds	*Best1*	Guziewiez et al. (2007) Zangerl et al. (2010)

Table 6. Examples of canine models of inherited retinal dystrophies. Models of progressive retinal dystrophies are shown in beige. Models of stationary diseases are shown in grey. Other pathologies are shown in white. ND, non-determined

Apoptosis is a mechanism of programmed cell death in which the cell plays an active role in its own demise. This form of cell death is energy consuming and involves transcription and protein synthesis. Apoptosis is associated with cytoskeletal destruction, membrane blubbing, nuclear condensation, DNA fragmentation and disassembling of the whole cell to produce membrane-enclosed vesicles in which organelles remain intact. This process prevents intracellular components from being released from the dying cells. Apoptosis most often involve the activation of caspases, a family of intracellular proteases that degrade a broad range of structural and regulatory proteins and activate DNases. Consequently, caspase activation is considered central to most definitions of apoptosis. However, accumulating evidences has also shown that apoptosis could also occur in a caspase-independent manner in neurodegenerative diseases, and that dying cells retain many morphological characteristics of apoptosis. Proteases involved in caspase-independent pathways of cell death include calpains, cathepsins and serine proteases.

Cathepsins and proteases are also features of autophagy, characterized by the formation of large vacuoles. Autophagy is also an active process driven by the cell itself, mainly as a protective response to stress. Cells undergoing autophagy may then undergo apoptosis.

III.2.2. Photoreceptor death in retinopathies is primarily through apoptosis

Although it is obvious that disease mechanism for each protein involved in inherited photoreceptor degeneration is different, it is assumed that most genetic mutations converge toward apoptosis. This was first suggested by Chang *et al*. in 1993, after demonstration of cleavage and fragmentation of photoreceptor DNA in three murine models of **rod-cone dystrophy** caused by a defect in the rod phototransduction cascade or photoreceptor structure [179]. Apoptosis was then reported to be the final outcome in all animal models and patients analyzed so far [88]. However, the exact apoptotic pathway engaged in the process is not fully understood.

III.2.2.1. Photoreceptor death during retinal development

The classical caspase-dependent cell death pathway is commonly used in eukaryotic cells to regulate cell numbers. In the retina, caspase-dependent apoptosis is involved during photoreceptor development.

Shortly before the complete elongation of photoreceptor outer segments, the population of photoreceptors is adjusted from its initial excess to a level appropriate for adult life. It was proposed that this mechanism reflects a lethal competition for energy and oxygen among photoreceptors due to onset of photoreceptor function (and thus of photoreceptor metabolism). The death of some photoreceptors reduces metabolic stress on the survivors so that the developmental death of photoreceptors slows, and then ends [25].

III.2.2.2. Photoreceptor death in inherited retinopathies involves caspases

Initially, caspases were attributed a central role in photoreceptor apoptosis in murine models of photoreceptor degeneration, including the *rd1* mouse [180]. However, these earlier studies were performed in murine models of early-onset and severe retinal degenerations, in which photoreceptor degeneration starts at the same time as the period of developmental cell death in this species (from postnatal day 5 to 30). This makes very difficult to analyze retinal degeneration at the tissue level, by histology, immunostaining, microarray or Western-Blot. In addition, it was demonstrated that caspases and pro-apoptotic proteins are down-regulated as development proceeds to protect terminally differentiated photoreceptors against apoptotic stimuli [181, 182]. Thus photoreceptors would be more prone to caspase-independent cell death or autophagy in face of genetic damages [183].

In this view, more recent work has demonstrated that caspase-mediated cell death is not sufficient to completely explain photoreceptor death in inherited retinopathies. Features of photoreceptor apoptosis are present in the absence of key caspases in murine models of retinal degenerations. In *rd1* mice, DNA fragmentation is still observed despite the absence of caspase-2, -3, -7, -8 and -9 activation, or cytochrome c release from the mitochondria [184]. In addition, the administration of caspase-3 inhibitor did not prevent DNA fragmentation in the *rd1* model [185]. Genetic ablation of caspase-3 provided only minimal protection against photoreceptor degeneration [186]. Clearly, alternative/additional mechanisms may be more critical role for the execution of photoreceptor apoptosis.

III.2.2.3. Photoreceptor death in inherited retinopathies involves calpains and cathepsin D

Recent studies have demonstrated that factors atypical for classical apoptosis, such as calpains and cathepsin D, are activated in rodent models of inherited retinal degeneration [187-190]. This further supports the notion that caspases are no longer the sole executioners of photoreceptor apoptosis. As caspase-3 and capsase-12 are activated by calpains, the different proteases may interact during photoreceptor cell death. Consistently, treating several mouse models of retinal dystrophies with a calpain inhibitor did not slow photoreceptor death.

III.2.3. Multiple molecular pathways overlap during photoreceptor death

Interestingly, calpain enzyme and cathepsins are activated by oxidative stress and altered glucose metabolism. They mediate necrosis or autophagy, in parallel or behind classical apoptosis. Thus, multiple cell death mechanisms may be predominant during different stages of the disease, or overlap at one particular stage, at least in murine models of retinal

dystrophies [191-193]. Energy availability in photoreceptors may determine the cell death pathway (for example, an energy-deprived photoreceptor may privilege necrosis, as it is a very lower-energy consuming process than apoptosis).
The presence of this continuum of destructive pathways clearly challenges the efficacy of potential therapies targeting a single pathway. This challenge would be likely even higher if (i) photoreceptor cell death is slow, (ii) there are temporal/geographical different waves of photoreceptor degeneration within the retina [194], and if (iii) rods and cones use different mechanisms to die [195], [29]. To date, these aspects remain largely unexplored.

III.3. Photoreceptors die in inherited retinopathies is response to disequilibrium

How different mutations converge to a similar apoptotic pathway in photoreceptor cells is not completely understood. Investigations are complicated by the diversity of inherited photoreceptor dystrophies associated proteins. In addition, in many cases, the biological role of the corresponding wild-type protein is unclear, so that the link between the dysfunction and the ultimate death of the photoreceptor is not evident.
Nevertheless, it is unlikely that there are more than 200 gene-specific photoreceptor mechanisms leading to apoptosis. Rather, it is expected to be a much smaller number of mechanisms that are share by several inherited retinal dystrophies loci.

III.3.1. Rapid rod degeneration in progressive PDE6β-deficiencies is correlated with disruption of Ca^{2+} and/or cGMP homeostasis

How *PDE6β* mutations cause cell death was particularly well described in the *rd1* mouse. As previously mentioned in **Chapter 2**, the *rd1* mouse carries a loss-of-function mutation in the *Pde6β* gene that predicts total loss of PDE6 activity. The onset of photoreceptor degeneration in *rd1* mice is exceptionally early (P8) and has a severe course, leading to an almost complete loss of photoreceptors before the complete maturation of the retina (at P20).

III.3.1.1. Loss of PDE6 activity is associated with toxic calcium overload through cGMP-gated channels

In the *rd1* mouse, it was found that loss of PDE6 activity is associated with massive accumulation of cGMP. As cGMP normally acts on cGMP-gated channels, it was proposed that elevated levels of cGMP in the outer retina increase the conductance of cGMP-gated channels and result in toxic Ca^{2+} overload in rods.
Evidence of the implication of cGMP-gated channels in the death of *rd1* rods has been elegantly obtained in the *rd1* x *Cngb1*$^{-/-}$ mouse, which lacks both PDE6β and rod cGMP-gated channels [196]. In this double mutant model, rod photoreceptor viability and outer segment morphology were greatly improved at P30, a stage in which almost all photoreceptors are lost in the *rd1* mouse [196].

Ca^{2+} overload activates the apoptotic machinery

How might Ca^{2+} overload affect photoreceptors? One hypothesis is that Ca^{2+} overload exceeds endogenous Ca^{2+} buffering systems, inactivates photoreceptor mitochondria and subsequently activates the apoptotic machinery. Supporting this idea, studies have found strong activation of Ca^{2+}-dependent enzymes in *rd1* photoreceptors. However, it is not known how elevated Ca^{2+} levels within the outer segments can activate Ca^{2+}-dependent mechanisms in the inner segment.

Ca^{2+} overload could place photoreceptors in a state of metabolic stress

An additional/alternative hypothesis is that Ca^{2+} overload places photoreceptors in a state of metabolic stress in requiring continuous activation of Ca^{2+}-ATPase and/or Na^{+}/K^{+}-ATPase to maintain electrochemical gradients.
It is likely that the disruption of the phototransduction cascade places the photoreceptors in a state equivalent to "permanent darkness". Thus, mutant rods need large quantities of ATP to re-equilibrate their membrane potential and died by prolonged disequilibrium of their metabolic homeostasis and energetic collapse.
In line with this hypothesis, increase in oxygen uptake, glucose utilization and lactic acid production is detectable at P8 in the *rd1* mouse retina, followed by a rapid decrease from P12 (correlating with the loss of photoreceptors and rod outer segments collapse).

III.3.1.2. Loss of PDE6 activity is associated with toxic cGMP accumulation

Massive cGMP accumulation in photoreceptors could also exert itself a cytotoxic effect in photoreceptors, independently of cGMP-gated channel activity and Ca^{2+} influx [197], [198]. It has been demonstrated in the *Cnga3*$^{-/-}$, *Gucy2e*$^{-/-}$ mouse that lacks both cGMP-gated channels and guanylate cyclase (and has elevated levels of cGMP). In this double mutant mouse, cone survival was significantly improved compared with the *Cnga3*$^{-/-}$ mouse, revealing cGMP as a trigger or accelerator of photoreceptor death [198].

Accumulation of cGMP *per se* could contribute to photoreceptor degeneration via the activation of cGMP-dependent protein kinases PKG. PKG are 100-fold more sensitive to cGMP than cGMP-channels [199]. Thus, cGMP-dependent PKG activation might occur earlier than cGMP-dependent Ca^{2+} influx through cGMP-gated channels [197]. Contribution of PKG signaling to photoreceptor death was demonstrated in the *rd1* mice [197]. In addition, in the *rd1* retina, inhibition of PKG was transiently but significantly neuroprotective [197]. However, PKG activity may directly or indirectly modulate the activity of cGMP-gated channels [196]. As neither non-functional cGMP-gated channels nor an inhibition of PKG was able to completely stop rod degeneration in the *rd1* mice, it is conceivable that both pathways are activated in parallel.

III.3.1.3. Mutations leading to disruption of Ca^{2+} and/or cGMP homeostasis can converge to the same mechanism of death

If the *rapid* death of rods in the *rd1* mouse is directly correlated with Ca^{2+} and/or cGMP accumulation, similar mechanism may be at play in other models of retinal dystrophies triggering aberrant Ca^{2+} and/or cGMP homeostasis.

It could concern other mutations directly affecting PDE6 function, such as loss-of-function mutations in *PDE6α* or *PDE6α'*. Consistently, cone death in the PDE6α'-deficient mouse was recently associated with an accumulation of cGMP and activation of PKG-target enzymes.

Mutations that indirectly affect PDE6 activity could also trigger the same mechanism of cell death. One example is mutations in the aryl hydrocarbon receptor-interacting protein-like (AIPL1) gene. In mice, *Aipl1* encodes a specialized chaperone protein required for assembly, trafficking and/or stability of PDE6 enzyme. In the *Aipl1*$^{-/-}$ mouse that carries a *null Aipl1* allele, the absence of AIPL1 leads to rapid degradation of rod PDE6 subunits by the proteasome. Limited light-induced decrease in cGMP and Ca^{2+} in darkness is observed in murine rods with low AIPL1 [200]. Elevated cGMP synthesis is also associated with gain-of-function of GCAP (guanylate cyclase activating protein), as in the *Gcap1* transgenic mice or GCAP1-deficient patients with dominant **cone-rod dystrophy** [201].

III.3.1.4. Severity of Ca^{2+} and/or cGMP imbalance determines the severity of photoreceptor death?

Interestingly, all animal models of retinopathies associated with a loss of PDE6 activity (and/or cGMP/Ca^{2+} overload) have an early-onset and fast retinal degeneration. For example, both *rd1* and *cpfl1* mice, that are characterized by homologous defects in either the rod or the cone PDE6, respectively, experience a fast degeneration with detectable onset of cell death as soon as P10 or P14, and almost complete disappearance of photoreceptors by P20 or P30 (**Figure 17**) [202].

In animal models with loss of PDE6 activity, the rate of photoreceptor loss seems correlated to the expected severity of the mutation (i.e. the reduction in PDE6 expression/function). The *rd1* mouse that carries a *null Pde6β* allele displays a slightly more severe degeneration that the *rd10* mouse, in which nonsense mutation is expected to reduce PDE6 activity. Likewise, analysis of the *null* and *hypomorphic* murine models of AIPL1-deficiency showed that retinal degeneration in *Aipl1* mutations is correlated to disturbance in the biosynthesis or stability of rod PDE6. *Aipl1*$^{-/-}$ mice have no PDE6 activity and display a kinetic of rod degeneration similar to that observed in *rd1* mice. In contrast, the hypomorphic *Aipl1*$^{h/h}$ mouse retains 20% of AIPL1 activity, and its retinal degeneration is much slower (only 50% of photoreceptors lost at 10 months of age).

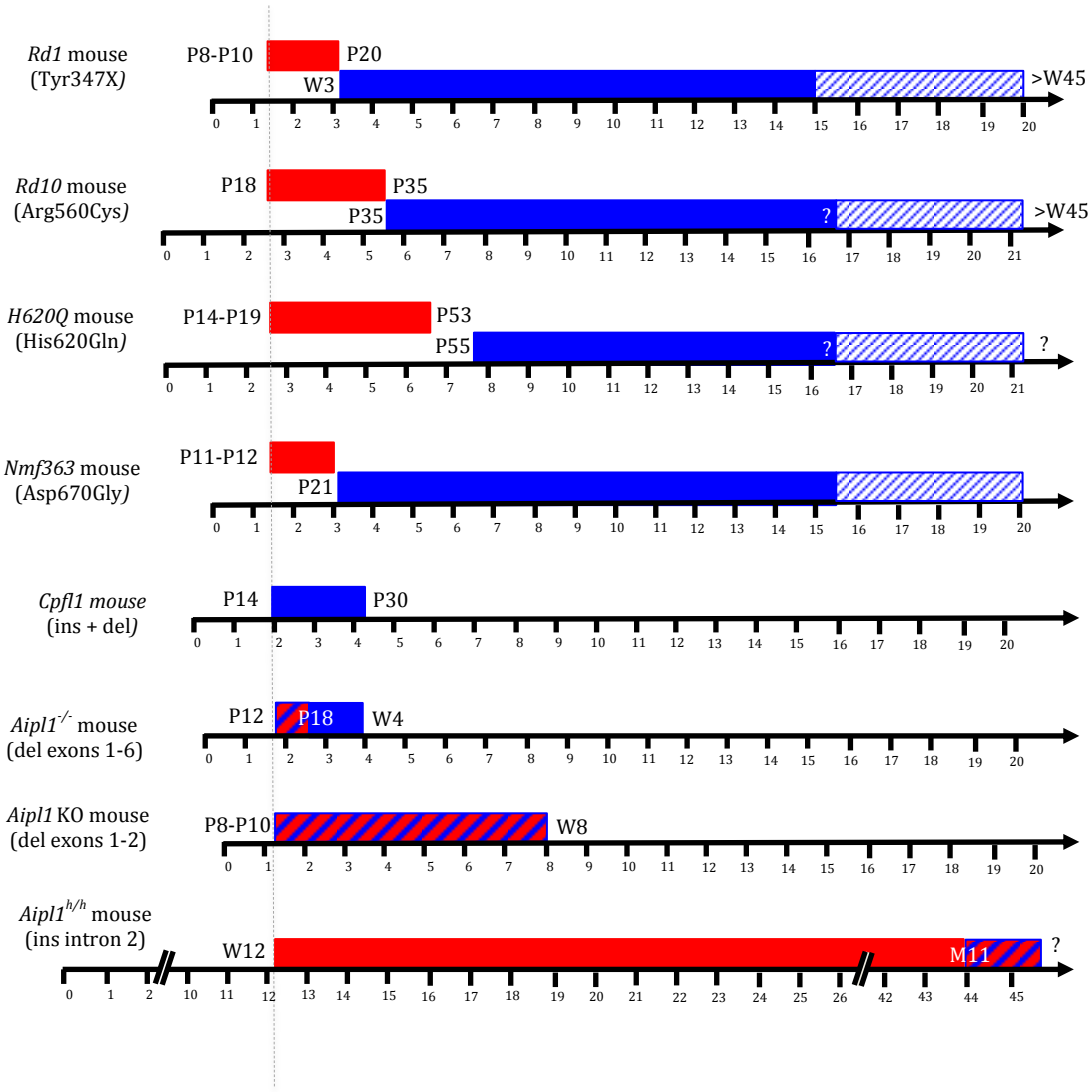

Figure 17. Schematic representation of the kinetics of rod (red) and cone (blue) degeneration that have been associated with murine models of PDE6-deficiencies. The rapid phase of photoreceptor degeneration are shown in full-colored boxes. The slow phase of photoreceptor degeneration are shown in hatched boxes. The onset of photoreceptor death is aligned. The corresponding time windows on the x axis are given in weeks post-birth. All animal models display similar kinetics of rod-cone degeneration.

Of note, photoreceptor degeneration in *Aipl1*$^{h/h}$ mice is much slower than that of *rd10* mice. This could be due to the fact that for one PDE6β subunit is required to form each PDE6 enzyme (stoichiometry PDE6α:PDE6β = 1:1), whereas one AIPL1 protein processes numerous PDE6 enzymes. Thus, a hypomorphic *Pde6β* allele could produce a more severe rod functional deficit than a hypomorphic *Aipl1* allele.

If this hypothesis is correct, is might be possible to slow the degeneration of photoreceptors by restoring the levels of cGMP/Ca^{2+} to the minimum level able to re-established photoreceptor *status quo*. It is in agreement with the observation that constitutive activation of PDE6 in GCAP1-deficient mice reduced cGMP and Ca^{2+} concentrations close to normal levels and spared rods from *severe* retinal degeneration (despite abnormal rod sensitivity)[201].

III.3.2. Slowly progressive rod degeneration in stationary PDE6β-retinopathies is correlated with loss of energy-consuming activity and excessive oxygen toxicity

III.3.2.1. *Pde6β* mutations leading to slow photoreceptor degeneration are not associated with elevated levels of cGMP and Ca^{2+}

The cGMP/Ca^{2+}model is a fascinating hypothesis to explain why some mutations do not produce rapid photoreceptor cell death, such as the *PDE6β*-H258N missense mutation, associated with non-progressive **congenital night blindness** in human patients [113], [114] and in mice [115].

The *PDE6β*-H258N mutation is located in a conserved region adjacent to the PDE6γ-interacting domain, and compromises the complete PDE6γ-dependent inhibition of PDE6 in the dark. This mutation is associated with a higher basal level of PDE6 activity (elevated noise) keeping dark-adapted cytoplasmic cGMP levels abnormally low. Consequently, cGMP-gated cation channels remain closed even in the dark, there is no increased transport of Ca^{2+} into the cell and rod photoreceptors remain permanently hyperpolarized. Mutant rods are unable to return to their dark-state and thus, to respond to light: they are desensitized. But, in these "sleeping" rods, there is no massive accumulation of cGMP, no calcium overload, no contribution to high-energy demand, and the disequilibrium of photoreceptor homeostasis remain mainly clustered into a functional defect. The mechanism that leads to fast cell death is absent, and mutant and dysfunctional photoreceptors do not *rapidly* degenerate.

III.3.2.2. Slowly-progressive death of photoreceptors is associated with continuous activation of the transduction cascade

Despite absence of Ca^{2+} and cGMP accumulation, mutant *PDE6β*-H258N rods slowly died overtime. Thus, another lethal disequilibrium must be at play in *PDE6β*-H258N rods. As PDE6 is continuously activated at high basal levels in mutant rods, continuous activation of

the transduction cascade even in darkness can be the initiator of this slow rod death (equivalent to constant exposure to low levels of light).

First evidences that an equivalent light exists in several inherited retinal dystrophies came from the observation that specific mutations in *Rhodopsin (Rho)* produce a protein that remains in its unliganded state for a prolonged period, and thus extensively activates the transduction cascade [203]. These mutations causes desensitization of the photoreceptors, slow late-onset photoreceptor death and are associated with **stationary congenital night blindness** in humans [204].

More convincing indication that spontaneous activation of transduction triggers photoreceptor degeneration was elegantly obtained in the *Rpe65*$^{-/-}$ mouse, a transgenic murine model of **LCA/cone-rod dystrophy**. The *Rpe65*$^{-/-}$ mouse carries a *null* mutation in *Rpe65* and develops a slowly progressive degeneration, leading to the loss of above 50% of photoreceptor cells by 12-18 months of age [205],[206]

In the *Rpe65*$^{-/-}$ mouse, there is no regeneration of 11-*cis*-retinaldehyde from all-*trans*-retinyl ester in the RPE cells, and thus a massive/total reduction of 11-*cis*-retinal in photoreceptors, in particular in rods that lack Müller-dependent retinoid cycle. Opsin remains permanently unliganded in mutant photoreceptors.

Several studies have indicated that the opsin apoprotein can constitutively activate the transduction cascade and cause the progressive death of photoreceptors in the *Rpe65*$^{-/-}$ mouse [206]. Indeed, photoreceptor degeneration was completely rescued when transducin activation was genetically abolished [206, 207]. It is estimated that 10^4 to 10^5 unliganded opsin molecules have the effect of one activated rhodopsin per second [207], but since there are many opsin molecules in the outer segment of *Rpe65*$^{-/-}$ mice, the accumulation of unliganded opsin may produce an activation equivalent to that produced by a nearly saturating bright light.

III.3.2.3. Contribution of low levels of Ca^{2+}

Excessive or constant hyperpolarization of photoreceptors may lead to apoptosis by decreasing Ca^{2+} concentration to a level that triggers apoptosis. Indeed, the “equivalent light” hypothesis suggests that aberrant activation of phototransduction decreases the probability of cGMP-gated channel opening and keeps the intracellular Ca^{2+} concentration at a constitutively low level. Consistently, dark Ca^{2+} is low in RPE65-deficient rods and dark rearing does not improve the survival of rods in the *Rpe65*$^{-/-}$ mouse.

The exact mechanism by which low Ca^{2+} concentration leads to apoptosis is not fully understood. Many studies have already shown that prolonged lowering of the Ca^{2+} concentration can kill neurons. In addition, rods have important protective mechanisms to regulate the rate of phototransduction and prevent the extensive reduction of Ca^{2+} concentration in bright light; supporting that low Ca^{2+} may be detrimental for rods.

III.3.2.4. Contribution of oxygen toxicity

Alternatively, mounting evidence supports the hypothesis that increased oxidative stress is an important effector of photoreceptor death in models of constitutively activated phototransduction. Recall that the retina has a high metabolic rate and hence a high rate of oxygen consumption, with mitochondrial oxidative phosphorylation consuming 90% of cellular oxygen (**Chapter 1**). Thus, due to inappropriate/constant phototransduction, photoreceptors are desensitized and their cellular metabolism falls. The reduction of cellular demand for ATP causes an overload of oxygen in inner and outer segments of photoreceptors, exacerbated by the inability of choroidal vessels to regulate blood flow in response to falling oxygen demand.

Oxygen can be highly toxic, as it can directly oxidize and inhibit phosphatases, kinases and other proteins or can be reduced to reactive oxygen species, which in excess can cause photoreceptor death. Elevated levels of oxygen can also mobilized Müller cells or microglia, which invade the degenerating photoreceptor layer, alter the expression of neuroprotective factors and/or exert cytotoxic function, further increasing the biochemical disequilibrium of photoreceptors. In addition, RPE cells can be severely impaired by increased oxidative stress, as they contain an abundance of photosensitizers (as lipofuscin, which is mainly derived from incomplete phagocytosis degradation of photoreceptor outer segments). Prolonged oxidative stress in RPE cells can affect RPE cellular activities, as glucose transport [208] or lysosomal degradative functions [209].
The oxygen toxicity hypothesis can explain why photoreceptor death is usually a slow process that takes months in these animal models, by a mechanism similar to an "accelerated aging"[2]. However, it is important to keep in mind that biological defenses against hyperoxia are not robust, so even small changes in cellular oxygen could also cause important damages at early stages of the disease, in particular in such vulnerable cells, as are photoreceptors.

III.3.2.5. Other mutations leading to continuous activation of transduction

Photoreceptor death caused by H258N *Pde6β* mutation could be equivalent to that seen in light damage models of retinal dystrophies, in which retinas exposed to prolonged low-levels of light experience severe desensitization and progressive photoreceptor death. In addition, a similar mechanism can also explain the slow degeneration of photoreceptors in forms of inherited retinal dystrophies caused by mutations in genes encoding proteins of the visual cycle (as *LRAT*), proteins involved in the shutoff of the transduction cascade (as *SAG*/arrestin or *RK*/rhodopsin kinase), proteins involved in cGMP synthesis (as *GUCY2D*/GC1), and cGMP-gated channels (as *CNGA3*, *CNGB3*, *CNGA1* and *CNGB1* if mutations result in lack of functional light-dependent conductance)[210].

[2] We can note here that increased oxidative stress could also be involved during the late stages of other forms of photoreceptor degenerations due to the loss of photoreceptor outer segments.

III.3.2.6. Severity of transduction inactivation determines the severity of photoreceptor death?

Interestingly, it was proposed that mutations causing continuous activation of the visual cascade lead to retinal degeneration, whereas mutations that can terminate signaling, even if only partially and intermittently, further slow the rate of degeneration sufficiently to give rise to stationary night blindness [211].

Numerous evidences support this hypothesis. For example, the *Rpe65*$^{-/-}$ mouse, that shows total loss of RPE65 expression in the RPE and no rhodopsin in photoreceptors, has photoreceptor degeneration relatively rapid with complete degeneration of M/L and S cones at P42 [207], [205]. In contrast, the *Rpe65* R91W knocking mouse, that shows partial expression of mutant RPE65 and rhodopsin up to 10% of wild-type levels, has a better preservation and slower degeneration of retinal morphology in comparison to *Rpe65*$^{-/-}$ mice [212]. In human *RPE65*-patients, the very mild cone impairment observed in one patient with Pro25Leu mutation in *RPE65* was correlated with the residual activity of the mutant RPE65 protein (above 10% of wild-type activity) [213].

Likewise, *null* mutations in *RK* or *arrestin* genes, that cause the abnormally prolonged activation of rhodopsin, are associated with minimal photoreceptor degeneration in murine models [214], [215] or human patients [216], [217]. It may be due to the remaining ability of rhodopsin to regenerate, preventing continuous activation of the signaling cascade as in *Rpe65*$^{-/-}$ mice [211].

If this hypothesis is correct, monitoring changes in Ca^{2+} and oxygen should provide insight into the fundamental differences in some forms of stationary and progressive retinal dystrophies. In addition, it might be possible to prevent photoreceptor degeneration in those forms of inherited dystrophies by decreasing the activation of the cascade, or by interrupting it for brief periods. Protection of photoreceptors by treatment with retinal derivatives that bind mutant opsin and hold the opsin in an inactive conformation in the dark is also conceivable [218]. Proof-of-concept of retinal derivatives were recently obtained in murine [219], [220] and canine models of RPE65-deficiency [221]. Oral retinoid therapy is currently evaluated in phase I clinical trials in patients with *Rpe65*- and *Lrat*-linked **rod-cone dystrophies** (NCT01014052, NCT01543906, NCT01521793).

III.3.3. Photoreceptor death in RPGRIP1-deficiency is related to outer segment defects

III.3.3.1. In the absence of proper outer segments, outer segment specific proteins localize to abnormal cellular locations

The mechanism of photoreceptor death in RPGRIP1-deficiency can be related to outer segment defects and outer segment proteins misrouting [222].

These two mechanisms are tightly related. Indeed, in the absence of proper outer segments, outer segment specific proteins continue to be produced but localize to abnormal cellular

locations. For example, deterioration of outer segments in the *Rpgrip1*$^{-/-}$ mice is associated with delocalization of rhodopsin and L/M opsin, normally expressed in the outer segments. Similar misrouting of outer segment proteins (including Peripherin/RDS and opsins) is observed after retinal detachment in other mammals (mechanical outer segment degradation) [223], [224]. As well, in the *Rds* mouse, outer segment disk morphogenesis is disrupted, which lead to accumulation of rhodopsin to the inner segment and cell body and progressive photoreceptor cell death.

III.3.3.2. Disrupted trafficking of outer segment proteins leads to photoreceptor cell death

As opsin constitutes over 90% of photoreceptor outer segment, it is not surprising that opsin mislocalization is stressful for photoreceptors. However, the mechanisms involved remained unclear.

Activation of cell death pathway: It was first proposed that mislocalized rhodopsin directly kills rod cells by stimulating normally inaccessible signaling pathways. In particular, activation of rhodopsin mislocalized in the inner segment may initiate a G-protein cascade leading to adenylate cyclase activation [225].

Alteration of synaptic homeostasis: Alternatively, it was proposed that the ectopic presence of high levels of opsin may have dramatic effects on photoreceptor neurite stability and signaling, such as neurotransmitter release in the synaptic termination [226]. Delocalized opsin could pack the synaptic or plasma membranes, diluting the effective concentration of normally occurring proteins.

Cellular stress: In addition, untargeted and/or unregulated delivery of rhodopsin in photoreceptor membrane might clearly favor reactive oxygen species (that cannot be eliminated by outer segment renewal). The ubiquitination/degradation of large amounts of misrouted proteins may also cause a damaging increase in the metabolic load placed on photoreceptors [227].
Moreover, the accumulation of mislocalized opsin in the endoplasmic reticulum (ER) may active the unfolded protein response (UPR) and cause ER stress. The UPR is a mechanism aimed at restoring homeostasis under conditions of ER stress. When proteins are misfolded, the cell activates several mechanisms to improve appropriate protein folding (by molecular chaperones) and to reverse, sequester and destroy misfolded proteins that affect function (by proteolysis). Misfolded proteins in the ER are also recognized by sensors that inhibit protein synthesis in order to alleviate the stress. However, when the amount of misfolded proteins exceeds the capacity of the protective UPR, cellular stress becomes chronic and the UPR signaling shifts to a pro-apoptotic cascade.

III.3.3.3. Misrouting of opsins is an early sign of photoreceptor degeneration is most forms of retinal dystrophies

Importantly, loss of photoreceptor outer segment and mislocalization of opsin to the membranes of the inner segment in photoreceptors is a feature of most known retinal dystrophies. It may constitute a general response to photoreceptor cell death, regardless of the cause of degeneration [228], [25].

In *rd1*, *rd10* and H620Q *Pde6β* mice, noticeable levels of mislocalized opsin and mitochondrial stress are detected at early stages of generation [229]. Progression of photoreceptor degeneration is closely associated with the UPR, suggesting that ER stress contributes to retinal pathogenesis [230].
In *Cnga3*$^{-/-}$ x *Nrl*$^{-/-}$ and *Cngb3*$^{-/-}$ x *Nrl*$^{-/-}$ mice (that lacks CNG-gated channels in a cone-rich retinas), enhanced levels of ER stress markers were recently observed, indicating a role of ER stress in cone degeneration in these models of cGMP-gated channel deficiencies. Alleviating ER stress by chemical chaperone effectively decreased levels of ER stress markers in the *Cnga3*$^{-/-}$ x *Nrl*$^{-/-}$ mouse, and was associated with prolonged cone survival [210]. It was hypothesized that cellular mechanism underlying the UPR and ER stress in those models of cGMP-gated channel deficiency involves opsin mistrafficking and/or mislocalization [231], [232], [233].
In addition, since 11-*cis*-retinal is a pharmacological chaperone for opsin, opsins are prone to aggregation in absence of 11-*cis*-retinal [234]. In studies in the *Lrat*$^{-/-}$ mouse model of **cone-rod dystrophy**, L/M and S opsins are mislocalized to the inner segments of cones, creating an increased burden on the cell. Interestingly, mislocalized L/M opsin is degraded, whereas mislocalized S opsin aggregates/accumulates in the RE and inner segment [235]. This observation explains the region-specific cone degeneration pattern observed in the retina of *Lrat*$^{-/-}$ mice since the ventral and central retina express higher levels of S-opsin than the dorsal retina in mice [234]. High S opsin toxicity might also explain the early loss of S-cone function in RPE65-deficient patients, while L and M cones remain initially functional [213, 236, 237].

III.4. Kinetics of photoreceptor death is determined by the level of photoreceptor disequilibrium and influenced by local environmental factors

III.4.1. Each genetic mutation provides to photoreceptors a different probability to death

From all these data, it emerges that different genetic insults can push photoreceptors into a common death pathway. However, it is evident that different loci are associated with different kinetics of photoreceptor death, varying from early-and-rapid to late-and-slow photoreceptor degeneration. This can be explained by the fact that each genetic mutation

provides to photoreceptors specific changes in photoreceptor equilibrium. These specific changes are not immediately harmful/lethal by themselves but they provide to photoreceptor a higher probability (or risk) to death. Mutations that initially bring a cell closer to a "cell death threshold" will exhibit a higher risk of cell death and thus a faster rate of photoreceptor degeneration.

In particular, mutations that induce accumulation of Ca^{2+} and metabolic collapse in photoreceptors appear to provide the highest probability of death: affected photoreceptor cells have to deal with massive increase in Ca^{2+} and/or cGMP and acute metabolic stress, which raises rapidly pathologic compound(s) closer to the critical level that will activate apoptosis. If they exist, adaptive compensatory processes are struggling to cope with these early and profound "degenerate and die messages", resulting in early and rapid loss of photoreceptor cells (and thus progressive disorders). In contrast, accumulation of reactive oxygen species-mediated damages, resulting from photo-oxidation, seems to be associated with a chronic stress and a lower risk of death: the degeneration of photoreceptor cells is slower.

III.4.2. Photoreceptor death is initiated by natural fluctuations in cellular physiology

This model was proposed by Clarke *et al*. to explain why in 11 animal models of inherited retinal dystrophies that photoreceptors are at constant risk of death [238]. This model indicates that (i) each mutant photoreceptor is at the same risk of death as every other mutant and that (ii) the time at which death will occur is random and independent of the time of death of other photoreceptors.
In other words, photoreceptor cells could start with an equal probability of cell death and the critical level of stress/disequilibrium that initiates apoptosis could be attained episodically by natural fluctuation in cellular physiology. Thus, stochastic factors result in the early death of some photoreceptors, whereas others (genetically equivalent) photoreceptors will survive for the lifetime in a steady state [42].

III.4.3. Geographic factors influence the initiation of photoreceptors death

Importantly, in patients of inherited retinal dystrophies, photoreceptor death is commonly not uniform across the retina, in particular at early stages [239]. For example, in patients with **rod-cone dystrophy**, photoreceptor death usually begins within the mid-peripheral retina, indicating that photoreceptors in this specific part of the retina have a greater risk of apoptosis [240]. In addition, several studies have demonstrated in patients with **rod-cone dystrophies** that the inferior retina is more vulnerable to rod degeneration that the central and superior retina [241], [242], [243]. Likewise, spatio-temporal patterns of photoreceptor degeneration have also been observed in murine (Jimenez, 1996 #432) and canine models of inherited retinopathies (Petit L *et al*. in preparation).

These observations seem inconsistent with the prediction that each mutant photoreceptor is at the same risk of death as every other mutant photoreceptor. However, this inconsistency can be reconciled by suggesting that local geographic factors are superimposed to the equal risk of death of photoreceptors. In the mid-peripheral retina of patients with **rod-cone dystrophies**, some local factors may increase the intrinsic risk of death in photoreceptors compared to photoreceptors located elsewhere [244].
The nature of the regional risk factors is unknown, but they may be: molecular heterogeneity within photoreceptors, variations in extra- and intracellular microenvironments, variations in the density or pigmentation of RPE cells, local differences in metabolism, vascularization, expression of neuroprotective factors and/or exposure to light...

III.4.4. Secondary pathology may influence photoreceptor death

The constant risk model indicates that progressive changes in the degenerative retina do not increase the risk of photoreceptor death overtime. However, this model is unlikely at middle and end-stage of degeneration, when the great majority of the cells are dead and severe secondary pathology seems likely to influence (positively or negatively) the risk of death.
For example, during the course of photoreceptor death, sustained changes occur in Müller and RPE cells, both cellular subtypes that ensheathe the photoreceptors and influence key metabolic pathway in rods and cones [245], [5, 6]. Changes in Müller and RPE cells are likely to participate in photoreceptor demise and death. It can be viewed as a photoreceptor-glial cell loop.

III.5. Secondary loss of cones in rod-initiated rod-cone dystrophies

To date, there are no known forms of retinal degenerations in humans or rod-dominated animal models where rod death is not followed by cone degeneration. While the cones account for only 5% of photoreceptors, they supply visual acuity and color perception, and their degeneration constitutes the most devastating aspect of the disease for affected patients. Therefore, the protection of cone function is the major goal of most therapeutic strategies. Unfortunately, little is known about the mechanisms that lead to this secondary cone death in **rod-cone dystrophies**, in particular in the vast majority of cases in which the causal mutation affects only rods. Consequently, factors critical to promote protection of cones in late stages of **rod-cone dystrophies** remain poorly understood.

Many evidences in animal models [101], [246-248] and patients with rod-initiated **rod-cone dystrophies** have indicated that cones degenerate in response to the death of rods, suggesting a cone dependency on rod survival. For example, Punzo *et al*. have elegantly demonstrated in murine models of **rod-cone dystrophies** with different kinetics of rod death that cone degeneration always starts after the end of the major rod death phase [101], As well, clinical examinations of patients with **rod-cone dystrophies** have suggested that

cone loss depends on the degree and the location of rod photoreceptor depletion [241], [3]. Interestingly, this cone dependency on rod survival is not reciprocal, as numerous forms of retinal dystrophies result only in cone death (as **cone dystrophies**)[249, 250].

There are several prevailing theories of why cones depend upon rods for their survival. These theories can fall into two non-exclusive categories:

- a direct influence of rods on cones via (i) the release of toxic factors by dying rods and/or (ii) a reduction in vital factors produced by normal rods
- an indirect influence of rods on cones by environmental perturbation via (i) an overload of oxygen, (ii) and/or a disruption of glucose delivery.

In both cases, secondary cone death in **rod-cone dystrophies** can be viewed as the consequence of prolonged cone stress and subsequent cone disequilibrium.

III.5.1. Rod factors directly influence cone survival/death

The first hypothesis involves the release by rods of toxic or vital factors that *directly* influence neighboring cone death or survival, respectively.

III.5.1.1. Preliminary data

Original results supporting this hypothesis were obtained in chimeric mice that contain various patches of mutant and normal photoreceptors [251], [252]. In these chimeric mice, a random mosaic pattern of photoreceptor death was expected. In contrast, the authors observed a uniform reduction of the ONL across the mutant and healthy patches, indicating that both mutant and healthy photoreceptors degenerate overtime. The degree of degeneration was independent of the size of the patches, but photoreceptor cell loss was delayed when the number of normal cells was increased [251]. It was hypothesized that release of a toxic factor by dying photoreceptors might kill the remnant cells, or alternatively, that normal photoreceptors release factors vital for the survival of the remnant cells.
Kedzierski and colleagues suggested that a similar process might be involved in the non-autonomous death of cones in rod-initiated **rod-cone dystrophies** [252].

III.5.1.2. Rod-derived toxic agents

The death of rods can be associated with the release of toxic factors that could themselves damage cones. Two potential toxic agents are usually cited: (i) glutamate and (ii) the products of apoptosis.

Glutamate: Glutamate is a well-known cause of neurotoxicity. However, glutamate toxicity as the principal cause of cone cell death is unlikely. Indeed, Müller cells expressed high level of glutamate transporters that serve to protect retinal neurons and there is no evidence that

photoreceptor release enough glutamate so as its extracellular concentration raises a toxic level. In addition, in animal models with advanced retinal degeneration, inner retinal signaling remains generally sensitive [253], [254].

Products of apoptosis: Other studies have raised the possibility that rod-derived toxic factors could be reactive oxygen species or products of apoptosis that accumulate in the subretinal space [252] or propagated from dying rods to healthy cones through rod-to-cone gap junctions [255].
This latter hypothesis was recently investigated in *rd1* and *Rho*$^{-/-}$ mice by deletion of the gap junction protein connexin36 [256]. Connexin36 is expressed on the cone side of gap junction and loss of connexin36 is sufficient to disrupt rod-cone coupling [90]. Connexin36-deficient *rd1* and *Rho*$^{-/-}$ mice showed the same kinetic of cone degeneration that their connexin36-expressing littermates. Thus, connexin36-dependent gap junction mediated bystander effect is not involved in secondary cone death in mouse models of **rod-cone dystrophies** [256].

Where a close temporal relationship between the peak of rod degeneration and the initiation of cone death would be expected, in practice cone cell death only begins after the major phase of rod death. Thus, if toxic factors play a role in cone death, they are not the predominant initiators of cone death.

III.5.1.3. Rod-derived vital factors

Transplantation of rod-enriched patches in *rd1* mice at late stage of rod degeneration demonstrated a limited preservation of host cones, including cones at distance from grafted cells [257], [258]. This suggests that transplanted rods could release diffusible trophic factor(s) that help cones to survive. To investigate this hypothesis, the authors have developed a co-culture system, avoiding direct contact between the retinal cells that secrete the putative factor(s) and the target retinal tissue [259], [260]. Explants of *rd1* retinas cultured in presence of retinas containing normal rods revealed a slightly greater number of cones than explants co-cultured with rod-deprivated retinas [259]. These data were supportive of a paracrine effect of rods on cone survival.

Rod-derived cone viability factor: Using cone-enriched retinal explants from chicken embryos, the same team has isolated one of the rod-derived factors capable of increasing the number of cone cells in culture, and name it rod-derived cone viability factor (RdCVF)[261].
Repeated subretinal injections of RdCVF protein promote short-term cone survival in *rd1* mice [261] and Pro23His *Rho* rats [261]. In addition, in the Pro23His rat, RdCVF injections prevent the loss of cone function by maintaining cone outer segments [262].

Putative mechanism of action: RdCVF is encoded by the *NXNL1* gene. It is predominantly expressed in photoreceptors (but also in inner retinal cells). RdCVF is homologous to the

family of thioredoxins, a group of proteins known to function as scavenger for reactive oxygen species. It was therefore suggested that RdCVF is involved in defense response against oxidative damage. However, RdCVF lacks oxidoreductase activity. It is not the case of the second protein product of *NXNL1*, RdCVFL, which has the characteristics of a thioredoxin-like enzyme.

Evidence of a physiological role of RdCVF against aging was obtained in the *Nxnl1*$^{-/-}$ mouse, in which cone function progressively declines with age [263]. This progressive photoreceptor degeneration was associated with increasing oxidative damage, suggesting a relation between RdCVF pathway and the maintenance of appropriate intracellular redox state of the cells. In addition, cones degenerated faster when *Nxnl1*$^{-/-}$ mice were raised under hyperoxic conditions [263]. As RdCVFL has an oxidoreductase activity, it was speculated that RdCVFL could be the sensor for oxidative conditions, coupling to the trophic protein RdCVF for an environmentally adapted protective response [264], [265], [266].

These data support a role of rod-derived signals in cone protection. However, as cones may survive for prolonged periods in the absence of rods (and therefore in the absence of rod-derived factors), loss of RdCVF seems also to contribute rather than govern secondary cone death [101]. Loss of RdCVF may rather increase the imbalance in cones during retinal degeneration.

III.5.2. Rod death disturbs the cone environment

In the outer retina, rods and cones are densely stacked together into a same layer. Their outer and inner segments are enclosed by RPE and Müller villi, respectively. This anatomical organization is remarkably conserved among the vertebrates and allows the life-long survival of photoreceptors despite the fact that these cells are continuously exposed to damaging factors (**Chapter 1**). As rods compose over 90% of the photoreceptor population, the loss of their activity, structure or clearance can disturb the physical and biochemical organization of the outer retina.

Disruption of the outer retina homeostasis can be the main factor that governs cone dysfunction and death in rod-initiated **rod-cone dystrophies** [29].

III.5.2.1. Photoreceptor density is a crucial determinant of cone survival

Supporting this idea, studies have found that photoreceptor cell density is a crucial determinant of cone death [267]. This was very elegantly demonstrated in a zebrafish deficient for the cone PDE6 enzyme [267].

In the zebrafish, the cone:rod ratio is reversed. At early stages of larval development, cones outnumbered rods by 8:1 and rods are initially concentrated in the ventral region. Then, approximately equal numbers of rods and cones are generated at the retinal margin by a population of mitotic progenitor cells. In addition, new rods are added in the central retina

by mitotic rod progenitors located in the outer nuclear layer. This neurogenesis continues throughout the all life of the fish.

In the *Pde6c*-mutant zebrafish larvae, central mutant cones died during the week of zebrafish development, following to the rapid death of the sparse central rods, strikingly analogous to the fate of cones in mammals.
In contrast, rods in the rod-rich ventral region are not affected by the loss of cones. As well, in *Pde6c*-mutant juvenile fish, although equal numbers of rods and (mutant/dying) cones are added at the retinal margin, the rods only persist in areas that always have a high density of rods. However, in *Pde6c*-mutant adult fish, when numerous rods have been added in the retinal margin and the central retina, rods appear healthy over the central and peripheral retina. This indicates that if rod cell density is sufficient, rods survive [267].

This model explains why cone degeneration always started after 90% of rods have died in animal models of rod-dominated species [101] and why, cone dysfunction is detectable by ERG only after the loss of 75% of rod function in human patients [241]. Such proportion of photoreceptor loss could represent the critical threshold after which the last-remaining healthy photoreceptors become affected and eventually died [101]. This model may also explain the long-term preservation of cones in the fovea of patients with rod-initiated **rod-cone dystrophies** [241], or in the cone-rich area centralis in canine models of retinal dystrophies [268], (Petit L. *et al*. in preparation). As well, it could explain why it is not uncommon to see "islands of cones remaining among rivers of degeneration" in animal models of **rod-cone dystrophies** [269], [270], (Petit L. *et al*. in preparation).

III.5.2.2. Loss of rods may affect the structural support of cones

How loss of the main proportion of photoreceptors could contribute to the secondary death of the healthy neighboring cells? One first hypothesis is the loss of structural support due to the collapse of the ONL. However, this hypothesis ignores that the apical processes of Müller cells envelop cone inner segments from early stages of rod cell death and that new junction complexes are formed between Müller and cones to firmly anchor the remaining cones to the outer limiting membrane [255] (Petit L. *et al*. in preparation).

III.5.2.3. Loss of rods may elevate oxidative stress in cones beyond the oxidant capacity of the cells

Another possible explanation for the slowly progressive death of cones after the death of rods is oxidative damage. Choroidal vessels are not subject to auto-regulation by tissue oxygen levels. After the dysfunction and loss of rods, which represent 95% of the photoreceptors and consume the majority of oxygen delivered to the outer retina, it is argued that the level of oxygen in the retina increases sharply. Oxidative stress in cones can

elevate beyond the antioxidant capacity of the cells, leading to the slow accumulation of oxidative damages in cones. This theory would explain why the peripheral retina, with its higher rod:cone ratio is the first affected in patients with rod-initiated **rod-cone dystrophies**, while the cone-exclusive fovea is not affected until very late stages of the disease.

Preliminary signs of oxygen toxicity

The narrowing of retinal vessels after rod death, due to their auto-regulation and constriction when tissue levels of oxygen are high, is consistent with high levels of oxygen in degenerated retinas. In addition, the average oxygen level significantly increases in the outer retina of rodent models of **rod-cone dystrophies** as rods degenerate [271, 272].
Photoreceptor cells are under constant environmental and intrinsic challenges that make them highly susceptible to oxidative stress (**Chapter 1**). Furthermore, hyperoxia leads to photoreceptor cell death in mice [273, 274]. These observations significantly emphasize the potential deleterious effects of high oxygen levels and oxidative stress to photoreceptors. Nevertheless, demonstrating that oxidative stress is the causative factor in secondary cone death is challenging.

Exogenous antioxidants delay cone death

Markers of lipid peroxidation and oxidative damage were evident in degenerating cones in a transgenic pig model of rod-initiated **rod-cone dystrophy** [275] and the *rd1* mouse [276], but it does not constitute a proof. More convincing, the systemic injection of exogenous antioxidant(s) at the onset of cone cell death delayed significantly M cone dysfunction and degeneration in the *rd1* mouse. This was associated with reduced markers of oxidative damage in *rd1* cones until P35 (the duration of the study) [276]. Similar results were obtained in the *rd10* and the transgenic Q344X mice [105].

Modulation of the endogenous antioxidant system delay cone death

Increased expression of components of the endogenous antioxidant defense system also reduced markers for oxidative damage, reduced cone cell loss and preserved cone function in the *rd10* mouse [277], [278]. These components did not cause an apparent reduction on rod death, indicating that they not acted by non-specifically slowing rod apoptosis. In the *rd1* and Q334X mice, similar results were obtained with systemic inhibition of NADPH oxidase, a cytoplasmic enzyme known to generate reactive oxygen species and expressed in photoreceptor inner segments (and also in ganglion, RPE and microglial cells) [279]. These results support a role of oxygen toxicity in secondary cone death. Nevertheless, cone-specific modulation of the antioxidant system would be desirable to confirm this hypothesis.

III.5.2.4. Loss of rods may disturb cone nutrition

Recently, it was proposed that cones have a nutrient shortage and/or imbalance in metabolism due to a change in retinal architecture [101], [29].

Phosphorylated mTOR is reduced in cones at early stages of cone degeneration

In a pioneer study, Punzo *et al*. evaluated changes in gene expression at the onset of cone death in four different mouse models of rod-initiated **rod-cone dystrophy** (among them the *rd1* mouse) [101]. In each of these models, the major phase of cone death was linked to upregulation of metabolic genes, as well as genes of the insulin/AKT/ mammalian Target of Rapamycin (mTOR) pathway, a key regulator of cellular metabolism [101].

mTOR serves as a signaling regulator, gathering information about the environment and helping the cell to decide whether it has enough nutrients to make new proteins. The activity of mTOR is controlled by nutrient availability, energy levels and growth factor signaling. When cellular energy levels are high, mTOR is phosphorylated and allows energy-consuming processes such as translation and prevents autophagy. In contrast, during nutrient deprivated conditions, mTOR is not phosphorylated and prevents energy consuming processes and autophagy may occur.
The authors found that phosphorylated (activated) mTOR was reduced in cones at the early stages of cone degeneration. In addition, the surviving cones had signs of autophagy and molecular marks of cellular starvation. Formation of autophagic vacuoles in dying cones was also observed in the *rd10* mouse [195] and in retinal tissues of human patients with extensive rod degeneration [280]. Thus, it was hypothesized that degeneration of cones is related to metabolic deregulation and/or shortage of nutrients [101].

Cones were not getting enough glucose

Further experiments suggested that the cones were not getting enough glucose after rod death. Indeed, cones overexpressed glucose transporter that allows the cell to take up more glucose. In addition, cone survival was prolonged for 4 weeks after systemic injection of insulin to stimulate the insulin/AKT/mTOR pathway and trick cones into thinking they had enough glucose.

Punzo *et al*. hypothesized that starvation in cones is due to the reduction in glucose flow from the RPE cells. In particular, they suggested that cones could be dependent on rod outer segments-RPE interactions to properly interact with RPE. Loss of 90% of outer segments-RPE breaching could represent the critical threshold by which cone-RPE interactions collapse and nutrient flow is disrupted [101], [194].
An alternative hypothesis is that metabolic function of RPE cells is impaired by the massive loss of rods. For example, it was recently demonstrated that oxidative stress leads to

subcellular redistribution of glucose transporter in a RPE cell line [208]. It could be of major interest to explore the molecular changes that occur in RPE cells during **rod-cone dystrophy**.

Consistent with the idea of reduced glucose in cones is cone dysfunction and reduced cone outer segment length. Indeed, cones use the majority of the glucose transported by the RPE to fuel lipid, protein and NADPH biosynthesis. Nevertheless, the lactate released by Müller cells could be used to produce high levels of ATP require for photoreceptor function [29], [195]. In addition or alternatively, ATP levels can be balanced by increased divergence of glucose to the Kreb Cycles (that produces 18 fold more ATP than glycolysis). It might explain why cones survive for extended periods in **rod-cone dystrophies** even in the absence of any outer segments. While glucose is limited in sleeping cones, ATP levels are not, allowing cones to survive. Consistent with this, cones suffer from autophagy, an energy-consuming process that provides nutrients but will consume more ATP that it can produce by degrading intracellular components.

However, sleeping cones are not as far out of troubles. The loss of outer segment is associated with opsin mislocalization to the inner segment. In addition, cones remain in a stressful environment due to high levels of oxygen. The endogenous antioxidant protective system of cones is limited (because NADPH, a critical antioxidant, and maybe RdCVF levels are limiting). Consequently, sleeping cones slowly die overtime, a process that could occur (at least) by necrosis [195].

CHAPTER **IV**

PROGRESS AND CHALLENGES TOWARD RESTORING PHOTORECEPTOR EQUILIBRIUM BY GENE ADDITION THERAPY

Many of the genes involved in inherited retinal dystrophies have now been identified and their function elucidated (**Chapter 2**), providing a major step towards the understanding of disease pathogenesis (**Chapter 3**). It is logical to ask how we can use this knowledge to correct the disease. One attractive solution for inherited recessive disorders is gene addition therapy, e.g. the correction of the genetic defect in affected cells. The theoretical hope of gene addition therapy is that addition of the wild-type cDNA of the disease gene would eliminate/alleviate the genetically induced stress and result in the preservation of photoreceptors.

Gene addition therapy in animal models RPE65-associated **LCA** has already been translated to human clinical trials with encouraging results. Treatment for the majority of inherited photoreceptor dystrophies in which the genetic defect lead to rapid degeneration of the photoreceptors, however, has not yet moved from proof-of-concept to the clinic.

In this chapter, we will examine the achievements in retinal gene addition therapy, and discuss the challenges to extrapolate the results to other forms of inherited retinal degenerations, in particular to severe photoreceptor diseases. These challenges include (i) the use of gene delivery vectors that efficiently transduce the outer retina, (ii) studies of the natural history of the diseases so that appropriate outcome measures can be planned regarding both photoreceptor dysfunction and degeneration components, and (iii) the requirement for testing new therapies in large animal models of photoreceptor defects with high cone:rod ratio and relevant photoreceptor density and distribution.

Contents

IV.1. Gene therapy for retinal diseases

To date, there is no effective treatment for inherited retinal dystrophies, but there are several lines of therapeutic approaches that hold promise. Among them, gene therapy (i.e. the use of genes as therapy) is an attractive therapeutic approach to cope with retinal dysfunction and photoreceptor death [281], [282], [283], [284].

IV.1.1. The theoretical advantages of gene therapy

Gene therapy takes advantage of the host machinery to locally produce bioactive substances. A nuclei acid is delivered to a target cell via a gene delivery system. The nuclei acid can directly bind the host sequences. Otherwise, the target cell can transcribe the delivered DNA to produce RNA that is itself active, or that will be translated into a specific protein. Therefore, one significant advantage of gene therapy over pharmacological therapy is that therapeutic levels can be maintained without the need for re-injection if delivered DNA remains stable. In addition, the combination of appropriate gene delivery vectors and cell-specific promoters can limit expression of a therapeutic gene (and thus protein) to the desired target cells, which is rarely possible even with local drug delivery methods.

IV.1.2. The retina is an ideal target tissue for gene therapy

The retina is particularly well suited as a target organ for gene therapy. The retina is easily accessible for surgical injection of gene delivery vehicles. Intravitreal injection releases gene delivery systems in the vitreous, at proximity of ganglion and amacrine cells. Subretinal injection deposits gene delivery systems in the subretinal space, between RPE and photoreceptor cells.

The eye is small and highly compartmentalized. It allows high vector concentrations in retinal cells after injection of relatively modest amounts of therapeutic vector. This compartmentalized anatomy limits systemic dissemination of the vector and reduces the risk of systemic adverse effects. It addition, subretinal injection allows a long contact time of the vector with the target cells.

The subretinal space has a relatively high degree of immune privilege. Tight junctions that form the blood-retina barrier separate the subretinal space from the blood supply, thus protecting it from most immune responses against gene products and/or vector antigens [281].

Another advantage for retinal gene therapy is that the target cell population (mainly the photoreceptors and the RPE cells) is post-mitotic. The lack of cell division allows the use of

non-integrating vector systems, limiting the risk of malignant transformation. Transgenes are not diluted in cell division.

Moreover, optical transparency of the intraocular structures and the neurosensory retina enable safe visualization of reporter gene expression and evaluation of gene therapy outcomes by non-invasive methods such as ophthalmoscopy, funduscopy, OCT and ERG.

Finally, as mammals have two eyes, the injection of only one eye allows the second uninjected eye to serve as a valuable internal control for experimental interventions. Although it is not possible to mask examiners to the treated eye versus the untreated eye after subretinal injections, unilateral injections are important to assess inter-individual and inter-examination variations. Retinal dystrophies are often symmetric in term of disease onset and progression.

IV.1.3. Gene therapies approaches for inherited retinal dystrophies

IV.1.3.1. Specific gene therapy is used to correct the causal gene defect

As the etiology of numerous forms of inherited retinal dystrophies has been now solved, one line of retinal gene therapy is to correct the primary gene defect in order to restore normal cell physiology and ameliorate the progression of the disease. This strategy is called “specific gene therapy”[282].

Loss-of-function mutations: For loss-of-function mutations (which typically show recessive or X-linked patterns of inheritance) specific gene therapy involves the introduction and expression of a functional allele of the defective gene into the appropriate cells, in order to correct the insufficiency or lack of functional wild-type protein. This approach is called gene *addition* therapy (provision of a new function).

Dominant-negative mutations: For dominant-negative mutations (which typically show dominance patterns of inheritance) specific gene therapy involves the introduction and expression of additional functional alleles into affected cells to overexpress the functional wild-type protein and compete with the mutant protein. This strategy is called gene *supplementation* therapy (provision of a supplement).

Toxic gain-of-function mutations: For dominant toxic gain-of-function mutations, the toxic effects of the abnormal gene product have to be reduced by silencing the mutant allele. It is gene *silencing* therapy. Several strategies exist to silence the mutant allele, including mutation-specific ribozymes or interference RNA. However, to circumvent the mutational heterogeneity among patients, the most commonly approach is to use mutation-independent *silencing* that will suppress both mutant and wild-type alleles (by targeting the promoter for

example), and to provide a suppression-resistant *replacement* gene (engineered using codon-redundancy or intragenic polymorphisms).

As most retinal degenerations caused by dominant genes cannot be addressed by single gene intervention, monogenic recessive dystrophies are the most suited diseases to specific gene therapy. For these recessive diseases, specific addition therapy is the most logical and very attractive curative approach. Nevertheless, specific gene therapy can only be applied when the cell type expressing the mutated alleles is still alive [285]. Consequently, early diagnosis and treatment in childhood may be necessary in the case of rapid photoreceptor degenerations. Another challenge of specific gene therapy is the large number of different genes that are involved and would need to be targeted individually in each group of patients [51], [9], [43], [286].

IV.1.3.2. Generic gene therapy is used to overcome the causal gene defect

For disorders that cannot be addressed by specific gene therapy (causative gene non identified, multigenic disorders,...) non-specific approaches of gene therapy have been developed [287], [288], [289]. Generic gene therapy involves the introduction of a gene that that is not primarily implicated in the pathogenesis of the disease but whose expression can ameliorate the clinical phenotype. Three different approaches are currently considered:

(i) Gene-based blocking of photoreceptor apoptosis: Genes encoding anti-apoptotic factors can be introduce to photoreceptor and/or RPE cells to interfere with the process of photoreceptor apoptosis[290].

(ii) Gene-based photoreceptor protection: Retinal cells can be transduced to provide long-term production of trophic factors, calcium channel antagonists or antioxidant enzymes to slow down photoreceptor degeneration. The idea behind neuroprotection is to raise the threshold required for the initiation of apoptosis, so that photoreceptor death is delayed or less frequent [288], [289]. This approach is particularly relevant when direct toward protection of cone function in **rod-cone dystrophies** because the slow time course of visual loss means that even a relatively subtle slowing of the process may be sufficient to preserve useful vision for the patient's lifetime [287].

***(iii) Gene-based restoration of visual perception*:** Finally, genes encoding light sensitive ion channels or opsins can be introduced into retinal cells to reactivate the endogenous retinal circuit and/or restore visual perception [285], [287], [289]. Several strategies targeting sleeping cones [45], ON-bipolar cells [291], [292] or ganglion cells [293], [294], [295], [296], [297], [298], [299], [300] are currently under development. One advantage of this approach is that it is applicable for late presentation (e.g. photoreceptor cell death nearly complete).

However, the genetic defect is not corrected in generic gene therapy. Thus, one common challenge of generic therapies it that the benefic effect is maintained for a relevant period of time, and is not disrupted by continuing cellular stress.
To date, there is still little evidence that a generic treatment may strongly influence the long-term progression of genetic retinal degenerations, despite several studies have provided encouraging results [301], [302].

As majority of inherited retinal dystrophies are caused by loss-of-function mutations acquired by recessive or X-linked inheritance, gene addition therapy will be the main focus of this chapter. The reader is directed to other recent reviews for in depth coverage of gene therapy for dominant retinal dystrophies [303], [304], gene-based neuroprotection of the photoreceptors [288] and optogenetic therapies for retinal disorders [285], [287], [289].

IV.2. Gene addition therapy for recessive inherited retinal dystrophies

IV.2.1. Gene transfer to the outer retina

Step one in designing a gene addition therapy for retinal diseases is to make sure that the vector system would target efficiently and/or specifically the appropriate cells. The key of transduction relies on two components: (i) the choice of an appropriate vector that permits efficient delivery of the nucleic acid in the target cells (ii) the choice of appropriate expression-restricting elements as promoter that determine the cell specificity and level of transgene expression. The great majority of inherited retinal dystrophies are caused by gene defects affecting the photoreceptors, and several other forms are caused by defects in the RPE. Therefore, the outer retina is the primary target site for gene addition therapy.
It is important that the vector system targets the photoreceptors and/or the RPE cells in stable manner, as most inherited retinal dystrophies take place over decades in humans. Transgene expression must also peak within the therapeutic window. In addition, the ideal vector delivery system should have low immunogenicity and not cause toxicity.

IV.2.1.1. Systems to evaluate expression patterns of vector systems

Studies investigating expression patterns of vector systems (tropism for specific cell subtypes, onset of gene expression, efficiency of expression, intensity of expression of the transgene duration of expression and toxicity) provided critical information for the design of gene addition therapy approaches.
These studies have largely involved marker systems with GFP (green fluorescent protein) or LacZ (encoding β-galactosidase), and *in vivo* application in animal models. Indeed, cell lines in culture often show different expression patterns than the analogous cells *in vivo*. In addition, *in vitro* experiments cannot be used to evaluate the variables that determine stability of gene expression and toxicity of therapy.

Alternatively, it has been recently proposed to use *ex vivo* explants of mammal retina for validation steps [305], [306]. Compared with monolayer culture, *ex vivo* tissue retains a normal tissue architecture and intact network activity. *Ex vivo* retinal explants could thus provide important information concerning comparative efficacies in cell targeting with different vector systems. Nevertheless, *ex vivo* retinal explants can be kept in culture for only 2 to 3 weeks of age, which can limit the use of vector systems that require more time for efficient transduction Busskamp, 2010 #161). In addition, *ex vivo* experiments are not relevant for safety and biodistribution assessments.

The most common animal model used for validating steps is the mouse. Indeed, accurate screening of vectors can be done quickly and efficiently in mice rather than in large animals (such as pigs, dogs and non-human primates) that are more expensive. By the large, the pattern of gene expression with regard to cellular tropism is similar in different species, but it not always the case. For example, the mouse has a very thin inner limiting membrane compared to large mammals, which could modify the tropism of the vectors after intravitreal injection [307]. In addition, only primates have a cone-rich macula and a cone-only fovea.
Large animal models are particularly useful in establishing efficacy and safety parameters prior to human trials. The large size of their eye allows the use of surgical maneuvers that are similar to those used in humans. In addition, they more closely resemble humans with respect to anatomy and host immune responses [166].

IV.2.1.2. Viral vectors are currently the most favored vectors for retinal gene transfer

Several systems are available for retinal gene transfer, but not all meet the criteria mentioned above. Vectors based on viruses are currently the most commonly used vectors for retinal gene transfer. One principal reason is that nonviral systems (as naked DNA, DNA complexed with cationic lipids or with polymers, DNA compacted in nanoparticles) typically provide poor transduction efficiency and transient gene expression. However, new improvements of nanoparticle-mediated gene transfer have been recently reported, with respect to intensity and duration of expression [308], [309]. For example, subretinal injection of VMD2-h*RPE65* complexed nanoparticles in the *Rpe65*$^{-/-}$ mouse was shown to lead to stable transgene expression and phenotypic improvements for at least 15 months postinjection [310].

IV.2.1.3. Adenoviral and lentiviral vectors are interesting to target RPE cells

Adenoviral vectors: Adenoviral vectors have the advantages to carry large inserts (up to 36kb) and to be non-integrative vectors (their genome persist as episomes in host cells). In

the mouse, they are able to transduce efficiently RPE and Müller cells after subretinal injection.

In contrast, high levels of photoreceptor transduction are only seen during retinal development and not in the post-mitotic adult retina [311]. As human photoreceptors are fully developed at birth, this significantly limits the relevance of adenoviral vectors for treating primary photoreceptor defects. In addition, adenoviral vectors suffer from significant immune responses due to the expression of viral genes in transduced cells. Thus, adenovirus-mediated gene expression is generally associated with cytotoxic removal of transduced cells, rapid loss of transgene expression and long-term toxicity.

Despite these limitations, one study has reported that adenovirus-mediated gene transfer provided short-term preservation of photoreceptors in the neonatal *rd1* mouse [312]. More convincing, but still moderate, therapeutic effect was obtained in the same model with a gutless adenoviral vector that was deleted of all viral coding sequences to avoid the immune responses to adenoviral proteins (subretinal injection at P5)[313]. Nevertheless, modification of adenoviral vector penton base has recently improved photoreceptor transduction after subretinal injection in adult mice (antibodies raised against GFP were not necessary to detect GFP in the photoreceptors) [314], [315]. This new result highlights the interest to pursue the evaluation of adenovirus as viral vectors for photoreceptor disorders.

Lentiviral vectors: Lentiviral vectors are RNA retroviruses with a cargo capacity of about 10kb. They can be developed from the human immunodeficiency virus [316], simian immunodeficiency virus (SIV), feline immunodeficiency virus (FIV) or equine infectious anemia virus (EIAV). Lentiviral vectors have been widely used for retinal gene therapy as they provide efficient, sustained, and nontoxic gene transfer to RPE and Müller cells after subretinal injection [317]. They have been effective in animal models of RPE diseases, including a murine [318] model of RPE65-linked **LCA** and a rat model of recessive **rod-cone dystrophy** due to MERTK mutations [319].

Photoreceptor transduction by lentiviral vectors is however less robust. Indeed, as for adenoviral vectors, photoreceptor transduction by lentiviral vectors is inversely correlated to photoreceptor differentiation. In one study, HIV vector pseudotyped with vesicular stomatitis virus surface protein VSV-G (which recognizes a ubiquitous phospholipid in the cell membrane) was shown to transduce photoreceptors in adult rats, but the levels of transduction were sporadic [320], [321].

Vectors based on EIAV have been reported to be more efficient at transduction of photoreceptors in adult primates [322], [323] (Zallochi ML et al. Poster 489-D1136, ARVO 2011). However, transduction pattern was also variable and antibodies raised against GFP have been used to allow detection of transgene expression [322]. Nonetheless, these results have set the basis to the development of two ongoing clinical trials for Stargardt and Usher syndromes using lentivirus vectors, despite the apparent failure of lentivirus-mediated

transduction of photoreceptors (the target cells in those clinical trials). The results of these trials are not yet available (Oxford BioMedica, NCT01367444 and NCT01505062).

IV.2.1.4. rAAV vectors are interesting to target RPE and/or photoreceptor cells

Over the last decade, AAV-based vectors have emerged as excellent gene transfer tools for retinal disorders because of (i) their ability to efficiently and stably transduce both RPE and photoreceptors after subretinal injection, (ii) their low immunogenicity when injected in the eye and (iii) their excellent safety profile [324].

AAV virus*:*

AAV is a small, non-envelop, single-stranded DNA Dependovirus that belongs to the family of *Parvoviridae*. It is a naturally replication-defective virus and requires "helper" functions for productive injection, usually provided by adeno- or herpes viruses. The 4.7 kb AAV single strand DNA is composed of two open reading frames, the *REP* and *CAP* genes, encoding four replication proteins [325] and three capsid structural proteins (VP1, VP2 and VP3), flanked by two 145 bp inverted terminal repeats (ITRs). The genome is enclosed in a capsid with icosahedral symmetry (**Figure 18a**).

To date, over 120 different natural capsid variants of AAV have been identified and thousands of laboratory-generated capsid variants have been created through rational mutagenesis or selected by directed evolution. Interestingly, capsid variations determine the host cell tropism of the vector by influencing the recognition of host cell surface cell receptors and co-receptors. The AAV capsid also affects intracellular processes related to AAV trafficking and uncoating, and is thus the primary player in transduction kinetics and intensity of transgene expression [324].

rAAV vectors:

Recombinant AAV vectors (rAAV) used for gene therapy are derived from the wild-type virus by deletion of the entire viral coding region and insertion of the expression cassette between the AAV ITRs (**Figure 18b**). Recombinant AAV vectors are gutless vectors.

Cell type expression patterns can be obtained using cell-specific promoters and by modifying the AAV capsids. Consequently, the majority of rAAV vectors used for gene therapy are pseudotypes, containing the transgene flanked by the ITRs of AAV2 within capsids from other AAV serotypes. They are referred to as rAAV2/n, where the first number indicates the origin of the ITRs and the second number the origin of the capsid (**Figure 18b**).

Recombinant AAV vectors are easy to produce. Their genome rarely integrates in the host cell genomes (events not yet evaluated in the retina) and persists in the host cells as stable episomal DNA aggregates. Therefore, rAAV-mediated transgene expression can be very efficient and stable for long periods in non-dividing cells.

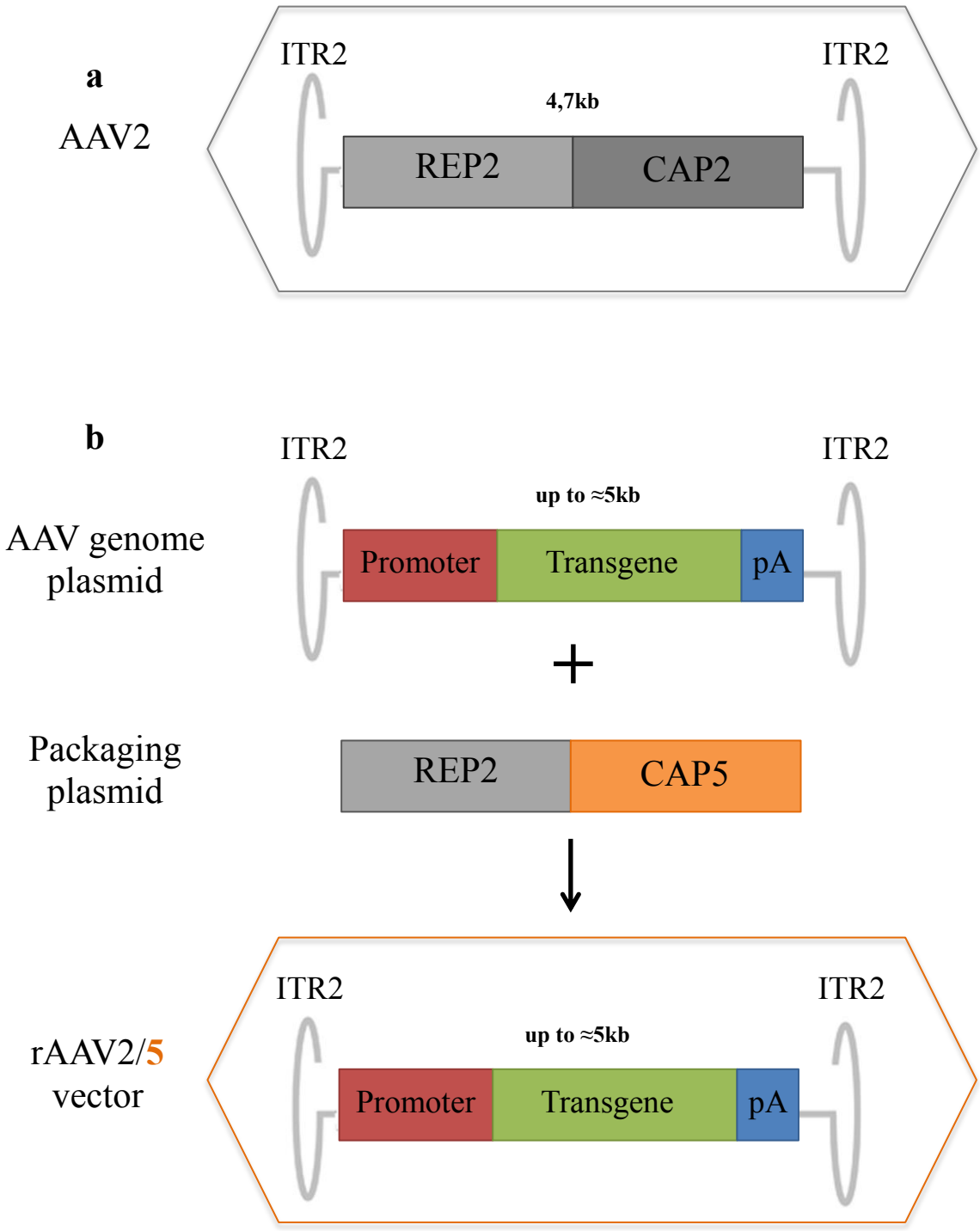

Figure 18. **Adeno-associated virus (AAV)-based vectors** (**a**) Wild-type AAV2 virus. AAV2 contains a single-stranded DNA genome of 4,7kb. The inverted terminal repeats [326] are necessary for conversion of the single-stranded genome to double-stranded DNA and packaging. The products of *REP* and *CAP* genes are necessary for replicating the AAV genome and for producing an AAV particle. (**b**) Recombinant AAV vector. Construction of a rAAV involves deleting the AAV coding sequences and replacing them with a transcription cassette containing the gene of interest and regulatory elements such as a promoter and a poly-adenylation signal. Assembly of the vector then requires supplying *REP* and *CAP* genes (and helper functions, not shown here).

Transduction:

The ability of rAAV serotypes to transduce the outer retina has been extensively documented using vectors encoding marker proteins in small and large species, mostly in wild-type animals. At present, at least nine standard rAAV serotypes have been evaluated (rAAV2/1 to rAA2/9), as well as several engineered rAAV serotypes. The specificity and the efficacy of outer retina transduction depend not only on the viral capsid, but also on the route of administration (subretinal or intravitreal) and the site of delivery within the retina [327], [324].

Outer retina transduction after subretinal injection: With the exceptions of rAAV2/3 that does not transduce retinal cells and rAAV2/6 that transduces RPE poorly [328], subretinal injection of all tested natural rAAV serotypes result in very efficient transduction of RPE cells (usually 100% of transduction in the area of subretinal detachment). In particular, rAAV2/4 is RPE-specific in the rat, the dog, and the non-human primate [329] (**Table 7**).

Interestingly, pseudotypes 2/2, 2/5, 2/7, 2/8 or 2/9 also mediate sustained transduction of 20 to 80% of the photoreceptors [324]. New AAV serotypes isolated from porcine tissues also demonstrate an attractive ability to transduce both RPE and photoreceptors in the mouse, and to a lesser extent in the pig [330], [331]. Less convincing photoreceptor transduction has been obtained using rAAV with chimeric capsids in the mouse retina [332] (**Table 7**).

Small [333], [328] and large [334], [335], [336] animal studies have demonstrated that rAAV2/5 or rAAV2/8 have higher photoreceptor transduction efficiencies and mediate more rapid onset of transgene expression than rAAV2/2.

In the mouse, rAAV2/8 and rAAV2/7 mediate 6-8 fold higher levels of photoreceptor transduction than rAAV2/5. Recombinant rAAV2/8 and rAAV2/9 also transduced higher number of cones (75%) than rAAV2/5 (35%)[337].

In the pig, rAAV2/8 mediates 3 and 1 fold higher levels of photoreceptor transduction than rAAV2/5 and rAAV2/9, respectively. However, all serotypes have comparable efficiency in transducing porcine cones in the cone-rich *area centralis* (cone : rod ratio = 1:3).

In the non-human primate, rAAV2/7, rAAV2/8 and rAAV2/9 mediate similar levels of photoreceptor transduction but rAAV2/9 transduced higher number of cones than other serotypes in the periphery (40% versus 10%) and perifovea (60% versus 20%). However, only rAAV2/9 was able to transduce the parafoveal cones (10%). The normal arrangement and ratios of cone and rod photoreceptors across the retina can thus be important variables affecting photoreceptor transduction.

To date, there is no side-by-side comparison of the efficiency of rAAV2/5 and rAAV2/8 for cone transduction in the non-human primate, but rAAV2/5 has been shown to efficiently transduce rods, foveal and parafoveal cones in the macula of monkeys [338]. Similarly, the efficacy of rAAV2/5, rAAV2/7, rAAV2/8 and rAAV2/9 for cone and rod transduction has not been yet compared in the dog.

Cell tropism of rAAV vectors across species after subretinal injection					
rAAV	**Rodent**	**Dog**	**Pig**	**NHP**	**References**
rAAV2/1	RPE, PR(few)	RPE	nd	nd	Auricchio et al. (2001) Acland et al. (2005)
rAAV2/2	RPE, PR, HC, MC, GC	RPE, PR (Rods + Cones)	nd	RPE, PR (Rods)	Ali et al. (1996) Bennett et al. (1999) Auricchio et al. (2001) Acland et al. (2001) Yang et al. (2002) Weber et al. (2003) Bainbridge et al. (2003) Vandenberghe et al. (2012, 2013) Charbel et al. (2013)
rAAV2/3	None	nd	nd	nd	Yang et al. (2002)
rAAV2/4	RPE	RPE	nd	RPE	LeMeur et al. (2007)
rAAV2/5	RPE, PR (Rods + Cones), MC (few)	RPE, PR (Rods + Cones), MC (few), HC (few)	RPE, PR (Rods + Cones), MC (few)	RPE, PR (Rods + Cones)	Auricchio et al. (2001) Yang et al. (2002) Lotery et al. (2003) Weber et al. (2003) LeMeur et al. (2007) Alloca M et al. (2007) Mancuso et al. (2007) Peterson-Jones et al. (2009) Mussolino et al. (2011) Boye et al. (2012) Manfredi et al. (2013) Charbel et al. (2013)
rAAV2/6	RPE, PR (few)	nd	nd	nd	Yang et al. (2002)
rAAV2/7	RPE, PR (Rods + Cones)	nd	nd	RPE, PR (Rods + Cones)	Allocca et al. (2007) Vandenberghe et al. (2013)
rAAV2/8	RPE, PR (Rods + Cones) , INL,MC, GC	RPE, PR (Rods + Cones), INL, GC	RPE, PR (Rods + Cones), MC (few)	RPE, PR (Rods + Cones)	Stieger et al. (2008) Vandenberghe et al. (2012, 2013) Allocca et al. (2007) Natkunarajah et al. (2008) Mussolino et al. (2011) Manfredi et al. (2013)
rAAV2/9	RPE, PR, INL, MC (Rods + Cones)	nd	RPE, PR (Rods + Cones)	RPE, PR (Rods + Cones)	Allocca et al. (2007) Vandenberghe et al. (2013) Manfredi et al. (2013)
rAAV2/rh.43	RPE, PR (Rods + Cones)	nd	nd	nd	Allocca et al. (2007)
rAAV2/rh.64 R1	RPE, PR (Rods + Cones)	nd	nd	RPE, PR (Rods + Cones)	Allocca et al. (2007) Vandenberghe et al. (2013)
rAAV2/hu.29 R	RPE, PR (Rods + Cones)	nd	nd	nd	Allocca et al. (2007)
rAAV2/rh.8R	nd	nd	nd	RPE, PR (Rods + Cones)	Vandenberghe et al. (2013)
rAAV2/po1	RPE, PR (Rods + Cones)	nd	RPE, PR (Rods + Cones)	nd	Bello A. et al. (2009) Puppo et al. (2013)
rAAV2/po2.1	RPE, PR (few)	nd	nd	nd	Puppo et al. (2013)
rAAV2/po4	RPE, PR	nd	RPE, PR (few)	nd	Puppo et al. (2013)
rAAV2/po5	RPE, PR (Rods + Cones)	nd	RPE, PR (Rods + Cones)	nd	Puppo et al. (2013)
rAAV2/po6	RPE, PR (few)	nd	RPE, PR (few)	nd	Puppo et al. (2013)
rAAV2/8 Y733F	RPE, PR, INL, MC	RPE, PR (Rods + Cones), INL, GC	nd	nd	Petrs-Silva et al. (2009) Mowat et al. (2013)
rAAV2/2 Y444F	RPE, PR, INL, GC	nd	nd	nd	Petrs-Silva et al. (2009)
rAAV2/9 Y446F	RPE, PR, INL	nd	nd	nd	Petrs-Silva et al. (2009)
rAAV2/Rec2	RPE, PR, MC (few)	nd	nd	nd	Charbel et al. (2013)
rAAV2/Rec3	RPE, PR	nd	nd	nd	Charbel et al. (2013)

The serotype of rAAV vectors also determined the kinetics of transgene expression after subretinal injection. For example, in the mouse, the onset of GFP expression in photoreceptor cells, as assessed by indirect ophthalmoscopy, is evident at 3 days after subretinal injection of rAAV2/8, at 4-5 days after injection of rAAV2/5 and 2/7, and at 11 days after injection of rAAV2/9 [337]. Recombinant AAV2/8 requires 1-2 weeks to reach maximal expression levels, whereas maximal transgene expression is seen at 2-4 weeks after subretinal injection of rAAV2/5. For rAAV2/2, this delay can be 4-6 weeks in the dog, and as long as 6-8 weeks postinjection in non-human primates [339].

Subretinal injection of rAAV2/2, rAAV2/5 and rAAV2/8 vectors have been used in gene therapy studies in rodents and/or canine models of inherited retinal dystrophies (caused by a genetic defect in cones and/or rods)[284]. Recombinant AAV2/5 has been used successfully in a non-human primate model of achromatopsia [170].

***Outer retina transduction after intravitreal injection*:** Efficient transduction of the outer retina following intravitreal injection could be a safer and less invasive technique, allowing a more widespread and homogeneous transgene expression. However, natural rAAV serotypes cannot efficiently transduce the outer retina after intravitreal injection [340] because the inner limiting membrane and neuronal and glial cells of the inner retina form a diffusive barrier with abundant binding sites for rAAV particles [307].

The development of mutant rAAV variants by mutagenesis of the viral capsid proteins has increased the efficiency of transduction and penetration of the vectors across the neuroretina. In particular, mutagenesis of specific capsid tyrosine residues, which limits rAAV intracellular ubiquitination and degradation (rAAV2-4YF), has allowed higher outer retina transduction from the vitreous in the mouse [341],[342]. However, it remains to be seen if these vectors are effective in large models where the delivery method and the inner limiting membrane are different.

Further improvement have involved *in vivo*-directed evaluation to engineer AAV variants able to target the outer retina from the vitreous [343]. A new variant (7m8) enabled substantially more photoreceptor and RPE transduction than rAAV2-4YF control in mice and in the fovea of non-human primates. More interestingly, this vector drived therapeutic level of transgene expression in the *Rs1h*$^{-/-}$ mouse model of **retinoshisis** (genetic defect in photoreceptor) and partially rescued the phenotype of the *rd12* mouse model of RPE65-**LCA** [343].

Safety:

AAV has never been shown to cause disease in humans or animals. It is mainly not toxic and it not associated with deleterious immune responses when injected in the eye.

In dogs, subretinal injection of AAV2/2-CMV-GFP, AAV2/4-CMV-GFP and AAV2/5-CMV-GFP (1,5-4.10^{11} vector genomes) has resulted in stable transgene expression up to 6 years postinjection [334], (Rolling F, unpublished data), in the absence of notable alterations of retinal anatomy and function. Similarly, in pigs, delivery of 1.10^{10} vector genomes of AAV2/5-CBA-eGFP or AAV2/8-CBA-eGFP has not been associated with ERG and morphological abnormalities at 6 weeks postinjection [326]. As well, in the non-human primate, delivery of up to 10^{10} vector genomes of AAV2/2-CBA-eGFP, 10^{10} vector genomes of AAV2/8-CBA-eGFP and 6.10^{10} vector genomes of AAV2/5-RK-GFP have been well tolerated [336], [338].

In human trials, safety of rAAV2/2-mediated gene therapy has been demonstrated in over 30 patients with *RPE65*-linked **LCA** (maximum reported dose: 1,5.10^{11} particles per eye)[344]. The longest follow-up is to date more than 3 years [282], [284]. No sustained inflammatory response has been attributed to rAAV vectors. Only minimal adaptive humoral response to the AAV2 capsid has been detected in two patients with transient increase of neutralizing antibodies in the serum. No notable cellular response to the vector or transgene product has been reported.

However, recent animal studies have highlighted the potential importance of determining dose-limiting toxicity. In the dog, subretinal injection of more than 2,3.10^{12} vector genomes of AAV2/5-RK-GFP or 7,2.10^{12} vector genomes of AAV2/5-CBA-GFP results in cone toxicity [345]. Similarly, in the non-human primate, subretinal injection of 1.10^{12} vector genomes of AAV2/2- or AAV2/8-CBA-eGFP is associated with histopathological evidence of inflammation and retinal degeneration [336].

These toxic or inflammatory responses probably reflect the high level of GFP expression in the RPE and/or photoreceptor cells. Indeed, GFP is toxic for retinal neurons at high doses (Rolling F. unpublished data). The delivery of 2,7.10^{13} vector genomes of AAV2/5-PR2.1-L-opsin restores cone function in dichromatic squirrel monkeys for more than 2 years, without sustained toxicity [170]. As well, doses of rAAV2/5 or 2/8 vectors from 1.10^{11} to 3.10^{12} vector genomes delivered are efficient in canine models of photoreceptor dystrophies [346], [347], [110], [348], with stable therapeutic effects recorded up to 36 months postinjection (Petit L, *et al*. unpublished data).

Another safety concern for retinal gene therapy using viral vectors could be vector biodistribution after intraocular delivery. Importantly, after subretinal or intravitreal injection, rAAV sequences are not detected in distant organs such as the liver or the gonads, indicating that widespread dissemination of the vector is minimal at the rAAV doses currently used [349], [350], [351], [326], [336], [338].

After subretinal injection, rAAV2/4 and rAAV2/5 sequences have been only detected in the optic nerve of injected dogs [350], pigs [326] and primates [350] [338]. In all cases, despite detection of genomes, no transgene expression has been observed outside the retina.
In contrast, after subretinal injection of rAAV2/8 in the rat, the dog and the non-human primate, vector DNA and sustained levels of GFP protein have been found in the lateral geniculate nucleus. In the dog, GFP-positive cells have been identified as ganglion cells axon projections and neurons of the lateral geniculate nucleus, suggesting that rAAV2/8 transport along neurons of the visual pathway is possible [351]. However, the NeuN marker used to specifically label brain neurons also labeled some subtypes of canine ganglion cells (Tshilenge K., Rolling F. *et al*. unpublished data). Furthermore, no GFP-positive cells have been observed after the first synapse in the rat and in the non-human primate retina [336]. No transgene expression in optic nerves has been observed in the pig after subretinal injection of AAV2/8-CBA-eGFP [326] and in GC1-deficient mice injected with AAV8 (Y733F)-smCBA-mGC1 [352], indicating possible inter-species or inter-manipulator variability. Indeed, transduction of ganglion cells after subretinal injection of rAAV2/8 vector may reflect the transduction of cells after spread of the subretinal bleb to the optic nerve or after leakage of vector into the vitreous [326], [336], [353].

After intravitreal injection of AAV2/2-CMV-GFP, early studies have shown that GFP protein can be detected in the brain and optic nerves of mice and dogs, for up to 6 months postinjection [349]. However, the DNA vector was only detected in the retina [349]. Similar results were obtained using other transgene products as LacZ in mice and guinea pigs [354]. These early data suggested that AAV2/2-mediated intravitreal gene transfer results in the transduction of retinal ganglion cells and that transgene products can be anterogradely transported along the visual pathway into the brain [327] .
In contrast, another study has demonstrated that vector DNA was present along the visual pathway in the brain (optic nerve, optic chiasm, optic tract, lateral geniculate nucleus and visual cortex) after intravitreal injection of rAAV2/2 in dogs[350]. Therefore, there could be an anterograde transport of rAAV2/2 from the retina to central visual structures. The use of cell-specific promoter may help to limit the expression of transgene products in the brain.

Small packaging capacity:

Despite its numerous advantages, the main drawback of rAAV vector is its relatively small packaging capacity, that is mainly restricted to 4,7 kb. This limits the treatment of several forms of inherited retinal dystrophies caused by mutations in genes whose functional cDNA exceed 5kb as *ABCA4*, *USH2A*, *USH2B* or *MYO7A* expressed in the photoreceptors.
Several strategies to overcome AAV packaging size are currently under investigation. They include (i) the use of dual rAAV vectors that reconstitute the full-length cDNA in transduced cells or (ii) the packaging of oversized genomes that contain heterogeneous transgenes.

Encouraging proof-of-concept results have been recently obtained in murine models of **Stargardt syndrome** [355], [356] and **Usher syndrome** [356] [357], [358].

IV.2.1.5. The importance of promoters

Promoter potency and specificity is the second key determinant of retinal cell transduction. The main requirement of a promoter is that, combined with an appropriate vector, it drives transgene expression in the target cell at a level that effects substantial amelioration of the disease phenotype. A minimum level of transgene expression in the target cell is essential to achieve a therapeutic effect. However, transgene overexpression may lead to cellular toxicity. Then, an ideal promoter should also restrict transgene expression to the appropriate cells to limit widespread expression of the transgene products and potential side effects. Expectedly, its size must fit with the packaging capacity of the chosen vector.

Targeting the RPE**:** *In vivo* gene transfer studies targeting the RPE has initially mostly used strong and ubiquitous promoters such as the immediate early cytomegalovirus (CMV) promoter or a chimeric chicken beta-actin (CBA)/CMV enhancer promoter (smCBA). However, other studies have revealed the efficacy of RPE-specific promoters as the human RPE65 (-1556 to +23bp) or the human VMD2 promoter (-585 to +38bp) that drives relatively weaker *in vitro* transgene expression compared with the ubiquitous promoters CMV or CBA (around 10%)[359], [360], [361], [362].

Targeting the photoreceptors**:** The majority of the vectors that efficiently transduce the photoreceptors still retain a preference for RPE cells. Therefore, when targeting the photoreceptors, it would be preferable to use cell-specific promoters to avoid high level of transgene products in the RPE.
A number of interesting photoreceptor specific promoters are capable of driving transgene expression to (i) cones and rods or to (ii) cones only. However, limited evidence exists for rod photoreceptor-specific transgene expression in the context of gene therapy. For example, the short murine rhodopsin promoter (mOP, -386 to +86bp) is known to express transgene in both rods and cones in rodents [363], [337] and the dog [345].

Rods and cones: Many preclinical studies have shown that the human rhodopsin kinase (RK, -112 to +87 or -112 to +180) promoter efficiently drives therapeutic transgene expression exclusively in the photoreceptors and restores function to murine and canine models of primary photoreceptor dystrophies [364, 365], [149], [352, 366], [347], [110], (Wert, 2013 #676), [348]. In combination with rAAV2/5, RK drives efficient transduction of photoreceptors in the non-human primate, indicating that this promoter could be ideal for a clinical setting [338].
The RK promoter drives transgene expression in both rods and cones in the mouse [367], rat (Petit L, unpublished data), dog [348], pig [368] and non-human primate retina [338].

Nevertheless, in the wild-type mouse, the RK promoter induces weaker levels of transgene expression per cones than the CMV promoter, and lower transduction of rods [368]. As well, in the wild-type pig, cone and rod transduction is markedly lower with RK than that obtained with CMV [368]. Higher level of cone transduction may be obtained with a 1,3kb promoter fragment of the human *IRBP* (interphotoreceptor retinoid binding protein) gene in the dog [347], but a direct comparison with the RK has not yet been performed.

Cones: The most commonly used cone-specific promoter is the human L/M opsin PR2.1 promoter, which has supported therapeutic transgene expression in one murine [369], two canine [346] and one non-human primate models of **achromatopsia** [170]. However, although PR2.1 can express transgenes in all cone subtypes in the murine retina, it is active only in L/M cones in the dog and the non-human primate [370], [170], [346]. In addition, its large size (2kb), limits remaining space for the transgene.
Another option for cone-specific expression may be the human cone arrestin promoter that allows efficient transgene expression in both S and M cones in the mouse [371]. Moreover, a 0,5kb fragment of the mouse blue opsin promoter, active in S cones and in a subset of M-cones [372], was recently successfully used in the context of gene therapy in the *Cnga3*$^{-/-}$ mouse [373]. It remains to be determined whether these two promoters are active in all cones in large animal models, such as the dog and the non-human primate.

IV.2.1.6. Summary

Along all the vectors that have been used for gene transfer to the outer retina, vectors derived from AAV are currently the most promising vectors in term of efficiency and safety. Novel AAV serotypes have been identified and they ability to transduce both RPE and photoreceptors is now demonstrated in small and large animal models. The ultimate proof of the potential of rAAV for retinal gene therapy is the correction of inherited retinal dystrophies in animal models before testing in humans. Consequently, the following part of this chapter will focus on rAAV-mediated gene addition therapy for inherited retinopathies, describing the preclinical and clinical success of gene therapy approaches for (i) slowly progressive RPE and photoreceptor-specific disorders, and (ii) the recent results obtained for more severe forms of photoreceptor degenerations. For a more complete review, please refer to [282], [374], [284].

IV.2. Proof-of-principle studies of rAAV-mediated gene therapy for RPE65-LCA

IV.2.1. Preclinical gene addition therapy in the *Rpe65*$^{-/-}$ canine model of congenital stationary night blindness

One of the first inherited retinal dystrophies for which retinal gene therapy has been developed is *RPE65*-**LCA**. RPE65 is almost exclusively expressed in the RPE and functions as the retinoid isomerase responsible for converting all-*trans* retinol to 11-*cis*-retinal during the retinoid cycle (**Chapter 1**). Improper functioning or absence of RPE65 results in a lack of 11-*cis*-retinal production and in a block in the visual cycle, hence affecting photoreceptor function. Large amount of opsin apoprotein in photoreceptors is thought to promote photoreceptor degeneration through the constant activation of the phototransduction cascade or through opsin mislocalization to the inner segment (**Chapter 3**). Meanwhile, it is conceivable that concomitant accumulation of large amounts of all-*trans*-retinyl esters in the RPE impact RPE health and cause secondary acute photoreceptor stress (**Chapter 3**).

Early and severe photoreceptor dysfunction is observed in all animal models of RPE65-deficiency, including the *Rpe65*$^{-/-}$ Briard dog, the *Rpe65* knockout mouse and the *rd12* mouse models. However, rate of photoreceptor degeneration vary substantially over the different models [375]. The *Rpe65*$^{-/-}$ dog shows no evidence of rod and cone degeneration for up to 1.5 years of age and many photoreceptors remain in the peripheral retina by 5-7 years of age [376], [377]. Similarly, rod degeneration in the *Rpe65*$^{-/-}$ and *rd12* mice progress slowly, with about 50-70% of photoreceptors remaining at 7 months of age, and about 30% at 24 months [378], [375]. However, in RPE65-deficient mice, massive degeneration of cones is observed before 1 month of age [379], [380], [381], [382]. Human *RPE65*-**LCA** patients show considerable retinal degeneration from early life, in particular in the fovea, but they have disproportionate functional loss for the amount of photoreceptors retained [375].

All animal models have been employed in the development of a gene addition therapy approach for the treatment of RPE65-deficiency [383], [384], [381], [385], [382], [386]. In particular, the canine model has been widely used because of its comparable eye anatomy and immune system as human [387], [388], [389], [390], [391], [392], [268], [393].
In the first study, subretinal delivery of AAV2/2-CBA-h*RPE65* at 4 months of age led to restoration of both rod and cone function to 16% of normal levels out of 3 months postinjection [387]. Subsequent follow-up studies confirmed and extended these results [389], as well as determined the efficacy of other serotypes including 2/1, 2/4 and 2/5 and other promoter (hRPE65) [388], [389], [390], [391], [392]. Most encouraging were the findings that the retinal function rescue remained stable overtime, up to 11 years postinjection [268]. In addition, successful restoration of both cone and rod ERG mediated responses was achieved in 20/22 eyes treated between 2 and 6 years of age [393] (-43% of rods and -15% of cones compared to a 3-month old *Rpe65*$^{-/-}$ dog) [377].

IV.2.2. Gene therapy clinical trials for *RPE65*-LCA

Successful gene addition therapy in RPE65-deficient dogs has led to several clinical trials, which were the first trials to use gene addition therapy for inherited retinopathies. Results of four clinical trials have been published. All employed rAAV2 vector carrying the h*RPE65* cDNA, but the promoter, the dose and volumes delivered were different [394], [395], [396], [397], [344], [398], [399], [268].

All trials, involving over 30 RPE65-deficient patients, showed sustained improvement of retinal and visual function, i.e. increased retinal light-sensitivity, increased visual acuity, increased visual field, reactivation of the visual cortex and improved vision-guided behavior [375]. These improvements remained stable through the longest follow-up period (>4.5 years) [268], constituting a first for an *in vivo* gene therapy approach to convincingly deliver both on safety and efficacy.

Nevertheless, contrary to what observed in pre-clinical studies, none of the reported treated patients have shown a detectable ERG improvement. The reason for the discrepancy in the therapeutic effect between animal models and humans could reflect the relatively faster rate of photoreceptor loss in human. Indeed, as retinal morphology in RPE65-deficient patients is already altered at early ages, all treatments have been performed in retina with ongoing neuronal degeneration and/or end-stage of the disease. The loss of significant number of photoreceptors and/or accumulation of changes in the remnant cells may influence the *overall* functional rescue obtained after gene therapy by:

(i) limiting the *total* level of RPE65 transduction (low number of transduced RPE cells and/or low efficiency of RPE transduction).

(ii) irreversibly compromising the function of the RPE and/or photoreceptors still present at the time of treatment

The level of total functional rescue obtained in treated *RPE65*-**LCA** patients can be too low to make a detectable difference by ERG, but not to make a detectable difference by visual acuity or visual-guided behavior (that could be more sensitive outcomes in humans). Indeed, in one *Rpe65*$^{-/-}$ dog injected after 5 years of age, there was no detectable rescue of ERG function, although dim-light vision was improved [393]. As well, *rcd1* dogs retain useful bright-light vision up to 8 years of age, whereas ERG response is not recordable from 2 years (Petit L *et al*. in preparation).

Analysis of photoreceptor degeneration in treated RPE65-deficients patients recently confirmed the idea that most of the photoreceptors present in the vector-exposed area at the time of treatment were not rescued by gene addition therapy. Indeed, Cideciyan *et al*. found no indication that the retinal degeneration (evaluated by measuring ONL thickness by OCT) had been halted in the treated areas, despite sustained improvement in visual function [268]. The overall number of rescued photoreceptor cells is also likely too small to contribute to preservation in thickness detectable by SD-OCT after only 3 years post-treatment [400].

IV.2.3. Summary

These early results indicate that despite the relative preservation of photoreceptor cells at the time of treatment, a therapeutic window exists for optimal gene therapy success. In addition, some subpopulations of photoreceptors, still present at the time of treatment, may not be capable to respond positively to the treatment.

Interestingly, the notion that the number of remaining photoreceptors at the time of effective treatment is not the only factor that influences the level of functional rescue was recently confirmed in one study moving back to the *Rpe65*$^{-/-}$ dog [393]. In this study, Annear *et al*. have treated *Rpe65*$^{-/-}$ dogs aged from 2 to 6 years of age and have analyzed ERG outcomes for correlation with age and the number of cones and rods in the vector-exposed area at 5 months postinjection. They found no correlation between the extent of ERG rescue and the age of dogs at the time of treatment and between the extent of ERG rescue and the number of photoreceptors, suggesting that additional factors might influence the degree of rescue [393].

Recently, Cideciyan *et al*. proposed that the health of photoreceptors cells at the time of treatment could be one limiting factor of the efficacy of gene therapy [268]. Indeed, they demonstrated that when *Rpe65*$^{-/-}$ dogs were treated prior the onset of degeneration (<2 years), the restoration of retinal function was associated with a preservation of further degeneration in the vector-exposed area of the retina. In contrast, when they used dogs treated after degeneration had begun (5-6 years), they claimed that gene addition therapy did not stem the degeneration of photoreceptors cells in the vector-exposed area. The authors conclude that a gene addition therapy approach does not arrest the degenerative process if intervention is initiated after a threshold of accumulative molecular changes has been reached in photoreceptors [268]. However, it is important to note here that old treated dogs were followed for only 1.5 year after treatment. As photoreceptor degeneration progresses very slowly in RPE65-deficient dogs, long-term follow-up of treated dogs is required to further support this conclusion. To date, advancing loss of photoreceptors in the vector-exposed and/or vector-unexposed area has not been totally demonstrated [268].

If photoreceptor alteration determines the ability of gene addition therapy to prevent photoreceptor loss, the spatio-temporal kinetics of retinal degeneration, the time of treatment, the injection location and the onset of transgene expression could be important factors affecting the overall efficacy of gene therapy. It makes gene therapy for photoreceptor defects more challenging. Indeed, efficiency of photoreceptor transduction is lower than that of RPE and photoreceptors are directly impaired by the genetic mutation in primary photoreceptor dystrophies. In particular, severe photoreceptor degenerations, could be the most difficult to treat, as the degeneration component progresses more rapidly.

IV.3. rAAV-mediated gene addition therapy for stationary photoreceptor diseases

Despite stationary photoreceptor diseases are relatively rare, they are ideal translational models for the development of gene addition therapies targeting the photoreceptors. Indeed, stationary disorders are often associated with congenital retinal dysfunction, and are thus diagnosed at early ages. In addition, their slowly progressive nature presents a wide window of opportunity for intervention.

IV.3.1. Preclinical gene addition therapy in animal models of achromatopsia

Achromatopsia is a severe visual impairment and yet a relatively stationary condition, despite it has recently been shown that slow cone degeneration begins early in childhood (**Chapter 1**)[46, 401, 402].

To date, at least four small and two large animal models of achromatopsia have been treated successfully using rAAV-mediated gene addition therapy, including: (i) one murine model of GNAT2-deficiency [369], (ii) two murine models of CNGA3-deficiency [373], [403] and (iii) one murine [371] and two canine models of CNGB3-deficiency [346], [404].

***The mutant GNAT2 mouse and gene therapy*:** GNAT2 encodes the Tα subunit of cone transducin and its absence results in little to no light-adapted ERG responses in humans.

The first report of gene therapy for **achromatopsia** was performed in the GNAT*2*-deficient *cpfl3* mouse [369]. This mouse model retains 25% of normal cone ERG responses at 4 weeks of age that become undetectable by 9 months of age. In contrast, cones appear to retain structural integrity for at least 14 weeks, as assessed by PNA staining.

Subretinal injection of 4.10^{10} genome particles of AAV2/5-PR2.1-m*Gnat2* in *cpfl3* mice at P23-29 restored cone ERG responses to levels indistinguishable from age-matched control in 80% of treated eyes, for at least 7 months [369]. Interestingly, when *cpfl3* mice were treated at 9 months, ERG rescue at 10 months of age was also observed, but levels of cone function was more variable, with only one eye showing cone ERG responses within the normal range [369].

***The mutant CNGA3 mice and gene therapy*:** Gene addition therapy has also been tested in two murine models of CNGA3-achromatopsia, the *Cnga3* knockout mouse [373] and the natural *cpfl5* mouse model [403].

CNGA3 encodes for the alpha subunit of cone cGMP-gated channel (stoichiometry CNGA3: CNGB3 = 3:1). CNGA3 is thought to confer the principal channel properties, thus, improper functioning or absence of CNGA3 results in non-functional cGMP-gated channels, hence affecting cone function.

In the *Cnga3*$^{-/-}$ mouse, absence of CNGA3 is associated with a total absence of cone function from birth, an early increase of intracellular levels of cGMP [373], mislocalization of opsins in the inner segment, followed by progressive degeneration of cones [231]. Loss of PNA-positive cones is first evident by 3 weeks of age. In the ventral retina, cone density is reduced to 50% at 4 weeks, and to 15% at 17 months of age. In contrast, 50% of cones remain present in the dorsal retina at 17 months of age.
The *cpfl5* mouse displays a similar phenotype, with no cone ERG responses and signs cone alteration from 3 weeks of age (opsin mislocalization to the inner segment)[405], [406].

In the *Cnga3*$^{-/-}$ mouse, Michalakis *et al.* demonstrated successful restoration of cone function 10 weeks after injection of 6-9.10^{9} genome particles of AAV2/5(Y719F)-mBP-m*Cnga3* in at P12-P14 [373]. Contrary to what seen in *Gnat2*$^{-/-}$ mice, ERG recovery was only 30% of wild-type levels. This possibly may be due to the use of a different promoter or to the faster rate of cone loss in the *Cnga3*$^{-/-}$ mouse, however levels of functional rescue was consistent with the surface directly exposed to the vector (25-30%).
In the *Cnga3*$^{-/-}$ mouse, treatment normalized the level of intracellular cGMP, reduced retinal inflammation and partially preserved PNA-positive cones in the treated area. More importantly, treated *Cnga3*$^{-/-}$ mice developed elaborated vision-guided behavior that was absent in untreated mice as assessed by water maze test [373]. The therapeutic effect remained stable for at least 8 months postinjection (Michalakis S. et al. Poster 490/D1137, ARVO 2011).

Comparable results were obtained in the *cpfl5* mouse using AAV2/5-CBA-m*Cnga3* vector [403]. Subretinal injection of 1.10^{10} genome particles in 2 weeks-old mice (detachment of the nearly entire retina) restored cone ERG responses to 60-70% of that recorded from wild-type controls. These responses remained stable for at least 10 weeks postinjection. At 5 months of age, better cone preservation in the treated area was also demonstrated with M- and S-opsin immunolabeling, as well as PNA staining [403]. Milder rescue had been observed with rAAV2/5 vector carrying m*Cnga3* cDNA under the control the human blue opsin promoter or the PR2.1 promoter (restoration of 50% of wild-type ERG responses, for at least 2 months postinjection)[407].

***The mutant CNGB3 murine and canine models and gene therapy*:** Successful gene therapy has also been demonstrated in animal models of CNGB3-deficiency. CNGB3 encodes for the β subunit of cone cGMP-gated channel. It is essential for the proper localization of CNGA3 in the outer segment and acts as a modulator of cGMP-gated channel properties.
In the *Cngb3* knockout mouse, a residual cone function (50% of wild-type) remains at P15, due to low levels of homomeric CNGA3 channels. This function is further reduced to 30% of wild-type levels by P30, to 20% by 12 months of age. At P30, cone outer segments are disorganized and cone density is reduced by 20%, as assessed by PNA staining or S-opsin immunolabeling. At 12 months of age, cone density is 50% of wild-type levels.

In both *Cngb3*$^{-/-}$ (*null* mutation) and Cngb3$^{m/m}$ (missense mutation) dogs, a residual cone function is also present at early stages of the disease (8 weeks of age), but is completely lost by 12 weeks of age. At 1 year of age, both L/M and S cone density is reduced by approximately 25%, with better preservation in the cone-rich visual streak [404].

In the murine *Cngb3* knockout mice, Carvalho *et al*. tested the efficacy of gene therapy using an AAV8 vector containing the human cone arrestin promoter driving the expression of the human *CNGB3* cDNA [371]. After subretinal injection 6-8.10^9 of genome particles at P15, CNGB3 was detected in both M- and S-cones and resulted in increased levels of CNGA3, as assessed by immunohistochemistry. PNA-positive cone density and survival was improved at 8 weeks postinjection, as well as cone outer segment structure. Moreover, the therapy also resulted in long-term restoration of cone-mediated ERG responses to 90% of wild-type levels for at least 9 months postinjection, and a significant improvement in visual acuity (evaluated as optokinetics reflex).
Interestingly, successful restoration of cone function was also achieved when *Cngb3*$^{-/-}$ mice were treated at P180. However, an ideal therapeutic window is present around P15-P30, as treatment performed at P90 and P180 resulted in functional rescue at 70-80% and 60-70% of wild-type levels respectively [371]. This could partially reflect the progression of cone degeneration in older *Cngb3*$^{-/-}$ mice. In addition, no significant improvement of visual acuity was observed in *Cngb3*$^{-/-}$ mice treated after P90 and P180. Without input from the photoreceptors, the inner retina and central visual pathways may permanently lose their ability to effectively process the input from the recovered cones.

AAV2/5-mediated h*CNGB3* addition therapy has been tested in the Cngb3$^{-/-}$ and Cngb3$^{m/m}$ dogs [346, 404]. Treated dogs exhibited restored cone function and visual-guided behavior, but, as observed in murine models of achromatopsia, the magnitude of therapy was dependent on both the age at treatment (from 3 weeks to 3,5 years of age) and the promoter used (PR2.1 or a shorter version PR0.5 that was shown to be less efficient to drive transgene expression to canine cones)[346]. Young dogs treated with rAAV2/5 vector carrying the human PR2.1 promoter displayed the more sustained therapeutic effects, with a restoration of cone function up to 5-10% of wild-type levels, and a restoration of visual-guided behavior in bright-light. Therapeutic effects were maintained for at least 33 months postinjection in two dogs [346]. In contrast, in dogs treated at older ages (n=10/11), or with other vector systems (n=5/7), transient or absent cone functional rescue was reported [404].

The reason for this age-dependency is still unknown. Analysis of transgene expression following rAAV-mediated gene transfer in CNGB3-deficeint dogs has excluded the possibility of a drastic reduction in the effectiveness of transgene expression over time [404]. However, this does not exclude a higher *heterogeneity* of transduction (for example: 40% of cones that express high levels of transgene and 60% of cones that express low levels of transgene ≠ 100% of cones express medium levels of transgene). Photoreceptor stress may result in

higher variability of rAAV transduction by decreasing the expression of AAV surface receptors and/or co-receptors, decreasing the activity of the promoter or reduces the stability of the mRNA and/or proteins products.
The authors hypothesized that the failure results from the improper reassembly of the components of the phototransduction cascade when retinas were treated at later stages of the disease. They used CNTF to promote cone outer segment deconstruction and reconstruction and reported an interesting increase of gene therapy efficacy. Another hypothesis is that CNTF down-regulates the cone phototransduction machinery and consequently reduces (i) the deleterious effects of the mutation and (ii) the *metabolic stress* on cells prone to degeneration (one of the major source of photoreceptor vulnerability, **Chapters 1** and **3**).

An important step in approaching this problem will be to understand the longitudinal changes that occur during phases of photoreceptor stress/degeneration at the level of both the *photoreceptors* and *rAAV vector pharmacology*. Recently, Punzo et al. have applied microarray technnology to identify cellular expression patterns of genes that change during cone death in murine models of **rod-cone dystrophy**, compared with wild-type mouse [101, 194] (**Chapter 3**). Such technology could be very interesting to understand the ability of subpopulation of transduced cones or rods to respond or not to rAAV-mediated gene addition therapy.

IV.3.2. Summary

Preclinical results of gene addition therapy for stationary photoreceptor disorders indicate that despite the relative slow progression of photoreceptor death in these diseases, a therapeutic window also exists for optimal gene therapy success.
In CNGB3-deficient dogs, despite the successful treatment by gene addition therapy in young animals, treatment with the same therapeutic vector is ineffective in animals older than 1 year [346], [404]. A similar effect of age was shown in the *Cngb3*$^{-/-}$ [371] and Gnat2-*cpfl5* mice [369], even if cone function (but no visual acuity) was restored in mice up to 6 months and 9 months of age, respectively. Several cones, still present at the time of treatment, may not be capable to respond positively to the treatment. There results further indicate that the health of photoreceptor cells at the time of treatment may be a limiting factor for functional rescue after rAAV-mediated gene transfer.

IV.4. rAAV-mediated gene addition therapy for progressive inherited photoreceptor diseases

Progressive photoreceptor degenerations are the most common causes of complete blindness in human. However, in the past, gene addition therapy has been marginally effective or ineffective when the photoreceptor degeneration starts too early or progresses too rapidly.

For instance, rAAV2-mediated addition of peripherin, a structural protein critical for stability of discs in the photoreceptor outer segments, results in restoration of 25% of wild-type ERG responses and improvements of neuronal responses in *Phrp2*$^{-/-}$ mice [408]. However, despite significant restoration of photoreceptor cell function in these mice, the duration of functional benefit was limited by progressive photoreceptor degeneration [408], [409]. As previously mentioned, in this disease linked with shortened outer segments, stopping disease progression would require the restoration of outer segment morphology and the re-activation of phototransduction to a sufficient large scale across the retina to restore the photoreceptor equilibrium. Consequently, if the quality of restored outer segments is too low, if the physiology of individual photoreceptors is altered during the course of the degeneration, or it many photoreceptors have been lost, this may never happen [42].

The discovery of novel rAAV vectors that allow more efficient level of transgene expression and minimize the interval between transduction and transgene expression, has offered novel opportunities to treat the severe forms of inherited retinal dystrophies [324]. Consequently, over the past 5 years, numerous animal models of progressive retinopathies have been successfully treated by rAAV-mediated gene addition therapy [281], [282], [374], [284]. Some of these results are discussed below.

IV.4.1. Preclinical studies in models of rod-initiated rod-cone dystrophies

***The mutant PDE6β mice and gene therapy*:** Mutations in the *PDE6β* gene, which encodes the β subunit of the rod PDE6 enzyme, are associated with one of the more common and aggressive forms of recessive rod-initiated **rod-cone dystrophies** (**Chapter 2**). In the absence of PDE6β, PDE6 activity is severely impaired and high levels of intracellular cGMP and Ca^{2+} accumulate, leading to rod death (**Chapter 3**). Rod dysfunction and early-onset degeneration is collectively seen in all animal models of PDE6β-associated **rod-cone dystrophies**, including the *rd1*, the *rd10* and the *H620Q* mice, as well as the PDE6β-deficient *rcd1* and *crd1* dogs (**Chapter 2**).

Gene therapy approaches to delay photoreceptor degeneration have been first employed in the *rd1* mouse, in which the majority of rod cells at lost by 3 weeks of age. Due to the early and rapid rate of photoreceptor cell loss in this *rd1* mouse, it is difficult to provide effective gene therapy in time.

Gene therapy approaches have been made using non-viral [410], [411], adenoviral [312],[313] lentiviral [412] or rAAV2/2 [413] vectors that allow poor photoreceptor transduction. Consequently, in all studies, despite treatment at early stages of retinal degeneration (between P2 and P8), preservation of photoreceptor cells was at best partial and transient (up to 6 weeks postinjection), whereas rod functional rescue was absent or limited [411].

The first convincing evidence of the benefits of gene addition therapy was obtained by combining the use of the rAAV2/5 serotype (that allow sustained restoration of retinal function in animal models of **achromatopsia**) and dark-rearing of the *rd10* mouse [364]. Dark rearing delays the onset of degeneration by as much as 4 weeks, however, rapid onset of photoreceptor degeneration occurs as soon as the animals are moved to a normal 12h/12h light environment.
Rd10 mice, that had been dark-reared from birth, were treated at P14 with AAV2/5-smCBA-m*Pde6β* (1.10^{10} genome particles) and maintained for 2 more weeks in the dark, before moving to a normal light environment [364]. At 3 weeks postinjection (1 week after removal of mice to light), 37% of rod ERG responses were maintained in treated eyes, which were 3 fold higher than responses recorded from contralateral untreated eyes. In addition, photoreceptor survival was prolonged up to P35, when only a few cells remain in untreated eyes [364]. However, the therapeutic effects faded 6 weeks after treatment [365].
This first result indicates that difficulties in achieving sustained long-term functional rescue in murine models of PDE6β-deficiency were probably not related to specific characteristics of the PDE6β subunit/mutations but to (i) excessively rapid loss of photoreceptors in these models and mainly to (ii) difficulties in achieving sufficient level of transgene expression in mutant photoreceptors in time to stop their degeneration.

Consistent with this hypothesis, the level of photoreceptor preservation in *rd10* mice following rAAV2/8-mediated gene supplementation therapy was superior to that obtained using rAAV2/5 [365]. However, the rescue was still relatively modest compared with those achieved using AAV2/5 vector in stationary photoreceptor disorders, and still transient (up to 8 weeks postinjection, 6 weeks after moving to the light).
More effective rescue of the dark-reared *rd10* mouse was achieved using the strong AAV2/8(Y733F) vector that can transduce most of the photoreceptors in a couple of days following *in vivo* delivery, and had the earliest onset and highest transduction efficiency of photoreceptors in the mouse. Indeed, subretinal injection of AAV2/8(Y733F)-smCBA-m*Pde6β* (1.10^{10} vector genomes) in dark-reared *rd10* mice at P14 preserved 58% of rod function, 68% of cone function and more than half of the photoreceptors for at least 6 months postinjection, as determined by ERG, spectral-domain OCT and histology [365]. This was the first long-term morphological and functional rescue of the *rd10* mouse. However, it is not clear whether this was due to the early onset of transgene expression or whether it

was because higher level of PDE6β expression was achieved in *rd10* rods. Kinetics of single stranded AAV2/8(Y733F)-mediated transgene expression has not been yet reported.

Interestingly, a more recent study demonstrated that subretinal injection of AAV2/5 or AAV2/8-CMV-h*PDE6β* (2,1.10^9 genome copies) in the dark-reared *rd10* mouse at P2 led to transient improvement in the number of photoreceptor nuclei in the ONL, and no preservation of retinal function at P35 (1 week after removal of mice to light)[414]. Similar results were obtained with rAAV vectors carrying the rhodopsin promoter or the m*Pde6β* cDNA [414]. These results are in disagreement with those obtained previously par Pang JJ et al [364, 365], indicating that the time of gene delivery (P2 versus P14), the area of retina treated (20-30% in this report versus 50% in the previous study) and/or the dose/titer of vector injected influence the overall efficacy of gene therapy.
In another study, it was reported that subretinal injection of AAV2/5-smCBA-mPde6*β* vector (1.10^{10} genome particles) in dark-reared *rd10* mice at P4 or P21, preserved ONL thickness and rod ERG responses up to 10 weeks postinjection (6 weeks after moving to the light)[415]. There was no difference in the ERG responses of P4 versus P21 treated retinas. However, at 4 weeks postinjection, untreated eyes showed higher ERG responses compared to the P4 or P21 treated eyes, indicating that gene therapy has a deleterious effect on the retina [415].

Of note, combination of rAAV2/5-h*PDE6β* or rAAV2/8-h*PDE6β* with nivaldipine, a pharmacological inhibitor of calcium channels, was not more effective than rAAV-h*PDE6β* alone in the *rd10* mice [414]. As well, co-delivery of AAV2/5-smCBA-m*Pde6β* and rAAV2/5 vector encoding the X-linked inhibitor of apoptosis protein (XIAP), only transiently modified the course of retinal degeneration in *rd10* mice, compared with co-delivery of AAV2/5-smCBA-m*Pde6β* and AAV2/5-smCBA-*GFP* [415].

***The mutant PDE6α mouse and gene therapy*:** As its PDE6β molecular partner, PDE6α is necessary for rod PDE6 holoenzyme activity. Mutations in the *PDE6α* mutations have been reported to cause severe recessive **rod-cone dystrophy** in several species, including mice dogs and humans. The *nmf363* murine model of PDE6α-deficiency has similar missense mutations in the catalytic domain of PDE6α found in human patients [416]. This mouse mimics the clinical phenotype found in humans, where there is a progressive loss of photoreceptors and visual function, at a faster rate of degeneration than occurs in the *rd10* mouse. In *nmf363* retina, no apparent photoreceptor degeneration is observed at P12, but 30% of photoreceptors have been lost by P14. At P38, only one row of photoreceptor nuclei remains in the ONL, and nearly all photoreceptor are lost by 5 months of age [416], [417].

Recently, Wert *et al*. evaluated the efficacy of gene addition therapy in the *nmf363* mouse using a rAAV2/8(Y733F) vector carrying the murine *Pde6α* cDNA under the control of a 1,1kb fragment of the murine rhodopsin promoter [417].

The *nmf236* mice received 9.10^{10} genome copies of AAV2/8(Y733F)-Rho-m*Pde6α* at P5 (before the onset of retinal degeneration) or at P21 (when approximately 50% of the photoreceptors have undergone degeneration)[417], [418].
In both eyes treated at P5 or P21, after an initial loss of cells between 1 and 2 months of age, a stable preservation of 3-4 rows of photoreceptor nuclei was showed in the vector-exposed area, for at least 6 months of age (the duration of the study). At this age, no photoreceptor cells remained in untreated fellow eyes. Thus, despite gene delivery after disease onset, photoreceptor degeneration was stopped in *nmf236* mice. In addition, treatment at either P5 or P21 resulted in preservation of mixed rod/cone ERG responses to 30% of wild type at 5-6 months of age, when no ERG responses remained detectable in untreated eyes. In contrast, no significant rod-specific ERG responses were detected in *nmf236* eyes treated either at P5 or P21, compared to untreated eyes. This indicates that in both cases, the overall rod functional rescue was too low to make a detectable difference by ERG. However, AAV2/8(Y733F)-Rho-*mPde6α* treatment was sufficient enough to significantly delay the secondary non-cell autonomous cone dysfunction in all *nmf236* treated eyes up to 6 months of age [418].

***The mutant CNGB1 mouse and gene therapy*:** rAAV-mediated gene therapy has also been recently validated in the *Cngb1* knockout murine model of CNGB1 retinopathy [419].
CNGB1 encodes for the beta subunit of rod cGMP-gated channel (stoichiometry CNGA1: CNGB1 = 3:1). As the cone CNGB3 subunits, CNGB1 is thought to act as a modulator of cGMP-gated channels properties. However, mutations in the *CNGB1* gene are associated with a much more progressive retinopathy than defects in *CNGB3*.
The knockout of *Cngb1* in mice results in a phenotype that mimics the pathology of patients, i.e. an early onset rod-initiated **rod-cone dystrophy**. In particular, the *Cngb1*$^{-/-}$ mouse lacks rod ERG responses from early ages. However, rod degeneration progresses much more slowly than murine models of PDE6-deficiency: around 10-20% of rods are lost by 4 months of age, 30-50% by 6 months and 80-90% at one year of age. Cone function is preserved until 6 months of age.
At P14, *Cngb1*$^{-/-}$ mice were treated using 1.10^{11} genome particles of rAAV2/8(Y733F) vector encoding the m*Cngb1a* cDNA under the control of a 417 bp mouse rhodopsin promoter (-386 to +86)[419]. At 5-6 weeks postinjection, both CNGA1 and CNGB1 expression was rescued in rod outer segments in the vector-exposed area of the treated eyes, as assessed by immunohistochemistry. Both proteins were absent in untreated eyes. Retinal histology at 12 months after treatment demonstrated preservation of 50-70% of rods in treated eyes and better preservation of cone morphology when only a few cells survive in untreated eyes. In addition, at 2 months postinjection, over 33% of wild-type rod-ERG responses were restored in *Cngb1a*$^{-/-}$ treated eyes, consistently with the surface of the retina directly exposed to the therapeutic rAAV vector [419].

IV.4.2. Preclinical studies models of progressive photoreceptor diseases involving both rods and cones

Although the majority of inherited retinal dystrophies are caused by genetic mutations in rods only, many forms of progressive retinopathies involve primarily both cones and rods.

***The mutant AIPL1 mice and gene therapy*:** AIPL1 is expressed predominantly in rods in the human and murine retina, but it is also expressed at lower levels in adult cones. AIPL1 is a molecular chaperone for the folding and/or assembly of cone and rod PDE6. Therefore AIPL1 deficiency is a disorder closely related to PDE6β-deficiency. Mutations in the *AIPL1* gene show allelic heterogeneity, with *null* alleles resulting in **LCA** and *hypomorphic* alleles resulting in **cone-rod dystrophy** in human and mice.
In *Aipl1*$^{-/-}$ retinas, there is no PDE6 activity as observed in *rd1* mice. In both models, kinetics of rod degeneration is similar, with the loss of almost all rods by 3 weeks of age. Cones also rapidly degenerate in the *Aipl1*$^{-/-}$ mouse as a consequence of their own genetic demise and concomitant rod cell death. This makes the *Aipl1*$^{-/-}$ mouse the animal model with the fastest rate of photoreceptor degeneration characterized so far.
However, the *Aipl1*$^{-/-}$ mouse appears more amenable to gene addition therapy than its PDE6β counterpart [420], [421], [281]. Indeed, subretinal injection of AAV2/8-CMV-m*Aipl1* ($1.5\text{-}3.10^9$ genome particles) into *Aipl1*$^{-/-}$ mice at P12 rescues scotopic and photopic ERG responses to 30-50% of wild-type levels for at least 6 weeks postinjection. Treatment also substantially prolongs the survival of the photoreceptors, so that 3-5 rows of ONL nuclei remained at 4 weeks of age [420]. The greater phenotypic rescue in *Aipl1*$^{-/-}$ mice compared to murine models of PDE6β-deficiency may reflect the fact that low levels of AIPL1 is less critical for PDE6 activity than low levels of PDE6β (stoichiometry PDE6α:PDE6β = 1:1)[281]. In addition, in the *rd10* mouse, mutant PDE6β may compete with wild-type PDE6β for interaction with PDE6α and/or PDE6γ subunits.

Nevertheless, the less effective rAAV2/2 serotype failed to work in the *Aipl1*$^{-/-}$ mouse, while it provides long-term therapeutic effect in the *Aipl1*$^{h/h}$ mouse that produces 20% of wild-type AIPL1 levels and displays a slower rate of degeneration (half of photoreceptors lost by 6-8 months)[420]. Superiority of rAAV2/8 over rAAV2/2 was also shown in the light-accelerated Aipl1$^{h/h}$ model that exhibited a 2-3 fold faster course of degeneration than the *Aipl1*$^{h/h}$ mouse reared in normal 12h/12h dark-light environment [420]. Therefore, as observed in PDE6β-deficient mice, the onset of transgene expression and/or the rate of photoreceptor degeneration influence the overall efficacy of gene therapy in the AIPL1-deficient mice.

More recently, it was demonstrated that AAV2/8-RK-h*AIPL1*, but not AAV2/5-RK-h*AIPL1*, rescue the phenotype of *Aipl1*$^{-/-}$ mice, even when mice were treated as early as P10 [421]. Subretinal injection of AAV2/8 vector ($5.10^8\text{-}1.10^9$ vector genomes) led to a 50% restoration of wild-type scotopic ERG responses for at least 4 weeks postinjection.

When the self-complementary AAV2/8(Y733F)-RK-hAIPL1 was used (1.10^{10} vector genomes), this rescued rod function was more sustained, persisting for at least P60 (the duration of the study)[422]. These improvements are likely due to the increased kinetics of transgene expression achieved with both the self-complementary genome and AAV8 (Y733F) used in this study.

***The Rpgrip1 mice and gene therapy*:** The *Rpgrip1* knockout mice undergo a rapid course of photoreceptor degeneration characterized by ongoing cell loss as early as P15, and profound disruption of outer segment formation.
Subretinal delivery of a rAAV2/2 vector carrying the murine *Rpgrip1* cDNA under the control of a fraction of the mouse rhodopsin promoter (-218 to +17) into 3 week-old *Rpgrip1*$^{-/-}$ mice restored the normal localization of RPGRIP1 and RPGR in the connecting cilium. This resulted in a slowing of rod function loss over the 5 month-follow up period (loss of 6% of ERG b-wave amplitude per month in treated eyes, compared with 22% per month in untreated eyes), consistent with the preservation of 6-7 rows of ONL nuclei in treated eyes, when only few cells remained in age-matched controls. Amelioration of the cone function or survival was not reported as the mouse Rho promoter primarily drove expression in rods [423].
Improving upon this study, treatment of 2-week-old *Rpgrip1*$^{-/-}$ mice with an AAV2/8-RK-h*RPGRIP1* vector resulted in photoreceptor-specific RPGRIP1 expression, significant preservation of photoreceptors and preservation of 33% of initial rod and cone function for at least 5 months of age. At this age, ERG responses cannot be further recorded in untreated eyes [149]. It is unclear whether the incomplete rescue was due to low levels of human RPGRIP1 expression and/or the divergence between human and mouse RPGRIP1 sequences.
Importantly, no therapeutic effect was obtained using AAV2/5-RK-h*RPGRIP1*, indicating that, as observed in the *Aipl1*$^{-/-}$ and *rd10* mice, rAAV2/8 is more efficient than rAAV2/5 in the *Rpgrip1*$^{-/-}$ mouse [149].

***The GC1 knockout mouse and gene therapy*:** Six studies have recently evaluated the impact of gene addition therapy for guanylate cyclase (GC1) deficiency using different rAAV serotypes in GC1 knockout mice, a model of *GUCY2D*-**LCA**.
In the GC1 knockout mouse, loss of cone function, based on ERG, precedes cone death. Nearly all cones have degenerated by 6 months of age. Rod photoreceptors maintain 30-50% of their function and, contrary to what seen in human patients, they do not degenerate. This absence of rod degeneration in the GC1 knockout mouse is likely due to the presence of a second guanylate cyclase in murine rods (guanylate cyclase 2, GC2).

Two gene therapies have been performed in the GC1 knockout mouse using the rAAV2/5 serotype, but with different therapeutic cDNA [424], [366].

In an initial study, subretinal injections of AAV2/5-smCBA vectors carrying the bovine GC1 cDNA were performed on 3-week-old GC1 knockout mice (1.10^9 delivered vector genomes). No restoration of cone ERG responses or preservation of cone cells was observed despite the confirmation of transgene expression in the cones at 5 weeks of age [424].
Subsequently, using AAV2/5-smCBA-m*GC1* (4.10^9 delivered vector genomes) or AAV2/5-RK-m*GC1* (4.10^{10} delivered vector genomes) in 2-weeks-old mice, the same group showed a 45% recovery of cone ERG responses, a robust improvement in cone-mediated visual acuity, as well as a partial preservation of cone cells, lasting at least 9 months postinjection [366], [352]. These results suggest that, contrary to what observed in *Aipl1*$^{-/-}$ or *Rpgrip1*$^{-/-}$ mice, the AAV2/5 vector is sufficient for targeting therapy to cones. However, no improvements in rod function were reported [366].
In contrast, Mihelec *et al*. demonstrated a 65% rescue of cone ERG responses, cone vision and cone survival for up to 6 months, as well as a 35% of rescue of rod function, after subretinal administration of AAV2/8-RK vectors carrying the murine or human *GC1* cDNA [425]. Several variables could account for the difference in efficacy including the age at intervention (P10 versus P14) and the vector dose/titer administered (1.10^{11} delivered genome vector versus 4.10^{10}). A recent study reported a restoration of 54% and 38% of cone ERG responses in 25% of *GC1*$^{-/-}$ mouse treated at P20 with $1{,}5.10^{10}$ genome copies of AAV2/8-CMV-h*GC1* or AAV2/8-short RK-h*GC1*, respectively [368].

A side-by-side comparison of AAV2/5-RK-m*GC1* (4.10^{10} genome particles) and AAV2/8(Y733F)-RK-m*GC1* (1.10^{10} genome particles) confirmed the superiority of AAV2/8(Y733F) in restoring cone function in the GC1 knockout mouse [352]. This result likely reflects that AAV8(Y733F) supports much faster onset of transgene expression than rAAV2/5 and that this temporal difference is important in terms of ability to restore function. However, it is unclear whether there is a higher overall number of preserved cones and/or a better functional rescue of transduced cones. Regarding rod function, there is no reported significant difference between the two vectors.
More recently, the ability of AAV2/8(Y733F)-RK-m*GC1* to rescue both cones and rods was confirmed in the GC1/GC2 double knockout mouse, which exhibits complete loss of both cone and rod ERG responses, as well as a slow degeneration of rods [426]. Both cone and rod functions were restored to 42-44% of wild-type following treatment at P18 and to 26-29% of wild type following treatment at P108. This functional rescue remained stable for at least 1 year post-treatment. However, over the follow-up of 1 year, only treatments before P108 slowed photoreceptor degeneration, as assessed by SD-OCT [426].

***The XLPRA1 and XLPRA2 dogs and gene therapy*:** The first evidence of the efficacy of gene addition therapy in large animal models of severe photoreceptor dystrophies has been recently obtained in the XLPRA1 and XLPRA2 canine models of *RPGR*-X linked **rod-cone dystrophy** [347].

Both models have different disease phenotypes [427]. In the XLPRA1 dog (nonsense mutation), any morphological alterations are observed from 20 and 24 weeks of age. Early events of rod death are detected at 1.4 years. Then, the disease slowly progresses over at least one decade. At 7.8 years of age, 4-5 rows of photoreceptor nuclei are still present. In contrast, in the XLPRA2 dog (frameshift mutation), the disease begins 5 weeks after birth, and is rapidly progressive. Differences in the location and the extent of retinal damage are observed in affected dogs, with 0 to 4 rows of remaining nuclei after 8 years of age [427].

In these two canine models, Beltran *et al*. evaluated the efficacy of rAAV2/5 vectors carrying the full-length h*RPGR* cDNA under the control of either the human IRBP or RK promoters (1.10^{11} injected genome copies). XLPRA1 dogs were treated at 28 weeks of age, before apparent signs of photoreceptor degeneration, and monitored to 77 weeks of age (around 1 year postinjection). XLPRA2 dogs were treated at 5 weeks of age, at early stages of photoreceptor degeneration, and followed up to 38 weeks of age (around 9 months postinjection).
The authors demonstrated convincing improvements in retinal structure in the vector-exposed areas of the retina in both models, with milder effective treatment seen in the XLPRA2 dog treated with the RK promoter. In all cases, secondary retinal remodeling was also prevented. However, in the XLPRA2 dog, advancing photoreceptor degeneration within the vector-exposed area was observed by SD-OCT from 4 to 8 months postinjection (see Figure S1 of the study) [347]. Evaluation of the effects of gene transfer on retinal function was difficult to evaluate due to the long-term preservation of ERG responses in these models and to high inter-individual variations. Nonetheless, improvements of rod and cone function were clearly seen in one XLPRA2 treated dog, and to a lesser extend in one XLPRA1 treated dog (age of animals at examination not reported). As mentioned by the authors, future studies should extend the post-treatment follow-up period to older ages when degeneration of non-exposed areas of the treated eyes would allow evaluating treatment consequences on visual-guided behavior [347].

IV.5. Summary and thesis aims

Over the last 5 years, gene addition therapy for inherited retinal diseases grew like wildfire. Proof-of-concept studies for the treatment of recessive disorders have been established in different animal models, particularly of retinal dystrophies caused by RPE-specific defects. Several clinical trials of rAAV-mediated gene therapy for RPE-deficiency are on going. The encouraging results relative to the safety and efficacy of gene transfer obtained in mice, dogs and humans, strongly supports the concept that rAAV-mediated gene therapy may be translated from animal models to humans.

The next level of challenge is to initiate treatment for the majority of retinal dystrophies in which the genetic defects are primarily in the photoreceptors. However, contrary to RPE-diseases, preclinical evidence of the potency and efficacy of gene transfer to retinal photoreceptors is less robust. Indeed, the relative low efficacy of photoreceptor transduction, the early physiological alterations of retinal cells or the rapid loss of photoreceptor cells seem to be important factors limiting the efficacy of gene therapy in severe photoreceptor degenerations. It could be particularly true in murine models with very rapid progressive degeneration, due to the relative slow onset of rAAV-mediated transgene expression.

The aim of this study was to evaluate the efficacy of gene addition therapy in two large animal models of severe photoreceptor dystrophies: (i) the PDE6β-deficient dog, a model of rod-cone dystrophy and (ii) the RPGRIP1-deficient dog, a model of cone-rod dystrophy.

Publications and results

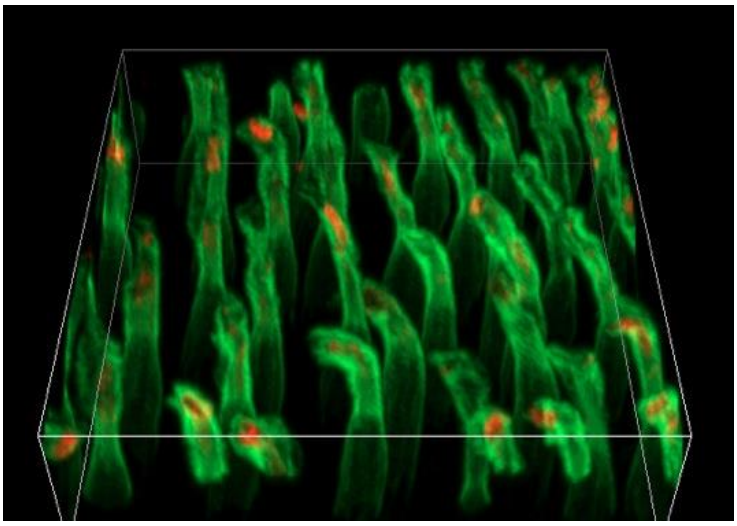

This image shows cone photoreceptors stained with peanut agglutinin (green) in the visual streak of a *Pde6β*$^{-/-}$ dog at 24 months of age. L/M opsin (red) are properly localized in the cone outer segments (Petit L. unpublished data)

Overview

The results obtained during my PhD work will be presented in two research articles (**Chapter 5** and **Chapter 6**).

The first article, published in *Molecular Therapy* in June 2012, deals with the treatment of the *rcd1* dog by rAAV-mediated gene addition therapy (**Chapter 5**) [110]. This dog displays a severe **rod-cone dystrophy** caused by a mutation in the rod-specific *Pde6β* gene. The idea was to introduce a wild-type copy of the canine *Pde6β* gene into mutant rods with rAAV2/5 and rAAV2/8 vectors. These vectors have been shown to efficiently transduce the rods in the rodent, canine and non-human primate retina. Treating 8 *rcd1* dogs at P21, before massive rod degeneration, I have evaluated whether rAAV-mediated c*Pde6β* expression restores rod function and subsequently lead to the preservation of rod photoreceptor cells in this model of severe retinal degeneration. In addition, as the secondary loss of cone function constitutes the most debilitating aspect of rod-cone dystrophy, I evaluated whether rAAV-mediated rod rescue was sufficient to long-term protect cone function and cone-mediated visual guided behavior in treated dogs.

The second article, published in *Molecular Therapy* in October 2013, evaluated the ability of rAAV-mediated gene addition therapy in the MLHD-*Cord1* dog, a canine model of cone-rod dystrophy caused by a genetic defect in both cones and rods (**Chapter 6**) [348] (study started in 2009 by Elsa Lhériteau). In this dog, the main objective was to restore cone function, but also to prevent massive rod degeneration for allowing long-term duration of the therapeutic cone rescue. The therapeutic strategy was analogous to that previously developed in the *rcd1* dog. To understand the therapeutic effects of gene transfer on photoreceptor function and survival components of the disease, we used electroretinography, funduscopy, optical coherence tomography and post-mortem histology.
I showed that contrary to what observed in treated PDE6β-deficient dogs, advancing retinal thinning is still observed in the treated area of MLHD-*Cord1* eyes, although this advancing photoreceptor degeneration is not associated with a gradual loss of restored cone function or preserved rod function. I hypothesized that advancing photoreceptor degeneration mainly reflects the gradual loss of functionally silent (non-rescued) photoreceptors. This hypothesis set the basis for the OFF/ON model of photoreceptor response that will be discussed at the end of this manuscript (**General Discussion**).

Justification of experimental models

I. The PDE6β- and RPGRIP1-deficient dogs are valuable translational models to develop gene addition therapy for severe photoreceptor diseases

The aim of this study was to evaluate the efficacy of gene addition therapy in two large animal models of severe photoreceptor dystrophies: (i) the PDE6β-deficient dog, a model of **rod-cone dystrophy** and (ii) the RPGRIP1-deficient dog, a model of **cone-rod dystrophy**.

I.1. The PDE6β- *and* RPGRIP1-deficient dogs have a retinal anatomy closed of primates

Large animal models are particularly interesting for translational research. Indeed, the size and anatomy of the eye in large animals provide a relevant model for determination of the therapeutic dose and appropriate surgical approaches. Moreover their longevity enables long-term follow-up, which is important in the treatment of retinal dystrophies than often takes years in humans [166].

More importantly, the retinal distribution, density and proportions of rods and cones in large animals more closely match those of primates than rodents, a potentially pre-clinical requirement for evaluating photoreceptor-targeting therapies. Indeed, the normal arrangement and ratios of cone and rod photoreceptors across the retina are important variables affecting disease presentation. For example, in rod-initiated **rod-cone dystrophy**, photoreceptor cell density has been suggested to be a crucial determinant of secondary non-autonomous cone death [29].

Only nonhuman primates have ocular anatomic features virtually identical to those of humans (including the macula), however, there are no models of severe photoreceptor degeneration in non-human primates.

Rodents, that display a distribution of rods and cones similar to the human peripheral retina are excellent models to evaluate the effects of the therapy on the early phases of secondary cone death. However, the absence of a distinct geographic region of high cone density makes the rodents imperfect models to predict long-term outcomes on foveal cones (which are preserved for decades in human patients, but whose loss of function is responsible for complete blindness). In contrast, long-term preservation of functional cones is observed in the cone-rich area centralis of the Pde6$\beta^{-/-}$ dog (Petit L, *et al.* in preparation).

I.2. The PDE6β- and RPGRIP1-deficient dogs are relevant models of severe photoreceptor diseases

The *rcd1* dog mimics the severe rod-cone dystrophy of patients

The *rcd1* dog is a natural model one of the most prevalent forms of recessive **rod-cone dystrophy** in Europe, with reported prevalence between 4-6% and estimated 36 000 patients affected worldwide (**Chapter 2**). This prevalence is one order of magnitude higher than the prevalence of *RPE65*-**LCA** that is currently evaluated in clinical trials.

Photoreceptor death in response to *PDE6β* mutations is directly correlated with the loss of PDE6 activity and subsequent toxic accumulation of Ca^{2+} and/or cGMP in rod outer segments. Consequently, the type of *PDE6β* mutation can directly influence the age of onset and the rate of photoreceptor degeneration of the disease. It is thus important to evaluate the efficacy of gene therapy in animal models that harbor similar types of mutations to those found in human patients. Interestingly, the *rcd1* dog carries a null mutation [69], similar to what found in almost half of the currently identified patients with PDE6β-deficiency (**Chapter 2**).

The *rcd1* dog mimics the phenotype of patients, where there is an early onset and severe progressive **rod-cone dystrophy**. This rapid rate of photoreceptor progression of the disease is interesting as it enables a rapid read out of treatment outcomes, in the form of either a restoration of rod function, a delay in the progression of photoreceptor cell loss or a preservation of dim-light vision. Such rapid assessment of therapeutic outcomes is not possible in all canine models of **rod-cone dystrophy**. For example, the XLPRA1 and XLPRA2 canine models of X-linked **rod-cone dystrophy**, in which rAAV-mediated gene therapy has been previously evaluated, retain sufficient rod and cone visual function to preclude accurate analysis of the effects of gene transfer by visual testing before (at least) 20 months of age [347].
In addition, the close temporal association of rod and cone death makes the *rcd1* dog an ideal model to evaluate the ability of rAAV-mediated rod rescue to protect long-term cone function.

Gene therapy for PDE6β-deficiency has previously been evaluated in murine models of the disease (**Chapter 4**). Accurate evaluation of the efficacy of gene therapy can be done quickly and efficiently in these small animals. However, the fast rate of photoreceptor degeneration in the murine models of PDE6β-deficiency can act as a double-edged sword. Indeed, the treatment of very rapid degenerations will require early intervention with rapid-onset treatment. The treatment of the *rd1* mouse model of PDE6β-deficiency, in which photoreceptor degeneration is almost complete by 4 weeks of age was particularly challenging. It is due to the time lag from vector delivery to onset of transgene expression,

reported as 3-4 weeks using rAAV2/2 vector [413]. The *rd10* mouse, in which retinal degeneration is delayed for up to 4 weeks, was also difficult to treat as rAAV2/5 and rAAV2/8 failed to provide long-term treatment [364], [382]. Only the combination of dark-rearing and fast-acting rAAV2/8 (Y733F) vector was shown to achieve long-term morphological and functional rescue in the *rd10* mouse [382]. Despite an early onset of retinal disease, the rate of photoreceptor loss is substantially slower in the *rcd1* dog. Thus, the *rcd1* dog could better emulate the typical progression of human rod-cone dystrophy that takes decades.

One possible limitation of the relevance of the *rcd1* dog as a model of severe photoreceptor degeneration is that retinal degeneration begins during retinal development (arrest of outer segment development at P14). Indeed, in newborn dogs, photoreceptor differentiation continues up to P20 and inner and outer segments elongate up to P35. This is in contrast with humans, in which retinal development is largely completed *in utero*.
The relative levels of Ca^{2+} inflowing into mutant rods as they differentiate and express cGMP gated channels may influence the rate of photoreceptor degeneration. Nevertheless, in the *rd1* mouse, the genetic depletion of cGMP-gated channels significantly reduces the rate of photoreceptor degeneration, indicating that rudimentary outer segments provide sufficient membrane area for the deleterious effect mediated by the cGMP-gated channels [196]. It is not known if rod degeneration begins *in utero* in patients with PDE6β-rod-cone dystrophy.

Finally, it is important to evaluate if missense PDE6β mutations may have latent dominant negative effects that become manifest following gene addition of the wild-type gene (by competition for interaction with PDE6α for example) (**Chapter 4**). It can determine the future success and widespread applicability of gene addition therapy in clinical practice. The *rcd1* dog does not allow such investigation because none of the commercially available antibodies against the mouse or human PDE6β subunit is specific in dogs due to cross-reactivity with the canine PDE6α subunit [110].

The MLHD-*Cord1* dog, mimics the severe cone-rod dystrophy of patients

The MLHD-*Cord1* dog is one of the two canine models of recessive **cone-rod dystrophy** for which the genetic basis is understood. The prevalence of **cone-rod dystrophies** caused by *RPGRIP1* mutations is approximately 2%, which represents a similar portion of cases than other known cone-rod dystrophy genes (1-2% of cases each, except the *ABCA4* gene associated with 40% of cases). In addition, *RPGRIP1* mutations are associated with 6% of **LCA** cases (**Chapter 2**).

In humans, genetic defects in *RPGRIP1* give rise to a heterogeneous set of clinical conditions that is also reflected in the animal models of RPGRIP1-deficiency (**Chapter 2**). This phenotypic diversity may be a potential obstacle (i) to determine which of the currently

available animal models most faithfully mimics the human retinopathy, and (ii) to select the patients. One solution could be to mainly focus on the common components of RPGRIP1-deficiency, i.e. the early and severe impairment of cone function and the progressive photoreceptor degeneration.

In the MLHD-*Cord1* dog, cone function is undetectable from the early age measured (1 month of age) whereas rod function is almost normal and rapidly declines thereafter [152], [153]. Whereas little is known about the progression of rod and cone degenerations in the MLHD-*Cord1* and in human patients with RPGRIP1-deficiency (**Chapter 2**), the functional phenotype of the MLHD-*Cord1* is particularly interesting. It enables a rapid read out of the outcome of treatment on cone function, as well as provides a good model to follow the degeneration of rods and its potential impact on rescued cone function.

However, the reason why RPGRIP1-deficiency is more detrimental to the cones than rods in the MLHD-*Cord1* dog is not known. Several non-exclusive hypotheses can be formulated:

(i) RPGRIP1 has a different function in cones and rods

(ii) RPGRIP1 has an additional function in cones

(iii) The threshold level of RPGRIP1 activity required for normal function is higher in cones than rods:

(iv) The residual RPGRIP1 activity in higher in mutant rods than in mutant cones

Consistent with the hypotheses (iii) and (iv), multiple mechanisms contribute to leakiness of the *Ins44* frameshift mutation in Rpgrip1$^{-/-}$ dogs, allowing continued RPGRIP1 production [159]. In addition, a modifier gene severely affects disease expression in the Rpgrip1$^{-/-}$ dog [158]. It is not known if such mechanisms exist in humans and if they can explain the large spectrum of phenotypes between RPGRIP1-family. This observation points to the need for further complete clarification of phenotype in the various animal models of *Rpgrip1* and individual patients.

2. Recombinant AAV2/5 and AAV2/8-RK vectors to target the photoreceptors

2.1. Subretinal injection

Subretinal injection releases the vector in the subretinal space between the photoreceptors and RPE cells. It allows a high concentration and long contact time of the vector with the target cells. Intravitreal injection is less invasive than subretinal injection but physical barriers and the widespread diffusion of vectors limit the transduction of the outer retina. We chose subretinal injection, as it is to date the favored delivery route to target efficiently the photoreceptors.

2.1. Recombinant AAV2/5 and AAV2/8 vectors

We chose to use AAV-derived vectors, as they are the only vectors able to transduce efficiently the adult photoreceptors (**Chapter 4**). In particular, we used rAAV2/5 and rAAV2/8 vectors for two reasons.

First, rAAV2/5 and rAAV2/8 efficiently transduce the photoreceptors in mice, dogs, pigs and nonhuman primates (**Chapter 4**). Self-complementary AAV vector constructs have a faster onset of transgene expression than conventional single-stranded AAV vectors in mice and dogs [428], [341], [429]. However, self-complementary rAAV vectors have significant restrictions on the size of gene that can be introduced (up to 2.2kb), limiting their potential for *PDE6β* (2,7kb) or *RPGRIP1* (3,6kb) addition.

Secondly, both rAAV2/5 and rAAV2/8 vectors have been used in previous gene therapy studies in murine models of PDE6β and RPGRIP1 deficiencies, as well as other models of severe photoreceptor dystrophies (**Chapter 4**). Thus, the mouse models can be discussed extensively together with our canine models.

The main objective of this study was not to compare the efficacy of rAAV2/5 and rAAV2/8 vectors but to identify a therapeutic strategy that allow sustained rescue of the phenotype. Therefore, rAAV vectors were used at their maximal production titer: 1.10^{11} vg/mL for rAAV2/5 and 1.10^{12} vg/mL for rAAV2/8 (100-120 µL injected). These doses are similar or below the doses that have been used in other preclinical studies. In human trials, the maximum reported dose that has been used to date is $1.5.10^{11}$ particles. This dose has been well tolerated.

2.2. The human rhodopsin kinase promoter

PDE6β is a rod-specific protein that is expressed in relative important amount in rod outer segments (1-2% of total protein content). Therefore an ideal vector system for *rcd1* dog would allow high level of transgene expression in rods only. However, there is to date no efficient rod-specific promoter. Consequently, we chose to use the human RK promoter that was shown to mediate efficient and specific transgene expression in rods and cones in the murine, dog and nonhuman primate retina (**Chapter 4**). Undesirable ectopic expression of PDE6β in transduced *rcd1* cones may occur. As cone function is normal in the *rcd1* dog until 9-12 months of age, the potential deleterious effects of ectopic expression of PDE6β in cones can be assessed by ERG (at least for this period).

RPGRIP1 gene is expressed in both cones and rods. Therefore, effective gene therapy in the MLHD-*Cord1* dog would require efficient transgene expression in both subtypes of photoreceptors. We also chose to use the human RK promoter. This promoter was used successfully in different animal models of inherited retinopathies linked to a defect in both rods and cones, including the *Rpgrip1*$^{-/-}$ mouse, the *Aipl1*$^{-/-}$ mouse, the *GC1*$^{-/-}$ mouse and the *XLPRA2* dog.

CHAPTER **V**

RESTORATION OF VISION IN THE PDE6β-DEFICIENT DOG, A LARGE ANIMAL MODEL OF CONE-ROD DYSTROPHY

Lolita Petit, Elsa Lhériteau, Michel Weber, Guylène LeMeur, Jack-Yves Deschamps, Nathalie Provost, Alexandra Mendes-Madeira, Lyse Libeau, Caroline Guihal, Marie-Anne Colle, Philippe Moullier and Fabienne Rolling

This work is published as a research article in Molecular Therapy
(Lolita Petit *et al*. Molecular Therapy **20**:11, 2019-2030, (2012))

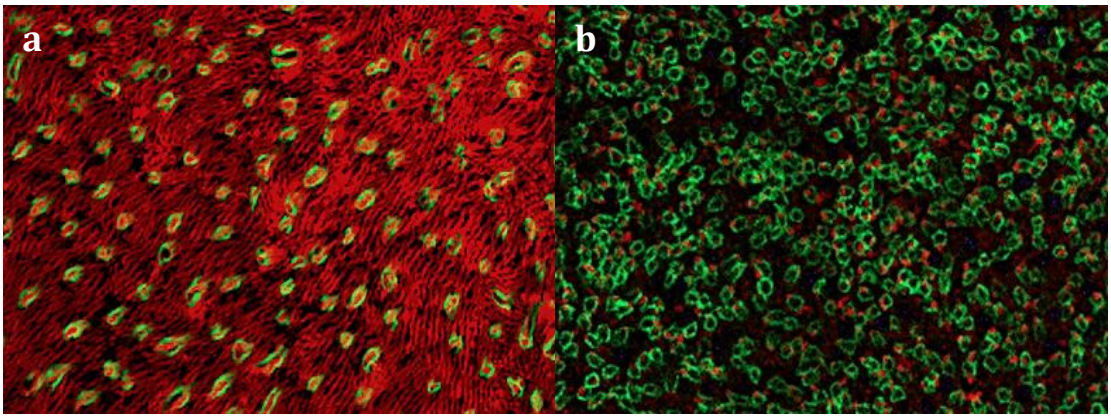

This image shows (**a**) preserved rods (red) in the vector-exposed area of a rAAV-treated *Pde6β*$^{-/-}$ retina at 4 months postinjection, while (**b**) only cones (green) are maintained in vector-unexposed areas of the same retina. (Petit L unpublished data)

Author contributions: LP, EL, PM and FR designed research. LP, EL, MW, GLM, JYD, NP, AMM, LL, CC and MAC performed research, LP, EL and FR analyzed data, LP and FR wrote the paper.

Restoration of Vision in the pde6β-deficient Dog, a Large Animal Model of Rod-cone Dystrophy

Lolita Petit[1], Elsa Lhériteau[1], Michel Weber[2], Guylène Le Meur[2], Jack-Yves Deschamps[3], Nathalie Provost[1], Alexandra Mendes-Madeira[1], Lyse Libeau[1], Caroline Guihal[1], Marie-Anne Colle[4], Philippe Moullier[1,5] and Fabienne Rolling[1]

[1]Translational Gene Therapy for Retinal and Neuromuscular Diseases, INSERM UMR 1089, Institut de Recherche Thérapeutique 1, Université de Nantes, Nantes, France; [2]CHU-Hôtel Dieu, Service d'Ophtalmologie, Nantes, France; [3]Emergency and Critical Care Unit, ONIRIS, Nantes-Atlantic College of Veterinary Medicine Food Science and Engineering, Nantes, France; [4]UMR 703 PAnTher INRA/ONIRIS, Nantes-Atlantic College of Veterinary Medicine Food Science and Engineering, Nantes, France; [5]Department of Molecular Genetics and Microbiology, College of Medicine, University of Florida, Gainesville, Florida, USA

Defects in the β subunit of rod cGMP phosphodiesterase 6 (PDE6β) are associated with autosomal recessive retinitis pigmentosa (RP), a childhood blinding disease with early retinal degeneration and vision loss. To date, there is no treatment for this pathology. The aim of this preclinical study was to test recombinant adeno-associated virus (AAV)-mediated gene addition therapy in the rod-cone dysplasia type 1 (*rcd1*) dog, a large animal model of naturally occurring PDE6β deficiency that strongly resembles the human pathology. A total of eight *rcd1* dogs were injected subretinally with AAV2/5RK.cpde6β (*n* = 4) or AAV2/8RK.cpde6β (*n* = 4). *In vivo* and *post-mortem* morphological analysis showed a significant preservation of the retinal structure in transduced areas of both AAV2/5RK.cpde6β- and AAV2/8RK.cpde6β-treated retinas. Moreover, substantial rod-derived electroretinography (ERG) signals were recorded as soon as 1 month postinjection (35% of normal eyes) and remained stable for at least 18 months (the duration of the study) in treated eyes. Rod-responses were undetectable in untreated contralateral eyes. Most importantly, dim-light vision was restored in all treated *rcd1* dogs. These results demonstrate for the first time that gene therapy effectively restores long-term retinal function and vision in a large animal model of autosomal recessive rod-cone dystrophy, and provide great promise for human treatment.

Received 17 March 2012; accepted 17 June 2012; advance online publication 24 July 2012. doi: 10.1038/mt.2012.134

INTRODUCTION

Retinitis pigmentosa (RP), or rod-cone dystrophy, comprises a wide spectrum of incurable hereditary retinal dystrophies characterized by sequential degeneration of rod and cone photoreceptors.[1] Early symptoms include night blindness and loss of peripheral vision due to progressive rod photoreceptors degeneration. This phase is followed by cone death and concomitant loss of central day vision. RP may be inherited as an autosomal recessive (50–60%), autosomal dominant (30–40%), X-linked (5–15%), or simplex/multiplex disease.[2] To date, about 45 genes associated with RP etiology have been identified; most of them are primarily expressed in photoreceptor cells.[3]

Mutations in the gene encoding the β subunit of rod cGMP-phosphodiesterase 6 (PDE6β) are associated with one of the most prevalent forms of autosomal recessive RP, accounting for ~1–2% of all human RP cases.[4–12] Rod PDE6 is localized on the disc membrane of rod outer segments where it plays a key role in the rod phototransduction cascade by controlling the level of cGMP and Ca^{2+} in the rod outer segments. Rod PDE6 is a heterotetrameric complex composed of two homologous catalytic subunits (PDE6α and PDE6β) and two copies of an inhibitory subunit (PDE6γ).[13] As both PDE6α and PDE6β subunits are required for rod PDE6 activity, loss-of-function mutations in the pde6β gene result in an improper function of PDE6 holoenzyme and an accumulation of cGMP and Ca^{2+} in the rod outer segments. This ultimately leads to rod then cone photoreceptor death through apoptosis by non-well defined mechanisms.[14–16]

There is currently no cure for RP caused by PDE6β deficiency. Addition gene therapy is an attractive approach for PDE6β-RP.

Gene therapy approaches to delay photoreceptors degeneration have already been employed in three murine models of PDE6β-RP, the rodless 1 (*rd1*),[17] the retinal degeneration 10 (*rd10*)[18,19] and the PDE6βH620Q.[20] Various vectors encoding murine or human pde6β gene have been tested, including adenovirus,[21] adeno-associated virus (AAV),[22–25] simian immunodeficiency virus,[26] herpes simplex virus,[27] and lentivirus.[20,28] In most studies functional rescue was limited, despite significant improvement of retinal morphology with an increased number of outer nuclear layer (ONL) nuclei and outer segment length. One of the best functional results (37% preservation of rod electroretinography (ERG) responses and prolonged photoreceptor survival up to postnatal day (P) 35) was obtained in dark-reared *rd10* mice, a model with a slower rate of degeneration than *rd1* mice, treated at P14 using an AAV2/5smCBA.mpde6β vector.[23] This suggest that difficulties in achieving sustained long-term functional

Correspondence: *Fabienne Rolling, Translational Gene Therapy for Retinal and Neuromuscular Diseases, INSERM UMR 1089, Institut de Recherche Thérapeutique 1, Université de Nantes, 8 quai Moncousu, 44007 Nantes Cedex 01, France. Email: fabienne.rolling@inserm.fr*

rescue in murine models of PDE6β-deficiency may not be related to specific characteristics of the PDE6β subunit but to (i) excessively rapid loss of photoreceptors in these models and mainly to (ii) difficulties in achieving sufficient level of transgene expression in mutant photoreceptors before their irreversible degeneration. This hypothesis was reinforced by a recent successful gene addition therapy in the same mouse model after subretinal injection of a fast-acting AAV2/8(Y733F)smCBA.mpde6β vector.[24] In this recent "proof-of-concept" study, the authors reported on a subsequent 58% preservation of rod ERG responses, rod-mediated vision-guided behavior and rod survival for up to 6 months.

Preclinical evaluation of recombinant AAV (rAAV)-mediated gene transfer in large animal models (*i.e.*, dogs, cats, pigs, and nonhuman primates) is a key step for future clinical development.[29] Indeed, the size and anatomy of the eye in large animals provide a more relevant model than rodents in terms of pathobiology and surgical approaches. Moreover, their longevity enables long-term evaluation of the treatment, which is crucial for pathologies such as PDE6β deficiency that typically progress over decades in humans.

The *Rcd1* dog is a natural large animal model of progressive retinal degeneration. The *Rcd1* dog carries a (2420G>A) nonsense mutation in the C-terminus of the PDE6β subunit[30] leading to truncation and destabilization of the gene product and a nonfunctional PDE6 holoenzyme.[31,32] Retinal development is normal in affected dogs until 13 days of age, at which point photoreceptor development is arrested. Rod degeneration then occurs gradually from 1 to 5 months of age, followed by cone loss within 1 to 2 years.[33,34] This clinical course of generalized retinal atrophy, which strongly mimics retinal degeneration in humans, makes this PDE6β deficient dog a valuable large animal model for the evaluation of gene therapy.

In the present study, we investigated the long-term efficacy of early rAAV-mediated pde6β gene transfer in the *rcd1* dog. Our findings demonstrate, for the first time, that gene transfer prevents long-term photoreceptor death and restores electrophysiological function and vision in this large animal model.

RESULTS

Recombinant AAV2/5 and AAV2/8 vector design and subretinal administration to *rcd1* dogs

We generated rAAV2/5 or rAAV2/8 vectors carrying the canine *pde6β* (*cpde6β*) gene under the control of the photoreceptor-specific human rhodopsin kinase (RK) promoter[35,36] to drive rapid and strong transgene expression in photoreceptors (**Figure 1**).

Rcd1 dogs display an early and severe rod-cone photoreceptor degeneration that starts in the central retina at P25, during postnatal differentiation of photoreceptor cells.[33,34] This rapid onset of retinal degeneration in *rcd1* dogs suggests that early therapeutic intervention is critical to prevent rod photoreceptor cell death in this model. To this end, we chose to treat *rcd1* dogs at P20, before extensive rod photoreceptor loss.

A total of eight *rcd1* dogs (A2–A9) were injected subretinally at the age of 20 days. Dogs A2 to A5 were treated with AAV2/5RK.cpde6β, whereas dogs A6 to A9 were injected with AAV2/8RK.cpde6β (**Table 1**). All injections were performed unilaterally in the right retina, except for dog A9 which received AAV2/8RK.cpde6β in both eyes due to the observation of significant vector reflux into the vitreous during the subretinal injection of the right eye. Subretinal blebs were restricted to the nasal superior retina and covered ~25% of the entire retinal surface, except in the right eye of dog A9 in which the bleb was much smaller.

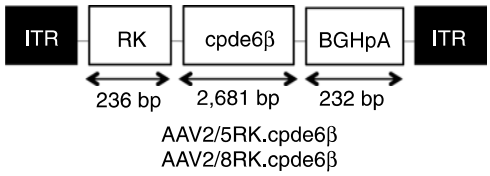

Figure 1 Schematic structure of recombinant adeno-associated virus (AAV) vectors. AAV2/5RK.cpde6β and AAV2/8RK.cpde6β vectors encode the canine pde6β cDNA under the control of a human RK promoter (–112 bp to +87 bp region of the proximal promoter[36]). BGHpA, bovine growth hormone polyadenylation signal; cpde6β, canine pde6β cDNA; ITR, inverted terminal repeats from AAV2; RK, human rhodopsin kinase promoter.

Table 1 List of dogs included in the study and ERG amplitudes

		Rod ERG (μV)			30Hz Flicker (μV)		
		1 mpi	9 mpi	18 mpi	1 mpi	9 mpi	18 mpi
Dog	Vector	T/U	T/U	T/U	T/U	T/U	T/U
NA1		169/166	215/182	140/128	45/46	67/65	43/42
NA2	None	141/191	[a]	[a]	33/39	[a]	[a]
A1		0/0	11/15	0/0	44/38	43/56	6/9
A2		47/0	43/10	53/0	45/53	54/53	40/14
A3	AAV2/5RK.cpde6β	34/0	34/0	42/0	39/35	17/15	25/13
A4	(10^{11} vg/ml)	40/0	52/0	nd	51/27	41/39	nd
A5		nd	[a]	[a]	nd	[a]	[a]
A6		37/0	87/0	63/0	21/46	38/15	30/11
A7	AAV2/8RK.cpde6β	45/0	37/0	28/0	42/29	23/17	19/9
A8	(10^{12} vg/ml)	41/0	41/0	nd	36/28	27/21	nd
A9		19[b]/64[b]	[a]	[a]	37[b]/30[b]	[a]	[a]

Abbreviations: 30 Hz Flicker, photopic 30 Hz Flicker amplitude; A, affected; mpi, month(s) postinjection; NA, nonaffected; nd, not done; rod ERG, scotopic rod-mediated b-wave amplitude; T, treated eye; U, untreated eye; vg, vector genome.
[a]Sacrificed for RT-PCR and/or histology. [b]Dog A9 received AAV2/8RK.cpde6β in both right and left eyes.

In all treated eyes, no apparent surgically induced retinal damage was noted by fundus photography or optical coherence tomography (OCT) at 2 months postinjection (mpi), despite the small size of the eye and the immaturity of the retina at the time of the subretinal injection (data not shown).

Assessment of transgene expression in *rcd1*-treated retinas

To evaluate pde6β transgene expression after subretinal injection of AAV2/5RK.cpde6β and AAV2/8RK.cpde6β vectors, presence of pde6β transcripts was assessed by reverse transcription (RT)-PCR in treated retinas of dogs A4 and A8, at 4 mpi (**Figure 2**).

As our preliminary RT-PCR analysis indicated that the *rcd1* dogs expressed mutant (2420G>A) pde6β transcripts at the

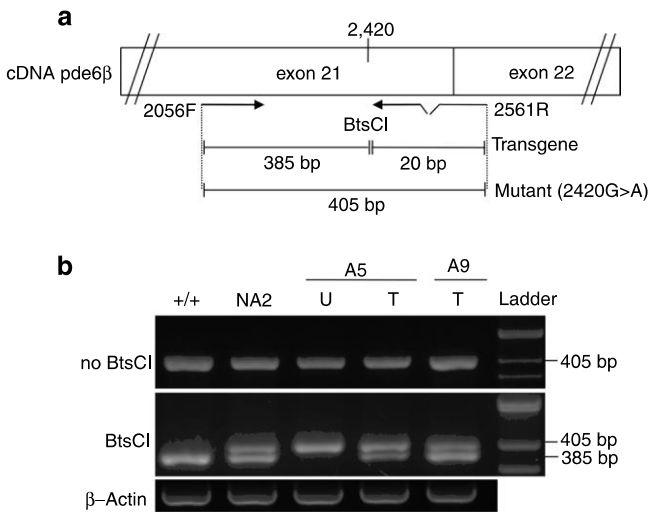

Figure 2 Detection of transgene (wild-type) and endogenous (mutant) pde6β transcripts in A5- and A9-treated retinas at 4 mpi. (**a**) Reverse transcription-PCR (RT-PCR) amplification of retinal cDNA using 2056F- and 2561R-specific primers generates a 405 bp product encompassing a portion of exons 21 and 22 of transgene and native pde6β transcripts. Mismatched 2561R specifically creates a unique *Bts*CI restriction site in PCR products arising from pde6β transgene transcripts, dividing the 405 bp product into 385 and 20 bp fragments. This *Bts*CI restriction site is not present in PCR products derived from mutant RNA templates. Arrows indicate the positions of the 2056F and 2561R primers used in RT-PCR. (**b**) Agarose gel electrophoresis of RT-PCR products after complete BtsCI digestion. Lines 1 and 2 show products from Pde6β$^{+/+}$ and Pde6β$^{+/-}$ (NA2) untreated control retinas, respectively. Lines 3 and 4 show products from untreated and AAV2/5RK.cpde6β-treated retinas of dog A5 at 4 mpi, respectively. Line 5 shows the AAV2/8RK.cpde6β-treated right retina of dog A9. +/+, Pde6β$^{+/+}$ retina; AAV, adeno-associated virus; bp, base pairs; ladder, 1 kb molecular size ladder; T, treated retina; U, untreated retina.

time of injection (P20) (data not shown), we used allele-specific RT-PCR to ensure discrimination between wild-type (transgene) and mutant 2420G>A (endogenous) pde6β transcripts in treated retinas.

Total retinal RNA was reverse-transcribed and subjected to PCR amplification designed to generate a 405 bp product encompassing a portion of exons 21 and 22 of both wild-type and mutant 2420G>A pde6β transcripts. A mismatched reverse primer specifically created a unique *Bts*CI restriction site in the PCR products arising from wild-type pde6β RNA templates, dividing the 405 bp product into 385 and 20 bp fragments (Figure 2a). This *Bts*CI restriction site was not created in the PCR products derived from mutant RNA templates. Thus, one could expect the complete digestion of RT-PCR products by BtsCI endonuclease to result in a 385-bp digestion product in RNA templates arising from Pde6β$^{+/+}$ retinas, a 405 bp product in RNA templates arising from untreated Pde6β$^{-/-}$ retinas and both 385 and 405 bp products in RNA templates arising from Pde6β$^{+/-}$ and rAAV-treated Pde6β$^{-/-}$ retinas.

The results were as expected (Figure 2b). Transgene-derived 385 bp product was detected in both AAV2/5RK.cpde6β- and AAV2/8RK.cpde6β-treated retinas. On the contrary, this 385 bp product was never detected in the untreated *rcd1* retina. These results clearly show that vector-encoded pde6β was expressed in both AAV2/5RK.cpde6β- and AAV2/8RK.cpde6β-treated retinas.

AAV2/5RK.cpde6*β* and AAV2/8RK.cpde6*β* preserve retinal structure

Fundus appearance and retinal thickness were evaluated in all dogs using color fundus photography and OCT. These noninvasive examinations were performed from 2 to 18 mpi for dogs A2, A3, A6, and A7, from 2 to 8 mpi for dogs A4 and A8, and from 2 to 3 mpi for dogs A5 and A9. Recordings on age-matched untreated Pde6β$^{+/-}$ (NA1) and Pde6β$^{-/-}$ (A1) dogs were performed as controls. All examinations were performed bilaterally to optimize the comparison between treated and untreated eyes.

Figure 3 shows the ophthalmoscopy results obtained for rAAV2/5-treated (A3), rAAV2/8-treated (A7) and age-matched Pde6β$^{+/-}$ control (NA1) dogs, at 4 and 18 mpi.

Fundus photography revealed a significant preservation of the retinal vasculature in both rAAV2/5- and rAAV2/8-treated eyes compared with an age-matched Pde6β$^{+/-}$ control. In contrast, severe retinal degeneration, hyper-reflective fundi and attenuated retinal vessels were observed in the untreated left eye of dogs A3 (Figure 3b, left) and A7 (Figure 3c, left) as early as 4 mpi. By 18 mpi, only few central retinal vessels were still visible in the untreated affected eyes and pallor of the optic nerve was observed (Figure 3b,c, right).

In all rAAV-treated eyes, this preservation of fundus appearance was associated with a preservation of central retinal thickness, as assessed by long-term OCT monitoring. At 4 and 18 mpi, the treated retina of dog A3 (224 and 207 µm) was 22 to 24% thicker than the contralateral untreated retina (174 and 157 µm) (Figure 3b). Meanwhile, the treated retina of dog A7 (240 µm) was 17–21% higher than the contralateral untreated retina (199 and 190 µm) (Figure 3c). At 18 mpi, the retinal thickness of A3 AAV2/5RK.cpde6β- and A7 AAV2/8RK.cpde6β-treated retinas was 207- and 240-µm thick, respectively, representing 83–97% of that observed in age-matched noninjected Pde6β$^{+/-}$ eyes (248 µm) (Figure 3a).

To more accurately define the therapeutic effect of rAAV-mediated gene transfer on retinal degeneration observed *in vivo* by OCT, we serially cryosectioned the entire treated retinas of dogs A5 and A9. The untreated left retinas of dogs A5 and NA2 were processed similarly and examined as controls.

The expression of the PDE6β subunit in treated *rcd1* eyes was not evaluated as all commercially available antibodies against the mouse or human PDE6β subunit were tested and found to be nonspecific in dogs due to crossreactivity with the canine PDE6**α** subunit (data not shown). Rod photoreceptors were thus identified by staining for the entire rod PDE6 holoenzyme or GNAT1.

Figure 4 shows photographs of hematoxylin and eosin stained sections and images of rod PDE6 and GNAT1 immunofluorescence obtained from nasal superior retinas of dogs A5 and NA2.

Low magnifications revealed a dramatic difference in retinal morphology between the vector-exposed and unexposed areas of the treated retina of dog A5 (Figure 4a,b). The vector-exposed region of the treated A5 retina retained a nearly normal morphology compared with the Pde6β$^{+/-}$ age-matched control retina (Figure 4c, top). The ONL from the treated A5 retina was 16–17 rows thick (39 ± 3 µm, n = 10), accounting for ~90% of the ONL thickness of the control retina (18–19 rows, 42 ± 2 µm, n = 10) (Figure 4c, top). Most importantly, the mean combined inner and

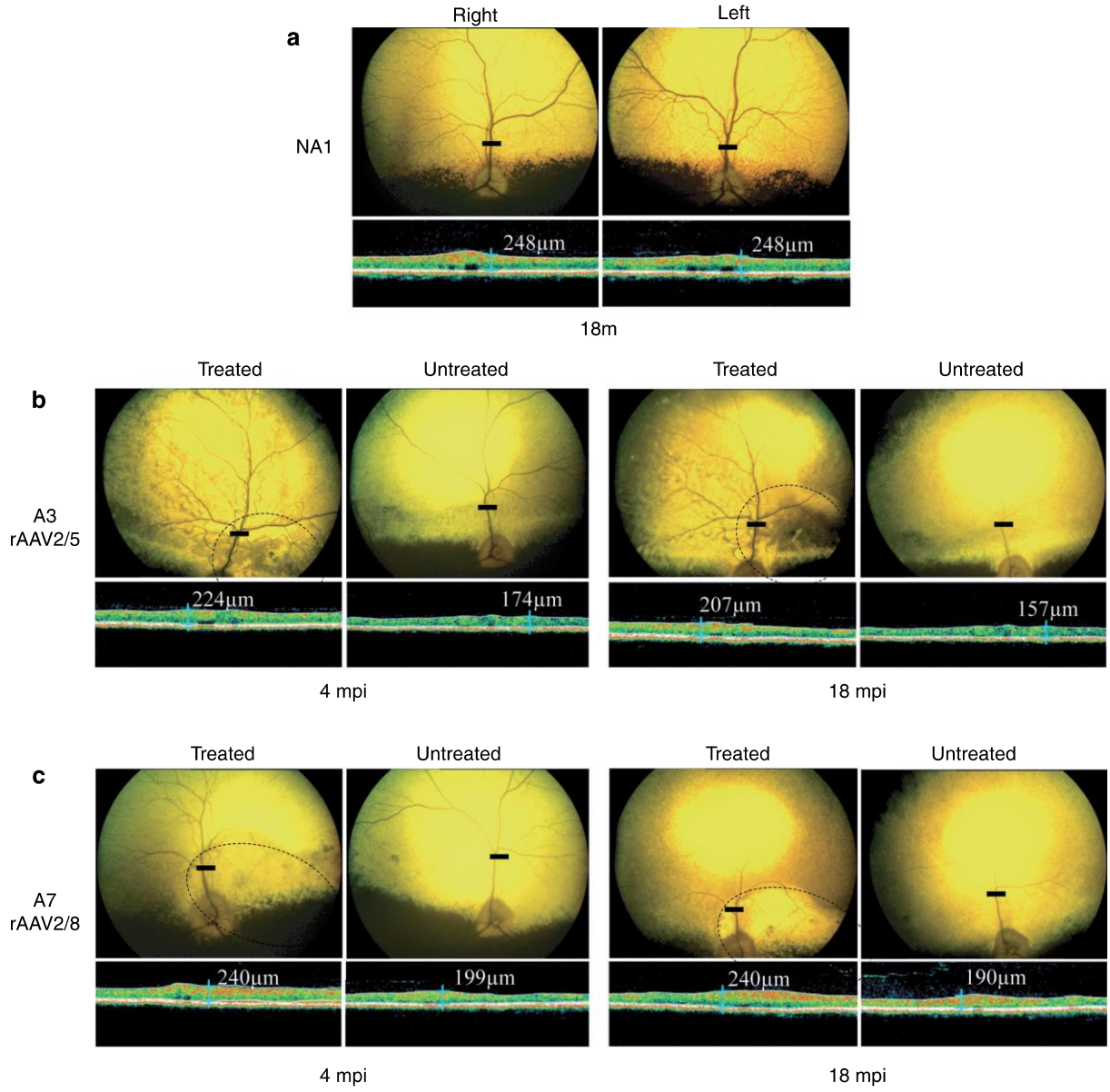

Figure 3 *In vivo* assessment of retinal morphology in dogs A3 and A7 at 4 and 18 mpi. (**a**) Fundus photographs and retinal cross-sectional images obtained from control nonaffected, untreated dog NA1 at 18 months of age. (**b**) Fundus photographs and retinal cross-sectional images obtained from dog A3 treated with AAV2/5RK.cpde6β at 4 and 18 mpi. (**c**) Fundus photographs and retinal cross-sectional images obtained from A7 treated with AAV2/8RK.cpde6β at 4 and 18 mpi. Dark circles on fundus photographs schematically represent areas of the treated retinas exposed to recombinant adeno-associated virus (rAAV) vectors. Optical coherence tomography (OCT) scans were acquired on a horizontal line shown on the fundus images (dark-line). The localization and the size of the dark-lines represent the localization and the size of the OCT scans. Retinal thicknesses at the same location were measured using calibrated calipers and indicated on the OCT scan. mpi, months postinjection; µm, micrometers.

outer segment thickness (22 ± 3 µm, n = 10) was indistinguishable from that of the Pde6β$^{+/-}$ control retina (22 ± 1 µm, n = 10).

In the vector-unexposed region of the A5 treated retina, however, a massive loss of photoreceptor cell nuclei was observed (Figure 4c, top) similarly to that seen in the noninjected contralateral retina. The ONL was reduced to 6–7 rows (20 ± 2 µm, n = 10) which represented only one-third to one-half of the number of rows observed in normal or in the vector-exposed retina respectively, and ~50% of normal or vector-exposed ONL thickness (Figure 4c, top). Moreover, photoreceptor inner and outer segments appeared to be shorter (16 ± 2 µm, n = 10), less dense and disorganized compared with the vector-exposed region and the nonaffected control retina.

Strong PDE6 labeling was found in outer segments in the vector-exposed region of the A5 treated retina (Figure 4c, middle), confirming the preservation of rod photoreceptor morphology after rAAV-mediated gene transfer. In contrast, only mild or undetectable PDE6 immunofluorescence was detected in the vector-unexposed region of the A5 treated retina and in the A5 untreated retina (Figure 4c, middle). A similar pattern of immunofluorescence was obtained using an antibody directed against GNAT1 (Figure 4c, bottom).

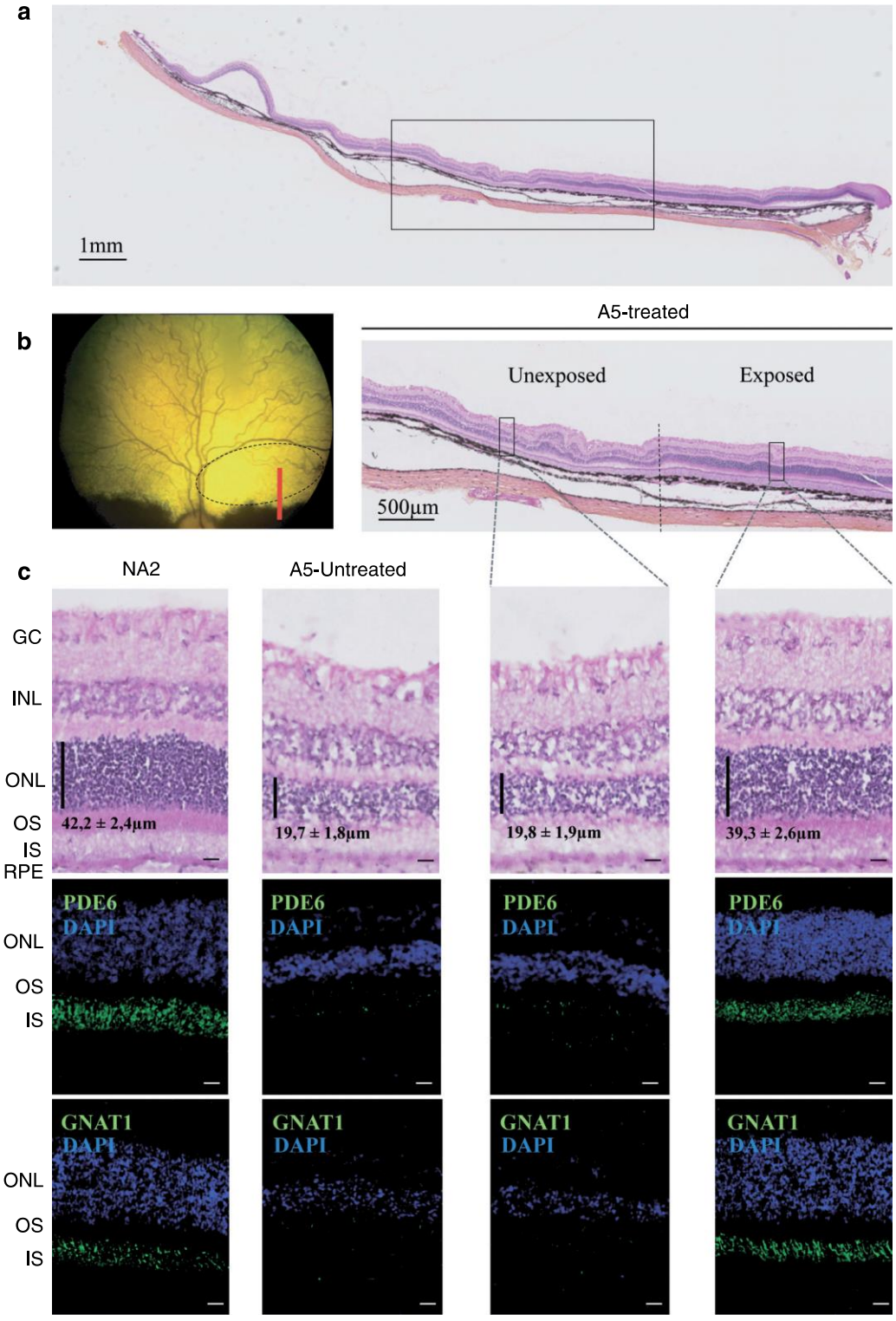

Figure 4 *Post-mortem* **assessment of retinal morphology in dog A5 at 4 months postinjection.** (**a–c**) Nasal retinal cryosections from the treated and untreated eyes of dog A5 at 4 months post subretinal delivery of rAAV2/5RK.cpde6β in the nasal superior retina. (**a**) Wide A5 retinal section displaying vector exposed and unexposed-areas. Retinal layers remained intact while the choroid has been partially detached from the retina during the embedding process. (**b**) Fundus photograph representing the A5 retina exposed to the rAAV2/5 vector (dark circle) and the localization of the wide retinal section (red line). (**c**) Nasal retinal cryosections from unaffected, untreated dog NA2 at 5 months of age and from the untreated and treated eyes of dog A5. Serial retinal cryosections were processed for hematoxylin and eosin coloration (top) and for immunohistochemistry using antibodies against rod PDE6 (middle) or GNAT1 (bottom). Primary antibodies were detected with Alexa 488-conjugated goat anti-rabbit IgG (green). Cell nuclei were counterstained with DAPI (blue). Bar = 10 µm. Vertical dark lines indicate ONL thickness (mean ± SEM, $n = 10$). GC, ganglion cells; INL, inner nuclear layer; IS, inner segments; ONL, outer nuclear layer; OS, outer segments; rAAV, recombinant adeno-associated virus; RPE, outer retinal pigment.

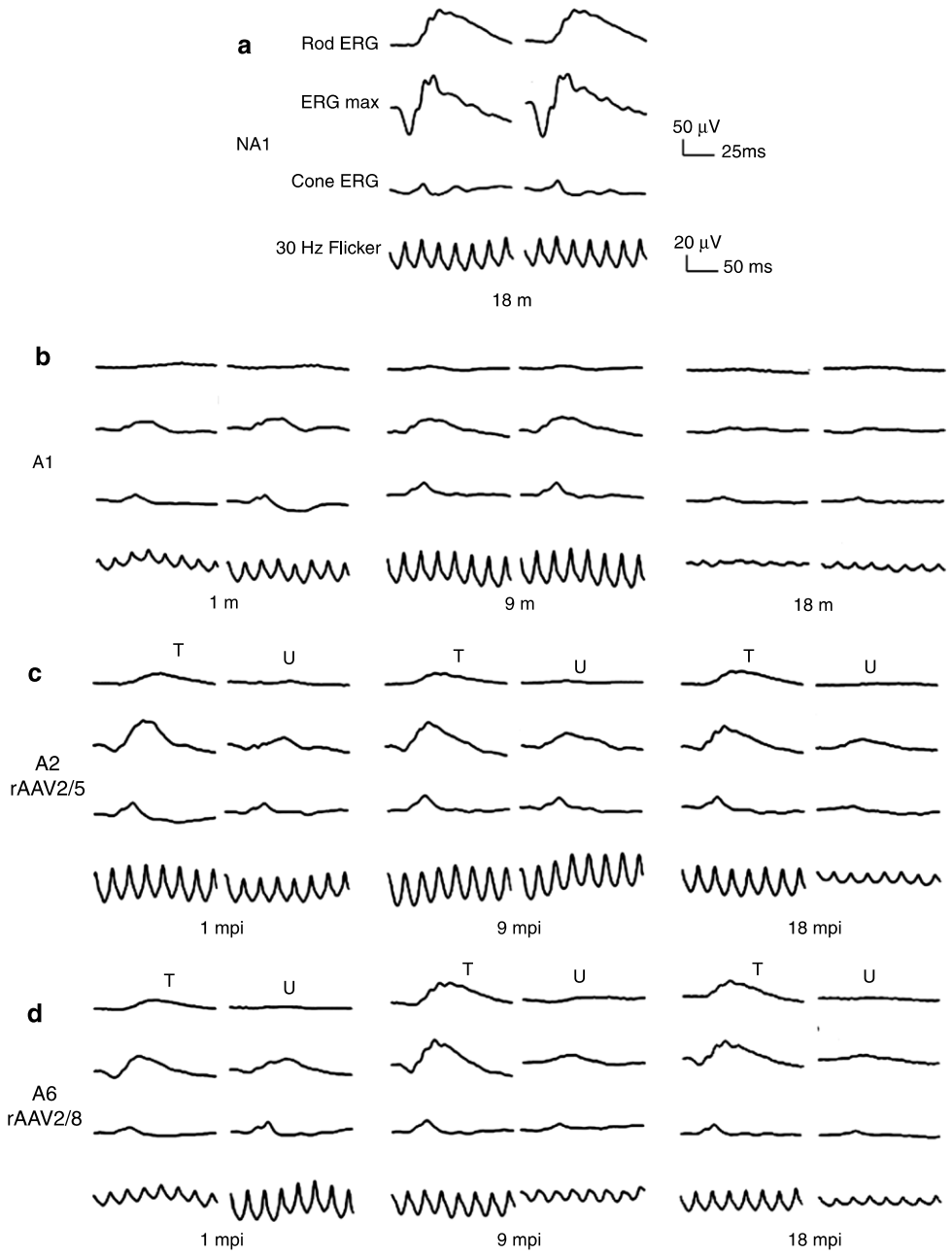

Figure 5 Bilateral full-field electroretinographic traces from dogs NA1, A1, A2, and A6 at 1, 9, and 18 months following subretinal injection. (**a**) Electroretinographic trace from control nonaffected, untreated dog NA1 at 18 months of age. (**b**) Electroretinographic traces from control affected, untreated dog A1 at 1 and 18 months of age. (**c**) Electroretinographic traces from dog A2 treated with AAV2/5RK.cpde6β. (**d**) Electroretinographic traces from dog A6 treated with AAV2/8RK.cpde6β. The top two recordings are low- and high-intensity dark-adapted responses, whereas the bottom two recordings show light-adapted responses (responses to single flash and 30 Hz flicker stimuli, respectively). AAV, adeno-associated virus; mpi, month(s) postinjection; T, treated eye; U, untreated eye.

The analysis of the entire retina showed that the preserved morphology covered ~25% of the total retinal surface (data not shown) and was mostly restricted to the region exposed to the vector.

AAV2/5RK.cpde6*β* and AAV2/8RK.cpde6*β* rescue retinal function

Retinal function was evaluated by the same investigator (L.L.) in all dogs using simultaneous bilateral full-field flash ERG. ERGs were performed on all treated dogs at different timepoints following vector delivery, starting at 1 mpi, except for dog A5 for which retinal function was first assessed at 3 mpi. Follow-up was 18 mpi for dogs A2, A3, A6 and A7, 9 mpi for dogs A4 and A8, and 4 mpi for dogs A5 and A9. Recordings on age-matched untreated Pde6β$^{+/-}$ (NA1) and Pde6β$^{-/-}$ (A1) dogs were performed as controls (Table 1).

Representative ERG waveforms for dogs A1, A2, and A6 at 1, 9, and 18 mpi are shown in Figure 5. The kinetics of functional recovery in dogs A2 and A6 are presented in Figure 6.

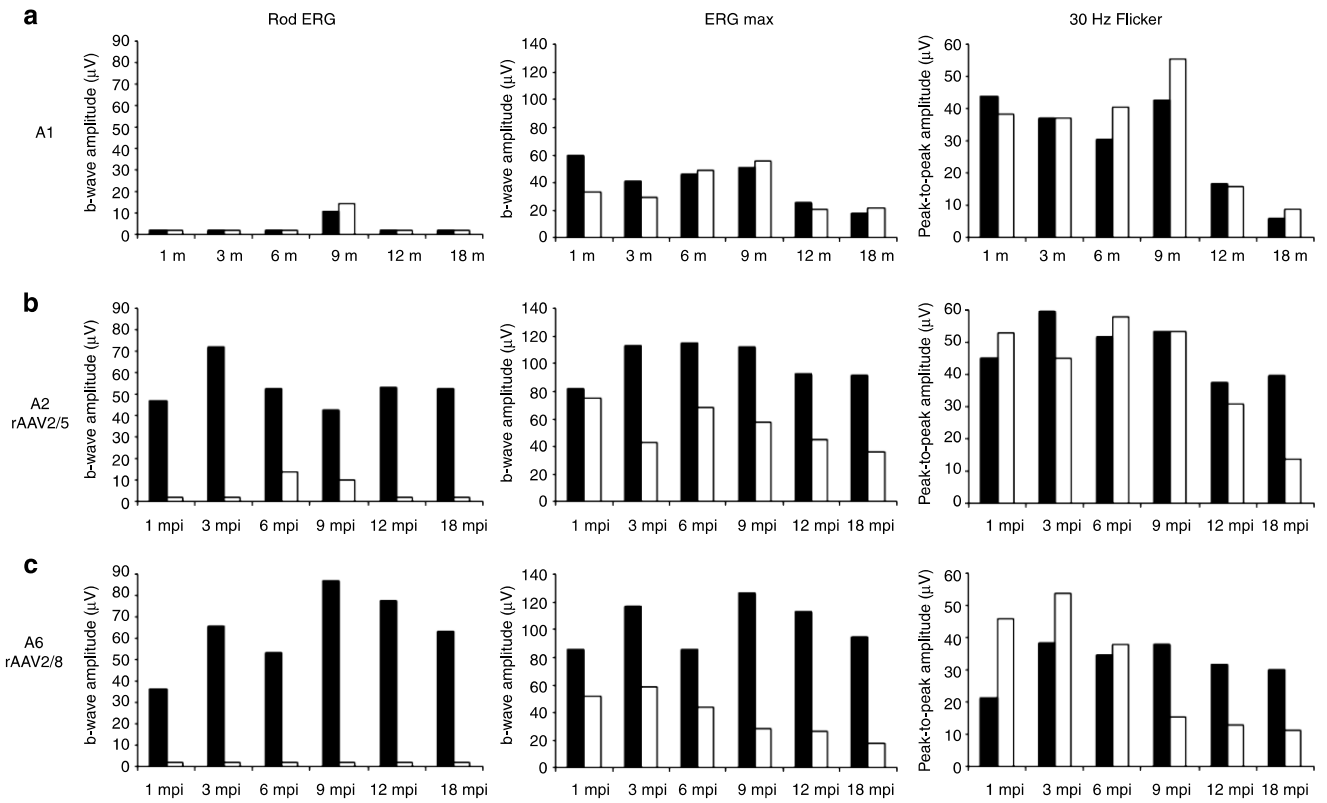

Figure 6 Kinetics of retinal function recovery in treated dogs A2 and A6. (**a**) Amplitudes of electroretinography (ERG) responses for control affected, untreated dog A1 from 1 to 18 months of age. (**b**) Amplitudes of ERG responses for dog A2 treated with AAV2/5RK.cpde6β from 1 to 18 mpi. (**c**) Amplitudes of ERG responses for dog A6 treated with AAV2/8RK.cpde6β from 1 to 18 mpi. The left and middle panels show scotopic rod and mixed cone-rod-mediated b-wave amplitudes, respectively. The right panel shows photopic 30 Hz flicker amplitude. Right eyes are shown in dark, left eyes in white. AAV, adeno-associated virus; mpi, month(s) postinjection.

We found that both AAV2/5RK.cpde6β and AAV2/8RK.cpde6β-subretinal delivery led to substantial restoration of rod function in all treated eyes as soon as 1 mpi (Table 1 and Figures 5c,d and 6b,c). In contrast, the rod responses were undetectable in the contralateral untreated eyes (Figures 5c,d and 6b,c) and in untreated control Pde6β$^{-/-}$ eyes (Table 1 and Figures 5b and 6a) at this timepoint.

Although the general trend of rod function recovery was similar in all rAAV2/5- or rAAV2/8-treated eyes, interindividual's variations were observed (Table 1) and might reflect small variations on the extent and/or localization of the vector bleb.

In all rAAV2/5- and rAAV2/8-treated dogs, the amplitude of rod function recovery increased slightly between 1 and 3 mpi and remained stable thereafter, up to 18 mpi, the longest period of observation (Figure 6b,c, left). In all treated dogs, restored rod function exhibited typical a- and b-wave components (Figure 5c,d).

At 18 mpi, the median b-wave amplitude recorded on AAV2/5RK.cpde6β- (47 ± 8 μV, n = 2) and AAV2/8RK.cpde6β- (46 ± 25 μV, n = 2) treated eyes represent 35% of that recorded on nonaffected eyes (134 ± 8 μV, n = 2) (**Supplementary Figure S1**). At 18 mpi, the maximal b-wave amplitudes were recorded on A2 AAV2/5RK.cpde6β- (53 μV, 38% of the normal rod function) and A6 AAV2/8RK.cpde6β- (63 μV, 45% of the normal rod function) treated retinas (Table 1 and Figure 6b,c, left).

The cone-mediated ERG (30 Hz Flicker) responses in treated and untreated eyes were similar in all AAV2/5RK.cpde6β- and AAV2/8RK.cpde6β-injected dogs over the first 8–12 month period postvector delivery (Figure 6b,c).

Interestingly, ERG max and 30 Hz flicker amplitudes remained stable in all treated eyes over the 12–18 mpi period while a progressive and consistent reduction of these responses was observed in all contralateral untreated eyes during this period (Table 1 and Figures 5c,d, and 6b,c).

At 18 mpi, the median amplitude of the 30 Hz flicker of AAV2/5RK.cpde6β- (33 ± 11 μV, n = 2) and AAV2/8RK.cpde6β- (25 ± 8 μV, n = 2) treated eyes represent 76 and 56% of that recorded on age-matched Pde6β$^{+/-}$ control eyes (43 ± 1μV, n = 2), respectively (**Supplementary Figure S1**). At 18 mpi, the maximal amplitudes of the 30 Hz flicker were recorded on A2 AAV2/5RK.cpde6β- (40 μV, 93% of the normal cone function) and A6 AAV2/8RK.cpde6β- (30 μV, 70% of the normal cone function) treated retinas (Table 1 and Figure 6b,c, left). They were approximately threefold higher than responses recovered for their contralateral untreated eyes (14 and 11μV).

Interestingly, the level of rod function restoration and cone function preservation obtained following delivery of rAAV2/5 was not significantly different from that achieved with the rAAV2/8 (**Supplementary Figure S1**).

AAV2/5RK.cpde6β and AAV2/8RK.cpde6β restore vision

Vision tests were performed on A2, A3, A6, and A7 treated Pde6β$^{-/-}$ dogs at 4, 8, 12, and 18 months postvector delivery (Table 2). Dim-light conditions were used to assess transmission of rescued rod activity to higher visual pathways and improvement of visually guided behavior. Bright light conditions were used to assess preservation of day vision in treated *rcd1* dogs.

Under dim-light conditions at 4 and 8 mpi, none of the treated dogs showed behavioral signs of blindness in both eyes (Table 2). However, at the latest timepoints (12 and 18 mpi), all treated dogs avoided obstacles when their untreated eye was occluded while they showed difficulty to navigate around the obstacle panels when their treated eye was occluded. They moved very cautiously with their nose to the ground and tried to feel the panels with their forelegs. Several collisions with obstacles were also noted. These results were confirmed by a significant increase in transit time. For example, dog A6 completed the obstacle course in 7 seconds with the untreated eye covered and in 30 seconds with the treated eye covered (**Supplementary Video S1**, part I). Dog A6 took a comparable time to complete the obstacle course with the untreated eye covered than a control nonaffected Pde6β$^{+/-}$ dog with one eye covered (9 seconds, data not shown).

In bright light conditions, none of the treated dogs showed behavioral signs of blindness from 4 to 18 mpi regardless of which eye was covered (Table 2 and **Supplementary Video S1**, part II).

Table 2 Evolution of dim- and bright-light vision in PDE6β$^{-/-}$ treated dogs

		Behavioral test					
		Dim-light			Bright-light		
		4 mpi	12 mpi	18 mpi	4 mpi	12 mpi	18 mpi
Dog	Vector	T/U	T/U	T/U	T/U	T/U	T/U
A2	AAV2/5RK.cpde6β	+/+	+/-	+/-	+/+	+/+	+/+
A3		+/+	+/-	+/-	+/+	+/+	+/+
A6	AAV2/8RK.cpde6β	+/+	+/-	+/-	+/+	+/+	+/+
A7		+/+	+/-	+/-	+/+	+/+	+/+

Abbreviations: –, impaired vision; +, correct vision; mpi, months postinjection; T, treated eye; U, untreated eye.
Vision tests were performed in dim (1.5 ± 0.8 lux) or bright (260 ± 13lux) light at different timepoints postinjection. An opaque lens was used to alternatively cover treated (right) and untreated (left) eyes.

DISCUSSION

In this study, a total of eight *rcd1* dogs were subretinally injected with rAAV2/5 and rAAV2/8 vectors carrying the cpde6β cDNA under the control of the photoreceptor-specific RK promoter. The results demonstrated that rAAV-mediated cpde6β expression restored rod function and consequently, prevented photoreceptor death and concomitant vision loss in treated dogs for at least 18 mpi (the duration of the study).

Interestingly, rod-mediated ERG responses were undetectable in the *rcd1* canine model from the earliest age measured[37] (1 month of age, Table 1). At this age, the PDE6β subunit was undetectable by immunoblot and rod PDE6 function was absent, suggesting that the *rcd1* dog carries a *null* mutation in the pde6β gene.[30] In this matter, this canine model of PDE6β deficiency is similar to the *rd1* murine model in which PDE6 function is also completely lacking,[17] but different from the hypomorphic *rd10* and Pde6βH620Q murine models in which photoreceptors develop and function almost normally before their degeneration.[18–20]

Here, we show that both AAV2/5RK.cpde6β and AAV2/8RK.cpde6β-gene transfer restored sustained and stable rod-mediated ERG responses in all treated *rcd1* eyes as early as 1 month postinjection (Figure 5). From 1 to 18 mpi, median amplitudes of dark-adapted b-waves in rAAV-treated eyes account for 28–35% of those recorded in normal eyes (**Supplementary Figure S1**), consistent with the estimated area of retina directly exposed to the vectors (~25% of the total retinal surface).

This is the first demonstration that gene therapy can restore a rod function in a *null* animal model of PDE6β deficiency as all attempts to treat the *rd1* mice by gene addition therapy have failed to provide functional rescue.[21,26,27] In contrast, in the *rd10* mouse, previous studies demonstrated that subretinal injection of AAV2/5smCBA.mpde6β led to the preservation of 37% of rod ERG responses up to P35,[23] and that subretinal injection of AAV2/8(Y733F)smCBA.mpde6β led to a preservation of 58% of rod ERG responses for up to 6 months after treatment.[24]

This finding has obvious clinical significance because among the 21 causative-mutations already identified in patients with PDE6β-recessive RP,[4–12] 8 (38%) are nonsense mutations predicted to lead to a complete loss of PDE6 function.[5–8,10] The most sustained rescue of rod function in *null* animal models of progressive photoreceptor defects reported to date was obtained in the Aipl1$^{-/-}$ mouse, in which both rod and cone functions are absent at birth. In this model, subretinal injection of AAV2/8RK.haipl1 at P10 led to a 50% restoration of wild-type scotopic ERG responses for at least 4 weeks postinjection.[38] When scAAV2/8(Y733F)RK.haipl1 was used,[39] this rescued rod function was more sustained persisting until P60 (the duration of the reported study).

In addition to this sustained restoration of rod function in treated *rcd1* retinas, long-term preservation of cone-mediated ERG responses were demonstrated up to 18 mpi (Table 1 and Figures 5 and 6). This result strongly suggests that rAAV-mediated gene therapy inhibited or delayed the initiation of secondary cone death in treated *rcd1* retinas. A similar beneficial effect of the primary rod treatment on the cone function has been previously obtained in *rd10* mice treated with AAV2/8(Y733F)smCBA.mpde6β for at least 6 weeks postinjection[24] (the duration of the reported study).

Several mechanisms have been proposed to explain the non-autonomous death of cones in rod-cone dystrophies: the loss of a rod-derived trophic support, the release of a toxic factor by dying rods, an increase in oxidative damage to cones once the rods have died or an imbalance in the metabolism of cones due to changes in retinal architecture.[14–16] In all these models, primary loss of rods is responsible for secondary cone death, indicating that protection of cones after rAAV-mediated gene transfer might be correlated with a preservation of rod cells in treated *rcd1* retinas.

Long-term preservation of central retinal thickness in treated *rcd1* eyes was observed by OCT from 4 to 18 mpi (Figure 3). Our histology data at 4 mpi suggested that this reflects the retention of rod photoreceptor cells in treated retinas (Figure 4).

Interestingly, this preservation of rod photoreceptors was not widespread but mainly restricted to nasal vector-exposed areas of treated retinas. Similar results have been recently shown in RPGR canine models of X-linked RP following subretinal injection of AAV2/5IRBP.hrpgr or AAV2/5RK.hrpgr.[40] This observation may have two notable clinical implications. First, it demonstrates that degenerating nontransduced photoreceptors have no major negative impact on transduced photoreceptor survival as previously suggested.[41] Second, it surprisingly indicates that localized preservation of rod photoreceptor cells in the nasal superior retina (that did not comprise the cone-rich *area centralis*[42]) is sufficient to maintain the nearly total cone function and subsequently delay initiation of cone loss. We do not have yet a clear explanation of the apparent complete retention of cone function observed in the treated *rcd1* retinas. It might be related to the physic and/or trophic interactions of preserved rods with other retinal cell populations.[14–16] Further monitoring of the cone function for months or years in treated *rcd1* dogs will be essential to confirm its stability overtime and injection of additional dogs will be required to identify the underlying molecular mechanism for this long-term preservation of cone function.

The effect of the rAAV-mediated gene therapy on the vision of treated *rcd1* dogs was assessed by behavioral tests under dim (1.5 ± 0.8 lux) and bright (260 ± 13 lux) light conditions. It is important to note that, in these two conditions, it was impossible to discriminate rod- from cone-mediated vision because both types of photoreceptors were stimulated.

In dim light, all treated dogs displayed normal vision behavior using either their untreated and treated eyes up to 8 mpi (**Table 2**), probably due to the preservation of normal cone function in both eyes (**Table 1** and **Figures 5** and **6**). Over the 8 to 18 mpi period, none of the treated dogs were still able to successfully negotiate the obstacle course using their untreated eye (**Supplementary Video S1**, part I) consistent with the progressive loss of cone function observed by ERG analysis at these late timepoints (**Table 1** and **Figures 5** and **6**). In contrast, they maintained normal vision-elicited behavior using their treated eyes (**Supplementary Video S1**, part I), demonstrating that rAAV-mediated restoration of rod function and/or preservation of cone function preserve long-term night vision in treated *rcd1* dogs.

In bright light, untreated dogs displayed vision over the 18-month period (**Supplementary Video S1**, part II) certainly due to the residual cone function in both eyes (**Table 1** and **Figures 5** and **6**). It will be necessary to further monitor the vision of treated rcd1 dogs over several years to determine whether the preservation of cone function observed by ERG analysis will also lead to long-term preservation of day vision over time.

In this study, the efficacy of rAAV2/5 and rAAV2/8 vectors was comparable with both vectors providing similar rod-mediated ERG responses in treated *rcd1* eyes (**Table 1**). This result was surprising as rAAV2/8 (10^{12} vg/ml) was injected at a tenfold higher titer than rAAV2/5 (10^{11} vg/ml) vector. One possible explanation might be the broader dispersion of rAAV2/8 in the canine retina after subretinal delivery.[43] The higher potential of rAAV2/8 for widespread diffusion across synapses may reduce the global number of rAAV-delivered vector genomes in photoreceptors cells and subsequently the level of pde6β expression. Alternatively or in addition, it is possible that in both rAAV2/5- and rAAV2/8-treated eyes, the saturation threshold of pde6β expression level was reached.

Interestingly, both rAAV2/5 and rAAV2/8 vectors provided long-term therapy in the *rcd1* dog. This result contradicts previous reports in mouse models of Pde6β,[24] Aipl1,[38] and Rpgrip1[44] deficiencies that have shown a strong functional advantage of rAAV2/8 and/or rAAV2/8(Y733F) vectors compared with the rAAV2/5 vector. This significant discrepancy in long-term rAAV2/5 efficiency between the *rcd1* dog and these murine models of retinal dystrophies probably reflects the slower rate of retinal degeneration in the *rcd1* dog.[33,34] This result should be considered in the context of PDE6β-patients as they typically describe impaired or absent night vision in childhood, followed by a reduction of their visual field from young adulthood, which slowly progresses over decades.[4–6]

In this study, we used rAAV vectors carrying the cpde6β under the control of the human RK promoter which has been demonstrated to drive transgene expression in both rods and cones after subretinal delivery,[35,36,40] whereas the β subunit of PDE6 is specifically expressed in rod photoreceptors.[13] Recombinant AAV-mediated gene therapy in *rcd1* retinas may thus led to undesirable ectopic expression of pde6β in transduced cones. It was unfortunately not possible to assess this pde6β expression in cones due to the limitations of pde6β immunostaining. However, based on the finding that rAAV-treated eyes exhibited no appreciable reduction of cone function over the 18-mpi period (**Table 1**), it is likely that this potential RK-mediated ectopic expression of pde6β has no toxic effects on the cone function, at least at this stage. These results have high clinical relevance because they suggest the potential safety of the human RK promoter for future treatment of pde6β defects.

In conclusion, this study demonstrated, for the first time, that rAAV-mediated gene transfer efficiently corrects the pde6β defect in a large animal model of pde6β deficiency, leading to (i) robust and stable restoration of rod function and (ii) concomitant long-term preservation of cone function and vision. As mutations in the *pde6β* gene are one of the leading causes of recessive RP[4–12] and as retinal degeneration in the *rcd1* dog is highly similar to the human disease, this preclinical study represent a major step towards the future development of this therapy in patients with PDE6β-deficiencies. In a larger sense, these PDE6β results offer great promise for the treatment of many other rapid recessive rod-cone dystrophies due to a rod-specific defect.

MATERIALS AND METHODS

Plasmid construction and production of rAAV vectors. Recombinant AAV2/5.RK.cpde6β and AAV2/8.RK.cpde6β vectors were produced by triple transfection of 293 cells according to previously reported methods,[45] using the SSV9RK.cpde6β vector plasmid. This construct carried the cpde6β cDNA (2,681 bp) directly under the control of the short human RK promoter (−112 bo to +87 bp region of the proximal promoter[36]) and the bovine growth hormone polyadenylation signal (BGHpA), flanked by two AAV2 inverted terminal repeat sequences.

For the SSV9RK.cpde6β construction, full-length cpde6β cDNA (NCBI RefSeq NM_001002934.1) was amplified by PCR from Pde6β$^{+/+}$ canine retinal cDNA. Two primers designed to cover the entire sequence of the *pde6β* gene were used for this purpose. The forward

primer encoded a *Hind*III end and the first 15 bp of the *cpde6β* gene (5′-AATTAAGCTTTAGACAGCCGGACAC-3′). The reverse primer (5′-CTTTATTCATAGTTGAGTTT-3′) encoded a 20 bp sequence of the *cpde6β* gene located 121 bp downstream of the stop codon. An endogenous EcoRV restriction site was present in the sequence of cpde6β 82 bp downstream of the stop codon. The PCR product (2,728 bp) was purified, digested by *Hind*III and *EcoRV* and cloned into a parental plasmid SSV9RK.crpgrip1, between the RK promoter and the bovine growth hormone polyadenylation site, after removal of the eGFP sequence (by *Hind*III and *EcoRV* digestion). The identity of the resulting SSV9RK.cpde6β construct was verified by sequencing.

Viral vector titers were determined by dot-blot and by quantitative real-time PCR and expressed as vector genomes (vg) per milliliter (vg/ml). The final vector titers of AAV2/5RK.cpde6β and AAV2/8RK.cpde6β were 1.10^{11} and 1.10^{12} vg/ml, respectively.

Animals. A total of nine affected Pde6β$^{-/-}$ and 1 Pde6β$^{+/-}$ control Irish Setter dogs were used in this study (**Table 1**). The first three Pde6β$^{-/-}$ individuals were kindly provided D.J. Maskell (University of Cambridge, Cambridge, UK). Animals were maintained at the Boisbonne Center (ONIRIS, Nantes-Atlantic College of Veterinary Medicine, Food Science and Engineering, Nantes, France) under a 12/12 hour light/dark cycle. All experiments involving animals were conducted in accordance with the Association for Research in Vision and Ophthalmology statement for the use of animals in ophthalmic and vision research.

Subretinal administration of rAAV vectors. Subretinal injections of AAV2/5RK.cpde6β and AAV2/8RK.cpde6β vectors were performed on 8 affected Pde6β$^{-/-}$ dogs at P20. For all dogs except A9, vector delivery was unilateral, leaving the contralateral eyes without injection as internal controls (**Table 1**). All subretinal injections were performed under general anesthesia induced by intramuscular injection of a mixture of diazepam (Hoffmann-La Roche, Basel, Switzerland) and ketamine (Rhone Merieux, Lyon, France) and maintained by inhalation of isofluorane gas. Pupils were fully dilated by topical administration of 0.3% atropine (Alcon Cusi SA, Barcelona, Spain), tropicamide (Novartis, Annonay, France) and phenylephrine hypochloride (Novartis).

Surgery was conducted using a transvitreal approach as previously described,[46] without vitrectomy. Under microscopic control, 80–120 µl of vector solution were injected into the subretinal space. Immediately after the injection, the localization and the extent of the retinal surface directly exposed to the vector were recorded on schematic fundus drafts as it was not possible to obtain clear fundus photography of the dog retina until 2 months of age. The precise orientation of the vector bleb was further determined by fundus photography at 2 mpi, by the observation of brighter areas that delineate the border of the treated area (data not shown).

Post-surgical care included one topical administration of 0.3% atropine (Alcon Cusi SA) and two topical administrations of Ocryl lotion (Laboratoire TVM, Lempdes, France) and gentamicin dexamethasonum (Virbac France S.A., Carros, France) daily for 10 days post-surgery.

Histology and immunohistochemistry. At 4 mpi, A5 and A9 dogs were euthanized by intravenous injection of pentobarbital sodium (Vétoquinol, Lure, France). Eyes were enucleated and fixed for 2 hours in 4% paraformaldehyde in phosphate-buffered saline (PBS) solution before removal of the anterior chamber and the lens. Eyecups were embedded in optimal cutting temperature compound (OCT Cryomount; Microm Microtech, Francheville, France), and flash-frozen in a dry ice isopentane bath. Ten to fifteen micrometer cryosections were prepared.

For morphological examinations, sections were stained with hematoxylin and eosin before imaging by transmitter light microscopy (Nikon, Champigny sur Marne, France). Photoreceptor survival was assessed by counting the number of photoreceptor nuclei rows in one ONL column. Mean combined outer and inner segment thickness values of vector-exposed and unexposed areas of the retina were determined by averaging ten counts, performed on ten different slices.

For immunohistochemical studies, cryosections were air-dried, washed in PBS solution and incubated in blocking solution [20% normal goat serum (Invitrogen Life Technologies, Saint Aubin, France), 0.05% Triton X-100 in PBS] for 1 hour at room temperature. The bovine rod PDE6 (1:500) (Cytosignal, Irvine, CA) or GNAT1 (1:250) (Santa-Cruz Technology, Heidelberg, Germany) antibodies were incubated overnight at 4 °C in blocking solution. After three washes in 0.05% Triton X-100 in PBS solution, slides were incubated with the secondary antibody Alexa 488 goat anti-rabbit IgG conjugate (Life Technologies, Grand Island, NY) at 1:250 for 2 hours at room temperature. Slides were washed three times with 0.05% Triton X-100 in PBS solution and once with PBS solution before counterstaining the nuclei with DAPI diluted at 1:500. Slides were mounted in Prolong Gold anti-fade reagent (Life Technologies), observed with a fluorescence microscope (Nikon) and images captured with a digital camera (Nikon).

Specificity of the primary bovine rod PDE6 antibody for canine retina was demonstrated in the Pde6β$^{+/+}$ retina by absence of co-labeling with peanut lectin agglutinin conjugated with fluorescein isothiocyanate (1:250; Vector Laboratories, Burlingame, CA) (data not shown).

RT-PCR

RNA extraction and retro-transcription. Total RNA was isolated from individual flash-frozen retinas or retinal cryosections of Pde6β$^{+/+}$, Pde6β$^{+/-}$, or Pde6β$^{-/-}$ dogs using TRIzol Reagent (Invitrogen Life Technologies). Rnase-free Dnase I (Ambion DNA-free kit; Invitrogen Life Technologies) was used according to the manufacturer's instructions to remove contaminating DNA before generation of cDNA by reverse-transcription. Five hundred nanograms of total RNA were reverse-transcribed using oligodT primers and M-MLV reverse transcriptase (Invitrogen Life Technologies) as per the manufacturer's instructions. Control assays without addition of reverse transcriptase were included and the products were used in the subsequent RT-PCR as negative controls.

Primers. Integrity of cDNA was determined by amplification of a 650 bp sequence of the β-actin gene using β-actinF (5′-TGACGGGGTCACCCACACTGTGCCCATCTA-3′) and β-actinR (5′-CTAGAAGCATTTGCGGTGGACGATGGAGGG-3′) primers.

For pde6β amplification, 2056F (5′-GAAGATCGTGGATGAGTCTAAGA-3′) and 2561R (5′-CTACTTATCATCAGTCAAGGCCA TC-3′) primers were designed to specifically create a BtsCI restriction site in RT-PCR products arising from wild-type RNA templates. The reverse primer was designed to neighbouring exon sequences to avoid amplification of genomic DNA (**Figure 2**). The forward 2056F primer was designed in a pde6β-specific sequence to avoid amplification of canine pde6α RNA.

To verify the specificity of the 2056F and 2561R primer set against pde6β, full-length canine pde6α cDNA (NCBI RefSeq NM_001003073.1) was amplified by PCR from Pde6α$^{+/+}$ canine retinal cDNA. The forward primer encoded a *BamH*I end and an 18 bp sequence located 72 bp upstream of the start codon of the cpde6α gene (5′-ATTAAGGATCCTGACTCTGTCTTGC-3′). The reverse primer encoded an EcoRV end and a 15 bp sequence located 353 bp downstream of the stop codon of the cpde6α gene (5′- TATTGATATCTGGGTGATGAGGAGG -3′). The PCR product (3,061 bp) was purified, digested by *BamH*I and *EcoRV* and cloned into the plasmid SSV9RK.cpde6β previously constructed, between the RK promoter and the bovine growth hormone polyadenylation site after removal of the cpde6β cDNA (by *BamH*I and *EcoRV* digestion). The identity of the resulting SSV9RK.cpde6α construct was verified by sequencing.

Amplification and BstCI digestion. The amount of cDNA used in β-actin and pde6β allele-specific PCR was 40 ng. Both PCR were performed using GoTaq DNA polymerase (Promega France, Charbonnicres, France) and a Veriti Applied Biosystems thermocycler.

The β-actin reaction profile was as follows: an initial denaturation step at 95 °C for 5 minutes, followed by 40 cycles at 94 °C for 30 seconds, 55 °C for 30 seconds, 72 °C for 30 seconds and a final incubation step at 72 °C for 7 minutes. For pde6β, conditions of amplification were: an initial denaturation step at 95 °C for 5 minutes, followed by 10 cycles at 94 °C for 30 seconds, 60 °C for 30 seconds, 72 °C for 30 seconds, 30 cycles at 94 °C for 30 seconds, 56 °C for 30 seconds, 72 °C for 30 seconds and a final incubation step at 72 °C for 7 minutes.

Actin PCR products were resolved on a 1.5% agarose gel electrophoresis. Pde6β PCR products were purified by Nucleospin Extract II (Macherey-Nagel, Hoerdt, France) before digestion by BtsCI (New England Biolabs, Ipswich, MA) for 2 hours at 50 °C according to the manufacturer's instructions and analyzed by 3.5% agarose gel electrophoresis.

Fundus photography and OCT. Fundus photography and OCT were performed bilaterally on all treated dogs every 2 months after treatment. Before clinical examinations, the pupils were topically dilated as described above. Dogs were anesthetized by intravenous injection of xylazine (BayerHealth Care, Shawnee Mission, KS) and ketamine (Rhone Merieux).

Fundus photographs were taken with a Canon UVI retinal camera connected to a digital imaging system (Lhedioph Win Software; Lheritier, Saint-Ouen-l'Aumône, France).

Optical coherence tomography was performed by doing a 3-mm horizontal line scan in vector-exposed or vector unexposed areas of the retina (Stratus 3000; Carl Zeiss S.A.S; Le Pecq, France).

Electroretinography. Retinal function of treated Pde6β$^{-/-}$ dogs and age-matched untreated Pde6β$^{-/-}$ and Pde6β$^{+/-}$ controls was evaluated using bilateral full-field flash ERG. Initial ERG measurements were recorded at 4 weeks postinjection and every subsequent 2 months up to 4 (dogs A5 and A9), 9 (dogs A4 and A8), or 18 mpi (dogs A2, A3, A6, and A7), the latest timepoints evaluated in this study. For all dogs, each contralateral eye served as intra-individual noninjected control (except for dog A9 who received injection in both eyes).

Both pupils of animals were topically dilated as described above. Dogs were dark-adapted for 20 minutes and anesthetized following premedication by intravenous injection of thiopental sodium (Specia Laboratories, Paris, France) followed by isofluorane gas inhalation. Hydroxypropulmethylcellulose (Laboratoires Théa, Clermont-Ferrand, France) was applied to each eye to prevent corneal dehydration during recordings.

A computer-based system MonColor (Metrovision, Pérenchies, France) and contact lens electrodes (ERG-jet; Microcomponents SA, Grenchen, Switzerland) were used.

ERGs were recorded in a standardized fashion according to the International Society for Clinical Electrophysiology of Vision (ISCEV) recommendations,[47] using a protocol described previously.[48]

Vision testing. Light and dim-light vision of selected treated Pde6β$^{-/-}$ dogs were evaluated at regular intervals from 7 to 18 mpi by recording ambulation of dogs through an obstacle avoidance course under 260 ± 13 lux and 1,5 ± 0.8 lux ambient light intensities, respectively. Details of the apparatus have been described previously.[48] Animals were adapted to each light condition for 1 hour before beginning the test. An opaque lens was used to alternatively cover the treated or the untreated eye. Obstacle panel combinations were randomly determined for each test to prevent the dogs memorizing the positions of the obstacle panels. A Nightshot camera recorder (Sony DCR-PC110E PAL; Sony, New York, NY) was used for filming the dimmest light condition. All dim-light films were cleared before mounting with commercial Final Cut Pro 7 software (Apple, Cork, Ireland) using a standardized protocol.

SUPPLEMENTARY MATERIAL

Figure S1. Median ERG responses of rAAV2/5- and rAAV2/8-treated eyes overtime.

Video S1. Assessment of dim and bright light vision in dog A6 at 18 mpi.

ACKNOWLEDGMENTS

We acknowledge K. Stieger (Justus-Liebig University, Giessen, Germany) for critical reading of this manuscript. We thank D.J. Maskell (University of Cambridge, Cambridge, UK) for the gift of the first *rcd1* dogs and S. Khani (State University of New York, Buffalo, NY) for the gift of the human RK promoter. We also thank the Vector Core (www.vectors.univ-nantes.fr) for production of the rAAV vectors, the staff of the Boisbonne Center for animals care and Mireille Ledevin for retinal cryosections. This work was supported by the Agence Nationale pour la Recherche, the Association Française contre les Myopathies, the INSERM, the Fondation pour la Thérapie Génique en Pays de la Loire and the Ministère Français de l'Enseignement Supérieur et de la Recherche.

REFERENCES

1. Dryja, TP (2001). Retinitis pigmentosa and stationary night blindness. *The Metabolic & Molecular Bases of Inherited Diseases* 5903–5933.
2. Hartong, DT, Berson, EL and Dryja, TP (2006). Retinitis pigmentosa. *Lancet* **368**: 1795–1809.
3. RETNET at <https://sph.uth.tmc.edu/Retnet/>. Last accessed 6 March 2012.
4. McLaughlin, ME, Sandberg, MA, Berson, EL and Dryja, TP (1993). Recessive mutations in the gene encoding the beta-subunit of rod phosphodiesterase in patients with retinitis pigmentosa. *Nat Genet* **4**: 130–134.
5. McLaughlin, ME, Ehrhart, TL, Berson, EL and Dryja, TP (1995). Mutation spectrum of the gene encoding the beta subunit of rod phosphodiesterase among patients with autosomal recessive retinitis pigmentosa. *Proc Natl Acad Sci USA* **92**: 3249–3253.
6. Danciger, M, Blaney, J, Gao, YQ, Zhao, DY, Heckenlively, JR, Jacobson, SG *et al.* (1995). Mutations in the PDE6B gene in autosomal recessive retinitis pigmentosa. *Genomics* **30**: 1–7.
7. Bayés, M, Giordano, M, Balcells, S, Grinberg, D, Vilageliu, L, Martínez, I *et al.* (1995). Homozygous tandem duplication within the gene encoding the beta-subunit of rod phosphodiesterase as a cause for autosomal recessive retinitis pigmentosa. *Hum Mutat* **5**: 228–234.
8. Danciger, M, Heilbron, V, Gao, YQ, Zhao, DY, Jacobson, SG and Farber, DB (1996). A homozygous PDE6B mutation in a family with autosomal recessive retinitis pigmentosa. *Mol Vis* **2**: 10.
9. Saga, M, Mashima, Y, Akeo, K, Kudoh, J, Oguchi, Y and Shimizu, N (1998). A novel homozygous Ile535Asn mutation in the rod cGMP phosphodiesterase beta-subunit gene in two brothers of a Japanese family with autosomal recessive retinitis pigmentosa. *Curr Eye Res* **17**: 332–335.
10. Hmani-Aifa, M, Benzina, Z, Zulfiqar, F, Dhouib, H, Shahzadi, A, Ghorbel, A *et al.* (2009). Identification of two new mutations in the GPR98 and the PDE6B genes segregating in a Tunisian family. *Eur J Hum Genet* **17**: 474–482.
11. Clark, GR, Crowe, P, Muszynska, D, O'Prey, D, O'Neill, J, Alexander, S *et al.* (2010). Development of a diagnostic genetic test for simplex and autosomal recessive retinitis pigmentosa. *Ophthalmology* **117**: 2169–77.e3.
12. Ali, S, Riazuddin, SA, Shahzadi, A, Nasir, IA, Khan, SN, Husnain, T *et al.* (2011). Mutations in the ß-subunit of rod phosphodiesterase identified in consanguineous Pakistani families with autosomal recessive retinitis pigmentosa. *Mol Vis* **17**: 1373–1380.
13. Ionita, MA and Pittler, SJ (2007). Focus on molecules: rod cGMP phosphodiesterase type 6. *Exp Eye Res* **84**: 1–2.
14. Sancho-Pelluz, J, Arango-Gonzalez, B, Kustermann, S, Romero, FJ, van Veen, T, Zrenner, E *et al.* (2008). Photoreceptor cell death mechanisms in inherited retinal degeneration. *Mol Neurobiol* **38**: 253–269.
15. Wright, AF, Chakarova, CF, Abd El-Aziz, MM and Bhattacharya, SS (2010). Photoreceptor degeneration: genetic and mechanistic dissection of a complex trait. *Nat Rev Genet* **11**: 273–284.
16. Punzo, C, Xiong, W and Cepko, CL (2012). Loss of daylight vision in retinal degeneration: are oxidative stress and metabolic dysregulation to blame? *J Biol Chem* **287**: 1642–1648.
17. Keeler, C (1966). Retinal degeneration in the mouse is rodless retina. *J Hered* **57**: 47–50.
18. Chang, B, Hawes, NL, Pardue, MT, German, AM, Hurd, RE, Davisson, MT *et al.* (2007). Two mouse retinal degenerations caused by missense mutations in the beta-subunit of rod cGMP phosphodiesterase gene. *Vision Res* **47**: 624–633.
19. Hart, AW, McKie, L, Morgan, JE, Gautier, P, West, K, Jackson, IJ *et al.* (2005). Genotype-phenotype correlation of mouse pde6b mutations. *Invest Ophthalmol Vis Sci* **46**: 3443–3450.
20. Davis, RJ, Tosi, J, Janisch, KM, Kasanuki, JM, Wang, NK, Kong, J *et al.* (2008). Functional rescue of degenerating photoreceptors in mice homozygous for a hypomorphic cGMP phosphodiesterase 6 b allele (Pde6bH620Q). *Invest Ophthalmol Vis Sci* **49**: 5067–5076.
21. Bennett, J, Tanabe, T, Sun, D, Zeng, Y, Kjeldbye, H, Gouras, P *et al.* (1996). Photoreceptor cell rescue in retinal degeneration (rd) mice by *in vivo* gene therapy. *Nat Med* **2**: 649–654.
22. Jomary, C, Vincent, KA, Grist, J, Neal, MJ and Jones, SE (1997). Rescue of photoreceptor function by AAV-mediated gene transfer in a mouse model of inherited retinal degeneration. *Gene Ther* **4**: 683–690.
23. Pang, JJ, Boye, SL, Kumar, A, Dinculescu, A, Deng, W, Li, J *et al.* (2008). AAV-mediated gene therapy for retinal degeneration in the rd10 mouse containing a recessive PDEbeta mutation. *Invest Ophthalmol Vis Sci* **49**: 4278–4283.
24. Pang, JJ, Dai, X, Boye, SE, Barone, I, Boye, SL, Mao, S *et al.* (2011). Long-term retinal function and structure rescue using capsid mutant AAV8 vector in the rd10 mouse, a model of recessive retinitis pigmentosa. *Mol Ther* **19**: 234–242.

25. Allocca, M, Manfredi, A, Iodice, C, Di Vicino, U and Auricchio, A (2011). AAV-mediated gene replacement, either alone or in combination with physical and pharmacological agents, results in partial and transient protection from photoreceptor degeneration associated with betaPDE deficiency. *Invest Ophthalmol Vis Sci* **52**: 5713–5719.
26. Kumar-Singh, R and Farber, DB (1998). Encapsidated adenovirus mini-chromosome-mediated delivery of genes to the retina: application to the rescue of photoreceptor degeneration. *Hum Mol Genet* **7**: 1893–1900.
27. Takahashi, M, Miyoshi, H, Verma, IM and Gage, FH (1999). Rescue from photoreceptor degeneration in the rd mouse by human immunodeficiency virus vector-mediated gene transfer. *J Virol* **73**: 7812–7816.
28. Tosi, J, Sancho-Pelluz, J, Davis, RJ, Hsu, CW, Wolpert, KV, Sengillo, JD *et al.* (2011). Lentivirus-mediated expression of cDNA and shRNA slows degeneration in retinitis pigmentosa. *Exp Biol Med (Maywood)* **236**: 1211–1217.
29. Stieger, K, Lhériteau, E, Lhéariteau, E, Moullier, P and Rolling, F (2009). AAV-mediated gene therapy for retinal disorders in large animal models. *ILAR J* **50**: 206–224.
30. Suber, ML, Pittler, SJ, Qin, N, Wright, GC, Holcombe, V, Lee, RH *et al.* (1993). Irish setter dogs affected with rod/cone dysplasia contain a nonsense mutation in the rod cGMP phosphodiesterase beta-subunit gene. *Proc Natl Acad Sci USA* **90**: 3968–3972.
31. Aquirre, G, Farber, D, Lolley, R, Fletcher, RT and Chader, GJ (1978). Rod-cone dysplasia in Irish setters: a defect in cyclic GMP metabolism in visual cells. *Science* **201**: 1133–1134.
32. Liu, YP, Krishna, G, Aguirre, G and Chader, GJ (1979). Involvement of cyclic GMP phosphodiesterase activator in an hereditary retinal degeneration. *Nature* **280**: 62–64.
33. Parry, HB (1953). Degenerations of the dog retina. II. Generalized progressive atrophy of hereditary origin. *Br J Ophthalmol* **37**: 487–502.
34. Aguirre, G, Farber, D, Lolley, R, O'Brien, P, Alligood, J, Fletcher, RT *et al.* (1982). Retinal degeneration in the dog. III. Abnormal cyclic nucleotide metabolism in rod-cone dysplasia. *Exp Eye Res* **35**: 625–642.
35. Khani, SC, Pawlyk, BS, Bulgakov, OV, Kasperek, E, Young, JE, Adamian, M *et al.* (2007). AAV-mediated expression targeting of rod and cone photoreceptors with a human rhodopsin kinase promoter. *Invest Ophthalmol Vis Sci* **48**: 3954–3961.
36. Beltran, WA, Boye, SL, Boye, SE, Chiodo, VA, Lewin, AS, Hauswirth, WW *et al.* (2010). rAAV2/5 gene-targeting to rods:dose-dependent efficiency and complications associated with different promoters. *Gene Ther* **17**: 1162–1174.
37. Buyukmihci, N, Aguirre, G and Marshall, J (1980). Retinal degenerations in the dog. II. Development of the retina in rod-cone dysplasia. *Exp Eye Res* **30**: 575–591.
38. Sun, X, Pawlyk, B, Xu, X, Liu, X, Bulgakov, OV, Adamian, M *et al.* (2010). Gene therapy with a promoter targeting both rods and cones rescues retinal degeneration caused by AIPL1 mutations. *Gene Ther* **17**: 117–131.
39. Ku, CA, Chiodo, VA, Boye, SL, Goldberg, AF, Li, T, Hauswirth, WW *et al.* (2011). Gene therapy using self-complementary Y733F capsid mutant AAV2/8 restores vision in a model of early onset Leber congenital amaurosis. *Hum Mol Genet* **20**: 4569–4581.
40. Beltran, WA, Cideciyan, AV, Lewin, AS, Iwabe, S, Khanna, H, Sumaroka, A *et al.* (2012). Gene therapy rescues photoreceptor blindness in dogs and paves the way for treating human X-linked retinitis pigmentosa. *Proc Natl Acad Sci USA* **109**: 2132–2137.
41. Sarra, GM, Stephens, C, de Alwis, M, Bainbridge, JW, Smith, AJ, Thrasher, AJ *et al.* (2001). Gene replacement therapy in the retinal degeneration slow (rds) mouse: the effect on retinal degeneration following partial transduction of the retina. *Hum Mol Genet* **10**: 2353–2361.
42. Mowat, FM, Petersen-Jones, SM, Williamson, H, Williams, DL, Luthert, PJ, Ali, RR *et al.* (2008). Topographical characterization of cone photoreceptors and the area centralis of the canine retina. *Mol Vis* **14**: 2518–2527.
43. Stieger, K, Colle, MA, Dubreil, L, Mendes-Madeira, A, Weber, M, Le Meur, G *et al.* (2008). Subretinal delivery of recombinant AAV serotype 8 vector in dogs results in gene transfer to neurons in the brain. *Mol Ther* **16**: 916–923.
44. Pawlyk, BS, Bulgakov, OV, Liu, X, Xu, X, Adamian, M, Sun, X *et al.* (2010). Replacement gene therapy with a human RPGRIP1 sequence slows photoreceptor degeneration in a murine model of Leber congenital amaurosis. *Hum Gene Ther* **21**: 993–1004.
45. Rabinowitz, JE, Rolling, F, Li, C, Conrath, H, Xiao, W, Xiao, X *et al.* (2002). Cross-packaging of a single adeno-associated virus (AAV) type 2 vector genome into multiple AAV serotypes enables transduction with broad specificity. *J Virol* **76**: 791–801.
46. Weber, M, Rabinowitz, J, Provost, N, Conrath, H, Folliot, S, Briot, D *et al.* (2003). Recombinant adeno-associated virus serotype 4 mediates unique and exclusive long-term transduction of retinal pigmented epithelium in rat, dog, and nonhuman primate after subretinal delivery. *Mol Ther* **7**: 774–781.
47. Narfström, K, Ekesten, B, Rosolen, SG, Spiess, BM, Percicot, CL and Ofri, R; Committee for a Harmonized ERG Protocol, European College of Veterinary Ophthalmology (2002). Guidelines for clinical electroretinography in the dog. *Doc Ophthalmol* **105**: 83–92.
48. Lhériteau, E, Libeau, L, Mendes-Madeira, A, Deschamps, JY, Weber, M, Le Meur, G *et al.* (2010). Regulation of retinal function but nonrescue of vision in RPE65-deficient dogs treated with doxycycline-regulatable AAV vectors. *Mol Ther* **18**: 1085–1093.

Supplementary Material:

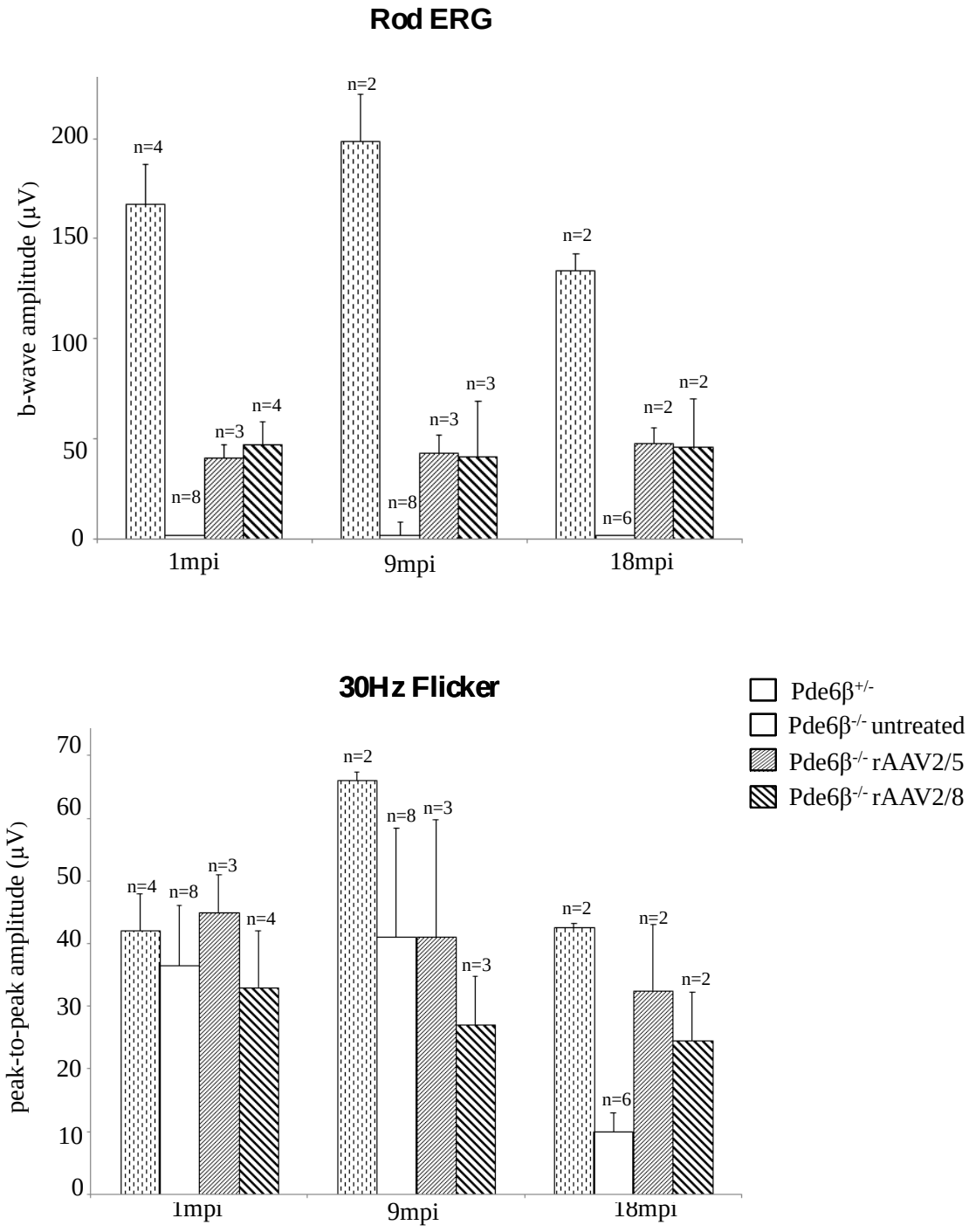

Figure S1. Median ERG responses of rAAV2/5- and rAAV2/8 treated eyes overtime. [17] Rod- (**a**) and cone-mediated (**b**) ERG responses amplitudes recorded at 1, 9 and 18mpi from groups of non-affected, affected, rAAV2/5-treated and rAAV2/8-treated affected eyes, respectively. The right eye of dog A9 was not included in the group of rAAV2/8-treated eyes at 1mpi due to important vector reflux observed during the subretinal injection. ERG responses amplitudes are expressed as median (± SEM) for each group. The number of eyes analyzed per group is indicated above each measure.

CHAPTER **VII**

SUCCESSFUL GENE THERAPY IN THE RPGRIP1-DEFICIENT DOG, A LARGE ANIMAL MODEL OF CONE-ROD DYSTROPHY

Elsa Lhériteau*, **Lolita Petit***, Michel Weber, Guylène LeMeur, Jack-Yves Deschamps, Lyse Libeau, Alexandra Mendes-Madeira, Caroline Guihal, Achille François, Richard Guyon, Nathalie Provost, Françoise Lemoine, Samatha Papal, Aziz El-Amraoui, Marie-Anne Colle, Philippe Moullier and Fabienne Rolling (*** equal contribution**)

This work is published as a research article in Molecular Therapy
(Elsa Lhériteau *et al*. Molecular Therapy, Epud ahead of print (2013))

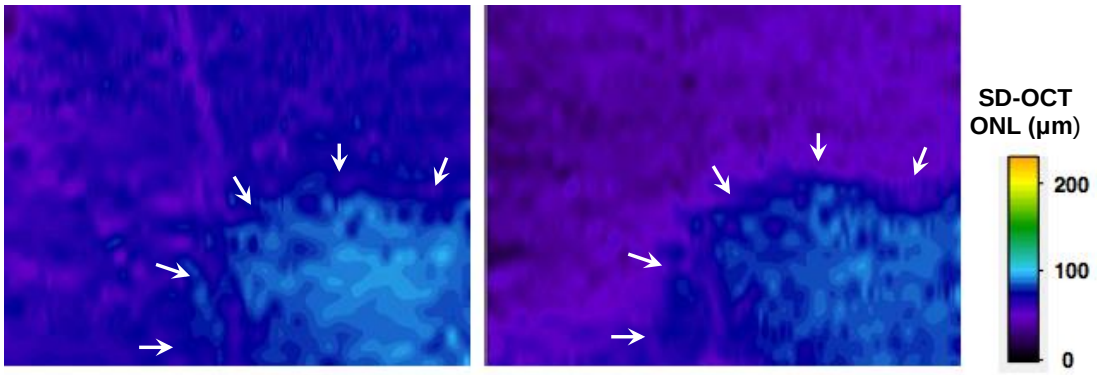

This image shows advancing ONL thinning in the vector-exposed area (arrows) of a rAAV-treated *Rpgrip1*$^{-/-}$ retina between (**a**) 12 months and (**b**) 24 months postinjection. Topography of ONL thickness has been obtained *in vivo* using spectral-domain OCT.

Author contributions: EL, PM and FR designed research. EL, LP, MW, GLM, JYD, LL, AMM, CC, AF, RG, NP, FL, SP, AEA and MAC performed research. EL, LP and FR analyzed data. LP and FR wrote the paper.

Successful Gene Therapy in the RPGRIP1-deficient Dog: a Large Model of Cone–Rod Dystrophy

Elsa Lhériteau[1], Lolita Petit[1], Michel Weber[2], Guylène Le Meur[2], Jack-Yves Deschamps[3], Lyse Libeau[1], Alexandra Mendes-Madeira[1], Caroline Guihal[1], Achille François[1], Richard Guyon[4], Nathalie Provost[1], Françoise Lemoine[5], Samantha Papal[6], Aziz El-Amraoui[6], Marie-Anne Colle[7], Philippe Moullier[1,8] and Fabienne Rolling[1]

[1]INSERM UMR 1089, Institut de Recherche Thérapeutique 1, Université de Nantes, Nantes, France; [2]CHU-Hôtel Dieu, Service d'Ophtalmologie, Nantes, France; [3]ONIRIS, Nantes-Atlantic College of Veterinary Medicine Food Science and Engineering, Emergency and Critical Care Unit, Nantes, France; [4]CNRS UMR 6061, Université de Rennes 1, Rennes, France; [5]Clinique Vétérinaire Atlantia, Nantes, France; [6]Institut Pasteur, INSERM UMRS 1120, Paris, France; [7]INRA/ONIRIS, Nantes-Atlantic College of Veterinary Medicine Food Science and Engineering, Nantes, France; [8]Department of Molecular Genetics and Microbiology, College of Medicine, University of Florida, Gainesville, Florida, USA

For the development of new therapies, proof-of-concept studies in large animal models that share clinical features with their human counterparts represent a pivotal step. For inherited retinal dystrophies primarily involving photoreceptor cells, the efficacy of gene therapy has been demonstrated in canine models of stationary cone dystrophies and progressive rod–cone dystrophies but not in large models of progressive cone–rod dystrophies, another important cause of blindness. To address the last issue, we evaluated gene therapy in the retinitis pigmentosa GTPase regulator interacting protein 1 (RPGRIP1)-deficient dog, a model exhibiting a severe cone–rod dystrophy similar to that seen in humans. Subretinal injection of AAV5 (n = 5) or AAV8 (n = 2) encoding the canine *Rpgrip1* improved photoreceptor survival in transduced areas of treated retinas. Cone function was significantly and stably rescued in all treated eyes (18–72% of those recorded in normal eyes) up to 24 months postinjection. Rod function was also preserved (22–29% of baseline function) in four of the five treated dogs up to 24 months postinjection. No detectable rod function remained in untreated contralateral eyes. More importantly, treatment preserved bright- and dim-light vision. Efficacy of gene therapy in this large animal model of cone–rod dystrophy provides great promise for human treatment.

Received 5 July 2013; accepted 22 September 2013; advance online publication 29 October 2013. doi:10.1038/mt.2013.232

INTRODUCTION

Inherited retinal dystrophies form a phenotypically and genetically heterogeneous group of blinding diseases characterized by the progressive degeneration of photoreceptor cells.[1] They are commonly classified according to the rate of photoreceptor cell loss, stationary or progressive disorders, and the subtype of photoreceptors functionally affected first: cone dystrophy (dysfunction of cones only),[2] cone–rod dystrophy (dysfunction of cones then rods),[2,3] and rod–cone dystrophy (dysfunction of rods then cones).[1] When both rod and cone responses are severely impaired within the first years of life (rod–cone or cone–rod dystrophies), the term Leber congenital amaurosis is usually used.

The pathological involvement of photoreceptors in inherited retinal degeneration (IRD) may be the result of mutations in genes/loci mainly expressed in photoreceptors themselves (cones and/or rods) or in the retinal pigment epithelium cells that are essential for the maintenance of the function, structural integrity, and survival of photoreceptors.[4] Primary genetic mutations in cones generally affect only cone function/survival (cone dystrophy).[2] By contrast, rod-specific mutations primarily affect rods but can often result in secondary loss of cone-mediated function and vision (rod–cone dystrophy).[1] When the causal gene is expressed in both subtypes of photoreceptors, cone function loss can slightly precede rod damage (cone–rod dystrophy) or inversely (rod–cone dystrophy) depending on the implicated gene, causal mutations, and/or genetic modifiers.[4] Retinal pigment epithelium–initiated dystrophies, which also hinder the function of both types of photoreceptors, can be associated with cone–rod or rod–cone phenotypes.[4]

IRDs are currently incurable, but for those acquired by recessive (50–60%) or X-linked (5–15%) inheritance,[1] gene addition therapy holds great promise. Indeed, over the past decade, gene transfer has resulted in significant morphological and/or functional improvements in a dozen different rodent models of IRD including models of cone, cone–rod and rod–cone dystrophies.[5–7]

Large models (dogs, cats, or pigs) are more amenable than rodents to vision testing, and their longevity enables long-term follow-up. More importantly, the retinal distribution, density, and proportion of rods and cones in these larger animals more closely match those of primates.[8]

Recently, gene therapy targeting photoreceptors was successfully used in two canine models of stationary cone dystrophy

The first two authors contributed equally to this work.

Correspondence: *Fabienne Rolling, PhD, INSERM UMR 1089, Institut de Recherche Thérapeutique 1, 8, quai Moncousu, 440007 Nantes Cedex 01, France. E-mail: fabienne.rolling@inserm.fr*

caused by a defect in the cone-specific *Cngb3* gene (*Cngb3*$^{-/-}$ and *Cngb3*$^{m/m}$ dogs),[9] in the *Rcd1* canine model of progressive rod–cone dystrophy caused by a defect in the rod-specific *Pde6β* gene[10], and in two canine models of progressive rod–cone dystrophy linked to a defect in the *Rpgr* gene, expressed in both rods and cones (*XLPRA1* and *XLPRA2* dogs).[11] These results strongly support the translation of gene therapy for stationary cone and progressive rod–cone dystrophies into the clinic. The efficacy of photoreceptor gene therapy in a large model of cone–rod dystrophy remains, however, to be demonstrated.

A closed research colony of miniature longhaired dachshund (MLHD) provides a highly relevant model for validating potential gene therapies for cone–rod dystrophies. Indeed, these dogs display a severe early onset cone–rod dystrophy (*Cord1*) that allows fairly rapid assessment of the effects of gene therapy on both retinal function and vision. Their cone function is totally absent at 2 months of age, and their rod function rapidly declines from 2 to 12 months of age.[12,13] In addition, their retinal degeneration has been linked to a locus containing the GTPase regulator interacting protein 1 (*Rpgrip1*) gene,[14] a known cause of recessive Leber congenital amaurosis (4–6% of all cases)[15–19] and cone–rod dystrophy (1% of all cases)[20] in humans. In mice, the *Rpgrip1* gene encodes multiple protein isoforms; among those, RPGRIP1α_1 is specifically expressed in the connecting cilium and outer segments of photoreceptor cells.[21–23] The RPGRIP1α_1 protein isoform anchors RPGR[21,24] and is thought to control microtubule organization in the connecting cilium and the molecular trafficking between the inner and outer segments of photoreceptors.[25] RPGRIP1 also appears to be required for the development and maintenance of photoreceptor outer segments.[26]

Gene therapy for RPGRIP1 deficiencies has previously been evaluated in the *Rpgrip1* knockout mouse, providing encouraging results.[27,28] In the initial study, delivery of the murine *Rpgrip1* cDNA into photoreceptors of *Rpgrip1*$^{-/-}$ mice at postnatal day 20 (P20) using a rAAV2/2 restored the localization of both RPGRIP1α_1 and RPGR in the connecting cilium and led to a significant slowing of photoreceptor function loss at 5 months postinjection (mpi) (loss of 6% of electroretinographic (ERG) b-wave amplitude per month in treated eyes compared with 22% per month in untreated contralateral eyes).[27] The second study used a rAAV2/8 and a human *RPGRIP1* cDNA, leading to a preservation of one-third of initial photoreceptor function in treated eyes at 5 mpi. At this age, ERG responses cannot be further recorded in untreated eyes.[28]

Herein, we evaluate the efficacy of rAAV-mediated *Rpgrip1* gene transfer in the MLHD-*Cord1* dog. We found that gene addition therapy can restore the functional deficit of cone photoreceptors and prevent the retinal degeneration and vision loss in this large animal model of cone–rod dystrophy.

RESULTS

An AAV2/5 vector carrying the eGFP under the control of the human RK promoter transduces both rods and cones in the canine retina

As RPGRIP1 deficiencies affect both cone and rod functions,[15–20] effective gene therapy in the MLHD-*Cord1* dog would require efficient transgene expression in both subtypes of photoreceptors. In this study, we chose to use rAAV2/5 or rAAV2/8 vectors, as they have been shown to be excellent vectors for transducing photoreceptors in mice, dogs,[29] pigs,[30] and nonhuman primates.[31,32] Concerning the promoter, several studies have demonstrated that the human RK promoter mediates efficient and specific transgene expression in both cones and rods, following subretinal injection, in the murine[28,33–38] and the nonhuman primate retina,[32] suggesting that this promoter may be ideally used in a clinical setting. This was reinforced with its recent successful use in a gene replacement therapy study in the XLPRA2 canine model of rod–cone dystrophy linked to a defect in both rods and cones.[11] However, these findings are inconsistent with previous results showing that in the dog, the human RK promoter drives rAAV-mediated expression exclusively in rods, except when high titer was used (3×10^{12} genome copies).[39]

To determine whether the human RK promoter can drive expression in both cones and rods in the dog and is suitable for our gene replacement study, we subretinally delivered a rAAV2/5 vector expressing enhanced green fluorescent protein (eGFP) under the control of the RK promoter (1×10^{11} genome copies, **Figure 1a**) into two dogs, NA2 and NA3 (**Table 1**). As reported earlier,[29] the area transduced, determined by live indirect ophthalmoscopy, perfectly matched with the vector subretinal bleb (**Figure 1b,c**). eGFP fluorescence peaked at 6 weeks postinjection (data not shown) and remained stable for at least 9 mpi, the time when the animals were sacrificed for histological assessment (**Figure 1c**). Histological sections were performed in the vector-exposed area. Epifluorescence microscopy showed eGFP expression limited to photoreceptor cells (cell bodies, inner/outer segments) (**Figure 1d**). Notably, a robust transduction of cones was detected (**Figure 1f–h**). Cones were identified based on two criteria: their well-defined shape and their labeling with L/M opsin (**Figure 1e–h**), a known marker of L/M cone outer segments, and at high exposure, of L/M cone inner segments (**Figure 1h**). Recombinant AAV2/5-RK-eGFP transduced on average 49±21% of L/M cones (number of double-labeled eGFP/opsin cones per field at ×20 magnification, n = 2 eyes). These results confirmed that the RK promoter could drive efficient and specific rAAV-mediated transgene expression into both cones (at least L/M) and rods in the canine retina, further supporting its application for gene transfer in MLHD-*Cord1* dog.

Production of therapeutic rAAV vectors and subretinal delivery in the MLHD-*Cord1* dog

Given the efficacy and specificity of the AAV-RK vector system, we subsequently produced rAAV2/5 and rAAV2/8 vectors encoding canine *Rpgrip1* (c*Rpgrip1*) under the control of the same promoter (**Figure 2a**). We first isolated and subcloned the c*Rpgrip1* cDNA. Seven overlapping fragments covering the entire *Rpgrip1* coding sequence were amplified using polymerase chain reaction (PCR) and RNA-ligase–mediated RACE (RLM-RACE) PCR (**Supplementary Figure S1a**) using primers designed against human, bovine and rodent *RPGRIP1* consensus sequences and putative canine sequences (**Supplementary Table S1**). The c*Rpgrip1* open reading frame spans 3630 bp, contains 24 coding exons, and encodes a predicted protein of 1209 amino acid (**Supplementary Figure S1b and Table S2**), as recently published.[40] Then, a total of seven MLHD-*Cord1* dogs (A2–A8) were injected subretinally

with these therapeutic vectors at 1 month of age (see below). Dogs A2–A6 received AAV2/5-RK-c*Rpgrip1*, whereas dogs A7 and A8 received AAV2/8-RK-c*Rpgrip1* (Table 1). All injections were performed unilaterally on the nasal superior quadrant of the retina, except for dog A3 that was treated in temporal.

During the progression of this study, dog A6 died accidentally at 3 weeks postinjection. Its retinas were collected to analyze the expression of c*Rpgrip1* by reverse transcriptase–PCR. Previous studies have suggested that a polyA tract insertion of 29 nucleotides flanked by a 15-bp duplication (Ins44), in the coding exon 2 of the c*Rpgrip1* gene, contributes to retinal degeneration in the MLHD-*Cord1* dog.[14] We, therefore, developed an allele-specific reverse transcriptase–PCR to ensure discrimination between wild-type (transgene) and Ins44 mutant (endogeneous) *Rpgrip1* transcripts in treated retinas (Figure 2b). The 154-bp amplification product derived from transgene RNA templates was detected in A6 treated retina (Figure 2c). On the contrary, untreated *Rpgrip1*$^{-/-}$ A6 eye yielded only the mutant RNA (198 bp) (Figure 2c). This result confirmed that vector-encoded *cRpgrip1* was expressed in transduced photoreceptors.

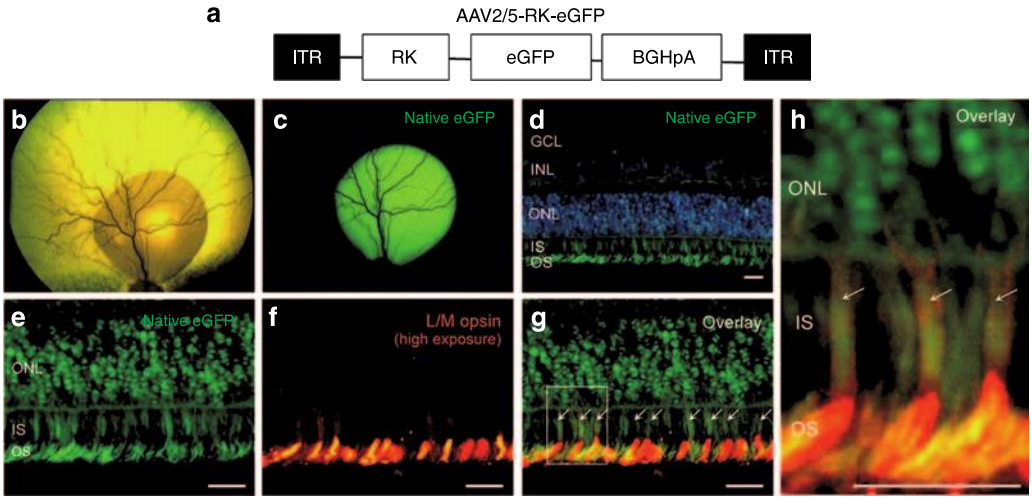

Figure 1 Green fluorescent protein (GFP) expression in rod and cone photoreceptors after subretinal injection of AAV2/5-RK-eGFP in the normal canine retina. (**a**) Schematic structure of recombinant AAV2/5-RK-eGFP vector. It encodes the eGFP reporter gene under the control of the human RK promoter (−112 to +87 bp region of the proximal promoter). (**b**) Retinal detachment created by the subretinal injection of AAV2/5-RK-eGFP vector 20 minutes after injection in the right eye of dog NA2. (**c**) Live fluorescent eGFP signal at 9 mpi in the right eye of dog NA2. (**d**) Image of native eGFP fluorescence (green) in the injected area of the right eye of dog NA2 after nuclei counterstaining with DAPI (blue). (**e**) Images of native eGFP (green) and (**f**) L/M opsin immunolabeling (red) in the injected area of the right eye of dog NA2. (**g–h**) Overlay images were taken at high exposure to 568 nm to allow the staining of cone inner segments (ISs). Arrows indicate eGFP-positive cones. Scale bar = 30 µm. BGHpA, bovine growth hormone polyadenylation signal; DAPI, 4′,6-diamidino-2-phenylindole; eGFP, enhanced GFP; GCL, ganglion cell layer; INL, inner nuclear layer; ITR, inverted terminal repeat; ONL, outer nuclear layer; OS, outer segment.

Table 1 List of dogs included in the study

			30 Hz flicker (µV)				Rod electroretinogram (µV)			
Dog	Vector	Follow-up (mpi)	1 mpi (T/U)	9 mpi (T/U)	12 mpi (T/U)	24 mpi (T/U)	1 mpi (T/U)	9 mpi (T/U)	12 mpi (T/U)	24 mpi (T/U)
NA1	None	24	ND	ND	ND	69/77	ND	ND	ND	186/199
A1		24	0/0	0/0	0/0	0/0	121/128	20/12	0/0	0/0
NA2	AAV2/5-RK-eGFP	9	ND	48/53[a]	†	†	ND	169/166[a]	†	†
NA3	(1.10^{11} vg/ml)	9	ND	67/65[a]	†	†	ND	215/182[a]	†	†
A2	AAV2/5-RK-cRpgrip1	24	18/0	21/0	29/0	33/0	185/197	27/16	32/0	41/0
A3	(1.10^{11} vg/ml)	12	20/0	15/0	16/0	ND	139/110	46/16	40/0	ND
A4		12	26/0	13/0	15/0	ND	194/184	45/12	48/0	ND
A5		6	19/0	20/0[a]	ND	ND	176/155	107/72[a]	ND	ND
A6		0,8	†	†	†	†	†	†	†	†
A7	AAV2/8-RK-cRpgrip1	24	15/0	27/0	13/0	13/0	113/114	28/0	0/0	0/0
A8	(1.10^{12} vg/ml)	24	48/0	53/0	49/0	53/0	197/118	62/44	56/0	50/0

30 Hz flicker, photopic 30 Hz flicker amplitude; A, affected; electroretinographic; mpi, months postinjection; NA, nonaffected; ND, not done; rod ERG, scotopic rod-mediated b-wave amplitude; T, treated eye; U, untreated eye; vg, vector genome.
†Died accidentally at 3 weeks postinjection from coccidiosis.
[a]Electroretinographic amplitudes at 6 months postinjection.

Gene therapy reduces the progressive photoreceptor degeneration in MLHD-*Cord1* retinas

In the MLHD-*Cord1* dog, photoreceptor degeneration becomes evident by histology at ~2 months of age and is almost complete at 28 months of age.[12,13] It is associated with a dramatic reduction of the retinal vasculature between 5 months and 2 years of age.[13] To determine whether rAAV-mediated c*Rpgrip1* gene addition can prevent, delay, slow, or stop this morphological damage, three complementary analyzes were performed in all treated dogs at different times after injection. First, funduscopy and time-domain optical coherence tomography (TD-OCT) were performed from 3 to 24 mpi to monitor the kinetic of retinal degeneration in treated and untreated eyes (**Figure 3** and **Supplementary Figure S2**). Second, spectral-domain OCT (SD-OCT) was performed at the latest time point to determine the extent of retinal preservation in treated eyes (**Figure 4a** and **Supplementary Figure S3a**). Finally, the eyes of the dog A2 were examined by histology and immunohistochemistry at 24 mpi to monitor the effect of gene transfer on the morphology of each photoreceptor cell type (**Figure 4b,c** and **Supplementary Figure S3b**).

Kinetics of retinal degeneration in MLHD-Cord1 untreated and treated eyes. The first analysis is illustrated by representative funduscopy and TD-OCT data obtained from dogs NA1 (nonaffected control; **Figure 3a**), A2 (rAAV2/5-treated; **Figure 3b**), and A8 (rAAV2/8-treated; **Figure 3c**) at 3, 9, 12, and 24 mpi.

In agreement with previous data,[13] an obvious reduction of retinal vasculature was observed from 3 to 24 mpi in untreated MLHD-*Cord1* eyes (**Figure 3b,c**, bottom) compared with normal eyes (**Figure 3a**). A reduction of retinal vasculature was also observed in both rAAV2/5- and rAAV2/8-treated eyes from 3 to 24 mpi (**Figure 3b,c**, top). However, this progressive attenuation of retinal vasculature in treated eyes seemed reduced compared with untreated eyes. Indeed, at 24 mpi, both rAAV2/5- and rAAV2/8-treated eyes displayed a partially preserved retinal vasculature (**Figure 3b,c**, top right), whereas only a few central vessels remained visible in the untreated eyes (**Figure 3b,c**, bottom right). This time course of preservation of retinal vasculature correlated with those of central retinal thickness. Indeed, both treated and untreated eyes showed a progressive reduction of the central retinal thickness from 3 to 24 mpi compared with normal eyes (**Figure 3a** and **Supplementary Figure S2**). However, at all the four time points explored, treated eyes had a thicker central retina than uninjected eyes, and the difference of thickness between both eyes remained relatively constant over time in all treated dogs (**Supplementary Figure S2**). For example, at both 3 and 24 mpi, the treated retina of dogs A2 (**Figure 3b** and **Supplementary Figure S2**) and A8 (**Figure 3c** and **Supplementary Figure S2**) were 4 and 10% thicker than their contralateral untreated retina, respectively. These results suggest an early therapeutic effect of gene transfer on retinal morphology. Despite the fact that this result was observed in the five treated dogs, we cannot exclude that they all randomly received the treatment in their better eye (it is not possible to perform a TD-OCT examination at the time of injection).

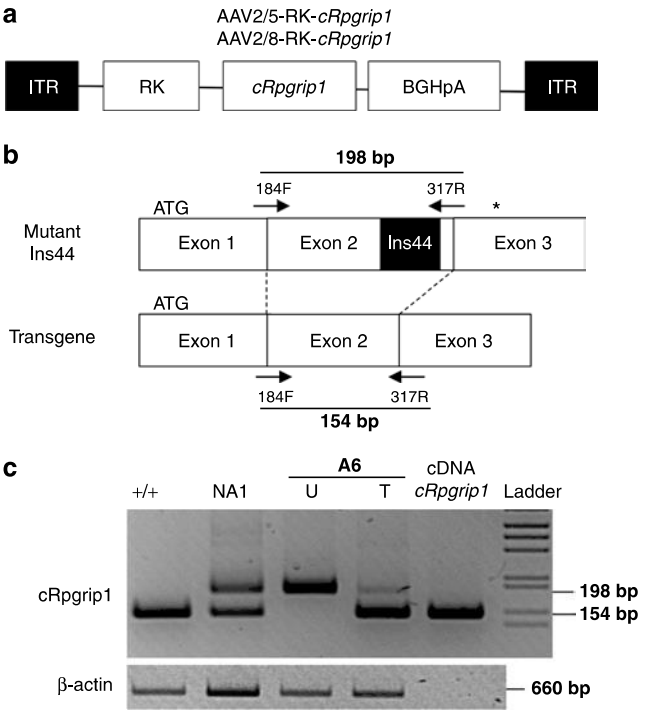

Figure 2 Reverse transcriptase–polymerase chain reaction (PCR) amplification of transgene (wild-type) and native (mutant) Rpgrip1 transcripts from A6 retinas at 3 weeks postinjection. (**a**) Schematic structure of recombinant AAV2/5-RK-c*Rpgrip1* and AAV2/8-RK-c*Rrpgrip1* vectors. Both encode the canine *Rpgrip1* cDNA (c*Rpgrip1*) under the control of the human RK promoter (–112 to +87 bp region of the proximal promoter). (**b**) PCR amplification using 184F and 317R primers encompasses a fraction of exons 1–3 of the canine *Rpgrip1* gene. MLHD-*Cord1* dogs have been shown previously to carry an insertion of 44 bp in exon 2 of the *cRpgrip1* gene (polyA tract insertion of 29 nucleotides flanked by 15-bp duplication). Thus, PCR amplification results in a 198-bp product when mutant Ins44 cDNAs are used as templates and in a 154-bp product when wild-type (vector-derived) cDNAs templates are used. Arrows indicate the positions of the 184F and 317R primers. The black box indicates the position of the Ins44 mutation in the *cRpgrip1* gene. (**c**) Agarose gel electrophoresis of c*Rpgrip1* and β-actin RT-PCR. Lanes 1 and 2 show products from *Rpgrip1*$^{+/+}$ and *Rpgrip1*$^{+/-}$ untreated control retinas, respectively. Lanes 3 and 4 show products from untreated and AAV2/5-RK-c*Rpgrip1*-treated retinas of dog A6 at 3 weeks postinjection, respectively. Lane 5 shows the product from the SSV9-RK-c*Rpgrip1* vector plasmid. +/+, *Rpgrip1*$^{+/+}$ retina; bp, base pairs; cDNA *Rpgrip1*; SSV9-RK-c*Rpgrip1* vector plasmid; Ins44, 44bp insertion mutation in the c*Rpgrip1* exon 2; ladder, 1 kb molecular size ladder; NA1, nonaffected *Rpgrip1*$^{+/-}$ retina; T, treated retina; U, untreated retina.

Topography of photoreceptor preservation in MLHD-Cord1 treated eyes. SD-OCT allows outer nuclear layer thickness assessment *in vivo*. This examination was performed at the latest time point for dogs A2, A3, A4, A5, A7, A8, and an age-matched control dog (NA1) to determine the extent of the therapeutic effects of gene therapy on retinal degeneration (**Figure 4a** and **Supplementary Figure S3a**).

For example, for the A2 treated eye, SD-OCT scans demonstrated a stark contrast between vector-exposed and vector-unexposed regions (**Figure 4a**). Vector-exposed regions (A2) had a much thicker outer nuclear layer (ONL) along with nearly normal appearing inner/outer segments (57 μm; **Figure 4a**), accounting for 69% of the photoreceptor layer thickness of the

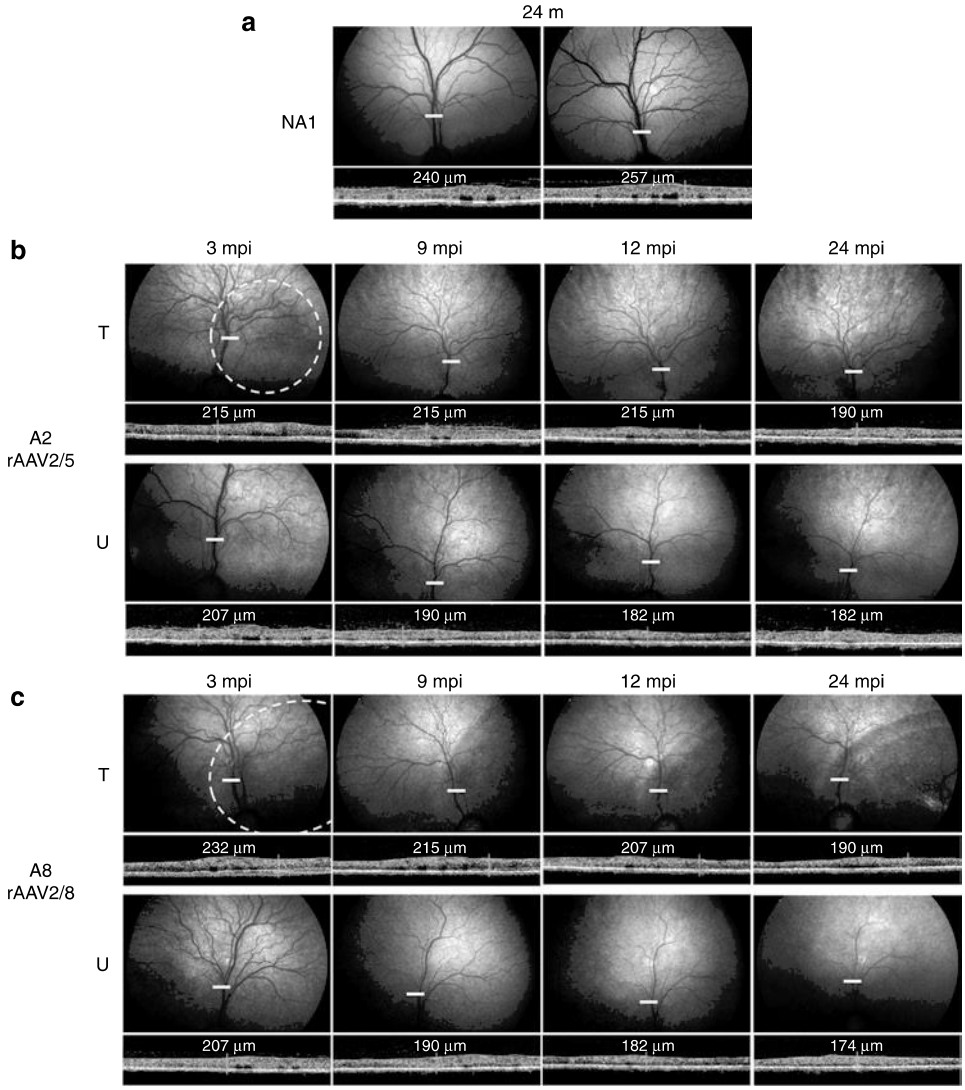

Figure 3 *In vivo* **assessment of retinal morphology in dogs A2 and A8 at 3, 9, 12, and 24 mpi.** (**a**) Fundus photographs and time-domain optical coherence tomography (OCT) images obtained for the right and left eyes of control nonaffected, untreated dog NA1 at 24 months of age. (**b**) Fundus photographs and retinal cross-sectional images obtained for the treated and untreated eyes of dog A2 treated with AAV2/5-RK-c*Rpgrip1* at 3, 9, 12, and 24 months postinjection (mpi). (**c**) Fundus photographs and retinal cross-sectional images obtained for the treated and untreated eyes of dog A8 treated with AAV2/8-RK-c*Rpgrip1* at 3, 9, 12, and 24 mpi. White-dotted circles on fundus photographs schematically represent areas of the treated retinas exposed to rAAV vectors. OCT scans were acquired on a horizontal line shown on the fundus images (white lines). The localization and the size of the white lines represent the localization and the size of the OCT scans. Retinal thicknesses at the same location (13 mm above the optic nerve head) were measured using calibrated calipers and are indicated on the OCT scans. m, months of age; T, treated eye; U, untreated eye.

control retina (NA1) in a similar region (82 µm; Figure 4a). By contrast, vector-unexposed regions had a homogeneously thin ONL and no inner/outer segments (23 µm; Figure 4a), which represented only 27% of the thickness observed in the normal retina (86 µm; Figure 4a). A similar pattern of localized photoreceptor thickness in the region exposed to the rAAV vector was observed across all retinas examined. It was more pronounced at late time points (**Supplementary Figure S3a**).

Morphology of long-term preserved photoreceptors in MLHD-Cord1 treated eyes. To further determine which subtypes of photoreceptors were maintained in transduced area of MLHD-*Cord1* treated eye, dog A2 was sacrificed at 24 mpi, and its retinas were analyzed by histology. Retina cryosections containing the vector-exposed region in the temporal half of the section and vector-unexposed regions in the nasal half were stained with eosin/hematoxylin (Figure 4b) or labeled against rod- (GNAT1) and cone-specific markers (peanut lectin agglutinin (PNA), L/M opsin, and S opsin) (Figure 4c and **Supplementary Figure S3b**). None of the four tested antibodies raised against the murine or human Rpgrip1 antigens showed specific staining on canine retinal flat mounts, cryo- or paraffin-embedded sections (data not shown).

Histological data (Figure 4b,c and **Supplementary Figure S3b**) confirmed our *in vivo* results (Figure 4a). The ONL in the vector-unexposed part of the treated retina was reduced to 2–3 rows of photoreceptor nuclei, indicating a near complete loss of photoreceptors. In this region, no staining of

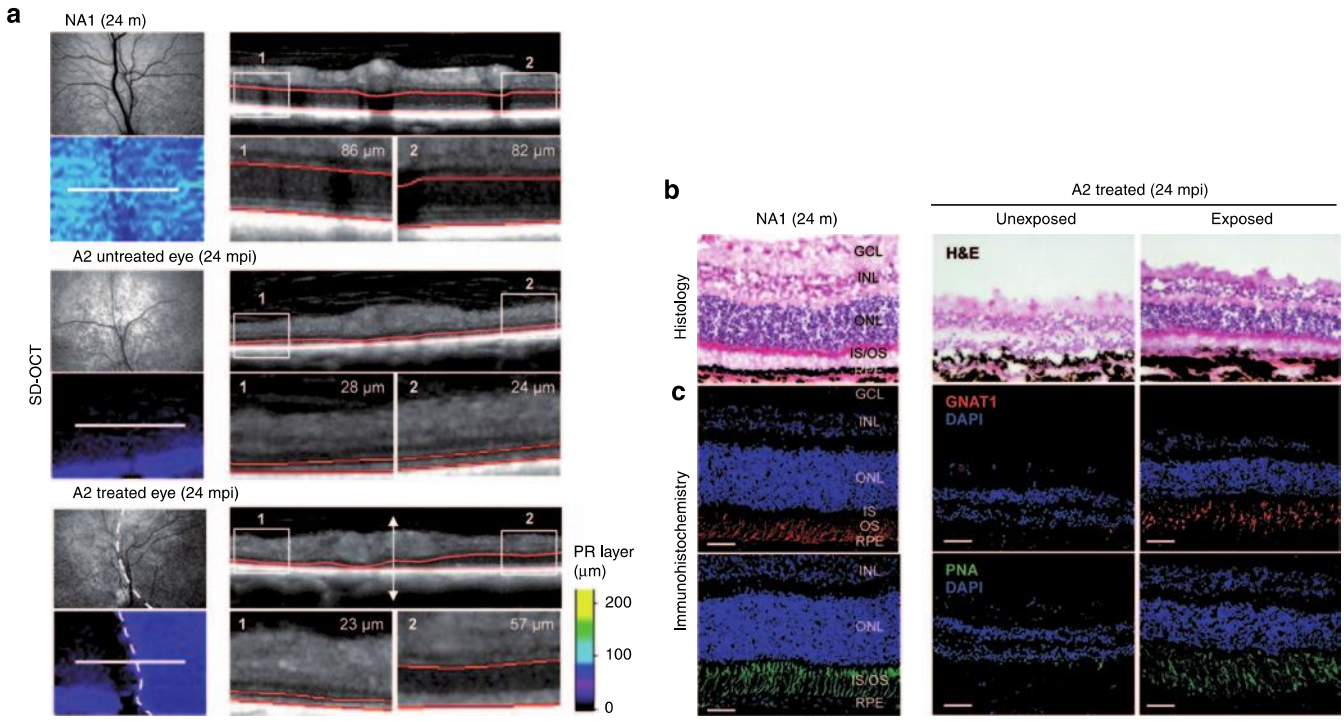

Figure 4 *In vivo* and postmortem assessment of photoreceptor (PR) layer thickness in dog A2 at 24 months postinjection (mpi). (**a**) Topographies of PR layer and spectral-domain optical coherence tomography (SD-OCT) scans (obtained 13 mm above the optic nerve head) from the right eye of dog NA1 (top) and both untreated (middle) and treated (bottom) eyes of dog A2 at 24 mpi. White-dotted circles on fundus photographs schematically represent the area of the treated A2 retina exposed to AAV2/5-RK-c*Rpgrip1* vector. OCT scans were acquired on a horizontal line shown on the fundus images (white lines). PR layer (outer nuclear layer (ONL) + outer segments (OSs) and inner segments (ISs)) was defined semi-automatically (red). PR layer thickness was measured in two normalized (1) temporal and (2) nasal locations. (**b**,**c**) Microscopic images of retinal sections from the treated eye of dog A2 at 24 mpi and the right eye of age-matched control dog NA1. Serial retinal cryosections encompassing the vector-exposed and the vector-unexposed areas of the treated retina were (**b**) stained with hematoxylin and eosin (H&E) (top) or (**c**) immunolabeled against GNAT1 (red, middle) or peanut agglutinin-FITC (green, bottom). Primary GNAT1 antibody was detected with Alexa 546–conjugated goat antirabbit IgG. Scale bar = 30 µm. GCL, ganglion cell layer; INL, inner nuclear layer; m, months of age; RPE, retinal pigment epithelium.

cone- or rod- outer segments can be detected (Figure 4c, left and **Supplementary Figure S3b**). By contrast, transduced regions showed a well-preserved ONL with 11–13 rows of photoreceptor nuclei remaining (Figure 4b, middle), representing 52–62% of normal ONL thickness (21 rows; Figure 4b, right). Preserved photoreceptors displayed well-organized outer segments and were positive for all tested cone and rod markers similar to the normal retina (Figure 4c and **Supplementary Figure S3b**). Thus, in the treated regions of MLHD-*Cord1* retina, both subtypes of photoreceptor seem to be morphologically preserved over the long term.

Gene therapy restores cone function and partially preserves rod function in *Rpgrip1*$^{-/-}$ dogs

We used full-field flash electroretinogram to analyze rescue of the hallmark functional deficits of Rpgrip1 deficiency in treated dogs. ERGs were performed at different time points following vector delivery, starting at 1 mpi. Time course analysis was over 24 mpi for dogs A2, A7, and A8, 12 mpi for dogs A3 and A4, and 6 mpi for dog A5 (Table 1).

Both AAV2/5 and AAV2/8 treatments led to a significant restoration of cone-mediated ERG responses compared with untreated contralateral eyes as early as 1 mpi (Table 1, Figures 5b,c and 6a,c, and **Supplementary Figures S4 and S5**). Importantly, this restored cone function remained stable over time, up to 24 mpi, the longest period of exploration (Table 1, Figures 5 and 6a,c, and **Supplementary Figure S5**). Restored cone function varied from 18% (13 µV) to 72% (53 µV) of the normal cone function (NA1, 73 µV; Table 1 and Figure 6e,g). This difference did not seem to be related to rAAV serotypes but can be explained by small interanimal variations in the extent/localization of the vector subretinal bleb and/or alteration of cones at the time of treatment.

At 1 mpi, no significant difference on rod b-wave amplitudes were observed between treated (113–197 µV) and untreated eyes (110–197 µV) of MLHD-*Cord1* dogs (Table 1, Figures 5 and 6b,d, and **Supplementary Figures S4 and S5**). These rod-mediated responses were all highly similar to that observed in the age-matched *Rpgrip1*$^{+/-}$ control dog (NA1, 192 µV) (Table 1 and Figure 6f). In the untreated eyes of MLHD-*Cord1* dogs, rod ERG responses initially present at 1 mpi decreased dramatically during the following months and were totally lost at 12 mpi (Table 1, Figures 5 and 6b,d, and **Supplementary Figure S4**). A similar decrease in rod b-wave amplitude was observed in the treated eye of dog A7 (Table 1 and **Supplementary Figure S4**). Interestingly, in dogs A2, A3, A4, and A8, although the rod ERG amplitude decreased during the first months following vector administration, it stabilized in the treated eyes from 9 mpi suggesting a partial and stable preservation of rod function (Table 1, Figure 6b,d, and

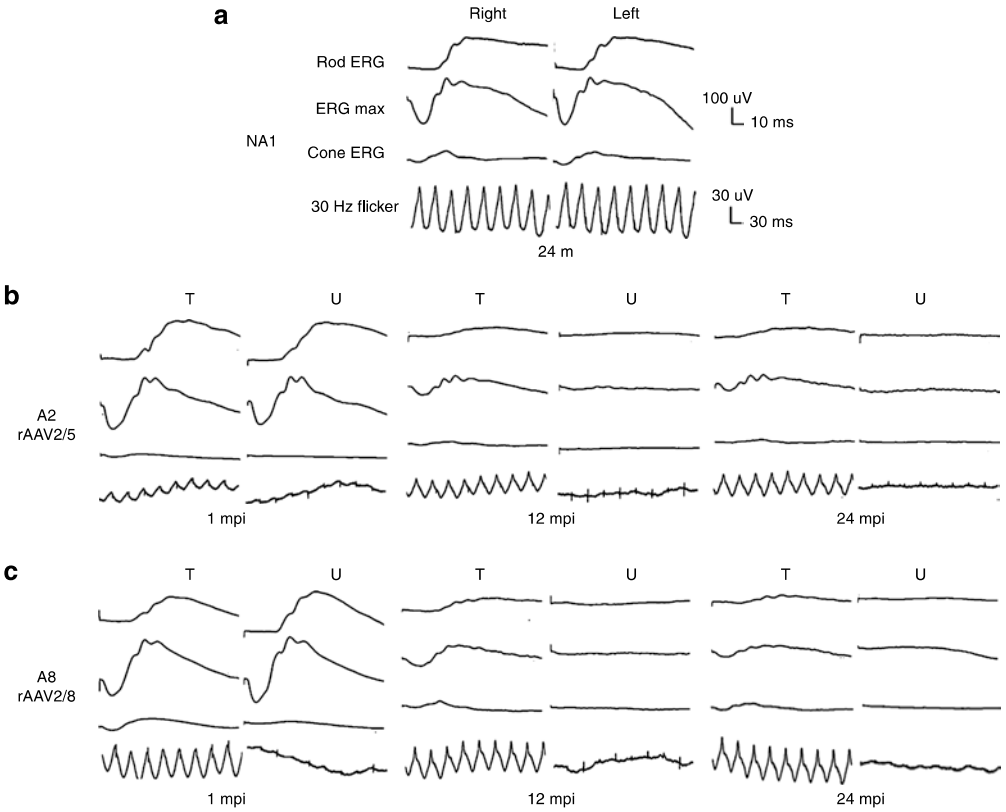

Figure 5 Bilateral full-field electroretinographic traces from dogs NA1, A2, and A8 at 1, 12, and 24 months following subretinal injection. (**a**) Electroretinographic trace from control nonaffected, untreated dog NA1 at 24 months of age. (**b**) Electroretinographic traces from dog A2 treated with AAV2/5-RK-c*Rpgrip1* at 1, 12, and 24 months postinjection (mpi). (**c**) Electroretinographic traces from dog A8 treated with AAV2/8-RK-c*Rpgrip1* at 1, 12 and 24 mpi. The top two recordings are low- and high-intensity dark-adapted responses, whereas the bottom two recordings show light-adapted responses (responses to single flash and 30 Hz flicker stimuli, respectively). m, months of age; T, treated eye; U, untreated eye.

Supplementary Figure S4). At 24 mpi, preserved rod responses of the rAAV2/5-treated eye of dog A2 represent 22% (41 µV) of those recorded at 1 mpi (185 µV) and 21% of that recorded in an age-matched *Rpgrip1*$^{+/-}$ dog (192 µV) (**Table 1** and **Figure 6h**). Likewise, rod responses of the rAAV2/8-treated eye of dog A8 were 25% (50 µV) of its baseline response (197 µV) and 26% of that recorded in the control dog (192 µV; **Table 1** and **Figure 6h**). At this age, no detectable response remained in untreated eyes.

Gene therapy preserves vision of MLHD-*Cord1* dogs in both dim and bright light

To determine whether cone function rescue and/or rod function preservation protected visual function, we used an obstacle avoidance course to evaluate visually guided behavior in dogs A2, A3, A4, A7, and A8 at different times after treatment. Dim- and bright-light conditions were used to evaluate rod- and cone-dominated vision, respectively (**Table 2**).

At 4 and 9 mpi, under both light conditions, none of the treated dogs showed behavioral signs of blindness regardless of which eye was covered (data not shown). However, at 12, 18, and 24 mpi, all dogs tested consistently avoided obstacles when their untreated eye was covered with an opaque lens, whereas they showed many difficulties in navigating around the panels when their treated eye was occluded (**Table 2**). These results were confirmed by a significant variation in transit time. For example, in bright light, dog A7 completed the obstacle course in 8 seconds with its untreated eye covered, whereas it took 27 seconds with its treated eye covered (**Supplementary Video S1**, part I). Similar results were obtained in dim-light condition, with dog A7 completing the obstacle course in 8 seconds with the untreated eye covered and in 33 seconds with the treated eye covered (**Supplementary Video S1**, part II). Together, these results strongly demonstrate that both rAAV2/5- and rAAV2/8-mediated c*Rpgrip1* expression preserved both dim- and bright-light vision in the MLDH-*Cord1* dog.

DISCUSSION

In this study, we have demonstrated the efficacy of gene replacement therapy in a large animal model of cone–rod dystrophy, the MLHD-*Cord1* dog.[12,13] Using rAAV2/5 and rAAV2/8 vectors expressing the c*Rpgrip1* cDNA under the control of the photoreceptor-specific human RK promoter, we have shown an increase of photoreceptor survival, a significant restoration of cone function, and a partial preservation of rod function for up to 24 mpi. Dim- and bright-light vision was also preserved in treated animals. Collectively, these results strongly indicate that gene therapy is a possible approach for treating recessive cone–rod dystrophies.

Animal models of retinal dystrophies that share clinical features with their human counterparts play a crucial role for the development and validation of new therapies. In this study, we confirmed that our MLHD-*Cord1* dogs manifest an early onset

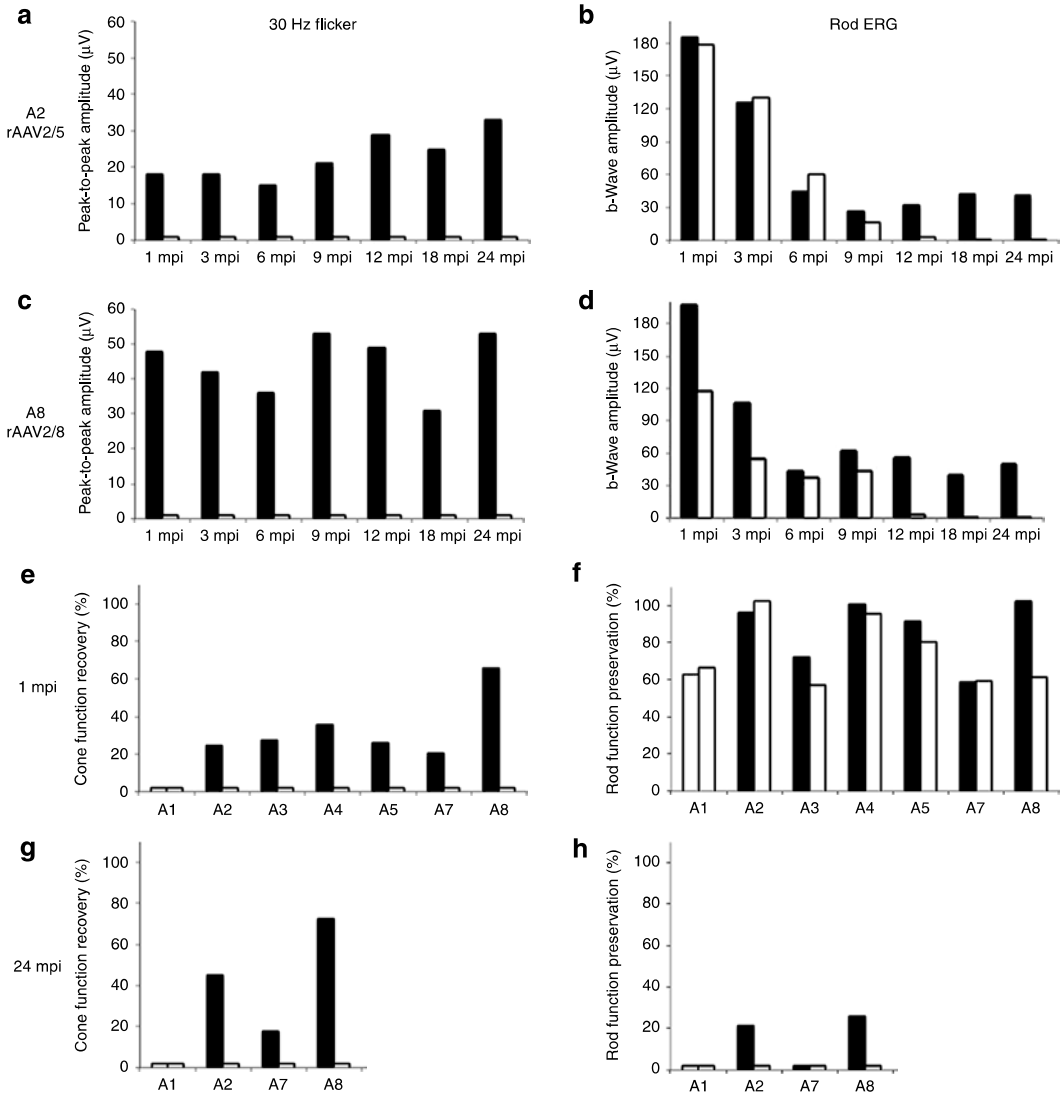

Figure 6 Kinetics of cone function recovery and rod function preservation in treated dogs. (**a**,**b**) Amplitudes of (**a**) 30 Hz flicker and (**b**) rod-b wave responses for dog A2 treated with AAV2/5-RK-c*Rpgrip1* from 1 to 24 months postinjection (mpi). (**c**,**d**) Amplitudes of (**c**) 30 Hz flicker and (**b**) rod-b wave responses for dog A8 treated with AAV2/8-RK-c*Rpgrip1* from 1 to 24 mpi. (**e**,**g**) Percentages of normal NA1 cone function (73 μV) recovered in MLHD-*Cord1* treated dogs at (**e**) 1 and (**g**) 24 mpi. (**f**,**h**) Percentages of normal NA1 rod function (192 μV) preserved in MLHD-*Cord1* treated dogs at (**f**) 1 and (**h**) 24 mpi. Treated eyes are shown in dark and untreated eyes in white. ERG, electroretinogram. MLHD, miniature long-haired dachshund.

Table 2 Evolution of bright- and dim-light vision in MLHD-*Cord1* treated dogs

			Bright-light				Dim-light			
Dog	Vector	Follow-up (mpi)	4 mpi (T/U)	9 mpi (T/U)	12 mpi (T/U)	24 mpi (T/U)	4 mpi (T/U)	9 mpi (T/U)	12 mpi (T/U)	24 mpi (T/U)
A2	AAV2/5-RK-cRpgrip1 (1.10^{11} vg/ml)	24	ND	+/+	+/–	+/–	ND	+/+	+/–	+/–
A3		12	+/+	+/+	+/–	ND	+/+	+/+	+/–	ND
A4		12	+/+	+/+	+/–	ND	+/+	+/+	+/–	ND
A5		6	+/+	ND	ND	ND	+/+	ND	ND	ND
A7	AAV2/8-RK-cRpgrip1 (1.10^{12} vg/ml)	24	ND	+/+	+/–	+/–	ND	+/+	+/–	+/–
A8		24	ND	+/+	+/–	+/–	ND	+/+	+/–	+/–

–, non–vision-guided behavior; +, vision-guided behavior; ND, not done; T, treated eye; U, untreated eye.
Vision tests were performed in bright (260±13 lux) and dim (1.5±0.8 lux) light at 4, 9, 12, 18, and 24 mpi. An opaque lens was used to alternatively cover treated and untreated eyes.

and severe progressive cone–rod dystrophy, consistent with previous characterization of this research colony.[12,13] All the dogs examined exhibited undetectable cone function from the earliest age measured (1 month of age). They had a nearly normal rod function at 1 month that rapidly declined thereafter. This dysfunction of photoreceptors was associated with a progressive loss of photoreceptor cells, as shown by the nearly complete loss of ONL nuclei at 24 months. This phenotype was highly conserved in all our *Rpgrip1*$^{-/-}$ dogs, despite small interindividual variations in the onset/speed of rod function and photoreceptor cell loss. This phenotype strongly correlates with the ophthalmologic abnormalities seen (i) in the *Rpgrip1* knockout mice in which photoreceptor degeneration begins at P15 and is almost complete by 5 months of age[25] and (ii) in patients with *RPGRIP1* mutations that display a degeneration of both rod and cone photoreceptors and experience a severe loss of color vision and central acuity early in life.[15–20] Of note, this MLHD-*Cord1* phenotype differs from that of other *Rpgrip1*$^{-/-}$ dogs in the pet population[41] or in a crossbred research colony[42] that have the same genetic mutation but display a variable cone function and no change of rod function over time. Several hypotheses have been formulated to explain this genotype/phenotype discrepancy, including that the *Cord1* phenotype involves a second gene that controls the penetrance or expression of c*Rpgrip1*[41,42] or that c*Rpgrip1* itself is the modifier gene.[43]

In this article, we showed that AAV2/5-RK-c*Rpgrip1* or AAV2/8-RK-c*Rpgrip1* gene transfer restored 18–72% of normal cone function in treated MLHD-*Cord1* eyes, as early as 1 mpi. Notably, this rescued cone function remained stable for at least 24 mpi (the longest time point explored), which supports a long-lasting and stable restoration of cone function after a single vector injection. This study demonstrates that gene therapy can restore cone function in a large animal model of RPGRIP1 deficiency. All previous reports of *Rpgrip1* gene therapy have been focusing on the *Rpgrip1* knockout mouse, which exhibits nearly normal cone function before photoreceptor degeneration.[25] In this *Rpgrip1*$^{-/-}$ mice, subretinal injection of AAV2/8-RK-h*RPGRIP1* at P14 led to the preservation of fourfold higher cone ERG responses compared with untreated eyes at 5 months of age, accounting for ~33% of wild-type levels. There was no decline in cone function in treated eyes from 2 to 5 months of age, whereas untreated eyes experienced a monthly decline of 25% of the cone amplitude.[28] In our MLHD-*Cord1* dogs, the cone function recovery (mean: 34±14% of nonaffected dog) was within the range of that previously obtained after rAAV-mediated gene therapy in murine models of cone–rod dystrophy with nonfunctional cones (primary genetic defect in both rods and cones), including the *GC1KO*[36,37,44] (from 20 to 65% of wild-type function) and *GC1/GC2* knockout mice (from 29 to 44% of wild-type function).[38]

In addition to this sustained cone function recovery, we evaluated the effect of c*Rpgrip1* gene replacement on rod photoreceptor function. Indeed, MLHD-*Cord1* dogs have been shown also to exhibit an extinction of rod function over time.[12,13] Interestingly, all along the first 6–9 months after treatment, this progressive loss of rod function remained unchanged in all treated *Rpgrip1*$^{-/-}$ dogs (n = 5). This indicates that subretinal delivery of AAV2/5-RK-c*Rpgrip1* or AAV2/8-RK-c*Rpgrip1* at 1 month of age, in over 35% of the total retinal surface, was insufficient to entirely stop or obviously delay the initiation of rod dysfunction in this model. Nevertheless, continuous monitoring of rod function up to 24 mpi revealed that in four out of the five treated dogs, c*Rpgrip1* gene transfer also had a significantly positive effect on rod function. Indeed, from 9 mpi, four dogs (rAAV2/5, n = 2 and rAAV2/8, n = 2) showed a better preservation of b-wave amplitude in treated eyes compared with their untreated eyes. At 12 mpi, rod-mediated responses of the untreated eye were almost flat, whereas the treated eye of dog A2, A3, A4, and A8 maintained a substantial ERG response (21, 29, 25, and 26% of normal eyes, respectively). Interestingly, in the two dogs followed up to 24 mpi, A2 (rAAV2/5) and A8 (rAAV2/8), this preserved rod function remained stable for the 12 following months, suggesting that rod function loss was halted in these treated eyes after the initial decrease. This long-term preserved rod function was 22 and 25% of baseline for A2 and A8 treated eye, respectively. It may represent a fraction of preserved rods with reduced but stabilized function and/or a smaller fraction of totally potent rods that remain healthy over time. It is interesting to note that 3 murine models of progressive cone–rod dystrophy with initial normal rod function, the *Rpgrip1*$^{-/-}$,[27] the *Aipl1*$^{h/h}$,[45] and the *Bbs4-null* mice,[46] displayed a similar kinetic of rod function preservation after gene therapy, i.e., an initial decrease of rod function followed by a stabilization.

Although the molecular events causing or leading to photoreceptor death in MLHD-*Cord1* dogs are not completely understood, all our *in vivo* and postmortem observations indicated that localized AAV2/5-RK-c*Rpgrip1* or AAV2/8-RK-c*Rpgrip1* injection at 1 month of age resulted in localized photoreceptor preservation up to 24 mpi. At this age, photoreceptor loss was nearly complete in vector-unexposed regions. This result is similar to the confined photoreceptor preservation previously observed in the *XLPRA1* and *XLPRA2* dog models that display a progressive rod–cone dystrophy linked to a genetic defect in both rods and cones[11] and in the *Rcd1* dog, a model of progressive rod–cone dystrophy that carries a genetic defect in rods only.[10]

Interestingly, our analysis also revealed that despite evidence of better photoreceptor preservation in the vector-exposed area of MLHD-*Cord1* treated eyes, advancing retinal thinning was still observed in all treated eyes from 3 to 24 mpi. A similar progressing retinal dystrophy has previously been observed in several canine gene therapy models, but remarkably, not all. In both *XLPRA2*[11] and *Rpe65*$^{-/-}$[47] dogs treated after the onset of apparent retinal degeneration, a gradual loss of photoreceptor nuclei was demonstrated in the vector-exposed area (from 3 to 24 mpi in the *XLPRA2* dog treated at 5 weeks of age (as clearly shown by SD-OCT on Supplementary Figure S1 of ref. 11) and at 1.3 years postinjection in the *Rpe65*$^{-/-}$ dog treated between 4.9 and 6.6 years of age). By contrast, in both *Rcd1*[10] and *Rpe65*$^{-/-}$[47,48] dogs treated before the onset of the disease, retinal degeneration was stably prevented in the vector-exposed area (up to 30 mpi for the *Rcd1* dog treated at P20 (Petit, L, unpublished data, 2013) and up to 11 years postinjection for the *Rpe65*$^{-/-}$ dog treated before 2.4 years of age).[47,48] The alteration stage of some photoreceptors at the age of the treatment/transgene expression may be responsible for this different outcome in dog models of IRD,[47] as previously suggested in murine models of IRD.[38,49,50] Interestingly, it was recently demonstrated in *Rpe65*$^{-/-}$ dogs and RPE65-deficient patients treated at

late stages of the disease that, advancing photoreceptor degeneration is not associated with a gradual loss of restored photoreceptor function,[47] strongly suggesting that it mainly reflects the gradual loss of functionally silent (nonrescued) photoreceptors. Long-term results from two of our treated dogs with persistent rescued cone and preserved rod function from 12 to 24 mpi suggest that it is also the case in the MLHD-*Cord1* dog.

The question then is whether these preclinical data on MLHD-*Cord1* dogs are predictive for future treatment of RPGRIP1-deficient patients? Human RPGRIP1 deficiencies are associated with Leber congenital amaurosis[15–19] and cone–rod dystrophy,[20] depending on the causative mutations and/or genetic modifiers. In all cases, RPGRIP1-deficient patients display an early onset and severe photoreceptor dysfunction and vision loss. However, the onset and progression of photoreceptor cell loss has been relatively poorly assessed. Importantly, a study reported that one patient with RPGRIP1 deficiencies retains central retinal architecture and a substantial ONL for long periods after the total loss of visual function.[17] In our study, both rAAV2/5- and rAAV2/8-mediated gene transfer had therapeutic effects in the MLHD-*Cord1* dog. Similar cone and rod function improvements were observed despite rAAV2/8 (10^{12} vg/ml) was injected at a 10-fold higher titer than rAAV2/5 (10^{11} vg/ml), as previously observed and discussed for the P*de6β*$^{-/-}$ treated dog.[10] This observation reinforces the potential of AAV2/5 associated with the human RK promoter for targeting photoreceptors in humans, as recently demonstrated in the nonhuman primate.[32] The positive effects on the major pathologic hallmarks that are found in the MLHD-*Cord1* dog suggest that patients with RPGRIP1 or other cone–rod dystrophies might benefit from gene addition therapy.

MATERIALS AND METHODS

Amplification of the canine *Rpgrip1* cDNA

Poly(A) mRNA isolation and cDNA synthesis. Poly(A) messenger RNAs (mRNAs) were extracted and purified from snap-frozen canine retinas using the Oligotex direct mRNA kit (Qiagen, Courtaboeuf, France) according to the manufacturer's instructions. cDNAs were synthesized using random hexamer primers and reverse transcriptase (Transcriptor High Fidelity, Roche Diagnostics, Meylan, France) according to the supplier's protocol.

PCR and RLM-RACE PCR. Human, bovine and rodent *RPGRIP1* cDNA sequences were aligned with the canine genomic sequence. Sequences of homology were used for primer design (Table S1) to amplify seven overlapping fragments covering the entire predicted c*Rpgrip1* coding sequence (Rpgrip1-1 to Rpgrip1-7) (**Supplementary Figure S1**). Both 3′ and 5′ ends of c*Rpgrip1* transcript were obtained with RLM-RACE PCR (Ambion, Applied Biosystems, Courtaboeuf, France) according to the manufacturer's instructions. The 5′ end of the c*Rpgrip1* cDNA was obtained in two steps using Rpgrip1-1F (5′ RACE adaptor primer)/Rpgrip1-1R (sequence specific primer in exon 6) as outer primers and 1nestedF (5′ RACE adaptor primer)/1nestedR (sequence specific primer in exon 4) as inner primers. The 3′ end of the *cRpgrip1* cDNA was obtained in two steps using Rpgrip1-7F (sequence specific primer in exon 19)/Rpgrip1-7R (3′ RACE adaptor primer) as outer primers and 7nestedF (sequence specific primer in exon 19–20/7nestedR (3′ RACE adaptor primer) as inner primers.

PCR amplification was performed using KOD Hot Start Polymerase (Novagen, Merck Eurolab, Fontenay sous Bois, France) under the following conditions: initiation at 95°C for 2 minutes, followed by 35 cycles of denaturation, annealing, and extension (depending on the amplicon; **Supplementary Table S1**). PCR products were then analyzed on a 1.5% agarose gel, extracted (NucleoSpin Extract II kit, Macherey Nagel, Hoerdt, France), cloned into the pS972 vector (Promega, Charbonnières, France), and sequenced with standard SP6 and T7 forward and reverse primers.

Rpgrip1-1 to Rpgrip1-7 PCR fragments were assembled using endogenous restriction sites present in the c*Rpgrip1* cDNA. The cloned c*Rpgrip1* cDNA was verified by sequencing and was identical to the recently published canine *Rpgrip1* reference sequence (GenBank HM021768).[40]

Vector plasmids construction and production of rAAV vectors. Recombinant AAV2/5-RK-eGFP, AAV2/5-RK-c*Rpgrip1*, and AAV2/8-RK-c*Rpgrip1* vectors were produced by triple transfection of 293 cells according to previously reported methods using the SSV9-RK-eGFP or SSV9-RK-c*Rpgrip1* vector plasmids.[10] These constructs expressed either eGFP or c*Rpgrip1* cDNA directly under the control of the short human RK promoter (−112 to +87 bp)[33] and the bovine growth hormone polyadenylation signal (BGHpA), flanked by two AAV2 inverted terminal repeat sequences.

For the SSV9-RK-eGFP vector plasmid construction, the 588-bp cytomegalovirus (CMV) promoter of a parental SSV9-CMV-eGFP plasmid was replaced with the 238-bp human RK promoter (kindly provided by Shahrokh Khani, State University of New-York, Buffalo, NY). For the SSV9-RK-c*Rpgrip1* plasmid construction, the 1340-bp eGFP-WRPE sequence of the SSV9-RK-eGFP plasmid was replaced with the 3861-bp c*Rpgrip1* cDNA. The resulting SSV9-RK-eGFP and SSV9-RK-c*Rpgrip1* constructs were verified by sequencing.

Viral vector titers were determined by dot blot and by quantitative real-time PCR and are expressed as vector genomes per millilitre (vg/ml). The final vector titers of AAV2/5-RK-eGFP, AAV2/5-RK-c*Rpgrip1*, and AAV2/8-RK-c*Rpgrip1* were 1×10^{11}, 1×10^{11}, and 1×10^{12} vg/ml, respectively.

Animals. A total of eight affected *Rpgrip1*$^{-/-}$ and 3 *Rpgrip1*$^{+/-}$ MLHD dogs were used in this study (**Table 1**). The first four *Rpgrip1*$^{-/-}$ individuals of the colony were kindly provided by Cathryn Mellersh (Animal Health Trust, Lanwades Park, Kentford, Newmarket, Suffolk, UK).[14] Animals were maintained at the Boisbonne Center (ONIRIS, Nantes-Atlantic College of Veterinary Medicine, Food Science and Engineering, Nantes, France) under a 12/12-hour light/dark cycle. All procedures involving animals were performed in compliance with the Association for Research in Vision and Ophthalmology statement for the use of animals in ophthalmic and vision research.

Subretinal administration of rAAV vectors. Subretinal injection of AAV2/5-RK-eGFP vector was performed bilaterally on two nonaffected *Rpgrip1*$^{+/-}$ dogs at 7 months of age. Subretinal injections of AAV2/5-RK-c*Rpgrip1* and AAV2/8-RK-c*Rpgrip1* were performed unilaterally on seven affected *Rpgrip1*$^{-/-}$ dogs at 1 month of age (**Table 1**). All subretinal injections were performed under general anesthesia as previously published.[10] All the vectors were injected at their maximal titer (AAV2/5-RK-eGFP, 10^{11} vg/ml; AAV2/5-RK-c*Rpgrip1*, 10^{11} vg/ml; and AAV2/8-RK-c*Rpgrip1*, 10^{12} vg/ml). The volume injected varied from 90 to 140 µl. At the time of injection, the location and extent of the subretinal blebs were recorded on fundus photographs or schematic fundus drafts when it was not possible to obtain clear fundus photography at the time of injection.

In vivo *GFP fluorescence imaging and GFP expression analysis.* GFP fluorescence in dogs NA2 and NA3 was monitored at weekly intervals by fluorescence retinal imaging using a Canon UVI retinal camera connected to a digital imaging system (Lhedioph Win Software, Lheritier SA, Saint-Ouen-l'Aumône, France).

At 9 mpi, dogs were euthanized by intravenous injection of pentobarbital sodium (Vétoquinol, Lure, France). Eyecups were fixed for 48 hours in Bouin's solution (Laurylab, Saint Fons, France), embedded in paraffin,

and 7-µm sections were prepared. Before immunostaining, sections were deparaffinized in toluene and rehydrated with phosphate-buffered saline solution. This method allows good preservation of cone photoreceptor shape but slightly reduces eGFP fluorescence. Nonspecific antigen binding was blocked by incubating sections in blocking solution (20% normal goat serum (Invitrogen), 0.1% Triton X-100 in phosphate-buffered saline) for 45 minutes at room temperature. Sections were then incubated overnight at 4°C with rabbit anti-LM opsin (1:200; Millipore, Molsheim, France) in blocking solution. After three washes in 0.1% Triton X-100 in phosphate-buffered saline solution, slides were incubated with the Alexa fluor 546–conjugated goat antirabbit IgG (1:250; Invitrogen) for 2 hours at room temperature. Cell nuclei were counterstained with 4′,6-diamidino-2-phenylindole (DAPI) (Invitrogen), and sections were mounted in Prolong Gold antifade reagent (Invitrogen). Sections were observed with an epifluorescence microscope (Nikon, Champigny-sur-Marne, France). eGFP signals were observed directly under 488 nm. To facilitate the colocalization of eGFP and L/M opsin, the immunolabeled sections were highly exposed to 568 nm to observe Alexa fluor 546 signals in cone inner segments. Images were captured with a digital camera (Nikon) (30 slices analyzed by canine retina, $n = 4$).

Reverse transcriptase–PCR. Total RNA was isolated from individual snap-frozen retinas of *Rpgrip1*$^{+/+}$, *Rpgrip1*$^{+/-}$, and *Rpgrip1*$^{-/-}$ dogs using TRIzol Reagent (Invitrogen). Rnase-free TURBO Dnase I (Ambion) was used according to the manufacturer's instructions to remove contaminating DNA before generation of cDNA by reverse transcription. Nine hundred nanograms of total RNA were reverse-transcribed using oligo-dT primers and Transcriptor High Fidelity reserve transcriptase (Roche Diagnostics) in a total volume of 20 µl as per the manufacturer's instructions.

Integrity of cDNA was determined by amplification of a 660-bp sequence of the canine β-actin gene using β-actinF (5′-TGA CGGGGTCACCCACACTGTGCCCATCTA-3′) and β-actinR (5′-CTAG AAGCATTTGCGGTGGACGATGGAGGG-3′) primers. For c*Rpgrip1* amplification, 184F (5′-CCAGTGTCGAAAGGTAAGAAT-3′) and 317R (5′-TCCTCGCCCTTTTGATCTCAT-3′) primers were designed to amplify a 154-bp or 198-bp product specific for the wild-type or mutant Ins44 cDNA, respectively (**Figure 3**). The amount of cDNA used in β-actin and c*Rpgrip1* PCR was 40 ng. Both PCRs were performed using KOD Hot Start DNA Polymerase (Novagen) and a Veriti thermocycler (Applied Biosystems). Conditions of amplification were as follows: an initial denaturation step at 95°C for 2 minutes, followed by 40 cycles at 95°C for 20 seconds, 58°C for 10 seconds, and 70°C for 7 seconds. Actin and c*Rpgrip1* PCR products were resolved on a 1.5 and 4% agarose gel electrophoresis, respectively.

Fundus photography and TD-OCT. Fundus photography and TD-OCT were performed bilaterally on all treated dogs every 2 months after treatment (except dog A6). Before clinical examinations, pupils were fully dilated by topical administration of 0.3% atropine (Alcon Cusi SA, Barcelona, Spain), tropicamide (Novartis, Annonay, France), and phenylephrine hypochloride (Novartis). Dogs were anesthetized by intravenous injection of xylazine (BayerHealth Care, Shawnee Mission, UK) and ketamine (Rhone Merieux, Lyon, France).

Fundus photographs were taken with a Canon UVI retinal camera connected to a digital imaging system (Lhedioph). TD-OCT was performed using a 3-mm horizontal line scan of the retina (Stratus 3000; Carl Zeiss S.A.S., Le Pecq, France). Mann–Whitney paired *t*-test was used to statistically analyze the results from treated and untreated eyes. A P value <0.05 was considered significant (confidence intervals = 95%). Statistical analyzes were performed using GraphPad Prism for Macintosh (GraphPad, Software, San Diego, CA).

Spectral-domain OCT. SD-OCT was performed bilaterally on dogs A2, A7, and A8 at 24 mpi. Pupils were dilated as described above, and dogs were anesthetized following premedication by intravenous injection of thiopental sodium (Specia Laboratories, Paris, France) followed by isoflurane gas inhalation.

SD-OCT was performed with 30° horizontal scans placed across the vector bleb temporal boundary (Spectralis Heidelberg Engineering, Heidelberg, Germany). Scans covered retinal regions of 13×8 mm (13 line scans of 1×8 mm, 23 averaging). Postacquisition processing of OCT data was performed with a commercial program following manufacturer's instructions (Heidelberg). The photoreceptor layer (ONL + outer and inner segments) was defined semi-automatically, and its thickness was automatically calculated.

Postmortem analysis of photoreceptor preservation in MLHD-Cord1–treated eyes. Dog A2 and age-matched untreated dog NA1 were sacrificed 24 mpi as described above. Eyes were fixed for 2 hours in 4% paraformaldehyde in phosphate-buffered saline solution before removal of the anterior chamber and the lens. Eyecups were embedded in optimal cutting temperature compound (OCT Cryomount, Microm Microtech, Francheville, France) and snap frozen in a dry isopentane bath. Cryosections of 12–15 µm thickness were prepared and stored until use.

For morphological examination, sections were stained with hematoxylin–eosin before imaging by transmitter light microscopy (Nikon). For immunohistochemical studies, sections were immunolabeled as previously described with the following antibodies: PNA-FITC (Vector Laboratories, Bulingame, CA, USA; 1:250), rabbit anti-L/M opsin (Millipore; 1:250), rabbit anti-S opsin (Millipore; 1:250), and rabbit anti-GNAT1 (Santa-Cruz Technology, Heidelberg, Germany; 1:250). Primary antibodies were revealed with the secondary antibody Alexa 546–conjugated goat antirabbit IgG (Invitrogen) at 1:250. Nuclei were counterstained with 4′,6-diamidino-2-phenylindole, and sections were mounted in Mowiol antifade reagent (Calbiochem, San Diego, CA). Tissues were viewed on an epifluorescence microscope (Nikon), and images were captured with a digital camera (Nikon).

Electroretinography. Retinal function of AAV2/5-RK-c*Rpgrip1*- or AAV2/8-RK-c*Rpgrip1*-treated *Rpgrip1*$^{-/-}$ dogs and age-matched untreated *Rpgrip1*$^{-/-}$ and *Rpgrip1*$^{+/-}$ controls were evaluated using bilateral full-field flash electroretinogram. Initial ERG measurements were recorded at 1 mpi and every subsequent 2 months, up to 4 (dog A5), 12 (dogs A3 and A4), or 24 mpi (dogs A2, A7, and A8).

Both pupils of animals were topically dilated as described above. Dogs were dark adapted for 20 minutes and anesthetized following premedication by intravenous injection of thiopental sodium (Specia Laboratories) followed by isoflurane gas inhalation. Hydroxypropulmethylcellulose (Laboratoires Théa, Clermont-Ferrand, France) was applied to each eye to prevent corneal dehydration during recordings.

A computer-based system (Neuropack MEB 9102K, Nikon KohdenO, Tokyo, Japan) and contact lens electrodes (ERG-jet; Microcomponents SA, Grenchen, Switzerland) were used. ERGs were recorded in a standardized fashion according to the International Society for Clinical Electrophysiology of Vision recommendations using a protocol described previously.[29] Mann–Whitney paired *t*-test was used to statistically analyze the results from treated and untreated eyes. A P value <0.05 was considered significant (confidence intervals = 95%). Statistical analyzes were performed using GraphPad Prism for Macintosh (GraphPad Software).

Behavioral studies. Ambulation of treated *Rpgrip1*$^{-/-}$ dogs through an obstacle avoidance course in bright- (260±13 lux) and dim-light (1.5±0.8 lux) conditions was evaluated at 4, 9, 12, 18, and 24 mpi as previously described.[10] An opaque lens was used to alternatively cover the treated or the untreated eye, and obstacle panel combinations were randomly determined for each test to prevent the dogs memorizing the positions of the obstacle panels. All dim-light films were cleared before mounting with commercial Final Cut Pro 7 software (Apple, Cork,

Ireland) using a standardized protocol. For each dog, the transit time and the number of collisions from three trials on the same day were used for data analysis. Vision-guided behavior (referred as + in Table 2) was determined for a mean transit time ≤10 seconds and a mean number of collisions ≤1. Non–vision-guided behavior (referred as – in Table 2) was determined for a mean transit time ≥20 seconds and/or a mean number of collisions ≥3.

SUPPLEMENTARY MATERIAL

Figure S1. Canine *Rpgrip1* amplification strategy.

Figure S2. Gene therapy did not halt retinal degeneration in treated MLHD-*Cord1* eyes.

Figure S3. Gene therapy prevented long-term photoreceptor degeneration in all treated MLHD-*Cord1* eyes.

Figure S4. Bilateral full-field electroretinographic traces from dogs A7, A3, A4, and A5.

Figure S5. Statistical analysis of ERG responses in treated and untreated MLHD-*Cord1* eyes.

Table S1. Primers used for the amplification of c*Rpgrip1* cDNA.

Table S2. Characterization of the exon–intron junctions of the c*Rpgrip1* gene.

Video S1. Assessment of bright- and dim-light vision of dog A7 at 12 months postinjection.

ACKNOWLEDGMENTS

We thank Cathryn Mellersh (Animal Health Trust, Newmarket, Suffolk, UK) for the gift of the first MLHD-*Cord1* dogs and Shahrokh Khani (State University of New-York, Buffalo, NY, USA) for the gift of the human RK promoter. We thank the Vector Core (www.vectors.univ-nantes.fr) for production of the rAAV vectors, the staff of the Boisbonne Center and Thibaut Larcher (INRA/ONIRIS, Nantes, France) for animal care, and Mireille Ledevin (INRA/ONIRIS, Nantes, France) for technical assistance. We also thank Knut Stieger (Justut-Liebig-University Giessen, Germany) for critical reading of the manuscript. This work was supported by unrestricted grants from the Association Française contre les Myopathies, the INSERM, the Fondation pour la Thérapie Génique en Pays de la Loire, and the Agence Nationale pour la Recherche.

REFERENCES

1. Hartong, DT, Berson, EL and Dryja, TP (2006). Retinitis pigmentosa. *Lancet* **368**: 1795–1809.
2. Michaelides, M, Hardcastle, AJ, Hunt, DM and Moore, AT (2006). Progressive cone and cone-rod dystrophies: phenotypes and underlying molecular genetic basis. *Surv Ophthalmol* **51**: 232–258.
3. Hamel, CP (2007). Cone rod dystrophies. *Orphanet J Rare Dis* **2**: 7.
4. den Hollander, AI, Black, A, Bennett, J and Cremers, FP (2010). Lighting a candle in the dark: advances in genetics and gene therapy of recessive retinal dystrophies. *J Clin Invest* **120**: 3042–3053.
5. Smith, AJ, Bainbridge, JW and Ali, RR (2012). Gene supplementation therapy for recessive forms of inherited retinal dystrophies. *Gene Ther* **19**: 154–161.
6. Colella, P and Auricchio, A (2012). Gene therapy of inherited retinopathies: a long and successful road from viral vectors to patients. *Hum Gene Ther* **23**: 796–807.
7. Boye, SE, Boye, SL, Lewin, AS and Hauswirth, WW (2013). A comprehensive review of retinal gene therapy. *Mol Ther* **21**: 509–519.
8. Stieger, K, Lhériteau, E, Lhéariteau, E, Moullier, P and Rolling, F (2009). AAV-mediated gene therapy for retinal disorders in large animal models. *ILAR J* **50**: 206–224.
9. Komáromy, AM, Alexander, JJ, Rowlan, JS, Garcia, MM, Chiodo, VA, Kaya, A *et al.* (2010). Gene therapy rescues cone function in congenital achromatopsia. *Hum Mol Genet* **19**: 2581–2593.
10. Petit, L, Lhériteau, E, Weber, M, Le Meur, G, Deschamps, JY, Provost, N *et al.* (2012). Restoration of vision in the pde6β-deficient dog, a large animal model of rod-cone dystrophy. *Mol Ther* **20**: 2019–2030.
11. Beltran, WA, Cideciyan, AV, Lewin, AS, Iwabe, S, Khanna, H, Sumaroka, A *et al.* (2012). Gene therapy rescues photoreceptor blindness in dogs and paves the way for treating human X-linked retinitis pigmentosa. *Proc Natl Acad Sci USA* **109**: 2132–2137.
12. Turney, C, Chong, NH, Alexander, RA, Hogg, CR, Fleming, L, Flack, D *et al.* (2007). Pathological and electrophysiological features of a canine cone-rod dystrophy in the miniature longhaired dachshund. *Invest Ophthalmol Vis Sci* **48**: 4240–4249.
13. Lhériteau, E, Libeau, L, Stieger, K, Deschamps, JY, Mendes-Madeira, A, Provost, N *et al.* (2009). The RPGRIP1-deficient dog, a promising canine model for gene therapy. *Mol Vis* **15**: 349–361.
14. Mellersh, CS, Boursnell, ME, Pettitt, L, Ryder, EJ, Holmes, NG, Grafham, D *et al.* (2006). Canine RPGRIP1 mutation establishes cone-rod dystrophy in miniature longhaired dachshunds as a homologue of human Leber congenital amaurosis. *Genomics* **88**: 293–301.
15. Dryja, TP, Adams, SM, Grimsby, JL, McGee, TL, Hong, DH, Li, T *et al.* (2001). Null RPGRIP1 alleles in patients with Leber congenital amaurosis. *Am J Hum Genet* **68**: 1295–1298.
16. Gerber, S, Perrault, I, Hanein, S, Barbet, F, Ducroq, D, Ghazi, I *et al.* (2001). Complete exon-intron structure of the RPGR-interacting protein (RPGRIP1) gene allows the identification of mutations underlying Leber congenital amaurosis. *Eur J Hum Genet* **9**: 561–571.
17. Jacobson, SG, Cideciyan, AV, Aleman, TS, Sumaroka, A, Schwartz, SB, Roman, AJ *et al.* (2007). Leber congenital amaurosis caused by an RPGRIP1 mutation shows treatment potential. *Ophthalmology* **114**: 895–898.
18. Fakhratova, M (2013). Identification of a novel LCA6 mutation in an Emirati family. *Ophthalmic Genet*, published online 2 January 2013 (doi:10.3109/13816810.2012.755552).
19. Khan, AO, Abu-Safieh, L, Eisenberger, T, Bolz, HJ and Alkuraya, FS (2013). The RPGRIP1-related retinal phenotype in children. *Br J Ophthalmol* **97**: 760–764.
20. Hameed, A, Abid, A, Aziz, A, Ismail, M, Mehdi, SQ and Khaliq, S (2003). Evidence of RPGRIP1 gene mutations associated with recessive cone-rod dystrophy. *J Med Genet* **40**: 616–619.
21. Roepman, R, Bernoud-Hubac, N, Schick, DE, Maugeri, A, Berger, W, Ropers, HH *et al.* (2000). The retinitis pigmentosa GTPase regulator (RPGR) interacts with novel transport-like proteins in the outer segments of rod photoreceptors. *Hum Mol Genet* **9**: 2095–2105.
22. Hong, DH, Yue, G, Adamian, M and Li, T (2001). Retinitis pigmentosa GTPase regulator (RPGRr)-interacting protein is stably associated with the photoreceptor ciliary axoneme and anchors RPGR to the connecting cilium. *J Biol Chem* **276**: 12091–12099.
23. Mavlyutov, TA, Zhao, H and Ferreira, PA (2002). Species-specific subcellular localization of RPGR and RPGRIP isoforms: implications for the phenotypic variability of congenital retinopathies among species. *Hum Mol Genet* **11**: 1899–1907.
24. Boylan, JP and Wright, AF (2000). Identification of a novel protein interacting with RPGR. *Hum Mol Genet* **9**: 2085–2093.
25. Zhao, Y, Hong, DH, Pawlyk, B, Yue, G, Adamian, M, Grynberg, M *et al.* (2003). The retinitis pigmentosa GTPase regulator (RPGR)- interacting protein: subserving RPGR function and participating in disk morphogenesis. *Proc Natl Acad Sci USA* **100**: 3965–3970.
26. Won, J, Gifford, E, Smith, RS, Yi, H, Ferreira, PA, Hicks, WL *et al.* (2009). RPGRIP1 is essential for normal rod photoreceptor outer segment elaboration and morphogenesis. *Hum Mol Genet* **18**: 4329–4339.
27. Pawlyk, BS, Smith, AJ, Buch, PK, Adamian, M, Hong, DH, Sandberg, MA *et al.* (2005). Gene replacement therapy rescues photoreceptor degeneration in a murine model of Leber congenital amaurosis lacking RPGRIP. *Invest Ophthalmol Vis Sci* **46**: 3039–3045.
28. Pawlyk, BS, Bulgakov, OV, Liu, X, Xu, X, Adamian, M, Sun, X *et al.* (2010). Replacement gene therapy with a human RPGRIP1 sequence slows photoreceptor degeneration in a murine model of Leber congenital amaurosis. *Hum Gene Ther* **21**: 993–1004.
29. Le Meur, G, Weber, M, Péréon, Y, Mendes-Madeira, A, Nivard, D, Deschamps, JY *et al.* (2005). Postsurgical assessment and long-term safety of recombinant adeno-associated virus-mediated gene transfer into the retinas of dogs and primates. *Arch Ophthalmol* **123**: 500–506.
30. Mussolino, C, della Corte, M, Rossi, S, Viola, F, Di Vicino, U, Marrocco, E *et al.* (2011). AAV-mediated photoreceptor transduction of the pig cone-enriched retina. *Gene Ther* **18**: 637–645.
31. Vandenberghe, LH, Bell, P, Maguire, AM, Cearley, CN, Xiao, R, Calcedo, R *et al.* (2011). Dosage thresholds for AAV2 and AAV8 photoreceptor gene therapy in monkey. *Sci Transl Med* **3**: 88ra54.
32. Boye, SE, Alexander, JJ, Boye, SL, Witherspoon, CD, Sandefer, KJ, Conlon, TJ *et al.* (2012). The human rhodopsin kinase promoter in an AAV5 vector confers rod- and cone-specific expression in the primate retina. *Hum Gene Ther* **23**: 1101–1115.
33. Khani, SC, Pawlyk, BS, Bulgakov, OV, Kasperek, E, Young, JE, Adamian, M *et al.* (2007). AAV-mediated expression targeting of rod and cone photoreceptors with a human rhodopsin kinase promoter. *Invest Ophthalmol Vis Sci* **48**: 3954–3961.
34. Sun, X, Pawlyk, B, Xu, X, Liu, X, Bulgakov, OV, Adamian, M *et al.* (2010). Gene therapy with a promoter targeting both rods and cones rescues retinal degeneration caused by AIPL1 mutations. *Gene Ther* **17**: 117–131.
35. Ku, CA, Chiodo, VA, Boye, SL, Goldberg, AF, Li, T, Hauswirth, WW *et al.* (2011). Gene therapy using self-complementary Y733F capsid mutant AAV2/8 restores vision in a model of early onset Leber congenital amaurosis. *Hum Mol Genet* **20**: 4569–4581.
36. Boye, SE, Boye, SL, Pang, J, Ryals, R, Everhart, D, Umino, Y *et al.* (2010). Functional and behavioral restoration of vision by gene therapy in the guanylate cyclase-1 (GC1) knockout mouse. *PLoS ONE* **5**: e11306.
37. Mihelec, M, Pearson, RA, Robbie, SJ, Buch, PK, Azam, SA, Bainbridge, JW *et al.* (2011). Long-term preservation of cones and improvement in visual function following gene therapy in a mouse model of leber congenital amaurosis caused by guanylate cyclase-1 deficiency. *Hum Gene Ther* **22**: 1179–1190.
38. Boye, SL, Peshenko, IV, Huang, WC, Min, SH, McDoom, I, Kay, CN *et al.* (2013). AAV-mediated gene therapy in the guanylate cyclase (RetGC1/RetGC2) double knockout mouse model of Leber congenital amaurosis. *Hum Gene Ther* **24**: 189–202.
39. Beltran, WA, Boye, SL, Boye, SE, Chiodo, VA, Lewin, AS, Hauswirth, WW *et al.* (2010). rAAV2/5 gene-targeting to rods:dose-dependent efficiency and complications associated with different promoters. *Gene Ther* **17**: 1162–1174.
40. Kuznetsova, T, Zangerl, B, Goldstein, O, Acland, GM and Aguirre, GD (2011). Structural organization and expression pattern of the canine RPGRIP1 isoforms in retinal tissue. *Invest Ophthalmol Vis Sci* **52**: 2989–2998.
41. Miyadera, K, Kato, K, Boursnell, M, Mellersh, CS and Sargan, DR (2012). Genome-wide association study in RPGRIP1(-/-) dogs identifies a modifier locus that determines the onset of retinal degeneration. *Mamm Genome* **23**: 212–223.
42. Kuznetsova, T, Iwabe, S, Boesze-Battaglia, K, Pearce-Kelling, S, Chang-Min, Y, McDaid, K *et al.* (2012). Exclusion of RPGRIP1 ins44 from primary causal

association with early-onset cone-rod dystrophy in dogs. *Invest Ophthalmol Vis Sci* **53**: 5486–5501.
43. Miyadera, K, Brierley, I, Aguirre-Hernández, J, Mellersh, CS and Sargan, DR (2012). Multiple mechanisms contribute to leakiness of a frameshift mutation in canine cone-rod dystrophy. *PLoS ONE* **7**: e51598.
44. Boye, SL, Conlon, T, Erger, K, Ryals, R, Neeley, A, Cossette, T *et al.* (2011). Long-term preservation of cone photoreceptors and restoration of cone function by gene therapy in the guanylate cyclase-1 knockout (GC1KO) mouse. *Invest Ophthalmol Vis Sci* **52**: 7098–7108.
45. Tan, MH, Smith, AJ, Pawlyk, B, Xu, X, Liu, X, Bainbridge, JB *et al.* (2009). Gene therapy for retinitis pigmentosa and Leber congenital amaurosis caused by defects in AIPL1: effective rescue of mouse models of partial and complete Aipl1 deficiency using AAV2/2 and AAV2/8 vectors. *Hum Mol Genet* **18**: 2099–2114.
46. Simons, DL, Boye, SL, Hauswirth, WW and Wu, SM (2011). Gene therapy prevents photoreceptor death and preserves retinal function in a Bardet-Biedl syndrome mouse model. *Proc Natl Acad Sci USA* **108**: 6276–6281.
47. Cideciyan, AV, Jacobson, SG, Beltran, WA, Sumaroka, A, Swider, M, Iwabe, S *et al.* (2013). Human retinal gene therapy for Leber congenital amaurosis shows advancing retinal degeneration despite enduring visual improvement. *Proc Natl Acad Sci USA* **110**: E517–E525.
48. Acland, GM, Aguirre, GD, Bennett, J, Aleman, TS, Cideciyan, AV, Bennicelli, J *et al.* (2005). Long-term restoration of rod and cone vision by single dose rAAV-mediated gene transfer to the retina in a canine model of childhood blindness. *Mol Ther* **12**: 1072–1082.
49. Koch, S, Sothilingam, V, Garcia Garrido, M, Tanimoto, N, Becirovic, E, Koch, F *et al.* (2012). Gene therapy restores vision and delays degeneration in the CNGB1(-/-) mouse model of retinitis pigmentosa. *Hum Mol Genet* **21**: 4486–4496.
50. Pang, JJ, Dai, X, Boye, SE, Barone, I, Boye, SL, Mao, S *et al.* (2011). Long-term retinal function and structure rescue using capsid mutant AAV8 vector in the rd10 mouse, a model of recessive retinitis pigmentosa. *Mol Ther* **19**: 234–242.

Supplementary Material:

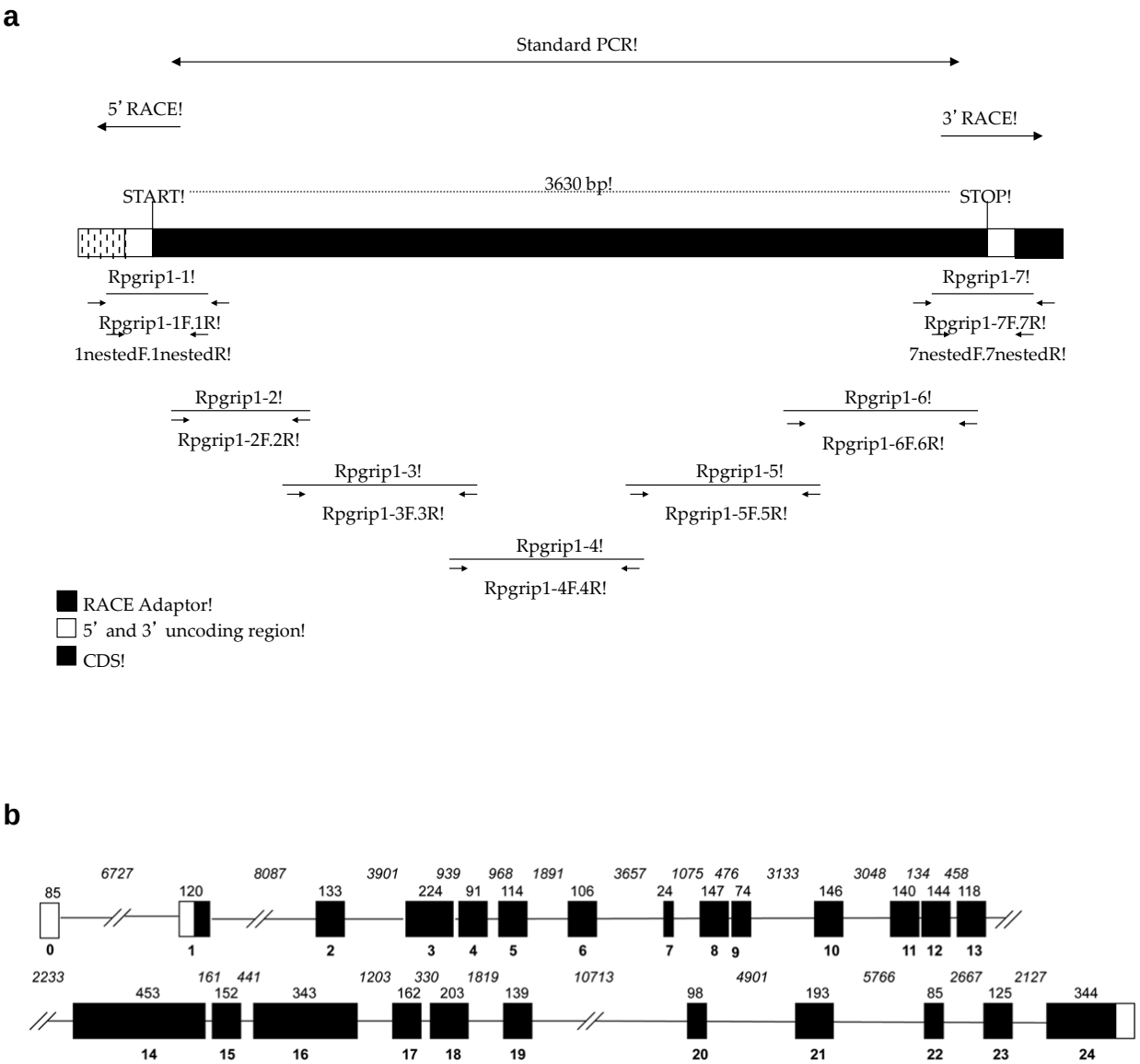

Figure S1. Canine *Rpgrip1* amplification strategy. (**a**) Standard PCR and RLM-RACE PCR amplification strategy. Seven overlapping fragments covering the entire coding region were amplified (Rpgrip1-1 to Rpgrip1-7). (**b**) Canine *Rpgrip1* gene organization. Exons are represented as boxes and introns as lines. White and black boxes represent non-coding and coding exons, respectively. Exon numbers are indicated behind exon boxes. Exon sizes are indicated above exon boxes in base pairs (bp). Intron sizes are indicated in italics above intron lines in base pairs.

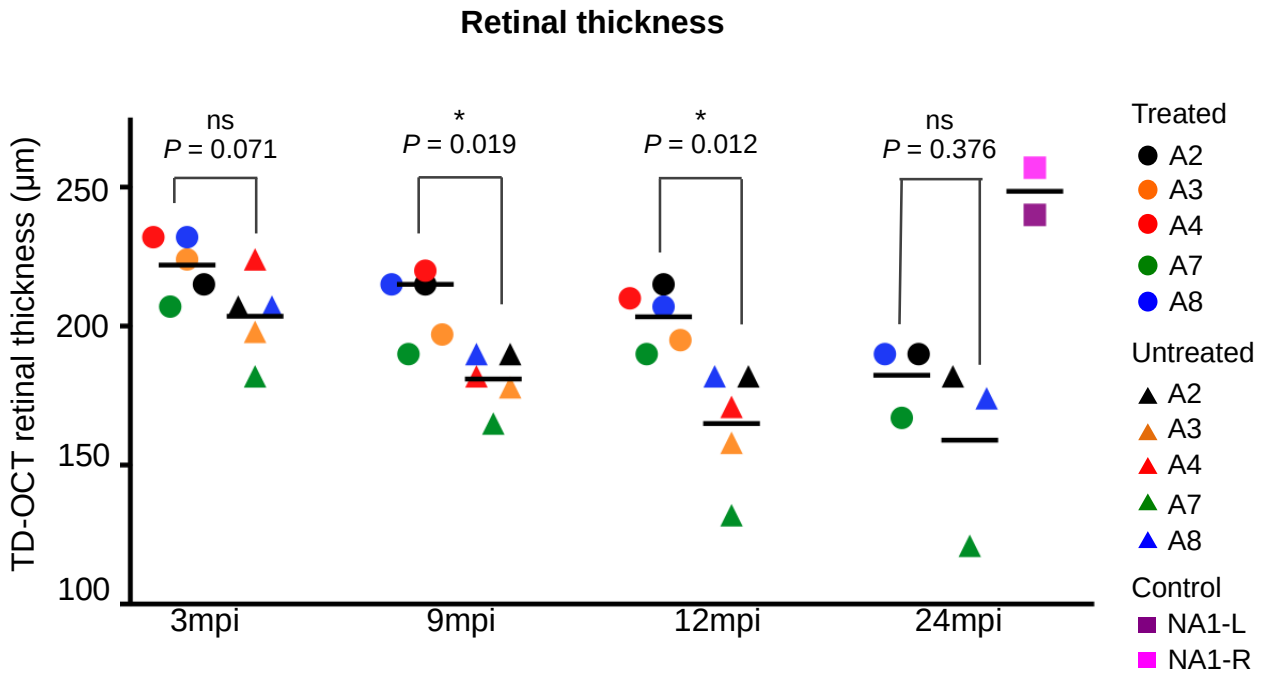

Figure S2. Gene therapy did not halt retinal degeneration in treated MLHD-*Cord1* eyes. Central retinal thickness were measured in treated and untreated eyes of dogs A2, A3, A4, A7 and A8 at 3, 9, 12 and 24 months postinjection (mpi) from TD-OCT scans obtained 13 mm above the optic nerve head. Results obtained in treated and untreated eyes were compared statistically at each time-point using unpaired Mann-Whitney t-test. One and two asterisk(s) indicate(s) significant difference between treated and untreated eyes with *P*-value <0.05 or <0.005, respectively. We note a significant higher retinal thickness in treated eyes compared to untreated eyes at 9 and 12 mpi. Dark bar represents the mean. Ns, non significant. NA1, non-affected *Rpgrip1*$^{+/-}$ dog. L, left eye; R, right eye.

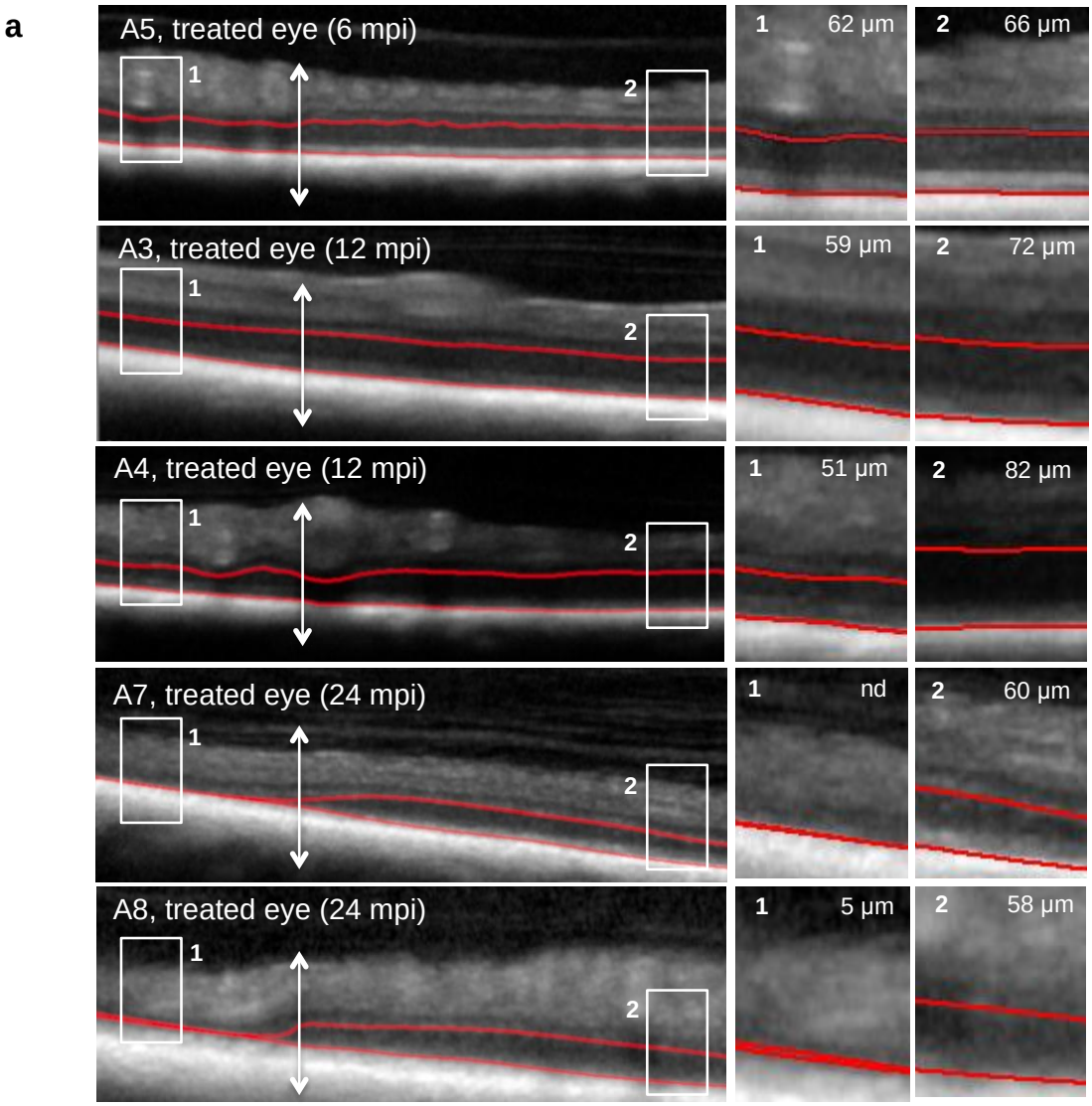
a
A5, treated eye (6 mpi)
1
2
1 62 µm
2 66 µm
A3, treated eye (12 mpi)
1
2
1 59 µm
2 72 µm
A4, treated eye (12 mpi)
1
2
1 51 µm
2 82 µm
A7, treated eye (24 mpi)
1
2
1 nd
2 60 µm
A8, treated eye (24 mpi)
1
2
1 5 µm
2 58 µm
b
A2 (24 mpi)
Unexposed
Exposed
NA1 (24 m)
LM opsin
DAPI
S opsin
DAPI
GCL
INL
ONL
IS
OS
RPE
GCL
INL
ONL
IS
OS
RPE

Figure S3. Gene therapy prevented long-term photoreceptor degeneration in all treated MLHD-*Cord1* eyes. (**a**) SD-OCT scans obtained 13 mm above the optic nerve head from the treated eye of dog A5, A3, A4, A7 and A8 at latest timepoint. Photoreceptor layer (ONL + outer and inner segments) was defined semi-automatically (red). Photoreceptor layer thickness was measured in two normalized temporal (1) and nasal (2) locations. (**b**) Microscopic images of retinal sections from the treated eye of dog A2 at 24 months postinjection (mpi) and the right eye of age-matched control dog NA1. Serial retinal cryosections encompassing the vector-exposed and the vector-unexposed areas of the treated retina were immunolabeled using L/M- (top) or S-opsin [430] antibodies. Primary antibodies were detected using Alexa 546-conjugated goat anti-rabbit IgG (red). Cell nuclei were counterstained with DAPI (blue). Scale bar = 30 µm. Abbreviations: m, months of age; GCL, ganglion cell layer; INL, inner nuclear layer; IS, inner segments; ONL, outer nuclear layer; OS, outer segments; RPE, retinal pigment epithelium; nd, not detectable.

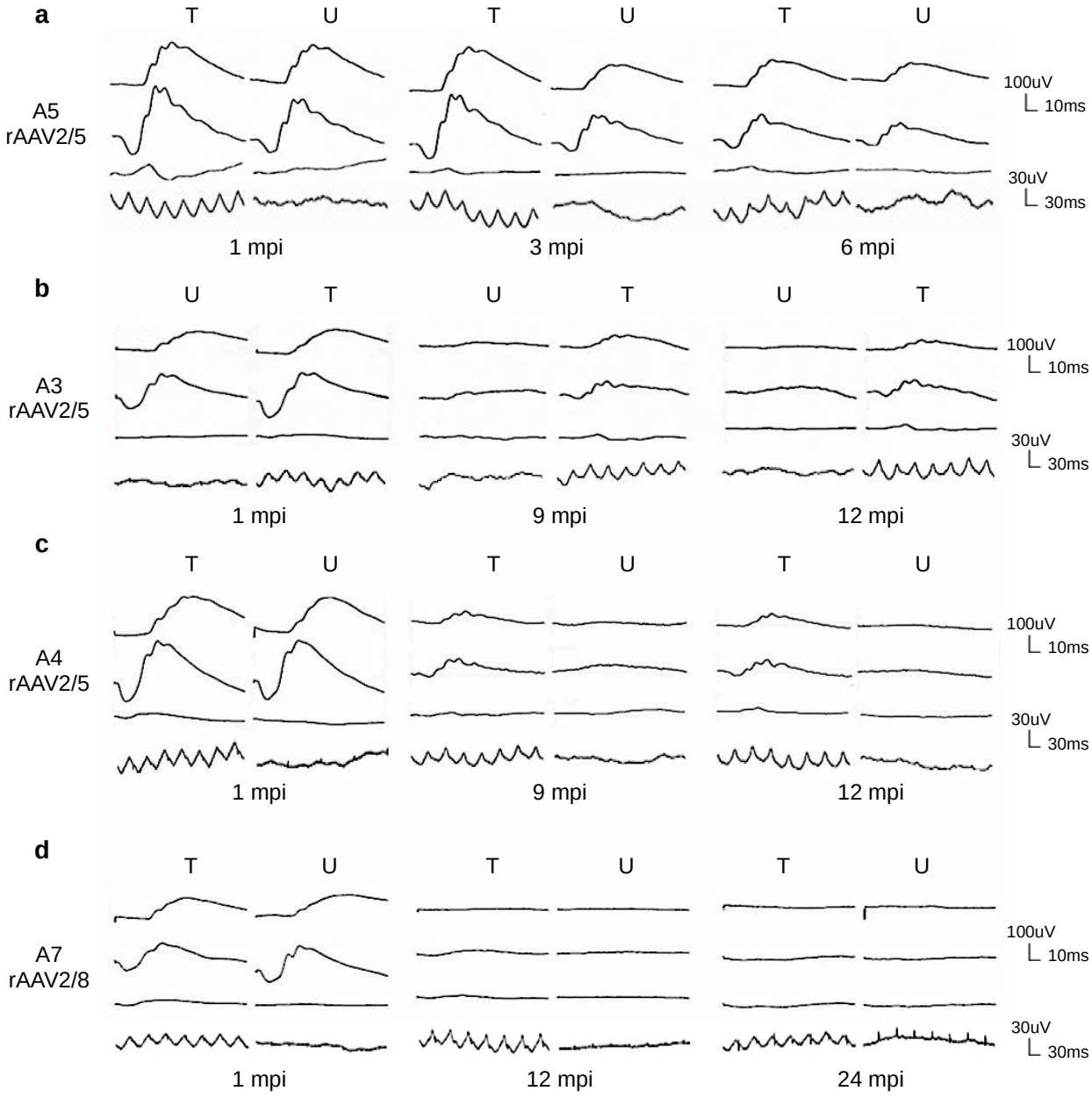

Figure S4. Bilateral full-field electroretinographic traces from dogs A7, A3, A4 and A5. (**a**) Electroretinographic trace from dog A5 treated with AAV2/5-RK-c*Rpgrip1* at 1, 3 and 6 months postinjection (mpi). (**b**) Electroretinographic traces from dog A3 treated with AAV2/5-RK-c*Rpgrip1* at 1, 9 and 12 mpi. (**c**) Electroretinographic traces from dog A4 treated with AAV2/5-RK-c*Rpgrip1* at 1, 9 and 12 mpi. (**d**) Electroretinographic traces from dog A7 treated with AAV2/8-RK-c*Rpgrip1* at 1, 12 and 24 mpi. The top two recordings are low- and high-intensity dark-adapted responses, whereas the bottom two recordings show light-adapted responses (responses to single flash and 30Hz flicker stimuli, respectively). Abbreviations: m, months of age; ms, milliseconds; μV, microvolts; T, treated eye; U, untreated eye.

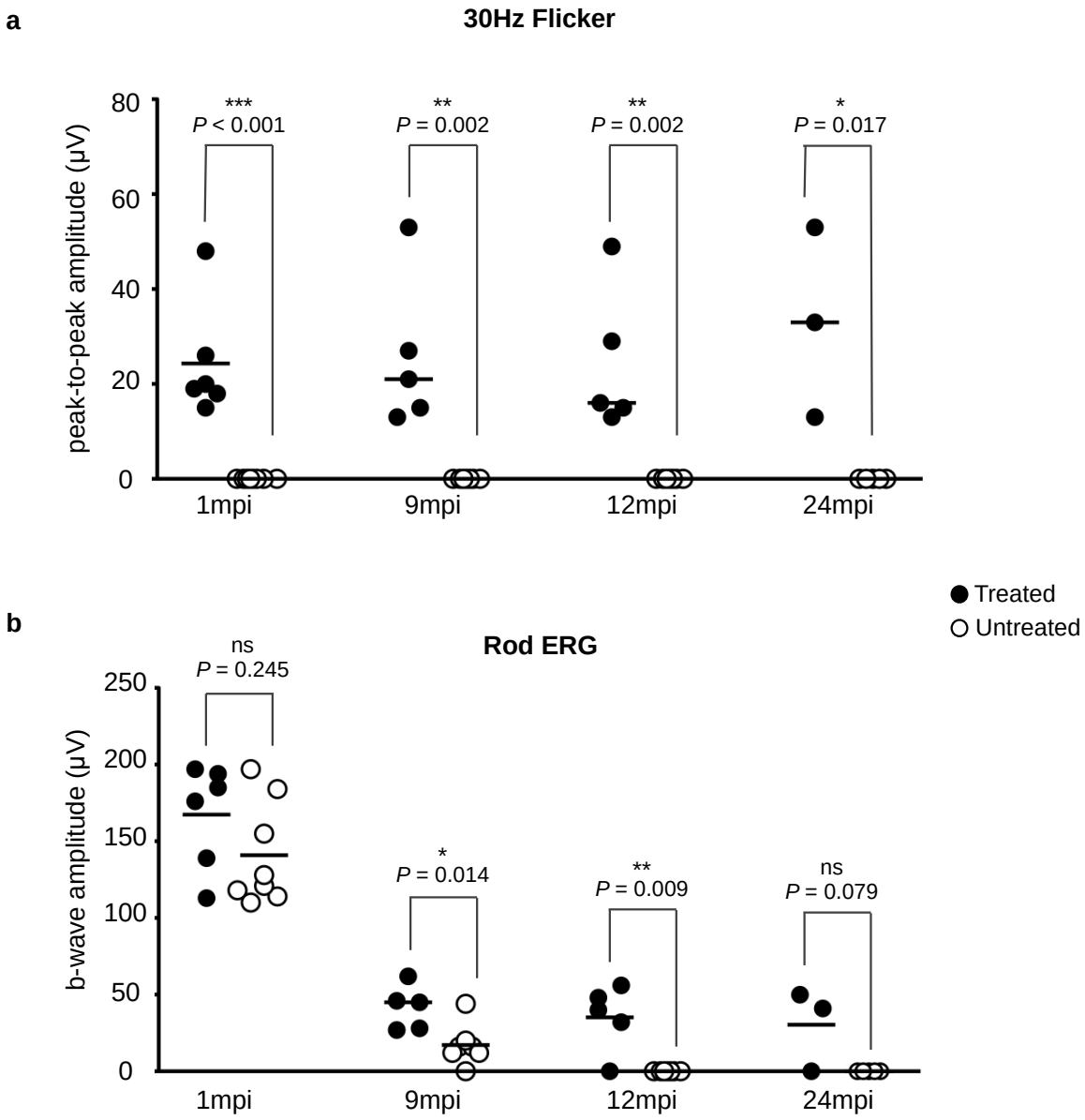

Figure S5. Statistical analysis of ERG responses in treated and untreated MLHD-*Cord1* eyes. (**a**) Cone 30Hz Flicker- and (**b**) rod-mediated ERG responses amplitudes obtained in treated (dark circles) and untreated eyes (white circles) of dogs A1, A2, A3, A4, A7 and A8 were compared statistically at 1, 9, 12 and 24 mpi with unpaired Mann-Whitney t-test. The number of eyes analyzed per group was a follows: injected at 1 mpi, n=6, uninjected at 1 mpi, n=8, injected at 9 mpi and 12 mpi, n=5, uninjected at 9 mpi and 12 mpi, n=7, injected at 24 mpi, n=3, uninjected at 24 mpi, n=5. One, two and three asterisk(s) indicate(s) significant difference between treated and untreated eyes with *P*-value <0.05, <0.005 or <0.001, respectively. We clearly note a significant restoration of cone function in treated eyes compared to untreated eyes at all time points. Regarding rod function, we note a significant better preserved function in treated eyes compared to untreated eyes at 9 and 12 mpi. At 24 mpi, no significant difference was found between treated and untreated eyes, probably due to the low number of examined eyes at this time point. Dark bars represent means. Abbreviations: ns, non significant.

Table S1. Primers used for the amplification of c*Rpgrip1* cDNA.

Primers	Sequences	Location	Tm(°C)	Product name and size
Rpgrip1-1F	GCTGATGGCGATGAATGAACACTG	5'RACE Adaptor	72	942bp+adaptor
Rpgrip1-1R	ACTTCTGTTAACTGTGCTTTTG	Exon 6	60	
1nestedF	CGCGGATCCGAACACTGCGTTTGCTGGCTTTGATG	5'RACE Adaptor	110	Rpgrip1-1
1nestedR	CGGTCTTCTCACTTGTTGC	Exon 4	58	(707bp+adaptor)
Rpgrip1-2F	AGAGCACATGTTGGTGAAGGA	Exon 2	62	Rpgrip1-2
Rpgrip1-2R	ACTTCTGTTAACTGTGCTTTTG	Exon 6	60	(582bp)
Rpgrip1-3F	CAGAGAAGCTCTTTGGAGTG	Exon 5	60	Rpgrip1-3
Rpgrip1-3R	GTCTCTGTGTGATCCTTACTG	Exon 13	62	(884bp)
Rpgrip1-4F	ATCAACGTGTGTTACCAGGA	Exon 12-13	58	Rpgrip1-4
Rpgrip1-4R	TGGTCAGAAAAGGTGAAGAA	Exon 16	56	(875bp)
Rpgrip1-5F	GGTGTTAGAATACTGGATGA	Exon 15	56	Rpgrip1-5
Rpgrip1-5R	TGGCCAGCTTCGGTGGGA	Exon 18	60	(675bp)
Rpgrip1-6F	AAGACTCAGAGCCTGGCTC	Exon 16	60	Rpgrip1-6
Rpgrip1-6R	TTCAATGCACATCTTCTCCGA	Exon 21	60	(704bp)
Rpgrip1-7F	ATTCAGTAGTGATGCAGAAAGAAG	Exon 19	66	Rpgrip1-7
Rpgrip1-7R	GCGAGCACAGAATTAATACGACT	3'RACE Adaptor	66	(898bp+adaptor)
7nestedF	CTAAATCCTGTGAATGATAAAGAATC	Exon 19-20	68	872bp+adaptor
7nestedR	CGCGGATCCGAATTAATACGACTCACTATAGG	3'RACE Adaptor	94	

Seven overlapping fragments (Rpgrip1-1 to Rpgrip1-7) covering the entire *cRpgrip1* coding sequence were amplified with PCR and RLM-RACE PCR using primers designed from human, bovine and rodent *RPGRIP1* consensus sequences and putative canine sequences. Abbreviations: bp, base pair; F, forward primer; R, reverse primer; Tm, primer melting temperature calculated with the 2*(A+T)+4*(G+C) method.

Table S2. Characterization of the exon-intron junctions of the c*Rpgrip1* gene.

Exon	Exon size (bp)	3'-Splice intron/exon acceptor sequence	5'-Splice exon/intron donor sequence	Intron	Intron size (bp)
0	ND	ND	CAAAAG**gt**ttgt	1	6727
1	120	ttt**ag**TGCCCT	CGAAAG**gt**aaat	2	8087
2	133	ctt**ag**GTAAGA	CAAAAG**gt**acct	3	3901
3	224	tcac**ag**GGCGAG	GGAGGG**gt**gagt	4	939
4	91	ttt**ag**AGCCCA	TGAGCC**gt**gagt	5	968
5	114	gacc**ag**CAATAC	GCTGCG**gt**aaga	6	1891
6	106	ttcc**ag**AGCTTC	CAAGAG**gt**gagg	7	3657
7	24	ttt**ag**GCATAT	CAGAAG**gt**actt	8	1075
8	147	cccc**ag**AATCAG	AAGGAG**gt**aaat	9	476
9	74	tctt**ag**TTTCAG	AGAAAA**gt**gagt	10	3133
10	146	tccc**ag**CATGCT	AGAAAG**gt**aggt	11	3048
11	140	cccc**ag**CCCAGA	GCCGAG**gt**aaga	12	134
12	144	ccgc**ag**CCCCGG	TACCAG**gt**gtgg	13	458
13	118	tctc**ag**GAGGAA	TGGAAG**gt**attt	14	2233
14	453	ctct**ag**AACAGC	TTACTG**gt**aagt	15	161
15	152	atcc**ag**GAGCTG	GATAAG**gt**gaga	16	441
16	343	ttcc**ag**TCCAGA	TTAAAG**gt**ggga	17	1203
17	162	tatc**ag**GTGATT	AAAGAG**gt**aaag	18	330
18	203	attt**ag**GACCAG	TTACAA**gt**aagg	19	1819
19	139	ctaa**ag**CAGGTG	TGAATG**gt**attg	20	10713
20	98	ttgc**ag**ATAAAG	AAGGCA**gt**aagt	21	4901
21	193	tgtc**ag**GACTCG	GCAAAG**gt**gacg	22	5766
22	85	gccc**ag**TGATCC	AGGACG**gt**aagg	23	2667
23	125	ctt**ag**TTTAAA	TAGAGA**gt**gagt	24	2127
24	nd	ccgc**ag**TCTTGA	nd	nd	nd

Exons are numbered beginning at the 5' end of the gene. Intron sequences are in lower case letters and exon sequences in uppercase letters. Conserved 3' splice acceptor sites (**ag**) and 5' splice donors sites [431] are in bold. Analysis of the exon-intro junctions demonstrated that boundaries followed the gt/ag consensus splicing rule. Abbreviations: bp, base pairs; nd, not determined.

General Discussion:

The aim of this study was to evaluate the efficacy of gene addition therapy for the treatment of severe photoreceptor dystrophies in (i) the PDE6β-deficient dog, a model of rod-cone dystrophy, and in (ii) the RPGRIP1-deficient dog, a model of cone-rod dystrophy.
The hallmark of these severe forms of inherited photoreceptor dystrophies is a combined **dysfunction** and **degeneration** of photoreceptor cells. In this chapter, the effects of rAAV-mediated gene therapy on both retinal function and retinal morphology will be discussed.

CAN AAV-MEDIATED GENE THERAPY IMPROVE THE DYSFUNCTION COMPONENT IN THE PDE6B- AND RPGRIP1-DEFICIENT DOGS?

The *rcd1* and MLHD-*Cord1* dogs lack rod or cone function from the earliest measured age, respectively. In the *rcd1* dog, the absence of rod function is thought to be directly correlated to the loss of rod PDE6 activity[69]. In the MLHD-*Cord1* dog, the reason of the total absence of cone function is still not known. Histopathological examination disclosed no change in cone outer segments at 6 weeks of age, but did not exclude the possibility that some of the cones are never normally formed [133]. The *Ins44* mutation in *Rpgrip1* is expected to produce a severely truncated protein lacking the RID domain, which is required for the interaction with RPGR. Disruption of RPGRIP1-RPGR interactions could explain the total absence of cone function in the MLHD-*Cord1* dog. Alternatively, a specific activity of RPGRIP1 may be absent in the MLHD-*Cord1* cones, or reduced below the threshold required for normal cone function.

1. rAAV-mediated gene therapy rescues rod function in the PDE6β-deficient dog

Retinal function was evaluated in all *rcd1* treated dogs using simultaneous bilateral full-field ERG. **In both rAAV2/5- and rAAV2/8-treated *rcd1* dogs, we demonstrated that rod function was substantially and stably rescued for at least 30 months postinjection** (the latest timepoint examined, **Figures 19** and **20**)**.** This is the most significant rescue a PDE6-defect reported to date. Indeed, previous gene therapy studies in the *rd1* [312], [313], [412] and the *nmf363 null* models of PDE6-deficiency did not reported functional rescue [417, 418].

In treated *rcd1* eyes, restored rod function accounts for 28-35% of those recorded in normal eyes, consistent with the area of retina directly exposed to the vector (25-30% of the total retinal surface). This could indicate that in the vector-exposed area (cone:rod ratio = 1: 41), approximately 100% of rods were transduced and that transduced rods recovered nearly 100% of their functionality. The idea that the maximum threshold of PDE6β expression was reached in transduced rods is consistent with the fact that similar levels of rod ERG responses were obtained in rAAV2/5- and rAAV2/8-treated dogs, despite the tenfold injection of rAAV2/8 (1.10^{12} vg/mL) compared to the rAAV2/5 injection (1.10^{11} vg/mL). PDE6β may be tittered by PDE6α and PDE6 activity is tiny regulated.

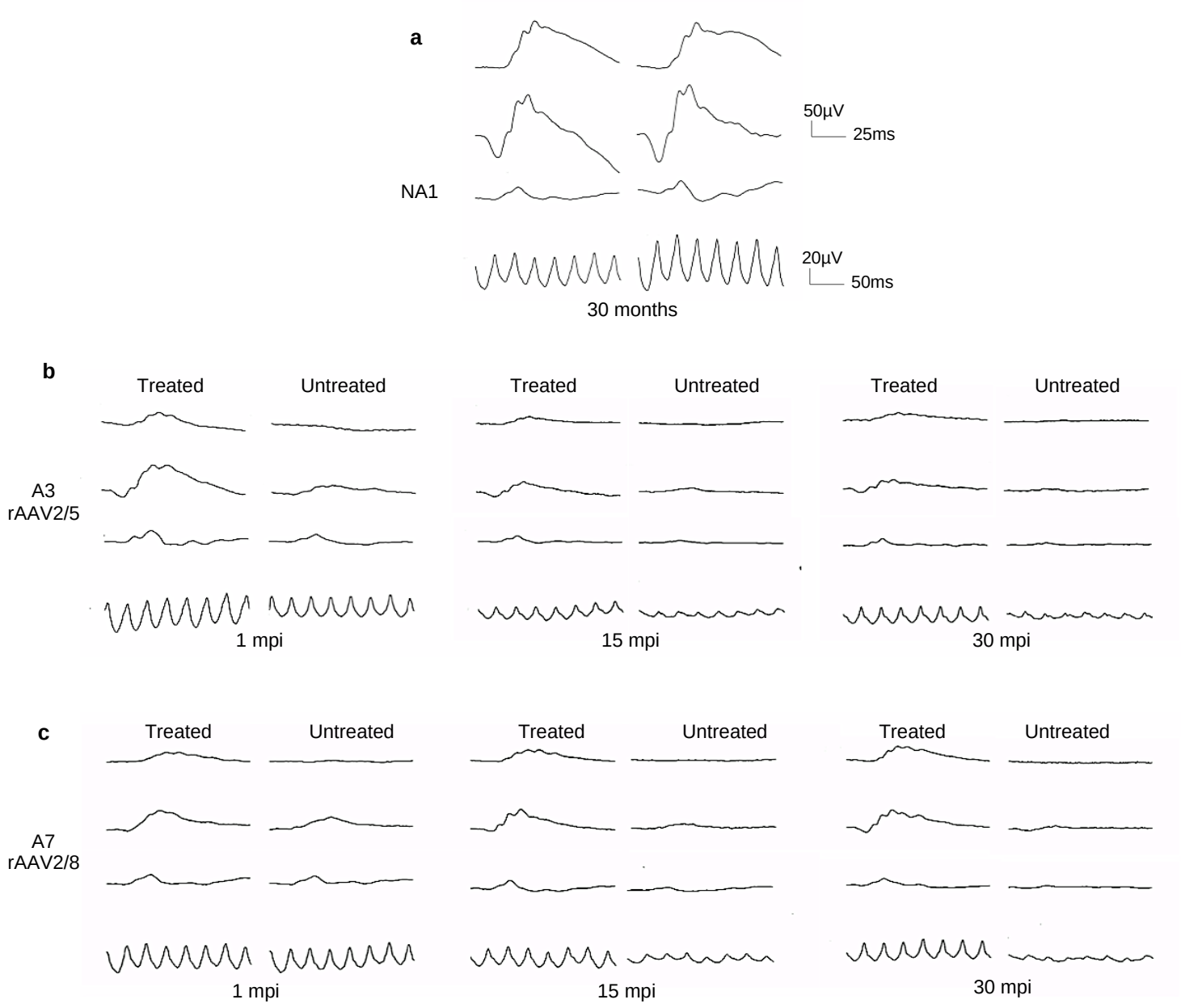

Figure 19. Bilateral full-field electroretinographic traces from dogs NA1, A3 and A7 at 1, 15 and 30 months following subretinal injection. (**a**) Electroretinographic trace from control non-affected dog NA1 at 30 months of age. (**b**) Electroretinographic traces from dog A3 treated with AAV2/5-RK-c*Pde6β*. (**c**) Electroretinographic traces from dog A7 treated with AAV2/8-RK-c*Pde6β*. The top two recordings are low- and high-intensity dark-adapted responses, whereas the bottom two recordings show light-adapted responses (responses to single flash and 30Hz flicker stimuli, respectively). AAV, adeno-associated virus; mpi, month(s) postinjection.

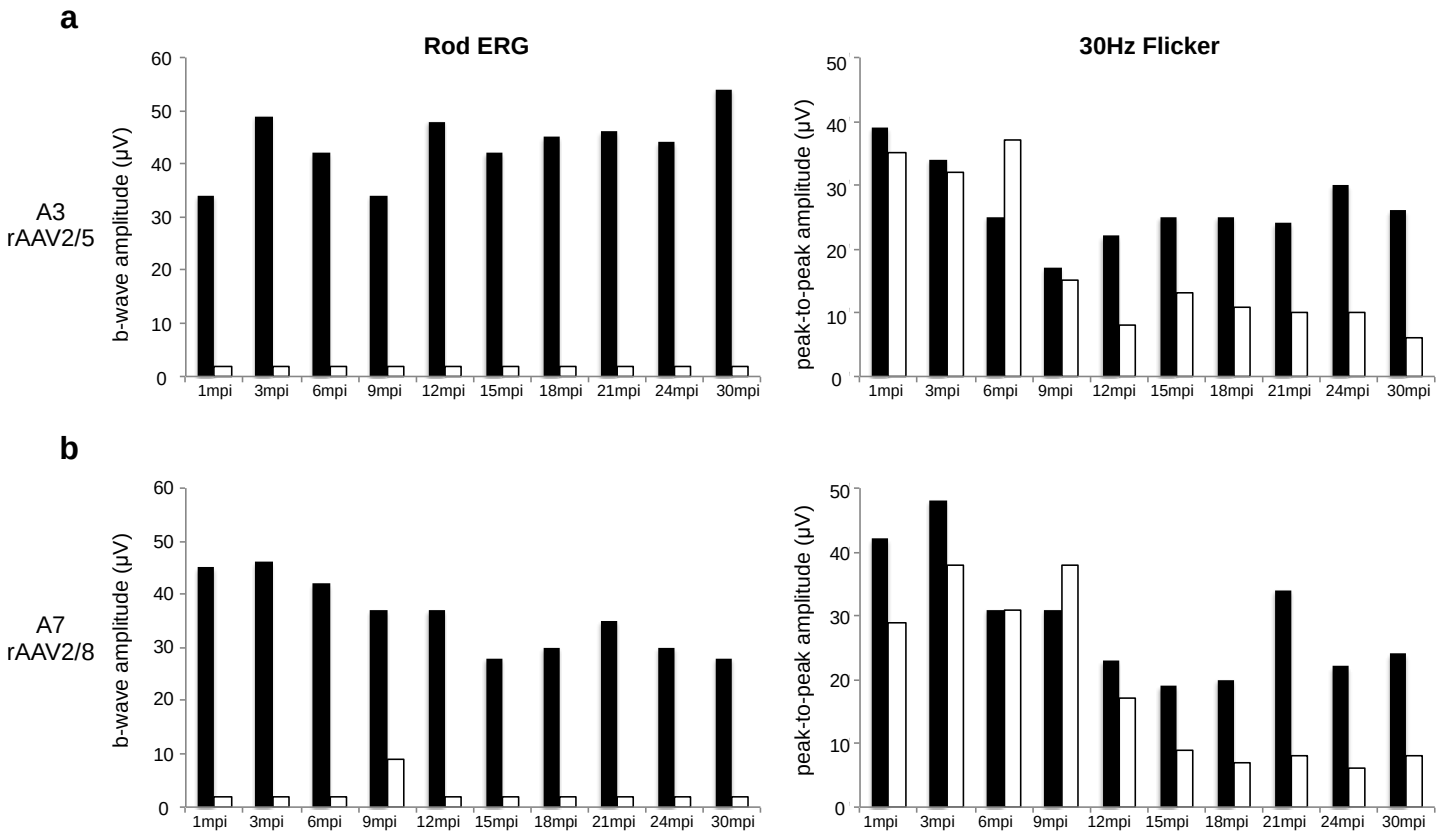

Figure 20. Kinetics of retinal function recovery in treated dogs A3 and A7.
(**a**) Amplitudes of electroretinography (ERG) responses for dog A3 treated with AAV2/5-RK-c*Pde6β* from 1 to 30 months postinjection. (**b**) Amplitudes of ERG responses for dog A7 treated with AAV2/8-RK-c*Pde6β* from 1 to 30 months postinjection. The left panels show scotopic rod b-wave amplitudes. The right panels show photopic 30Hz flicker amplitude. Treated eyes are shown in dark, untreated eyes in white. AAV, adeno-associated virus; mpi, month(s) postinjection.

Unfortunately it was not possible to test this hypothesis, as we did not manage to quantify the relative levels of PDE6β expression in rAAV2/5- and rAAV2/8-treated *rcd1* eyes. We developed an allele-specific qRT-PCR to quantify the expression levels of both mutant and wild-type PDE6β mRNA (which differs by only one base pair), but the method was not enough robust to give answer (Petit L, data not shown). We tested by Western-Blot all the commercially available antibodies raised against the mouse or human PDE6β for their ability to recognize the canine PDE6β, and we amplified the canine PDE6α cDNA to test the specificity of the antibodies. None of the antibody tested was specific to the canine PDE6β subunit (Petit L, unpublished data). Attempts to separate the canine mutated PDE6β subunit from the canine wild-type PDE6β-PDE6α proteins by (i) size and (ii) size plus isoelectric point did not raise consistent results (in collaboration with GENETHON, Paris, France, data not shown). Alternatively, it would be interesting to develop a PDE6 assay to quantify the level of restored PDE6 activity in treated *rcd1* retinas.

Interestingly, in the *Cngb1*$^{-/-}$ mouse model of **rod-cone dystrophy** subretinal injection of AAV2/8 (Y733F)-mOP-m*Cngb1a* at P14 also restored rod-specific ERG responses to about one-third of what is recorded in age-matched control, in accordance with the approximate size of the treated area (about 30% of the total retinal surface)[419]. In this model, levels of endogenous CNGA1 subunit, the molecular partner of CNGB1, could also ensure that amounts of transgene expression not exceed wild-type levels [419].

2. rAAV-mediated gene therapy rescues cone function in the RPGRIP1-deficient dog

As performed in the *Rcd1* dogs, retinal function was evaluated in all MLHD-*Cord1* treated dogs using simultaneous bilateral full-field ERG. **In both rAAV2/5- and rAAV2/8-treated MLHD-*Cord1* dogs, we demonstrated that cone function was substantially and stably rescued for at least 24 months postinjection** (the latest timepoint examined)**.**

Intriguingly, restored cone function varied from 18 to 72% of the normal responses, despite that subretinal blebs always covered over one third of the total retinal surface. This heterogeneity of functional rescue did not seem to be related to the rAAV serotypes, although additional rAAV2/8-treated dogs would be needed to draw a definitive conclusion (only 2 dogs received rAAV2/8).

We can hypothesize that the differences of cone rescue reflect inter-individual variations in the efficiency of cone transduction and/or physiological alteration of cones at the time of treatment.

In addition, this result can reflect a correlation between restored cone function and the location of the subretinal bleb. Indeed, contrary to rods, cone topography across the canine retina is particularly heterogeneous[168], (Petit L *et al*, in preparation). Most of the treated MLHD-*Cord1* dogs received subretinal injection in the nasal superior part of the

retina (cone:rod ratio = 1:41) and vector blebs partially covered the nasal part of the cone-rich visual streak (cone:rod ratio = 1:10).

Given the relative high proportion of cones in the cone-rich visual streak, the inclusion of this particular region in the injected area is expected to lead to substantial variation in the number of total targeted cones (and thus of the total functional rescue). **Moreover, there could be a relative better preservation of mutant cones in the MLHD-*Cord1* cone-rich visual streak compared with the rod-rich mid-peripheral retina.**

In *Rpe65*$^{-/-}$ dogs, a significant positive correlation with cone flicker amplitudes and with inclusion of the area centralis in the injected area was recently reported. It was also hypothesized that this correlation reflects the greater number of cones per unit area in the *area centralis* than in the peripheral retina [393].

CAN AAV-MEDIATED GENE THERAPY IMPROVE THE DEGENERATION COMPONENT IN THE PDE6B- AND RPGRIP1-DEFICIENT DOGS?

To be clinically relevant, gene addition therapy needs to restore the function of mutant photoreceptors, but also to prevent their progressive death. Indeed, the effect of gene therapy on photoreceptor function has to be maintained for a valuable period of time, and not rapidly overcome by persistent photoreceptor degeneration.

1. rAAV-mediated Pde6β gene transfer restored a physiological equilibrium in transduced *rcd1* rods

In the *rcd1* dog, rod death is thought to be directly correlated to the loss of PDE6 activity. To determine whether *Pde6β* gene transfer in rods is sufficient to prevent rod death, retinal thickness was evaluated by OCT and SD-OCT over time. In addition, we performed a *post-mortem* histological analysis of two rAAV-treated retinas at 4 and 30 months postinjection.

We observed a preservation of 90% of the photoreceptors in the vector-exposed area of rAAV2/5- and rAAV2/8-treated *rcd1* retinas for at least 30 months postinjection. At this age, no photoreceptor cells remained in the vector-unexposed regions (with the exception of one or two rows of cones in the *visual streak* and in the central superior retina) (**Figure 21**). **This observation indicates that early *Pde6β* gene transfer restored the physiological equilibrium in transduced rods, stopping photoreceptor degeneration.**

This result was the most sustained rescue of a severe form of photoreceptor degenerations reported so far**.** Similar almost complete rescue of photoreceptors has been previously observed in the *Rpe65*$^{-/-}$ dog, a canine model of RPE defect, treated before the onset of photoreceptor loss [268]. In *Rpe65*$^{-/-}$ dogs, ONL thickness in the vector-exposed area (superior retina) remained within the normal range for at least 9 years postinjection, whereas ONL thickness was undetectable outside the injected region (except in the cone-rich visual streak) [268].

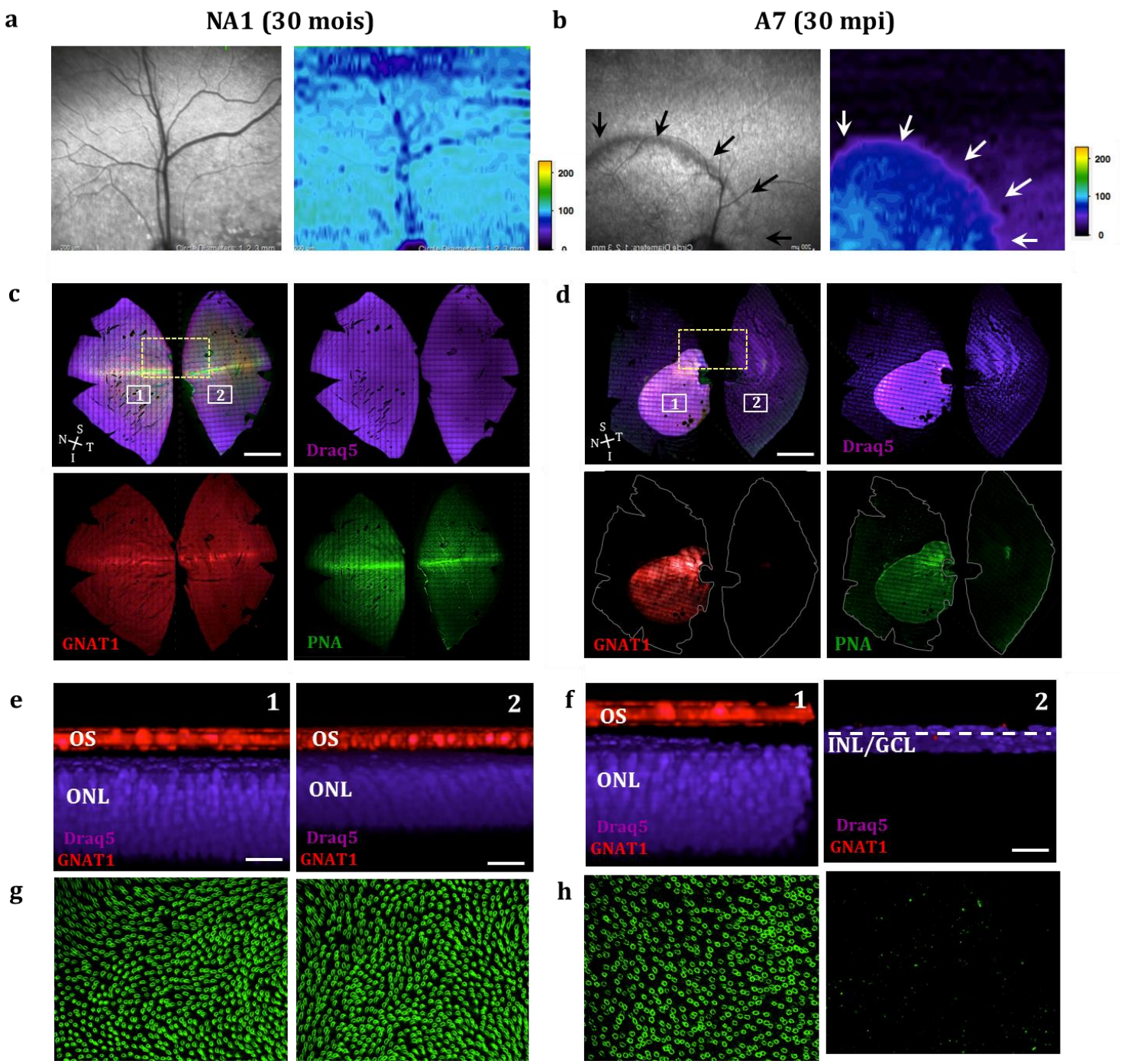

Figure 21. *In vivo* and *post-mortem* assessment of photoreceptor preservation in dogs (a,c,e,g) NA1 and (b,d,f,h) A7 at 30 months postinjection. **a,b)** Fundus photograph and topography of photoreceptor layer obtained by spectral-domain optical coherence tomography (SD-OCT). White arrows indicate the area of the treated A7 retina exposed to AAV2/8-RK-cPde6β vector. **c,d)** Confocal images of flat-mount retinas stained with Draq5 (nuclei marker, purple), GNAT (rod outer segment marker, red) and PNA (cone inner and outer segment marker, green). Images were taken from the outer segments of photoreceptors to the outer plexiform layer. Yellow squares represent the area previously observed in vivo by SD-OCT. **e,f**: Image from representative z plan showing ONL thickness (purple) and rod outer segment labeling with an antibody raised against GNAT1. **g,h**: Confocal images of flat mount retinas stained with PNA. The focal plan of the images is at the level of outer segments. We can note that in the A7 treated retina, the rod and cone photoreceptors are only preserved in the vector-exposed area. S, superior retina, T, temporal retina, I, inferior retina, N, nasal retina, ONL, outer nuclear layer, OS, outer segments. (Petit L *et al*. in preparation).

In both *rcd1* and *Rpe65*$^{-/-}$ dogs, while transduced rods represented only 25-30% of the total rod population, the degeneration of the residual 65-70% non-transduced photoreceptors had no major negative impact on rod survival in the treated area (at least for the examined period). The phenomenon of non-cell autonomous degeneration had however been described in chimeric mice that express patches of rhodopsin-mutant and wild-type photoreceptors. In chimeric mice, healthy rods rapidly degenerate in the presence of the mutant rods, even when 42% of the retina is composed by normal photoreceptors [251].

It is possible that PDE6β- and RPE65-deficiencies involve a different mechanism that the death of rods in rhodopsin-deficiency.
Alternatively, differences between dogs and chimeric mice may reflect the **high spatial density of "rescued" rods in the treated area of (our) dogs**. Indeed, in chimeric mice, wild-type rods were intermingled with mutant rods and rate of degeneration depended upon the proportion of healthy cells in the retina [251]. In contrast, in the treated dogs there is a clear demarcation between treated and untreated areas **(Figure 21).** This hypothesis is consistent with the observations in the zebrafish which show that relative photoreceptor cell density is a crucial determinant of photoreceptor death [267],[29]. This result should be considered in the context of PDE6β-deficient patients as they typically have advanced rod degeneration in the peripheral retina at the time of diagnosis (**Chapter 2**).

2. rAAV-mediated Pde6β gene transfer prevents cone cell death in *rcd1* treated retinas

In the *rcd1* dog, and in other models of rod-initiated **rod-cone dystrophies**, death of rods causes non-autonomous death of cones. Therefore, if the number of rescued rods is too low in the treated retinas, cones may not long-term survive and the benefits of the therapy may be greatly reduced.

Coherent with the long-term amelioration of rod survival in the vector-exposed area of *rcd1* dogs, we showed that the initiation of secondary cone dysfunction was significantly delayed in treated eyes (Figures **19** and **20**).
A similar beneficial effect of the primary rod treatment on cone function has been previously obtained in murine models of rod-initiated **rod-cone dystrophy**:
(i) in the *rd10* mouse treated with AAV2/8(Y733F)-smCBA-m*Pde6β* at P14, in which cone function was totally preserved for at least 6 months postinjection in treated eyes, although photopic responses were lost at 8 weeks of age in untreated eyes. In this mouse model, gene therapy preserved up to 70% of the normal ONL thickness in the vector-exposed area (>90% of retinal detachment)[365].
(ii) in the *Cngb1* knockout mouse treated with AAV2/8(Y733F)-mOP-m*Cngb1a* at P14, in which morphology of cones was preserved for at least 12 months of age in treated eyes, although cone degeneration becomes evident after 6 months of age in untreated mice. In this

model, gene therapy preserved 60-72% of photoreceptor cells in the vector-exposed area [419].
(iii) in the *nmf363* mouse model of PDE6α-deficiency treated with AAV2/8(Y733F)-Rho-m*Pde6α* at P5 or P21, in which cone dysfunction was slightly slowed from 3 to 6 months post-treatment, despite the absence of rescued rod ERG responses. The therapeutic effect of gene therapy on cone survival was attributed to the stable preservation of up to 50% of the ONL thickness in the vector-exposed area of the treated eye [417, 418].

Given the high similitude of cone:rod photoreceptor ratio, distribution and degeneration between the canine and the human PDE6β-deficient retinas, the regional rescue of rods in treated *rcd1* dogs provides an ideal tool to study functional and physical links between rod and cone survival in rod-cone dystrophies. Further characterizations of the long-term preservation of cone function in treated *rcd1* dogs are pending.
Preliminary results indicate that long-term preservation of cone function corresponds to the preservation of cones in the vector-exposed area of treated dogs, which are normally rapidly lost between 9-12 and 18 months of age. The cones in the vector-exposed area are totally preserved for at least 24 months postinjection (the latest timepoint explored). In contrast, within the rest of the retina, the kinetics of cone degeneration remains largely unchanged (Petit L *et al*. in preparation). The drastic fall of cone survival at the boundaries of the vector-exposed area provides preliminary evidences of the dependence of cones on the *physical* presence of neighboring rods for their long-term survival.

3. MLHD-*Cord1* treated retinas show advancing retinal degeneration

In the MLHD-*Cord1* dog, the pathway that links the causal mutation and the death of cone and/or rod photoreceptors is still not known.
Using *in vivo* and *post-mortem* morphological analyses, we observed improved photoreceptor cell survival and preservation of outer segment morphology in the vector-exposed area of MLHD-*Cord1* treated eyes for at least 24 months postinjection (the duration of the study).
However, contrary to the observation made in the *rcd1* and the young *Rpe65*$^{-/-}$ dogs, rAAV-mediated *Rprip1* gene transfer did not completely prevent loss of photoreceptor cells and continuous retinal thinning was observed in the vector-exposed area from 3 to 24 months postinjection. Consequently, at 24 months postinjection, while *rcd1* treated dogs retained 90% of photoreceptor cells in the vector-exposed area, only 50-60% of photoreceptors were still present in the MLHD-*Cord1* dogs.
Similar advancing retinal thinning in the vector-exposed area has been reported in the XLPRA2 dog treated at early stages of retinal degeneration [347] and in *Rpe65*-LCA patients treated at late stages of retinal degeneration [268].

There may be several reasons to explain why photoreceptor degeneration proceeds despite treatment. First, the course of degeneration can be under way in the MLHD-*Cord1* or the XLPRA2 dogs at the time of maximal transgene expression. In the subpopulation of photoreceptors, which have begun to degenerate, introducing the wild-type gene may not allow prevention of apoptosis.

In addition, advancing retinal degeneration might be the result of inappropriate level of transgene expression in a subpopulation of photoreceptors. Interestingly, in the XLPRA2 dog, Beltran *et al*. demonstrated that the human IRBP promoter used to drive expression of their transgene to rods and cones was more effective in halting photoreceptor degeneration than the RK promoter [347]. A higher expression of transgene could be necessary for prevention of photoreceptor death in both MLHD-*Cord1* and XLPRA2 dogs. Alternatively, the physiological state of photoreceptor may impair the expression of the transgene by limiting the entry or the trafficking of rAAV particles or decreasing the stability of the mRNA and/or the protein products.

ANIMAL MODELS OF SEVERE PHOTORECEPTOR DYSTROPHIES DEMONSTRATE PRELIMINARY EVIDENCE OF AN "ON/OFF" PHOTORECEPTOR RESPONSE TO GENE THERAPY

In the *rcd1* dog, rAAV-mediated gene addition therapy stably prevented rod degeneration, a result correlated with the stable restoration of the rod function in treated area. In contrast, in the MLHD-*Cord1* dog, we have shown advancing photoreceptor degeneration in the vector-exposed area. However, advancing retinal thinning in the MLHD-*Cord1* vector-exposed area was not associated with a loss of restored cone function (that remained stable from 1 to 24 months postinjection or preserved rod function (that remained stable from 12 to 24 months postinjection). **This indicates that advanced photoreceptor degeneration mainly reflected the loss of a subpopulation of silent (non-rescued- photoreceptors within the vector-exposed area.**

A similar response of photoreceptors to gene therapy has been recently described in RPE65-LCA patients treated at late stage of retinal degeneration [268]. In these patients, serial measurements of ONL thickness over 3 years post-treatment demonstrated that photoreceptor loss continued within the vector-exposed area. However, the patients showed remarkable lasting improvements in visual function.

To explain this result in the RPE65-LCA patients, Cideciyan *et al*. proposed that functionally rescued cells could be the cells that will longer survive. In this case, function loss will be initially slow (during the loss of non-rescued cells). **Then, at later stages, functional rescue will be more and more affected, as last-remaining rescued cells will start to die** [268].

This hypothesis is highly consistent with the fact that retinal degeneration is non-homogeneous in humans or animals affected by inherited retinal degenerations (**Chapter 3**) (Petit L *et al*. in preparation). **However, as photoreceptor degeneration progress slowly in RPE65 patients, further monitoring of retina function for years will be required to confirm this hypothesis and determine the real therapeutic potential of gene addition therapy for inherited retinal dystrophies** [400]**.** The challenge is the same in RPE65-deficient dogs, in which, only 40% of photoreceptor cells are lost by 6 years of age [377], [268], [393].

The MLHD-*Cord1* dog displays a severe early onset cone-rod dystrophy that allows fairly rapid assessment of the effects of gene therapy on both retinal function and degeneration. Almost complete loss of ONL nuclei is observed after 24 months of age, but **rod dysfunction, which is an early sign of rod degeneration, progresses from 1 to 12 months of age** [153], [348].
Our *in vivo* analysis of rod function in treated MLHD-Cord1 dogs revealed that, along the first 6-9 months after treatment, the progressive loss of rod function remained unchanged in all treated *Rpgrip1*$^{-/-}$ dogs. **However, continuous monitoring of rod function up to 24 months postinjection, revealed that in 4/5 treated dogs, rod function was stabilized and then remained stable for the 12 following months**. This function may represent a fraction of stably preserved rods and further longitudinal measurements of the ONL thickness in treated MLHD-Cord1 by SD-OCT will be essential to determine whether, as for the rod function, there will or wont be a detectable stabilization of photoreceptor cell loss in treated areas at later stages of the disease.

Very interestingly, **these preliminary results suggest that the last-remaining rescued cells do not die as the disease progresses. Rather, they might be a mixed population of *at least* two groups of photoreceptor cells within the treated area at the time of intervention (Figure 22):**

- the photoreceptors that **do not respond <u>at all</u> to the treatment**: the photoreceptors are functionally non-rescued and physically degenerate ("**OFF**" photoreceptors)
- the photoreceptors that **entirely respond to the treatment**: they are **stably** functionally **<u>and</u>** physically rescued ("**ON**" photoreceptors).

In this context, it is very interesting to note now that 3 murine models of rapid progressive photoreceptor dystrophy with initial rod function, the *Rpgrip1*$^{-/-}$ [423], the *Aipl1*$^{h/h}$ [420] and the *Bbs4 null* mice [432], displayed a similar kinetic of rod function preservation after gene therapy, **i.e. an initial decrease of rod function followed by a stabilization**.

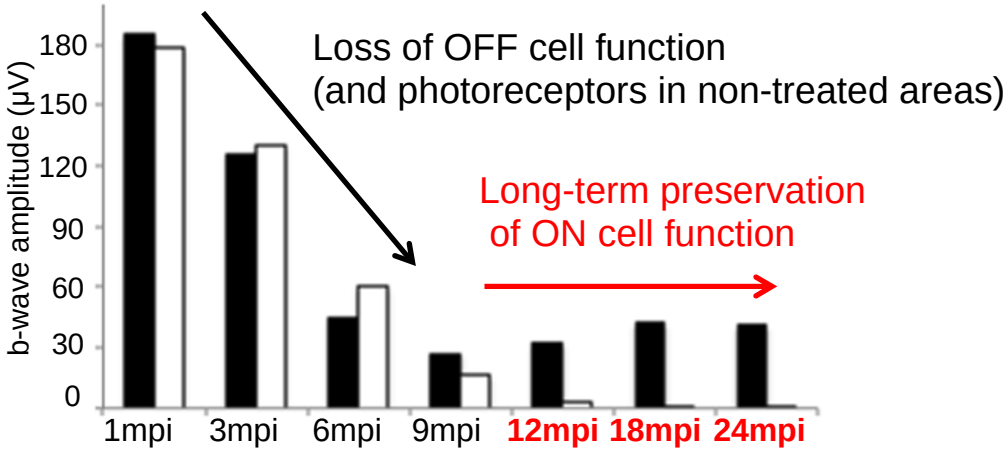

Figure 22. Preliminary evidences of an "OFF/ON" photoreceptor response to gene therapy. Kinetics of rod function preservation in A2 treated dog. Treated eye is shown in dark, untreated eye in white. Mpi, month(s) postinjection.

Particularly, in the *Aipl1*$^{h/h}$ mouse, the stabilization of rod function in treated eyes appeared earlier when the rate of retinal degeneration was increased by constant light exposure (9 weeks versus 12 weeks postinjection) [420]. **This suggests that the population of rescued rods is present from early timepoints after treatment, but this population is small and cannot be detected by full-field ERG before that most of the non-rescued rods have lost their function**.

The presence of mixed populations of "ON" and "OFF" photoreceptors from early stages of retinal degeneration may be consistent with the previous observation that functional rescue of some subpopulations of photoreceptors is not possible in animal models of stationary cone dystrophy despite the slow rate of photoreceptor degeneration [346, 404], [371]. The health of photoreceptors at the time of treatment may determine their subsequent "ON" and "OFF" fate. As well, when the disease progresses, the proportion of "OFF/ON" cells might change with a potential rapid decrease of the number of "ON" cells.

Importantly, also the "OFF/ON" photoreceptor response can be viewed as a limit for the application of such rAAV-mediated gene therapy in patients with advances retinal degeneration, the recent study in the RPE65-LCA patients, which has demonstrated a preserved restored vision despite a progressive retinal thinning, indicates that some "ON" cells could still exist at late stage of the disease [268].
Moreover, despite the presence of only few "ON" cells in degenerated retina, some patients demonstrated strong improvements of their retinal function and life-quality. These results indicate that gene therapy has still a great potential for treating inherited retinal dystrophies. This potential could be even more important if the remaining "ON" cells are located in a particular retinal area, and it they are synonymous with a long-term therapeutic effects.
Evidences of the efficacy of early gene addition therapy in the PDE6β- and the RPGRIP1-deficient dogs provides thus great promise for human treatment, even if the efficacy of gene therapy at later stages of the disease must now to be accurately evaluated.

List of references

1. Baccus, S.A., *Timing and computation in inner retinal circuitry.* Annu Rev Physiol, 2007. **69**: p. 271-90.

2. Masland, R.H., *The neuronal organization of the retina.* Neuron, 2012. **76**(2): p. 266-80.

3. Holopigian, K., et al., *Local cone and rod system function in patients with retinitis pigmentosa.* Invest Ophthalmol Vis Sci, 2001. **42**(3): p. 779-88.

4. Young, R.W., *The renewal of rod and cone outer segments in the rhesus monkey.* J Cell Biol, 1971. **49**(2): p. 303-18.

5. Strauss, O., *The retinal pigment epithelium in visual function.* Physiol Rev, 2005. **85**(3): p. 845-81.

6. Sparrow, J.R., D. Hicks, and C.P. Hamel, *The retinal pigment epithelium in health and disease.* Curr Mol Med, 2010. **10**(9): p. 802-23.

7. Calvert, P.D., et al., *Light-driven translocation of signaling proteins in vertebrate photoreceptors.* Trends Cell Biol, 2006. **16**(11): p. 560-8.

8. Rosenbaum, J.L. and G.B. Witman, *Intraflagellar transport.* Nat Rev Mol Cell Biol, 2002. **3**(11): p. 813-25.

9. Berger, W., B. Kloeckener-Gruissem, and J. Neidhardt, *The molecular basis of human retinal and vitreoretinal diseases.* Prog Retin Eye Res, 2010. **29**(5): p. 335-75.

10. Mustafi, D., A.H. Engel, and K. Palczewski, *Structure of cone photoreceptors.* Prog Retin Eye Res, 2009. **28**(4): p. 289-302.

11. Wang, J.S. and V.J. Kefalov, *An alternative pathway mediates the mouse and human cone visual cycle.* Curr Biol, 2009. **19**(19): p. 1665-9.

12. Wang, J.S. and V.J. Kefalov, *The cone-specific visual cycle.* Prog Retin Eye Res, 2011. **30**(2): p. 115-28.

13. Saari, J.C., *Vitamin A metabolism in rod and cone visual cycles.* Annu Rev Nutr, 2012. **32**: p. 125-45.

14. Wang, J.S., et al., *Intra-retinal visual cycle required for rapid and complete cone dark adaptation.* Nat Neurosci, 2009. **12**(3): p. 295-302.

15. Ebrey, T. and Y. Koutalos, *Vertebrate photoreceptors.* Prog Retin Eye Res, 2001. **20**(1): p. 49-94.

16. Fu, Y. and K.W. Yau, *Phototransduction in mouse rods and cones.* Pflugers Arch, 2007. **454**(5): p. 805-19.

17. Goc, A., et al., *Structural characterization of the rod cGMP phosphodiesterase 6.* J Mol Biol, 2010. **401**(3): p. 363-73.

18. Kolandaivelu, S., B. Chang, and V. Ramamurthy, *Rod phosphodiesterase-6 (PDE6) catalytic subunits restore cone function in a mouse model lacking cone PDE6 catalytic subunit.* J Biol Chem, 2011. **286**(38): p. 33252-9.

19. Deng, W.T., et al., *Cone Phosphodiesterase-6alpha' Restores Rod Function and Confers Distinct Physiological Properties in the Rod Phosphodiesterase-6beta-Deficient rd10 Mouse.* J Neurosci, 2013. **33**(29): p. 11745-53.

20. Olshevskaya, E.V., A.N. Ermilov, and A.M. Dizhoor, *Factors that affect regulation of cGMP synthesis in vertebrate photoreceptors and their genetic link to human retinal degeneration.* Mol Cell Biochem, 2002. **230**(1-2): p. 139-47.

21. Weiss, E.R., et al., *Species-specific differences in expression of G-protein-coupled receptor kinase (GRK) 7 and GRK1 in mammalian cone photoreceptor cells: implications for cone cell phototransduction.* J Neurosci, 2001. **21**(23): p. 9175-84.

22. Ames, A., 3rd, et al., *Energy metabolism of rabbit retina as related to function: high cost of Na+ transport.* J Neurosci, 1992. **12**(3): p. 840-53.

23. Kawamura, S. and S. Tachibanaki, *Rod and cone photoreceptors: molecular basis of the difference in their physiology.* Comp Biochem Physiol A Mol Integr Physiol, 2008. **150**(4): p. 369-77.

24. Miyazono, S., et al., *Highly efficient retinal metabolism in cones.* Proc Natl Acad Sci U S A, 2008. **105**(41): p. 16051-6.

25. Stone, J., et al., *Mechanisms of photoreceptor death and survival in mammalian retina.* Prog Retin Eye Res, 1999. **18**(6): p. 689-735.

26. Coffe, V., R.C. Carbajal, and R. Salceda, *Glycogen metabolism in the rat retina.* J Neurochem, 2004. **88**(4): p. 885-90.

27. Nihira, M., et al., *Primate rod and cone photoreceptors may differ in glucose accessibility.* Invest Ophthalmol Vis Sci, 1995. **36**(7): p. 1259-70.

28. Braun, R.D., R.A. Linsenmeier, and T.K. Goldstick, *Oxygen consumption in the inner and outer retina of the cat.* Invest Ophthalmol Vis Sci, 1995. **36**(3): p. 542-54.

29. Punzo, C., W. Xiong, and C.L. Cepko, *Loss of daylight vision in retinal degeneration: are oxidative stress and metabolic dysregulation to blame?* J Biol Chem, 2012. **287**(3): p. 1642-8.

30. Winkler, B.S., *An hypothesis to account for the renewal of outer segments in rod and cone photoreceptor cells: renewal as a surrogate antioxidant.* Invest Ophthalmol Vis Sci, 2008. **49**(8): p. 3259-61.

31. Kevany, B.M. and K. Palczewski, *Phagocytosis of retinal rod and cone photoreceptors.* Physiology (Bethesda), 2010. **25**(1): p. 8-15.

32. Young, R.W. and D. Bok, *Participation of the retinal pigment epithelium in the rod outer segment renewal process.* J Cell Biol, 1969. **42**(2): p. 392-403.

33. Mayhew, T.M. and D. Astle, *Photoreceptor number and outer segment disk membrane surface area in the retina of the rat: stereological data for whole organ and average photoreceptor cell.* J Neurocytol, 1997. **26**(1): p. 53-61.

34. Vander Heiden, M.G., L.C. Cantley, and C.B. Thompson, *Understanding the Warburg effect: the metabolic requirements of cell proliferation.* Science, 2009. **324**(5930): p. 1029-33.

35. Besharse, J.C., J.G. Hollyfield, and M.E. Rayborn, *Turnover of rod photoreceptor outer segments. II. Membrane addition and loss in relationship to light.* J Cell Biol, 1977. **75**(2 Pt 1): p. 507-27.

36. Murga-Zamalloa, C.A., et al., *Interaction of ciliary disease protein retinitis pigmentosa GTPase regulator with nephronophthisis-associated proteins in mammalian retinas.* Mol Vis, 2010. **16**: p. 1373-81.

37. Murga-Zamalloa, C., A. Swaroop, and H. Khanna, *Multiprotein complexes of Retinitis Pigmentosa GTPase regulator (RPGR), a ciliary protein mutated in X-linked Retinitis Pigmentosa (XLRP).* Adv Exp Med Biol, 2010. **664**: p. 105-14.

38. Patil, H., et al., *Selective loss of RPGRIP1-dependent ciliary targeting of NPHP4, RPGR and SDCCAG8 underlies the degeneration of photoreceptor neurons.* Cell Death Dis, 2012. **3**: p. e355.

39. Zhang, H., et al., *Deletion of PrBP/delta impedes transport of GRK1 and PDE6 catalytic subunits to photoreceptor outer segments.* Proc Natl Acad Sci U S A, 2007. **104**(21): p. 8857-62.

40. Zhang, H., et al., *Trafficking of membrane-associated proteins to cone photoreceptor outer segments requires the chromophore 11-cis-retinal.* J Neurosci, 2008. **28**(15): p. 4008-14.

41. Karan, S., et al., *A model for transport of membrane-associated phototransduction polypeptides in rod and cone photoreceptor inner segments.* Vision Res, 2008. **48**(3): p. 442-52.

42. Wright, A.F., et al., *Photoreceptor degeneration: genetic and mechanistic dissection of a complex trait.* Nat Rev Genet, 2010. **11**(4): p. 273-84.

43. den Hollander, A.I., et al., *Lighting a candle in the dark: advances in genetics and gene therapy of recessive retinal dystrophies.* J Clin Invest, 2010. **120**(9): p. 3042-53.

44. Jacobson, S.G., et al., *Retinal optogenetic therapies: clinical criteria for candidacy.* Clin Genet, 2013. **84**(2): p. 175-82.

45. Busskamp, V., et al., *Genetic reactivation of cone photoreceptors restores visual responses in retinitis pigmentosa.* Science, 2010. **329**(5990): p. 413-7.

46. Thiadens, A.A., et al., *Progressive loss of cones in achromatopsia: an imaging study using spectral-domain optical coherence tomography.* Invest Ophthalmol Vis Sci, 2010. **51**(11): p. 5952-7.

47. Genead, M.A., et al., *Photoreceptor structure and function in patients with congenital achromatopsia.* Invest Ophthalmol Vis Sci, 2011. **52**(10): p. 7298-308.

48. Thomas, M.G., et al., *Early signs of longitudinal progressive cone photoreceptor degeneration in achromatopsia.* Br J Ophthalmol, 2012. **96**(9): p. 1232-6.

49. Koenekoop, R.K., et al., *Genetic testing for retinal dystrophies and dysfunctions: benefits, dilemmas and solutions.* Clin Experiment Ophthalmol, 2007. **35**(5): p. 473-85.

50. Hamel, C.P., *Cone rod dystrophies.* Orphanet J Rare Dis, 2007. **2**: p. 7.

51. Hartong, D.T., E.L. Berson, and T.P. Dryja, *Retinitis pigmentosa.* Lancet, 2006. **368**(9549): p. 1795-809.

52. Bonnet, C. and A. El-Amraoui, *Usher syndrome (sensorineural deafness and retinitis pigmentosa): pathogenesis, molecular diagnosis and therapeutic approaches.* Curr Opin Neurol, 2012. **25**(1): p. 42-9.

53. Forsythe, E. and P.L. Beales, *Bardet-Biedl syndrome.* Eur J Hum Genet, 2013. **21**(1): p. 8-13.

54. Mockel, A., et al., *Retinal dystrophy in Bardet-Biedl syndrome and related syndromic ciliopathies.* Prog Retin Eye Res, 2011. **30**(4): p. 258-74.

55. Weber, B., et al., *Genomic organization and complete sequence of the human gene encoding the beta-subunit of the cGMP phosphodiesterase and its localisation to 4p 16.3.* Nucleic Acids Res, 1991. **19**(22): p. 6263-8.

56. Khramtsov, N.V., et al., *The human rod photoreceptor cGMP phosphodiesterase beta-subunit. Structural studies of its cDNA and gene.* FEBS Lett, 1993. **327**(3): p. 275-8.

57. Lugnier, C., *Cyclic nucleotide phosphodiesterase (PDE) superfamily: a new target for the development of specific therapeutic agents.* Pharmacol Ther, 2006. **109**(3): p. 366-98.

58. Conti, M. and J. Beavo, *Biochemistry and physiology of cyclic nucleotide phosphodiesterases: essential components in cyclic nucleotide signaling.* Annu Rev Biochem, 2007. **76**: p. 481-511.

59. Reichenbach, A., et al., *The structure of rabbit retinal Muller (glial) cells is adapted to the surrounding retinal layers.* Anat Embryol (Berl), 1989. **180**(1): p. 71-9.

60. Aravind, L. and C.P. Ponting, *The GAF domain: an evolutionary link between diverse phototransducing proteins.* Trends Biochem Sci, 1997. **22**(12): p. 458-9.

61. Guo, L.W., et al., *Asymmetric interaction between rod cyclic GMP phosphodiesterase gamma subunits and alphabeta subunits.* J Biol Chem, 2005. **280**(13): p. 12585-92.

62. Mou, H. and R.H. Cote, *The catalytic and GAF domains of the rod cGMP phosphodiesterase (PDE6) heterodimer are regulated by distinct regions of its inhibitory gamma subunit.* J Biol Chem, 2001. **276**(29): p. 27527-34.

63. Muradov, H., K.K. Boyd, and N.O. Artemyev, *Rod phosphodiesterase-6 PDE6A and PDE6B subunits are enzymatically equivalent.* J Biol Chem, 2010. **285**(51): p. 39828-34.

64. Piriev, N.I., et al., *Rod photoreceptor cGMP-phosphodiesterase: analysis of alpha and beta subunits expressed in human kidney cells.* Proc Natl Acad Sci U S A, 1993. **90**(20): p. 9340-4.

65. Piriev, N.I., et al., *Expression of cone photoreceptor cGMP-phosphodiesterase alpha' subunit in Chinese hamster ovary, 293 human embryonic kidney, and Y79 retinoblastoma cells.* Mol Vis, 2003. **9**: p. 80-6.

66. Qin, N., S.J. Pittler, and W. Baehr, *In vitro isoprenylation and membrane association of mouse rod photoreceptor cGMP phosphodiesterase alpha and beta subunits expressed in bacteria.* J Biol Chem, 1992. **267**(12): p. 8458-63.

67. Qin, N. and W. Baehr, *Expression and mutagenesis of mouse rod photoreceptor cGMP phosphodiesterase.* J Biol Chem, 1994. **269**(5): p. 3265-71.

68. Zhang, F.L. and P.J. Casey, *Protein prenylation: molecular mechanisms and functional consequences.* Annu Rev Biochem, 1996. **65**: p. 241-69.

69. Suber, M.L., et al., *Irish setter dogs affected with rod/cone dysplasia contain a nonsense mutation in the rod cGMP phosphodiesterase beta-subunit gene.* Proc Natl Acad Sci U S A, 1993. **90**(9): p. 3968-72.

70. Parry, H.B., *Degenerations of the dog retina. II. Generalized progressive atrophy of hereditary origin.* Br J Ophthalmol, 1953. **37**(8): p. 487-502.

71. Aguirre, G.D. and L.F. Rubin, *Rod-cone dysplasia (progressive retinal atrophy) in Irish setters.* J Am Vet Med Assoc, 1975. **166**(2): p. 157-64.

72. Artemyev, N.O., et al., *Subunit structure of rod cGMP-phosphodiesterase.* J Biol Chem, 1996. **271**(41): p. 25382-8.

73. McLaughlin, M.E., et al., *Mutation spectrum of the gene encoding the beta subunit of rod phosphodiesterase among patients with autosomal recessive retinitis pigmentosa.* Proc Natl Acad Sci U S A, 1995. **92**(8): p. 3249-53.

74. McLaughlin, M.E., et al., *Recessive mutations in the gene encoding the beta-subunit of rod phosphodiesterase in patients with retinitis pigmentosa.* Nat Genet, 1993. **4**(2): p. 130-4.

75. Danciger, M., et al., *Mutations in the PDE6B gene in autosomal recessive retinitis pigmentosa.* Genomics, 1995. **30**(1): p. 1-7.

76. Danciger, M., et al., *A homozygous PDE6B mutation in a family with autosomal recessive retinitis pigmentosa.* Mol Vis, 1996. **2**: p. 10.

77. Bayes, M., et al., *Homozygous tandem duplication within the gene encoding the beta-subunit of rod phosphodiesterase as a cause for autosomal recessive retinitis pigmentosa.* Hum Mutat, 1995. **5**(3): p. 228-34.

78. Saga, M., et al., *A novel homozygous Ile535Asn mutation in the rod cGMP phosphodiesterase beta-subunit gene in two brothers of a Japanese family with autosomal recessive retinitis pigmentosa.* Curr Eye Res, 1998. **17**(3): p. 332-5.

79. Hmani-Aifa, M., et al., *Identification of two new mutations in the GPR98 and the PDE6B genes segregating in a Tunisian family.* Eur J Hum Genet, 2009. **17**(4): p. 474-82.

80. Clark, G.R., et al., *Development of a diagnostic genetic test for simplex and autosomal recessive retinitis pigmentosa.* Ophthalmology, 2010. **117**(11): p. 2169-77 e3.

81. Simpson, D.A., et al., *Molecular diagnosis for heterogeneous genetic diseases with targeted high-throughput DNA sequencing applied to retinitis pigmentosa.* J Med Genet, 2011. **48**(3): p. 145-51.

82. Tsang, S.H., et al., *A novel mutation and phenotypes in phosphodiesterase 6 deficiency.* Am J Ophthalmol, 2008. **146**(5): p. 780-8.

83. Kim, C., et al., *Microarray-based mutation detection and phenotypic characterization in Korean patients with retinitis pigmentosa.* Mol Vis, 2012. **18**: p. 2398-410.

84. Gal, A., et al., *Heterozygous missense mutation in the rod cGMP phosphodiesterase beta-subunit gene in autosomal dominant stationary night blindness.* Nat Genet, 1994. **7**(1): p. 64-8.

85. Gao, Y.Q., et al., *Screening of the PDE6B gene in patients with autosomal dominant retinitis pigmentosa.* Exp Eye Res, 1996. **62**(2): p. 149-54.

86. Goldenberg-Cohen, N., et al., *Genetic heterogeneity and consanguinity lead to a "double hit": homozygous mutations of MYO7A and PDE6B in a patient with retinitis pigmentosa.* Mol Vis, 2013. **19**: p. 1565-71.

87. Jacobson, S.G., et al., *Evidence for retinal remodelling in retinitis pigmentosa caused by PDE6B mutation.* Br J Ophthalmol, 2007. **91**(5): p. 699-701.

88. Portera-Cailliau, C., et al., *Apoptotic photoreceptor cell death in mouse models of retinitis pigmentosa.* Proc Natl Acad Sci U S A, 1994. **91**(3): p. 974-8.

89. Ali, S., et al., *Mutations in the beta-subunit of rod phosphodiesterase identified in consanguineous Pakistani families with autosomal recessive retinitis pigmentosa.* Mol Vis, 2011. **17**: p. 1373-80.

90. Abd-El-Barr, M.M., et al., *Genetic dissection of rod and cone pathways in the dark-adapted mouse retina.* J Neurophysiol, 2009. **102**(3): p. 1945-55.

91. Keeler, C.E., *The Inheritance of a Retinal Abnormality in White Mice.* Proc Natl Acad Sci U S A, 1924. **10**(7): p. 329-33.

92. Bowes, C., et al., *Retinal degeneration in the rd mouse is caused by a defect in the beta subunit of rod cGMP-phosphodiesterase.* Nature, 1990. **347**(6294): p. 677-80.

93. Pittler, S.J. and W. Baehr, *Identification of a nonsense mutation in the rod photoreceptor cGMP phosphodiesterase beta-subunit gene of the rd mouse.* Proc Natl Acad Sci U S A, 1991. **88**(19): p. 8322-6.

94. Farber, D.B. and R.N. Lolley, *Enzymic basis for cyclic GMP accumulation in degenerative photoreceptor cells of mouse retina.* J Cyclic Nucleotide Res, 1976. **2**(3): p. 139-48.

95. Farber, D.B., S. Park, and C. Yamashita, *Cyclic GMP-phosphodiesterase of rd retina: biosynthesis and content.* Exp Eye Res, 1988. **46**(3): p. 363-74.

96. Blanks, J.C., A.M. Adinolfi, and R.N. Lolley, *Photoreceptor degeneration and synaptogenesis in retinal-degenerative (rd) mice.* J Comp Neurol, 1974. **156**(1): p. 95-106.

97. LaVail, M.M. and R.L. Sidman, *C57BL-6J mice with inherited retinal degeneration.* Arch Ophthalmol, 1974. **91**(5): p. 394-400.

98. Tansley, K., *Hereditary degeneration of the mouse retina.* Br J Ophthalmol, 1951. **35**(10): p. 573-82.

99. Carter-Dawson, L.D., M.M. LaVail, and R.L. Sidman, *Differential effect of the rd mutation on rods and cones in the mouse retina.* Invest Ophthalmol Vis Sci, 1978. **17**(6): p. 489-98.

100. Jimenez, A.J., et al., *The spatio-temporal pattern of photoreceptor degeneration in the aged rd/rd mouse retina.* Cell Tissue Res, 1996. **284**(2): p. 193-202.

101. Punzo, C., K. Kornacker, and C.L. Cepko, *Stimulation of the insulin/mTOR pathway delays cone death in a mouse model of retinitis pigmentosa.* Nat Neurosci, 2009. **12**(1): p. 44-52.

102. Chang, B., et al., *Retinal degeneration mutants in the mouse.* Vision Res, 2002. **42**(4): p. 517-25.

103. Chang, B., et al., *Two mouse retinal degenerations caused by missense mutations in the beta-subunit of rod cGMP phosphodiesterase gene.* Vision Res, 2007. **47**(5): p. 624-33.

104. Gargini, C., et al., *Retinal organization in the retinal degeneration 10 (rd10) mutant mouse: a morphological and ERG study.* J Comp Neurol, 2007. **500**(2): p. 222-38.

105. Komeima, K., B.S. Rogers, and P.A. Campochiaro, *Antioxidants slow photoreceptor cell death in mouse models of retinitis pigmentosa.* J Cell Physiol, 2007. **213**(3): p. 809-15.

106. Cronin, T., A. Lyubarsky, and J. Bennett, *Dark-rearing the rd10 mouse: implications for therapy.* Adv Exp Med Biol, 2012. **723**: p. 129-36.

107. Hart, A.W., et al., *Genotype-phenotype correlation of mouse pde6b mutations.* Invest Ophthalmol Vis Sci, 2005. **46**(9): p. 3443-50.

108. Davis, R.J., et al., *Functional rescue of degenerating photoreceptors in mice homozygous for a hypomorphic cGMP phosphodiesterase 6 b allele (Pde6bH620Q).* Invest Ophthalmol Vis Sci, 2008. **49**(11): p. 5067-76.

109. Clements, P.J., et al., *Confirmation of the rod cGMP phosphodiesterase beta subunit (PDE beta) nonsense mutation in affected rcd-1 Irish setters in the UK and development of a diagnostic test.* Curr Eye Res, 1993. **12**(9): p. 861-6.

110. Petit, L., et al., *Restoration of vision in the pde6beta-deficient dog, a large animal model of rod-cone dystrophy.* Mol Ther, 2012. **20**(11): p. 2019-30.

111. Goldstein, O., et al., *IQCB1 and PDE6B Mutations Cause Similar Early Onset Retinal Degenerations in Two Closely Related Terrier Dog Breeds.* Invest Ophthalmol Vis Sci, 2013. **54**(10): p. 7005-19.

112. Wright, A.F., et al., *Lifespan and mitochondrial control of neurodegeneration.* Nat Genet, 2004. **36**(11): p. 1153-8.

113. Gal, A., et al., *Heterozygous missense mutation in the rod cGMP phosphodiesterase beta-subunit gene in autosomal dominant stationary night blindness.* Nat Genet, 1994. **7**(4): p. 551.

114. Muradov, K.G., A.E. Granovsky, and N.O. Artemyev, *Mutation in rod PDE6 linked to congenital stationary night blindness impairs the enzyme inhibition by its gamma-subunit.* Biochemistry, 2003. **42**(11): p. 3305-10.

115. Tsang, S.H., et al., *Transgenic mice carrying the H258N mutation in the gene encoding the beta-subunit of phosphodiesterase-6 (PDE6B) provide a model for human congenital stationary night blindness.* Hum Mutat, 2007. **28**(3): p. 243-54.

116. Dryja, T.P., et al., *Null RPGRIP1 alleles in patients with Leber congenital amaurosis.* Am J Hum Genet, 2001. **68**(5): p. 1295-8.

117. Gerber, S., et al., *Complete exon-intron structure of the RPGR-interacting protein (RPGRIP1) gene allows the identification of mutations underlying Leber congenital amaurosis.* Eur J Hum Genet, 2001. **9**(8): p. 561-71.

118. Roepman, R., et al., *The retinitis pigmentosa GTPase regulator (RPGR) interacts with novel transport-like proteins in the outer segments of rod photoreceptors.* Hum Mol Genet, 2000. **9**(14): p. 2095-105.

119. Boylan, J.P. and A.F. Wright, *Identification of a novel protein interacting with RPGR.* Hum Mol Genet, 2000. **9**(14): p. 2085-93.

120. Hong, D.H., et al., *Retinitis pigmentosa GTPase regulator (RPGRr)-interacting protein is stably associated with the photoreceptor ciliary axoneme and anchors RPGR to the connecting cilium.* J Biol Chem, 2001. **276**(15): p. 12091-9.

121. Demirci, F.Y., et al., *X-linked cone-rod dystrophy (locus COD1): identification of mutations in RPGR exon ORF15.* Am J Hum Genet, 2002. **70**(4): p. 1049-53.

122. Ayyagari, R., et al., *X-linked recessive atrophic macular degeneration from RPGR mutation.* Genomics, 2002. **80**(2): p. 166-71.

123. Vervoort, R., et al., *Mutational hot spot within a new RPGR exon in X-linked retinitis pigmentosa.* Nat Genet, 2000. **25**(4): p. 462-6.

124. Meindl, A., et al., *A gene (RPGR) with homology to the RCC1 guanine nucleotide exchange factor is mutated in X-linked retinitis pigmentosa (RP3).* Nat Genet, 1996. **13**(1): p. 35-42.

125. Mavlyutov, T.A., H. Zhao, and P.A. Ferreira, *Species-specific subcellular localization of RPGR and RPGRIP isoforms: implications for the phenotypic variability of congenital retinopathies among species.* Hum Mol Genet, 2002. **11**(16): p. 1899-907.

126. Lu, X. and P.A. Ferreira, *Identification of novel murine- and human-specific RPGRIP1 splice variants with distinct expression profiles and subcellular localization.* Invest Ophthalmol Vis Sci, 2005. **46**(6): p. 1882-90.

127. Lu, X., et al., *Limited proteolysis differentially modulates the stability and subcellular localization of domains of RPGRIP1 that are distinctly affected by mutations in Leber's congenital amaurosis.* Hum Mol Genet, 2005. **14**(10): p. 1327-40.

128. Mollet, G., et al., *The gene mutated in juvenile nephronophthisis type 4 encodes a novel protein that interacts with nephrocystin.* Nat Genet, 2002. **32**(2): p. 300-5.

129. Otto, E., et al., *A gene mutated in nephronophthisis and retinitis pigmentosa encodes a novel protein, nephroretinin, conserved in evolution.* Am J Hum Genet, 2002. **71**(5): p. 1161-7.

130. Castagnet, P., et al., *RPGRIP1s with distinct neuronal localization and biochemical properties associate selectively with RanBP2 in amacrine neurons.* Hum Mol Genet, 2003. **12**(15): p. 1847-63.

131. Zhao, Y., et al., *The retinitis pigmentosa GTPase regulator (RPGR)- interacting protein: subserving RPGR function and participating in disk morphogenesis.* Proc Natl Acad Sci U S A, 2003. **100**(7): p. 3965-70.

132. Won, J., et al., *RPGRIP1 is essential for normal rod photoreceptor outer segment elaboration and morphogenesis.* Hum Mol Genet, 2009. **18**(22): p. 4329-39.

133. Patil, H., et al., *Structural and functional plasticity of subcellular tethering, targeting and processing of RPGRIP1 by RPGR isoforms.* Biol Open, 2012. **1**(2): p. 140-60.

134. Nir, I. and D.S. Papermaster, *Immunocytochemical localization of opsin in degenerating photoreceptors of RCS rats and rd and rds mice.* Prog Clin Biol Res, 1989. **314**: p. 251-64.

135. Jacobson, S.G., et al., *Leber congenital amaurosis caused by an RPGRIP1 mutation shows treatment potential.* Ophthalmology, 2007. **114**(5): p. 895-8.

136. Seong, M.W., et al., *LCA5, a rare genetic cause of leber congenital amaurosis in Koreans.* Ophthalmic Genet, 2009. **30**(1): p. 54-5.

137. Fakhratova, M., *Identification of a Novel LCA6 Mutation in an Emirati Family.* Ophthalmic Genet, 2013. **34**(4): p. 234-7.

138. Khan, A.O., et al., *The RPGRIP1-related retinal phenotype in children.* Br J Ophthalmol, 2013. **97**(6): p. 760-4.

139. Chen, Y., et al., *Comprehensive mutation analysis by whole-exome sequencing in 41 Chinese families with Leber congenital amaurosis.* Invest Ophthalmol Vis Sci, 2013. **54**(6): p. 4351-7.

140. Hameed, A., et al., *Evidence of RPGRIP1 gene mutations associated with recessive cone-rod dystrophy.* J Med Genet, 2003. **40**(8): p. 616-9.

141. Huang, L., et al., *Exome sequencing of 47 chinese families with cone-rod dystrophy: mutations in 25 known causative genes.* PLoS One, 2013. **8**(6): p. e65546.

142. Fernandez-Martinez, L., et al., *Evidence for RPGRIP1 gene as risk factor for primary open angle glaucoma.* Eur J Hum Genet, 2011. **19**(4): p. 445-51.

143. Tan, M.H., et al., *Leber congenital amaurosis associated with AIPL1: challenges in ascribing disease causation, clinical findings, and implications for gene therapy.* PLoS One, 2012. **7**(3): p. e32330.

144. Jacobson, S.G., et al., *Determining consequences of retinal membrane guanylyl cyclase (RetGC1) deficiency in human Leber congenital amaurosis en route to therapy: residual cone-photoreceptor vision correlates with biochemical properties of the mutants.* Hum Mol Genet, 2013. **22**(1): p. 168-83.

145. Cremers, F.P., J.A. van den Hurk, and A.I. den Hollander, *Molecular genetics of Leber congenital amaurosis.* Hum Mol Genet, 2002. **11**(10): p. 1169-76.

146. Cheng, C.L. and R.S. Molday, *Changes in gene expression associated with retinal degeneration in the rd3 mouse.* Mol Vis, 2013. **19**: p. 955-69.

147. Koenekoop, R.K., *RPGRIP1 is mutated in Leber congenital amaurosis: a mini-review.* Ophthalmic Genet, 2005. **26**(4): p. 175-9.

148. Li, L., et al., *Detection of variants in 15 genes in 87 unrelated Chinese patients with Leber congenital amaurosis.* PLoS One, 2011. **6**(5): p. e19458.

149. Pawlyk, B.S., et al., *Replacement gene therapy with a human RPGRIP1 sequence slows photoreceptor degeneration in a murine model of Leber congenital amaurosis.* Hum Gene Ther, 2010. **21**(8): p. 993-1004.

150. Swaroop, A., D. Kim, and D. Forrest, *Transcriptional regulation of photoreceptor development and homeostasis in the mammalian retina.* Nat Rev Neurosci, 2010. **11**(8): p. 563-76.

151. Mellersh, C.S., et al., *Canine RPGRIP1 mutation establishes cone-rod dystrophy in miniature longhaired dachshunds as a homologue of human Leber congenital amaurosis.* Genomics, 2006. **88**(3): p. 293-301.

152. Turney, C., et al., *Pathological and electrophysiological features of a canine cone-rod dystrophy in the miniature longhaired dachshund.* Invest Ophthalmol Vis Sci, 2007. **48**(9): p. 4240-9.

153. Lheriteau, E., et al., *The RPGRIP1-deficient dog, a promising canine model for gene therapy.* Mol Vis, 2009. **15**: p. 349-61.

154. Miyadera, K., et al., *Phenotypic variation and genotype-phenotype discordance in canine cone-rod dystrophy with an RPGRIP1 mutation.* Mol Vis, 2009. **15**: p. 2287-305.

155. Busse, C., et al., *Ophthalmic and cone derived electrodiagnostic findings in outbred Miniature Long-haired Dachshunds homozygous for a RPGRIP1 mutation.* Vet Ophthalmol, 2011. **14**(3): p. 146-52.

156. Narfstrom, K., et al., *Assessment of hereditary retinal degeneration in the English springer spaniel dog and disease relationship to an RPGRIP1 mutation.* Stem Cells Int, 2012. **2012**: p. 685901.

157. Kuznetsova, T., et al., *Exclusion of RPGRIP1 ins44 from primary causal association with early-onset cone-rod dystrophy in dogs.* Invest Ophthalmol Vis Sci, 2012. **53**(9): p. 5486-501.

158. Miyadera, K., et al., *Genome-wide association study in RPGRIP1(-/-) dogs identifies a modifier locus that determines the onset of retinal degeneration.* Mamm Genome, 2012. **23**(1-2): p. 212-23.

159. Miyadera, K., et al., *Multiple mechanisms contribute to leakiness of a frameshift mutation in canine cone-rod dystrophy.* PLoS One, 2012. **7**(12): p. e51598.

160. Kuznetsova, T., et al., *Structural organization and expression pattern of the canine RPGRIP1 isoforms in retinal tissue.* Invest Ophthalmol Vis Sci, 2011. **52**(6): p. 2989-98.

161. Applebury, M.L., et al., *The murine cone photoreceptor: a single cone type expresses both S and M opsins with retinal spatial patterning.* Neuron, 2000. **27**(3): p. 513-23.

162. Rohlich, P., T. van Veen, and A. Szel, *Two different visual pigments in one retinal cone cell.* Neuron, 1994. **13**(5): p. 1159-66.

163. Bobu, C., et al., *Photoreceptor organisation and phenotypic characterization in retinas of two diurnal rodent species: potential use as experimental animal models for human vision research.* Vision Res, 2008. **48**(3): p. 424-32.

164. Gaillard, F., et al., *Retinal anatomy and visual performance in a diurnal cone-rich laboratory rodent, the Nile grass rat (Arvicanthis niloticus).* J Comp Neurol, 2008. **510**(5): p. 525-38.

165. Ortin-Martinez, A., et al., *Automated quantification and topographical distribution of the whole population of S- and L-cones in adult albino and pigmented rats.* Invest Ophthalmol Vis Sci, 2010. **51**(6): p. 3171-83.

166. Stieger, K., et al., *AAV-mediated gene therapy for retinal disorders in large animal models.* ILAR J, 2009. **50**(2): p. 206-24.

167. Kemp, C.M. and S.G. Jacobson, *Rhodopsin levels in the central retinas of normal miniature poodles and those with progressive rod-cone degeneration.* Exp Eye Res, 1992. **54**(6): p. 947-56.

168. Mowat, F.M., et al., *Topographical characterization of cone photoreceptors and the area centralis of the canine retina.* Mol Vis, 2008. **14**: p. 2518-27.

169. Ahnelt, P.K. and H. Kolb, *The mammalian photoreceptor mosaic-adaptive design.* Prog Retin Eye Res, 2000. **19**(6): p. 711-77.

170. Mancuso, K., et al., *Gene therapy for red-green colour blindness in adult primates.* Nature, 2009. **461**(7265): p. 784-7.

171. Ollivier, F.J., et al., *Comparative morphology of the tapetum lucidum (among selected species).* Vet Ophthalmol, 2004. **7**(1): p. 11-22.

172. Petters, R.M., et al., *Genetically engineered large animal model for studying cone photoreceptor survival and degeneration in retinitis pigmentosa.* Nat Biotechnol, 1997. **15**(10): p. 965-70.

173. Li, Z.Y., et al., *Rhodopsin transgenic pigs as a model for human retinitis pigmentosa.* Invest Ophthalmol Vis Sci, 1998. **39**(5): p. 808-19.

174. Ross, J.W., et al., *Generation of an inbred miniature pig model of retinitis pigmentosa.* Invest Ophthalmol Vis Sci, 2012. **53**(1): p. 501-7.

175. Reicher, S., E. Seroussi, and E. Gootwine, *A mutation in gene CNGA3 is associated with day blindness in sheep.* Genomics, 2010. **95**(2): p. 101-4.

176. Narfstrom, K., *Progressive retinal atrophy in the Abyssinian cat. Clinical characteristics.* Invest Ophthalmol Vis Sci, 1985. **26**(2): p. 193-200.

177. Rah, H., et al., *Early-onset, autosomal recessive, progressive retinal atrophy in Persian cats.* Invest Ophthalmol Vis Sci, 2005. **46**(5): p. 1742-7.

178. Miyadera, K., G.M. Acland, and G.D. Aguirre, *Genetic and phenotypic variations of inherited retinal diseases in dogs: the power of within- and across-breed studies.* Mamm Genome, 2012. **23**(1-2): p. 40-61.

179. Chang, G.Q., Y. Hao, and F. Wong, *Apoptosis: final common pathway of photoreceptor death in rd, rds, and rhodopsin mutant mice.* Neuron, 1993. **11**(4): p. 595-605.

180. Jomary, C., M.J. Neal, and S.E. Jones, *Characterization of cell death pathways in murine retinal neurodegeneration implicates cytochrome c release, caspase activation, and bid cleavage.* Mol Cell Neurosci, 2001. **18**(4): p. 335-46.

181. Donovan, M. and T.G. Cotter, *Caspase-independent photoreceptor apoptosis in vivo and differential expression of apoptotic protease activating factor-1 and caspase-3 during retinal development.* Cell Death Differ, 2002. **9**(11): p. 1220-31.

182. Donovan, M., F. Doonan, and T.G. Cotter, *Decreased expression of pro-apoptotic Bcl-2 family members during retinal development and differential sensitivity to cell death.* Dev Biol, 2006. **291**(1): p. 154-69.

183. Bramall, A.N., et al., *The genomic, biochemical, and cellular responses of the retina in inherited photoreceptor degenerations and prospects for the treatment of these disorders.* Annu Rev Neurosci, 2010. **33**: p. 441-72.

184. Doonan, F., M. Donovan, and T.G. Cotter, *Caspase-independent photoreceptor apoptosis in mouse models of retinal degeneration.* J Neurosci, 2003. **23**(13): p. 5723-31.

185. Yoshizawa, K., et al., *Caspase-3 inhibitor transiently delays inherited retinal degeneration in C3H mice carrying the rd gene.* Graefes Arch Clin Exp Ophthalmol, 2002. **240**(3): p. 214-9.

186. Zeiss, C.J., J. Neal, and E.A. Johnson, *Caspase-3 in postnatal retinal development and degeneration.* Invest Ophthalmol Vis Sci, 2004. **45**(3): p. 964-70.

187. Doonan, F., M. Donovan, and T.G. Cotter, *Activation of multiple pathways during photoreceptor apoptosis in the rd mouse.* Invest Ophthalmol Vis Sci, 2005. **46**(10): p. 3530-8.

188. Paquet-Durand, F., et al., *Calpain is activated in degenerating photoreceptors in the rd1 mouse.* J Neurochem, 2006. **96**(3): p. 802-14.

189. Sanges, D., et al., *Apoptosis in retinal degeneration involves cross-talk between apoptosis-inducing factor (AIF) and caspase-12 and is blocked by calpain inhibitors.* Proc Natl Acad Sci U S A, 2006. **103**(46): p. 17366-71.

190. Paquet-Durand, F., L. Johnson, and P. Ekstrom, *Calpain activity in retinal degeneration.* J Neurosci Res, 2007. **85**(4): p. 693-702.

191. Sancho-Pelluz, J., et al., *Photoreceptor cell death mechanisms in inherited retinal degeneration.* Mol Neurobiol, 2008. **38**(3): p. 253-69.

192. Lohr, H.R., et al., *Multiple, parallel cellular suicide mechanisms participate in photoreceptor cell death.* Exp Eye Res, 2006. **83**(2): p. 380-9.

193. Rohrer, B., et al., *Multidestructive pathways triggered in photoreceptor cell death of the rd mouse as determined through gene expression profiling.* J Biol Chem, 2004. **279**(40): p. 41903-10.

194. Punzo, C. and C. Cepko, *Cellular responses to photoreceptor death in the rd1 mouse model of retinal degeneration.* Invest Ophthalmol Vis Sci, 2007. **48**(2): p. 849-57.

195. Murakami, Y., et al., *Receptor interacting protein kinase mediates necrotic cone but not rod cell death in a mouse model of inherited degeneration.* Proc Natl Acad Sci U S A, 2012. **109**(36): p. 14598-603.

196. Paquet-Durand, F., et al., *A key role for cyclic nucleotide gated (CNG) channels in cGMP-related retinitis pigmentosa.* Hum Mol Genet, 2011. **20**(5): p. 941-7.

197. Paquet-Durand, F., et al., *PKG activity causes photoreceptor cell death in two retinitis pigmentosa models.* J Neurochem, 2009. **108**(3): p. 796-810.

198. Xu, J., et al., *cGMP Accumulation Causes Photoreceptor Degeneration in CNG Channel Deficiency: Evidence of cGMP Cytotoxicity Independently of Enhanced CNG Channel Function.* J Neurosci, 2013. **33**(37): p. 14939-48.

199. Lincoln, T.M. and T.L. Cornwell, *Intracellular cyclic GMP receptor proteins.* FASEB J, 1993. **7**(2): p. 328-38.

200. Ramamurthy, V., et al., *Leber congenital amaurosis linked to AIPL1: a mouse model reveals destabilization of cGMP phosphodiesterase.* Proc Natl Acad Sci U S A, 2004. **101**(38): p. 13897-902.

201. Woodruff, M.L., et al., *Constitutive excitation by Gly90Asp rhodopsin rescues rods from degeneration caused by elevated production of cGMP in the dark.* J Neurosci, 2007. **27**(33): p. 8805-15.

202. Trifunovic, D., et al., *cGMP-dependent cone photoreceptor degeneration in the cpfl1 mouse retina.* J Comp Neurol, 2010. **518**(17): p. 3604-17.

203. Robinson, P.R., et al., *Constitutively active mutants of rhodopsin.* Neuron, 1992. **9**(4): p. 719-25.

204. McAlear, S.D., T.W. Kraft, and A.K. Gross, *1 rhodopsin mutations in congenital night blindness.* Adv Exp Med Biol, 2010. **664**: p. 263-72.

205. Rohrer, B., et al., *Correlation of regenerable opsin with rod ERG signal in Rpe65-/- mice during development and aging.* Invest Ophthalmol Vis Sci, 2003. **44**(1): p. 310-5.

206. Woodruff, M.L., et al., *Spontaneous activity of opsin apoprotein is a cause of Leber congenital amaurosis.* Nat Genet, 2003. **35**(2): p. 158-64.

207. Fan, J., et al., *Opsin activation of transduction in the rods of dark-reared Rpe65 knockout mice.* J Physiol, 2005. **568**(Pt 1): p. 83-95.

208. Fernandes, R., K. Hosoya, and P. Pereira, *Reactive oxygen species downregulate glucose transport system in retinal endothelial cells.* Am J Physiol Cell Physiol, 2011. **300**(4): p. C927-36.

209. Holz, F.G., et al., *Inhibition of lysosomal degradative functions in RPE cells by a retinoid component of lipofuscin.* Invest Ophthalmol Vis Sci, 1999. **40**(3): p. 737-43.

210. Ma, H., et al., *Loss of cone cyclic nucleotide-gated channel leads to alterations in light response modulating system and cellular stress response pathways: a gene expression profiling study.* Hum Mol Genet, 2013. **22**(19): p. 3906-19.

211. Lem, J. and G.L. Fain, *Constitutive opsin signaling: night blindness or retinal degeneration?* Trends Mol Med, 2004. **10**(4): p. 150-7.

212. Samardzija, M., et al., *R91W mutation in Rpe65 leads to milder early-onset retinal dystrophy due to the generation of low levels of 11-cis-retinal.* Hum Mol Genet, 2008. **17**(2): p. 281-92.

213. Lorenz, B., et al., *A comprehensive clinical and biochemical functional study of a novel RPE65 hypomorphic mutation.* Invest Ophthalmol Vis Sci, 2008. **49**(12): p. 5235-42.

214. Chen, C.K., et al., *Abnormal photoresponses and light-induced apoptosis in rods lacking rhodopsin kinase.* Proc Natl Acad Sci U S A, 1999. **96**(7): p. 3718-22.

215. Xu, J., et al., *Prolonged photoresponses in transgenic mouse rods lacking arrestin.* Nature, 1997. **389**(6650): p. 505-9.

216. Cideciyan, A.V., et al., *Null mutation in the rhodopsin kinase gene slows recovery kinetics of rod and cone phototransduction in man.* Proc Natl Acad Sci U S A, 1998. **95**(1): p. 328-33.

217. Fuchs, S., et al., *A homozygous 1-base pair deletion in the arrestin gene is a frequent cause of Oguchi disease in Japanese.* Nat Genet, 1995. **10**(3): p. 360-2.

218. Perusek, L. and T. Maeda, *Vitamin A derivatives as treatment options for retinal degenerative diseases.* Nutrients, 2013. **5**(7): p. 2646-66.

219. Van Hooser, J.P., et al., *Rapid restoration of visual pigment and function with oral retinoid in a mouse model of childhood blindness.* Proc Natl Acad Sci U S A, 2000. **97**(15): p. 8623-8.

220. Ablonczy, Z., et al., *11-cis-retinal reduces constitutive opsin phosphorylation and improves quantum catch in retinoid-deficient mouse rod photoreceptors.* J Biol Chem, 2002. **277**(43): p. 40491-8.

221. Gearhart, P.M., et al., *Improvement of visual performance with intravitreal administration of 9-cis-retinal in Rpe65-mutant dogs.* Arch Ophthalmol, 2010. **128**(11): p. 1442-8.

222. Pierce, E.A., *Pathways to photoreceptor cell death in inherited retinal degenerations.* Bioessays, 2001. **23**(7): p. 605-18.

223. Fariss, R.N., et al., *Evidence from normal and degenerating photoreceptors that two outer segment integral membrane proteins have separate transport pathways.* J Comp Neurol, 1997. **387**(1): p. 148-56.

224. Linberg, K.A., et al., *Experimental retinal detachment in the cone-dominant ground squirrel retina: morphology and basic immunocytochemistry.* Vis Neurosci, 2002. **19**(5): p. 603-19.

225. Alfinito, P.D. and E. Townes-Anderson, *Activation of mislocalized opsin kills rod cells: a novel mechanism for rod cell death in retinal disease.* Proc Natl Acad Sci U S A, 2002. **99**(8): p. 5655-60.

226. Deretic, D., *A role for rhodopsin in a signal transduction cascade that regulates membrane trafficking and photoreceptor polarity.* Vision Res, 2006. **46**(27): p. 4427-33.

227. Green, E.S., et al., *Characterization of rhodopsin mis-sorting and constitutive activation in a transgenic rat model of retinitis pigmentosa.* Invest Ophthalmol Vis Sci, 2000. **41**(6): p. 1546-53.

228. Gorbatyuk, M. and O. Gorbatyuk, *Review: Retinal degeneration: Focus on the unfolded protein response.* Mol Vis, 2013. **19**: p. 1985-xxx.

229. Vlachantoni, D., et al., *Evidence of severe mitochondrial oxidative stress and a protective effect of low oxygen in mouse models of inherited photoreceptor degeneration.* Hum Mol Genet, 2011. **20**(2): p. 322-35.

230. Yang, L.P., et al., *Activation of endoplasmic reticulum stress in degenerating photoreceptors of the rd1 mouse.* Invest Ophthalmol Vis Sci, 2007. **48**(11): p. 5191-8.

231. Michalakis, S., et al., *Impaired opsin targeting and cone photoreceptor migration in the retina of mice lacking the cyclic nucleotide-gated channel CNGA3.* Invest Ophthalmol Vis Sci, 2005. **46**(4): p. 1516-24.

232. Thapa, A., et al., *Endoplasmic reticulum stress-associated cone photoreceptor degeneration in cyclic nucleotide-gated channel deficiency.* J Biol Chem, 2012. **287**(22): p. 18018-29.

233. Duricka, D.L., R.L. Brown, and M.D. Varnum, *Defective trafficking of cone photoreceptor CNG channels induces the unfolded protein response and ER-stress-associated cell death.* Biochem J, 2012. **441**(2): p. 685-96.

234. Zhang, T., et al., *Cone opsin determines the time course of cone photoreceptor degeneration in Leber congenital amaurosis.* Proc Natl Acad Sci U S A, 2011. **108**(21): p. 8879-84.

235. Zhang, T. and Y. Fu, *A Phe-rich region in short-wavelength sensitive opsins is responsible for their aggregation in the absence of 11-cis-retinal.* FEBS Lett, 2013. **587**(15): p. 2430-4.

236. Jacobson, S.G., et al., *Human cone photoreceptor dependence on RPE65 isomerase.* Proc Natl Acad Sci U S A, 2007. **104**(38): p. 15123-8.

237. Lorenz, B., et al., *Chromatic pupillometry dissects function of the three different light-sensitive retinal cell populations in RPE65 deficiency.* Invest Ophthalmol Vis Sci, 2012. **53**(9): p. 5641-52.

238. Clarke, G., C.J. Lumsden, and R.R. McInnes, *Inherited neurodegenerative diseases: the one-hit model of neurodegeneration.* Hum Mol Genet, 2001. **10**(20): p. 2269-75.

239. Pacione, L.R., et al., *Progress toward understanding the genetic and biochemical mechanisms of inherited photoreceptor degenerations.* Annu Rev Neurosci, 2003. **26**: p. 657-700.

240. Milam, A.H., Z.Y. Li, and R.N. Fariss, *Histopathology of the human retina in retinitis pigmentosa.* Prog Retin Eye Res, 1998. **17**(2): p. 175-205.

241. Cideciyan, A.V., et al., *Disease sequence from mutant rhodopsin allele to rod and cone photoreceptor degeneration in man.* Proc Natl Acad Sci U S A, 1998. **95**(12): p. 7103-8.

242. Jacobson, S.G., et al., *Disease expression of RP1 mutations causing autosomal dominant retinitis pigmentosa.* Invest Ophthalmol Vis Sci, 2000. **41**(7): p. 1898-908.

243. Jacobson, S.G., et al., *Photoreceptor layer topography in children with leber congenital amaurosis caused by RPE65 mutations.* Invest Ophthalmol Vis Sci, 2008. **49**(10): p. 4573-7.

244. Clarke, G. and C.J. Lumsden, *Heterogeneous cellular environments modulate one-hit neuronal death kinetics.* Brain Res Bull, 2005. **65**(1): p. 59-67.

245. Bringmann, A., et al., *Muller cells in the healthy and diseased retina.* Prog Retin Eye Res, 2006. **25**(4): p. 397-424.

246. Garcia-Ayuso, D., et al., *Changes in the Photoreceptor Mosaic of P23H-1 Rats During Retinal Degeneration: Implications for Rod-Cone Dependent Survival.* Invest Ophthalmol Vis Sci, 2013. **54**(8): p. 5888-900.

247. Ji, Y., et al., *Rearrangement of the cone mosaic in the retina of the rat model of retinitis pigmentosa.* J Comp Neurol, 2012. **520**(4): p. 874-88.

248. Piano, I., et al., *Cone survival and preservation of visual acuity in an animal model of retinal degeneration.* Eur J Neurosci, 2013. **37**(11): p. 1853-62.

249. Michaelides, M., et al., *Progressive cone and cone-rod dystrophies: phenotypes and underlying molecular genetic basis.* Surv Ophthalmol, 2006. **51**(3): p. 232-58.

250. Michaelides, M., D.M. Hunt, and A.T. Moore, *The cone dysfunction syndromes.* Br J Ophthalmol, 2004. **88**(2): p. 291-7.

251. Huang, P.C., et al., *Cellular interactions implicated in the mechanism of photoreceptor degeneration in transgenic mice expressing a mutant rhodopsin gene.* Proc Natl Acad Sci U S A, 1993. **90**(18): p. 8484-8.

252. Kedzierski, W., D. Bok, and G.H. Travis, *Non-cell-autonomous photoreceptor degeneration in rds mutant mice mosaic for expression of a rescue transgene.* J Neurosci, 1998. **18**(11): p. 4076-82.

253. Bush, R.A., K.W. Hawks, and P.A. Sieving, *Preservation of inner retinal responses in the aged Royal College of Surgeons rat. Evidence against glutamate excitotoxicity in photoreceptor degeneration.* Invest Ophthalmol Vis Sci, 1995. **36**(10): p. 2054-62.

254. Strettoi, E., et al., *Morphological and functional abnormalities in the inner retina of the rd/rd mouse.* J Neurosci, 2002. **22**(13): p. 5492-504.

255. Ripps, H., *Cell death in retinitis pigmentosa: gap junctions and the 'bystander' effect.* Exp Eye Res, 2002. **74**(3): p. 327-36.

256. Kranz, K., et al., *Testing for a gap junction-mediated bystander effect in retinitis pigmentosa: secondary cone death is not altered by deletion of connexin36 from cones.* PLoS One, 2013. **8**(2): p. e57163.

257. Mohand-Said, S., et al., *Photoreceptor transplants increase host cone survival in the retinal degeneration (rd) mouse.* Ophthalmic Res, 1997. **29**(5): p. 290-7.

258. Mohand-Said, S., et al., *Selective transplantation of rods delays cone loss in a retinitis pigmentosa model.* Arch Ophthalmol, 2000. **118**(6): p. 807-11.

259. Mohand-Said, S., et al., *Normal retina releases a diffusible factor stimulating cone survival in the retinal degeneration mouse.* Proc Natl Acad Sci U S A, 1998. **95**(14): p. 8357-62.

260. Fintz, A.C., et al., *Partial characterization of retina-derived cone neuroprotection in two culture models of photoreceptor degeneration.* Invest Ophthalmol Vis Sci, 2003. **44**(2): p. 818-25.

261. Leveillard, T., et al., *Identification and characterization of rod-derived cone viability factor.* Nat Genet, 2004. **36**(7): p. 755-9.

262. Yang, Y., et al., *Functional cone rescue by RdCVF protein in a dominant model of retinitis pigmentosa.* Mol Ther, 2009. **17**(5): p. 787-95.

263. Cronin, T., et al., *The disruption of the rod-derived cone viability gene leads to photoreceptor dysfunction and susceptibility to oxidative stress.* Cell Death Differ, 2010. **17**(7): p. 1199-210.

264. Fridlich, R., et al., *The thioredoxin-like protein rod-derived cone viability factor (RdCVFL) interacts with TAU and inhibits its phosphorylation in the retina.* Mol Cell Proteomics, 2009. **8**(6): p. 1206-18.

265. Leveillard, T. and J.A. Sahel, *Rod-derived cone viability factor for treating blinding diseases: from clinic to redox signaling.* Sci Transl Med, 2010. **2**(26): p. 26ps16.

266. Jaillard, C., et al., *Nxnl2 splicing results in dual functions in neuronal cell survival and maintenance of cell integrity.* Hum Mol Genet, 2012. **21**(10): p. 2298-311.

267. Stearns, G., et al., *A mutation in the cone-specific pde6 gene causes rapid cone photoreceptor degeneration in zebrafish.* J Neurosci, 2007. **27**(50): p. 13866-74.

268. Cideciyan, A.V., et al., *Human retinal gene therapy for Leber congenital amaurosis shows advancing retinal degeneration despite enduring visual improvement.* Proc Natl Acad Sci U S A, 2013. **110**(6): p. E517-25.

269. Marc, R.E. and D. Cameron, *A molecular phenotype atlas of the zebrafish retina.* J Neurocytol, 2001. **30**(7): p. 593-654.

270. Ogilvie, J.M., et al., *Age-related distribution of cones and ON-bipolar cells in the rd mouse retina.* Curr Eye Res, 1997. **16**(3): p. 244-51.

271. Yu, D.Y., et al., *Intraretinal oxygen levels before and after photoreceptor loss in the RCS rat.* Invest Ophthalmol Vis Sci, 2000. **41**(12): p. 3999-4006.

272. Yu, D.Y., et al., *Photoreceptor death, trophic factor expression, retinal oxygen status, and photoreceptor function in the P23H rat.* Invest Ophthalmol Vis Sci, 2004. **45**(6): p. 2013-9.

273. Yamada, H., et al., *Fibroblast growth factor-2 decreases hyperoxia-induced photoreceptor cell death in mice.* Am J Pathol, 2001. **159**(3): p. 1113-20.

274. Okoye, G., et al., *Increased expression of brain-derived neurotrophic factor preserves retinal function and slows cell death from rhodopsin mutation or oxidative damage.* J Neurosci, 2003. **23**(10): p. 4164-72.

275. Shen, J., et al., *Oxidative damage is a potential cause of cone cell death in retinitis pigmentosa.* J Cell Physiol, 2005. **203**(3): p. 457-64.

276. Komeima, K., et al., *Antioxidants reduce cone cell death in a model of retinitis pigmentosa.* Proc Natl Acad Sci U S A, 2006. **103**(30): p. 11300-5.

277. Usui, S., et al., *Increased expression of catalase and superoxide dismutase 2 reduces cone cell death in retinitis pigmentosa.* Mol Ther, 2009. **17**(5): p. 778-86.

278. Usui, S., et al., *Overexpression of SOD in retina: need for increase in H2O2-detoxifying enzyme in same cellular compartment.* Free Radic Biol Med, 2011. **51**(7): p. 1347-54.

279. Usui, S., et al., *NADPH oxidase plays a central role in cone cell death in retinitis pigmentosa.* J Neurochem, 2009. **110**(3): p. 1028-37.

280. Szamier, R.B. and E.L. Berson, *Histopathologic study of an unusual form of retinitis pigmentosa.* Invest Ophthalmol Vis Sci, 1982. **22**(5): p. 559-70.

281. Smith, A.J., J.W. Bainbridge, and R.R. Ali, *Gene supplementation therapy for recessive forms of inherited retinal dystrophies.* Gene Ther, 2012. **19**(2): p. 154-61.

282. Colella, P. and A. Auricchio, *Gene therapy of inherited retinopathies: a long and successful road from viral vectors to patients.* Hum Gene Ther, 2012. **23**(8): p. 796-807.

283. McClements, M.E. and R.E. MacLaren, *Gene therapy for retinal disease.* Transl Res, 2013. **161**(4): p. 241-54.

284. Boye, S.E., et al., *A comprehensive review of retinal gene therapy.* Mol Ther, 2013. **21**(3): p. 509-19.

285. Busskamp, V., et al., *Optogenetic therapy for retinitis pigmentosa.* Gene Ther, 2012. **19**(2): p. 169-75.

286. Farrar, G.J., P.F. Kenna, and P. Humphries, *On the genetics of retinitis pigmentosa and on mutation-independent approaches to therapeutic intervention.* EMBO J, 2002. **21**(5): p. 857-64.

287. Cepko, C.L., *Emerging gene therapies for retinal degenerations.* J Neurosci, 2012. **32**(19): p. 6415-20.

288. Trifunovic, D., et al., *Neuroprotective strategies for the treatment of inherited photoreceptor degeneration.* Curr Mol Med, 2012. **12**(5): p. 598-612.

289. Sahel, J.A. and B. Roska, *Gene therapy for blindness.* Annu Rev Neurosci, 2013. **36**: p. 467-88.

290. Marigo, V., *Programmed cell death in retinal degeneration: targeting apoptosis in photoreceptors as potential therapy for retinal degeneration.* Cell Cycle, 2007. **6**(6): p. 652-5.

291. Lagali, P.S., et al., *Light-activated channels targeted to ON bipolar cells restore visual function in retinal degeneration.* Nat Neurosci, 2008. **11**(6): p. 667-75.

292. Doroudchi, M.M., et al., *Virally delivered channelrhodopsin-2 safely and effectively restores visual function in multiple mouse models of blindness.* Mol Ther, 2011. **19**(7): p. 1220-9.

293. Bi, A., et al., *Ectopic expression of a microbial-type rhodopsin restores visual responses in mice with photoreceptor degeneration.* Neuron, 2006. **50**(1): p. 23-33.

294. Tomita, H., et al., *Visual properties of transgenic rats harboring the channelrhodopsin-2 gene regulated by the thy-1.2 promoter.* PLoS One, 2009. **4**(11): p. e7679.

295. Tomita, H., et al., *Channelrhodopsin-2 gene transduced into retinal ganglion cells restores functional vision in genetically blind rats.* Exp Eye Res, 2010. **90**(3): p. 429-36.

296. Zhang, Y., et al., *Ectopic expression of multiple microbial rhodopsins restores ON and OFF light responses in retinas with photoreceptor degeneration.* J Neurosci, 2009. **29**(29): p. 9186-96.

297. Thyagarajan, S., et al., *Visual function in mice with photoreceptor degeneration and transgenic expression of channelrhodopsin 2 in ganglion cells.* J Neurosci, 2010. **30**(26): p. 8745-58.

298. Caporale, N., et al., *LiGluR restores visual responses in rodent models of inherited blindness.* Mol Ther, 2011. **19**(7): p. 1212-9.

299. Polosukhina, A., et al., *Photochemical restoration of visual responses in blind mice.* Neuron, 2012. **75**(2): p. 271-82.

300. Wu, C., et al., *rAAV-mediated subcellular targeting of optogenetic tools in retinal ganglion cells in vivo.* PLoS One, 2013. **8**(6): p. e66332.

301. Rex, T.S., et al., *Systemic but not intraocular Epo gene transfer protects the retina from light-and genetic-induced degeneration.* Mol Ther, 2004. **10**(5): p. 855-61.

302. Chen, B. and C.L. Cepko, *HDAC4 regulates neuronal survival in normal and diseased retinas.* Science, 2009. **323**(5911): p. 256-9.

303. Farrar, G.J., et al., *Gene-based therapies for dominantly inherited retinopathies.* Gene Ther, 2012. **19**(2): p. 137-44.

304. Rossmiller, B., H. Mao, and A.S. Lewin, *Gene therapy in animal models of autosomal dominant retinitis pigmentosa.* Mol Vis, 2012. **18**: p. 2479-96.

305. Fradot, M., et al., *Gene therapy in ophthalmology: validation on cultured retinal cells and explants from postmortem human eyes.* Hum Gene Ther, 2011. **22**(5): p. 587-93.

306. Baba, Y., et al., *In vitro cell subtype-specific transduction of adeno-associated virus in mouse and marmoset retinal explant culture.* Biochimie, 2012. **94**(12): p. 2716-22.

307. Dalkara, D., et al., *Inner limiting membrane barriers to AAV-mediated retinal transduction from the vitreous.* Mol Ther, 2009. **17**(12): p. 2096-102.

308. Han, Z., et al., *DNA nanoparticle-mediated ABCA4 delivery rescues Stargardt dystrophy in mice.* J Clin Invest, 2012. **122**(9): p. 3221-6.

309. Koirala, A., S.M. Conley, and M.I. Naash, *A review of therapeutic prospects of non-viral gene therapy in the retinal pigment epithelium.* Biomaterials, 2013. **34**(29): p. 7158-67.

310. Koirala, A., et al., *Persistence of non-viral vector mediated RPE65 expression: Case for viability as a gene transfer therapy for RPE-based diseases.* J Control Release, 2013.

311. Pang, J., et al., *Adenoviral-mediated gene transfer to retinal explants during development and degeneration.* Exp Eye Res, 2004. **79**(2): p. 189-201.

312. Bennett, J., et al., *Photoreceptor cell rescue in retinal degeneration (rd) mice by in vivo gene therapy.* Nat Med, 1996. **2**(6): p. 649-54.

313. Kumar-Singh, R. and D.B. Farber, *Encapsidated adenovirus mini-chromosome-mediated delivery of genes to the retina: application to the rescue of photoreceptor degeneration.* Hum Mol Genet, 1998. **7**(12): p. 1893-900.

314. Cashman, S.M., L. McCullough, and R. Kumar-Singh, *Improved retinal transduction in vivo and photoreceptor-specific transgene expression using adenovirus vectors with modified penton base.* Mol Ther, 2007. **15**(9): p. 1640-6.

315. Sweigard, J.H., S.M. Cashman, and R. Kumar-Singh, *Adenovirus vectors targeting distinct cell types in the retina.* Invest Ophthalmol Vis Sci, 2010. **51**(4): p. 2219-28.

316. Valverde, D., et al., *A novel mutation in exon 17 of the beta-subunit of rod phosphodiesterase in two RP sisters of a consanguineous family.* Hum Genet, 1996. **97**(1): p. 35-8.

317. Pang, J., et al., *Efficiency of lentiviral transduction during development in normal and rd mice.* Mol Vis, 2006. **12**: p. 756-67.

318. Bemelmans, A.P., et al., *Lentiviral gene transfer-mediated cone vision restoration in RPE65 knockout mice.* Adv Exp Med Biol, 2008. **613**: p. 89-95.

319. Tschernutter, M., et al., *Long-term preservation of retinal function in the RCS rat model of retinitis pigmentosa following lentivirus-mediated gene therapy.* Gene Ther, 2005. **12**(8): p. 694-701.

320. Bemelmans, A.P., et al., *Retinal cell type expression specificity of HIV-1-derived gene transfer vectors upon subretinal injection in the adult rat: influence of pseudotyping and promoter.* J Gene Med, 2005. **7**(10): p. 1367-74.

321. Bainbridge, J.W., M.H. Tan, and R.R. Ali, *Gene therapy progress and prospects: the eye.* Gene Ther, 2006. **13**(16): p. 1191-7.

322. Balaggan, K.S., et al., *Stable and efficient intraocular gene transfer using pseudotyped EIAV lentiviral vectors.* J Gene Med, 2006. **8**(3): p. 275-85.

323. Kong, J., et al., *Correction of the disease phenotype in the mouse model of Stargardt disease by lentiviral gene therapy.* Gene Ther, 2008. **15**(19): p. 1311-20.

324. Vandenberghe, L.H. and A. Auricchio, *Novel adeno-associated viral vectors for retinal gene therapy.* Gene Ther, 2012. **19**(2): p. 162-8.

325. Kreppel, F., et al., *Long-term transgene expression in the RPE after gene transfer with a high-capacity adenoviral vector.* Invest Ophthalmol Vis Sci, 2002. **43**(6): p. 1965-70.

326. Mussolino, C., et al., *AAV-mediated photoreceptor transduction of the pig cone-enriched retina.* Gene Ther, 2011. **18**(7): p. 637-45.

327. Stieger, K., et al., *Adeno-associated virus mediated gene therapy for retinal degenerative diseases.* Methods Mol Biol, 2011. **807**: p. 179-218.

328. Yang, G.S., et al., *Virus-mediated transduction of murine retina with adeno-associated virus: effects of viral capsid and genome size.* J Virol, 2002. **76**(15): p. 7651-60.

329. Weber, M., et al., *Recombinant adeno-associated virus serotype 4 mediates unique and exclusive long-term transduction of retinal pigmented epithelium in rat, dog, and nonhuman primate after subretinal delivery.* Mol Ther, 2003. **7**(6): p. 774-81.

330. Bello, A., et al., *Isolation and evaluation of novel adeno-associated virus sequences from porcine tissues.* Gene Ther, 2009. **16**(11): p. 1320-8.

331. Puppo, A., et al., *Recombinant vectors based on porcine adeno-associated viral serotypes transduce the murine and pig retina.* PLoS One, 2013. **8**(3): p. e59025.

332. Charbel Issa, P., et al., *Assessment of tropism and effectiveness of new primate-derived hybrid recombinant AAV serotypes in the mouse and primate retina.* PLoS One, 2013. **8**(4): p. e60361.

333. Auricchio, A., et al., *Exchange of surface proteins impacts on viral vector cellular specificity and transduction characteristics: the retina as a model.* Hum Mol Genet, 2001. **10**(26): p. 3075-81.

334. Le Meur, G., et al., *Postsurgical assessment and long-term safety of recombinant adeno-associated virus-mediated gene transfer into the retinas of dogs and primates.* Arch Ophthalmol, 2005. **123**(4): p. 500-6.

335. Lotery, A.J., et al., *Adeno-associated virus type 5: transduction efficiency and cell-type specificity in the primate retina.* Hum Gene Ther, 2003. **14**(17): p. 1663-71.

336. Vandenberghe, L.H., et al., *Dosage thresholds for AAV2 and AAV8 photoreceptor gene therapy in monkey.* Sci Transl Med, 2011. **3**(88): p. 88ra54.

337. Allocca, M., et al., *Novel adeno-associated virus serotypes efficiently transduce murine photoreceptors.* J Virol, 2007. **81**(20): p. 11372-80.

338. Boye, S.E., et al., *The human rhodopsin kinase promoter in an AAV5 vector confers rod- and cone-specific expression in the primate retina.* Hum Gene Ther, 2012. **23**(10): p. 1101-15.

339. Bennett, J., et al., *Cross-species comparison of in vivo reporter gene expression after recombinant adeno-associated virus-mediated retinal transduction.* Methods Enzymol, 2000. **316**: p. 777-89.

340. Hellstrom, M., et al., *Cellular tropism and transduction properties of seven adeno-associated viral vector serotypes in adult retina after intravitreal injection.* Gene Ther, 2009. **16**(4): p. 521-32.

341. Petrs-Silva, H., et al., *High-efficiency transduction of the mouse retina by tyrosine-mutant AAV serotype vectors.* Mol Ther, 2009. **17**(3): p. 463-71.

342. Petrs-Silva, H., et al., *Novel properties of tyrosine-mutant AAV2 vectors in the mouse retina.* Mol Ther, 2011. **19**(2): p. 293-301.

343. Dalkara, D., et al., *In vivo-directed evolution of a new adeno-associated virus for therapeutic outer retinal gene delivery from the vitreous.* Sci Transl Med, 2013. **5**(189): p. 189ra76.

344. Maguire, A.M., et al., *Age-dependent effects of RPE65 gene therapy for Leber's congenital amaurosis: a phase 1 dose-escalation trial.* Lancet, 2009. **374**(9701): p. 1597-605.

345. Beltran, W.A., et al., *rAAV2/5 gene-targeting to rods:dose-dependent efficiency and complications associated with different promoters.* Gene Ther, 2010. **17**(9): p. 1162-74.

346. Komaromy, A.M., et al., *Gene therapy rescues cone function in congenital achromatopsia.* Hum Mol Genet, 2010. **19**(13): p. 2581-93.

347. Beltran, W.A., et al., *Gene therapy rescues photoreceptor blindness in dogs and paves the way for treating human X-linked retinitis pigmentosa.* Proc Natl Acad Sci U S A, 2012. **109**(6): p. 2132-7.

348. Lheriteau, E., et al., *Successful Gene Therapy in the RPGRIP1-deficient Dog: a Large Model of Cone-Rod Dystrophy.* Mol Ther, 2013.

349. Dudus, L., et al., *Persistent transgene product in retina, optic nerve and brain after intraocular injection of rAAV.* Vision Res, 1999. **39**(15): p. 2545-53.

350. Provost, N., et al., *Biodistribution of rAAV vectors following intraocular administration: evidence for the presence and persistence of vector DNA in the optic nerve and in the brain.* Mol Ther, 2005. **11**(2): p. 275-83.

351. Stieger, K., et al., *Subretinal delivery of recombinant AAV serotype 8 vector in dogs results in gene transfer to neurons in the brain.* Mol Ther, 2008. **16**(5): p. 916-23.

352. Boye, S.L., et al., *Long-term preservation of cone photoreceptors and restoration of cone function by gene therapy in the guanylate cyclase-1 knockout (GC1KO) mouse.* Invest Ophthalmol Vis Sci, 2011. **52**(10): p. 7098-108.

353. Bruewer, A.R., et al., *Evaluation of lateral spread of transgene expression following subretinal AAV-mediated gene delivery in dogs.* PLoS One, 2013. **8**(4): p. e60218.

354. Guy, J., et al., *Reporter expression persists 1 year after adeno-associated virus-mediated gene transfer to the optic nerve.* Arch Ophthalmol, 1999. **117**(7): p. 929-37.

355. Allocca, M., et al., *Serotype-dependent packaging of large genes in adeno-associated viral vectors results in effective gene delivery in mice.* J Clin Invest, 2008. **118**(5): p. 1955-64.

356. Trapani, I., et al., *Effective delivery of large genes to the retina by dual AAV vectors.* EMBO Mol Med, 2013.

357. Lopes, V.S., et al., *Retinal gene therapy with a large MYO7A cDNA using adeno-associated virus.* Gene Ther, 2013. **20**(8): p. 824-33.

358. Colella, P., et al., *Myosin7a deficiency results in reduced retinal activity which is improved by gene therapy.* PLoS One, 2013. **8**(8): p. e72027.

359. Alexander, J.J. and W.W. Hauswirth, *Adeno-associated viral vectors and the retina.* Adv Exp Med Biol, 2008. **613**: p. 121-8.

360. Conlon, T.J., et al., *Preclinical potency and safety studies of an AAV2-mediated gene therapy vector for the treatment of MERTK associated retinitis pigmentosa.* Hum Gene Ther Clin Dev, 2013. **24**(1): p. 23-8.

361. Guziewicz, K.E., et al., *Recombinant AAV-Mediated BEST1 Transfer to the Retinal Pigment Epithelium: Analysis of Serotype-Dependent Retinal Effects.* PLoS One, 2013. **8**(10): p. e75666.

362. Deng, W.T., et al., *Tyrosine-mutant AAV8 delivery of human MERTK provides long-term retinal preservation in RCS rats.* Invest Ophthalmol Vis Sci, 2012. **53**(4): p. 1895-904.

363. Glushakova, L.G., et al., *Does recombinant adeno-associated virus-vectored proximal region of mouse rhodopsin promoter support only rod-type specific expression in vivo?* Mol Vis, 2006. **12**: p. 298-309.

364. Pang, J.J., et al., *AAV-mediated gene therapy for retinal degeneration in the rd10 mouse containing a recessive PDEbeta mutation.* Invest Ophthalmol Vis Sci, 2008. **49**(10): p. 4278-83.

365. Pang, J.J., et al., *Long-term retinal function and structure rescue using capsid mutant AAV8 vector in the rd10 mouse, a model of recessive retinitis pigmentosa.* Mol Ther, 2011. **19**(2): p. 234-42.

366. Boye, S.E., et al., *Functional and behavioral restoration of vision by gene therapy in the guanylate cyclase-1 (GC1) knockout mouse.* PLoS One, 2010. **5**(6): p. e11306.

367. Khani, S.C., et al., *AAV-mediated expression targeting of rod and cone photoreceptors with a human rhodopsin kinase promoter.* Invest Ophthalmol Vis Sci, 2007. **48**(9): p. 3954-61.

368. Manfredi, A., et al., *Combined Rod and Cone Transduction by Adeno-Associated Virus 2/8.* Hum Gene Ther, 2013.

369. Alexander, J.J., et al., *Restoration of cone vision in a mouse model of achromatopsia.* Nat Med, 2007. **13**(6): p. 685-7.

370. Komaromy, A.M., et al., *Targeting gene expression to cones with human cone opsin promoters in recombinant AAV.* Gene Ther, 2008. **15**(14): p. 1049-55.

371. Carvalho, L.S., et al., *Long-term and age-dependent restoration of visual function in a mouse model of CNGB3-associated achromatopsia following gene therapy.* Hum Mol Genet, 2011. **20**(16): p. 3161-75.

372. Akimoto, M., et al., *Transgenic mice expressing Cre-recombinase specifically in M- or S-cone photoreceptors.* Invest Ophthalmol Vis Sci, 2004. **45**(1): p. 42-7.

373. Michalakis, S., et al., *Restoration of cone vision in the CNGA3-/- mouse model of congenital complete lack of cone photoreceptor function.* Mol Ther, 2010. **18**(12): p. 2057-63.

374. Pang, J.J., et al., *AAV-mediated gene therapy in mouse models of recessive retinal degeneration.* Curr Mol Med, 2012. **12**(3): p. 316-30.

375. Cideciyan, A.V., *Leber congenital amaurosis due to RPE65 mutations and its treatment with gene therapy.* Prog Retin Eye Res, 2010. **29**(5): p. 398-427.

376. Hernandez, M., et al., *Altered expression of retinal molecular markers in the canine RPE65 model of Leber congenital amaurosis.* Invest Ophthalmol Vis Sci, 2010. **51**(12): p. 6793-802.

377. Mowat, F.M., et al., *RPE65 gene therapy slows cone loss in Rpe65-deficient dogs.* Gene Ther, 2013. **20**(5): p. 545-55.

378. Gouras, P., J. Kong, and S.H. Tsang, *Retinal degeneration and RPE transplantation in Rpe65(-/-) mice.* Invest Ophthalmol Vis Sci, 2002. **43**(10): p. 3307-11.

379. Znoiko, S.L., et al., *Downregulation of cone-specific gene expression and degeneration of cone photoreceptors in the Rpe65-/- mouse at early ages.* Invest Ophthalmol Vis Sci, 2005. **46**(4): p. 1473-9.

380. Pang, J.J., et al., *Retinal degeneration 12 (rd12): a new, spontaneously arising mouse model for human Leber congenital amaurosis (LCA).* Mol Vis, 2005. **11**: p. 152-62.

381. Pang, J.J., et al., *Gene therapy restores vision-dependent behavior as well as retinal structure and function in a mouse model of RPE65 Leber congenital amaurosis.* Mol Ther, 2006. **13**(3): p. 565-72.

382. Pang, J., et al., *Self-complementary AAV-mediated gene therapy restores cone function and prevents cone degeneration in two models of Rpe65 deficiency.* Gene Ther, 2010. **17**(7): p. 815-26.

383. Dejneka, N.S., et al., *In utero gene therapy rescues vision in a murine model of congenital blindness.* Mol Ther, 2004. **9**(2): p. 182-8.

384. Chen, Y., et al., *RPE65 gene delivery restores isomerohydrolase activity and prevents early cone loss in Rpe65-/- mice.* Invest Ophthalmol Vis Sci, 2006. **47**(3): p. 1177-84.

385. Bemelmans, A.P., et al., *Lentiviral gene transfer of RPE65 rescues survival and function of cones in a mouse model of Leber congenital amaurosis.* PLoS Med, 2006. **3**(10): p. e347.

386. Li, X., et al., *Gene therapy rescues cone structure and function in the 3-month-old rd12 mouse: a model for midcourse RPE65 leber congenital amaurosis.* Invest Ophthalmol Vis Sci, 2011. **52**(1): p. 7-15.

387. Acland, G.M., et al., *Gene therapy restores vision in a canine model of childhood blindness.* Nat Genet, 2001. **28**(1): p. 92-5.

388. Narfstrom, K., et al., *Functional and structural recovery of the retina after gene therapy in the RPE65 null mutation dog.* Invest Ophthalmol Vis Sci, 2003. **44**(4): p. 1663-72.

389. Acland, G.M., et al., *Long-term restoration of rod and cone vision by single dose rAAV-mediated gene transfer to the retina in a canine model of childhood blindness.* Mol Ther, 2005. **12**(6): p. 1072-82.

390. Narfstrom, K., et al., *Assessment of structure and function over a 3-year period after gene transfer in RPE65-/- dogs.* Doc Ophthalmol, 2005. **111**(1): p. 39-48.

391. Jacobson, S.G., et al., *Safety of recombinant adeno-associated virus type 2-RPE65 vector delivered by ocular subretinal injection.* Mol Ther, 2006. **13**(6): p. 1074-84.

392. Le Meur, G., et al., *Restoration of vision in RPE65-deficient Briard dogs using an AAV serotype 4 vector that specifically targets the retinal pigmented epithelium.* Gene Ther, 2007. **14**(4): p. 292-303.

393. Annear, M.J., et al., *Successful gene therapy in older Rpe65-deficient dogs following subretinal injection of an adeno-associated vector expressing RPE65.* Hum Gene Ther, 2013. **24**(10): p. 883-93.

394. Maguire, A.M., et al., *Safety and efficacy of gene transfer for Leber's congenital amaurosis.* N Engl J Med, 2008. **358**(21): p. 2240-8.

395. Bainbridge, J.W., et al., *Effect of gene therapy on visual function in Leber's congenital amaurosis.* N Engl J Med, 2008. **358**(21): p. 2231-9.

396. Hauswirth, W.W., et al., *Treatment of leber congenital amaurosis due to RPE65 mutations by ocular subretinal injection of adeno-associated virus gene vector: short-term results of a phase I trial.* Hum Gene Ther, 2008. **19**(10): p. 979-90.

397. Cideciyan, A.V., et al., *Human RPE65 gene therapy for Leber congenital amaurosis: persistence of early visual improvements and safety at 1 year.* Hum Gene Ther, 2009. **20**(9): p. 999-1004.

398. Simonelli, F., et al., *Gene therapy for Leber's congenital amaurosis is safe and effective through 1.5 years after vector administration.* Mol Ther, 2010. **18**(3): p. 643-50.

399. Jacobson, S.G., et al., *Gene therapy for leber congenital amaurosis caused by RPE65 mutations: safety and efficacy in 15 children and adults followed up to 3 years.* Arch Ophthalmol, 2012. **130**(1): p. 9-24.

400. Wojno, A.P., E.A. Pierce, and J. Bennett, *Seeing the light.* Sci Transl Med, 2013. **5**(175): p. 175fs8.

401. Thomas, M.G., et al., *High-resolution in vivo imaging in achromatopsia.* Ophthalmology, 2011. **118**(5): p. 882-7.

402. Carroll, J., S.S. Choi, and D.R. Williams, *In vivo imaging of the photoreceptor mosaic of a rod monochromat.* Vision Res, 2008. **48**(26): p. 2564-8.

403. Pang, J.J., et al., *AAV-mediated cone rescue in a naturally occurring mouse model of CNGA3-achromatopsia.* PLoS One, 2012. **7**(4): p. e35250.

404. Komaromy, A.M., et al., *Transient photoreceptor deconstruction by CNTF enhances rAAV-mediated cone functional rescue in late stage CNGB3-achromatopsia.* Mol Ther, 2013. **21**(6): p. 1131-41.

405. Chang, B., et al., *A homologous genetic basis of the murine cpfl1 mutant and human achromatopsia linked to mutations in the PDE6C gene.* Proc Natl Acad Sci U S A, 2009. **106**(46): p. 19581-6.

406. Schon, C., M. Biel, and S. Michalakis, *Gene replacement therapy for retinal CNG channelopathies.* Mol Genet Genomics, 2013. **288**(10): p. 459-67.

407. Pang, J.J., et al., *Achromatopsia as a potential candidate for gene therapy.* Adv Exp Med Biol, 2010. **664**: p. 639-46.

408. Ali, R.R., et al., *Restoration of photoreceptor ultrastructure and function in retinal degeneration slow mice by gene therapy.* Nat Genet, 2000. **25**(3): p. 306-10.

409. Sarra, G.M., et al., *Gene replacement therapy in the retinal degeneration slow (rds) mouse: the effect on retinal degeneration following partial transduction of the retina.* Hum Mol Genet, 2001. **10**(21): p. 2353-61.

410. Andrieu-Soler, C., et al., *Single-stranded oligonucleotide-mediated in vivo gene repair in the rd1 retina.* Mol Vis, 2007. **13**: p. 692-706.

411. Souied, E.H., et al., *Non-invasive gene transfer by iontophoresis for therapy of an inherited retinal degeneration.* Exp Eye Res, 2008. **87**(3): p. 168-75.

412. Takahashi, M., et al., *Rescue from photoreceptor degeneration in the rd mouse by human immunodeficiency virus vector-mediated gene transfer.* J Virol, 1999. **73**(9): p. 7812-6.

413. Jomary, C., et al., *Rescue of photoreceptor function by AAV-mediated gene transfer in a mouse model of inherited retinal degeneration.* Gene Ther, 1997. **4**(7): p. 683-90.

414. Allocca, M., et al., *AAV-mediated gene replacement, either alone or in combination with physical and pharmacological agents, results in partial and transient protection from photoreceptor degeneration associated with betaPDE deficiency.* Invest Ophthalmol Vis Sci, 2011. **52**(8): p. 5713-9.

415. Yao, J., et al., *Caspase inhibition with XIAP as an adjunct to AAV vector gene-replacement therapy: improving efficacy and prolonging the treatment window.* PLoS One, 2012. **7**(5): p. e37197.

416. Sakamoto, K., et al., *New mouse models for recessive retinitis pigmentosa caused by mutations in the Pde6a gene.* Hum Mol Genet, 2009. **18**(1): p. 178-92.

417. Wert, K.J., et al., *Gene therapy provides long-term visual function in a pre-clinical model of retinitis pigmentosa.* Hum Mol Genet, 2013. **22**(3): p. 558-67.

418. Wert, K.J., J. Sancho-Pelluz, and S.H. Tsang, *Mid-stage intervention achieves similar efficacy as conventional early-stage treatment using gene therapy in a pre-clinical model of retinitis pigmentosa.* Hum Mol Genet, 2013.

419. Koch, S., et al., *Gene therapy restores vision and delays degeneration in the CNGB1(-/-) mouse model of retinitis pigmentosa.* Hum Mol Genet, 2012. **21**(20): p. 4486-96.

420. Tan, M.H., et al., *Gene therapy for retinitis pigmentosa and Leber congenital amaurosis caused by defects in AIPL1: effective rescue of mouse models of partial and complete Aipl1 deficiency using AAV2/2 and AAV2/8 vectors.* Hum Mol Genet, 2009. **18**(12): p. 2099-114.

421. Sun, X., et al., *Gene therapy with a promoter targeting both rods and cones rescues retinal degeneration caused by AIPL1 mutations.* Gene Ther, 2010. **17**(1): p. 117-31.

422. Ku, C.A., et al., *Gene therapy using self-complementary Y733F capsid mutant AAV2/8 restores vision in a model of early onset Leber congenital amaurosis.* Hum Mol Genet, 2011. **20**(23): p. 4569-81.

423. Pawlyk, B.S., et al., *Gene replacement therapy rescues photoreceptor degeneration in a murine model of Leber congenital amaurosis lacking RPGRIP.* Invest Ophthalmol Vis Sci, 2005. **46**(9): p. 3039-45.

424. Haire, S.E., et al., *Light-driven cone arrestin translocation in cones of postnatal guanylate cyclase-1 knockout mouse retina treated with AAV-GC1.* Invest Ophthalmol Vis Sci, 2006. **47**(9): p. 3745-53.

425. Mihelec, M., et al., *Long-term preservation of cones and improvement in visual function following gene therapy in a mouse model of leber congenital amaurosis caused by guanylate cyclase-1 deficiency.* Hum Gene Ther, 2011. **22**(10): p. 1179-90.

426. Boye, S.L., et al., *AAV-mediated gene therapy in the guanylate cyclase (RetGC1/RetGC2) double knockout mouse model of Leber congenital amaurosis.* Hum Gene Ther, 2013. **24**(2): p. 189-202.

427. Beltran, W.A., G.M. Acland, and G.D. Aguirre, *Age-dependent disease expression determines remodeling of the retinal mosaic in carriers of RPGR exon ORF15 mutations.* Invest Ophthalmol Vis Sci, 2009. **50**(8): p. 3985-95.

428. Natkunarajah, M., et al., *Assessment of ocular transduction using single-stranded and self-complementary recombinant adeno-associated virus serotype 2/8.* Gene Ther, 2008. **15**(6): p. 463-7.

429. Mowat, F.M., et al., *Tyrosine capsid-mutant AAV vectors for gene delivery to the canine retina from a subretinal or intravitreal approach.* Gene Ther, 2013.

430. Longbottom, R., et al., *Genetic ablation of retinal pigment epithelial cells reveals the adaptive response of the epithelium and impact on photoreceptors.* Proc Natl Acad Sci U S A, 2009. **106**(44): p. 18728-33.

431. Gt, L., et al., *1 Prominent proptosis in childhood thyroid eye disease. Abbreviated source.* Strabismus, 1997. **5**(1): p. 57-8.

432. Simons, D.L., et al., *Gene therapy prevents photoreceptor death and preserves retinal function in a Bardet-Biedl syndrome mouse model.* Proc Natl Acad Sci U S A, 2011. **108**(15): p. 6276-81.

Résumé substantiel en Français

(30 pages)

La rétine

La perception visuelle débute dans la rétine, un tissu neuronal situé dans le fond de l'œil. La rétine détecte les signaux lumineux, les convertis en signaux électriques et traite cette information avant son transfert vers les centres visuels supérieurs.

Chez les mammifères, la rétine contient 5 types principaux de neurones, organisés en 3 couches de corps cellulaires (**Figure 1**). La couche nucléaire externe contient les corps cellulaires des photorécepteurs. La couche nucléaire interne contient les corps cellulaires des cellules amacrines, bipolaires et horizontales. La couche de cellules ganglionnaires contient les corps cellulaires des cellules ganglionnaires et de quelques cellules amacrines.

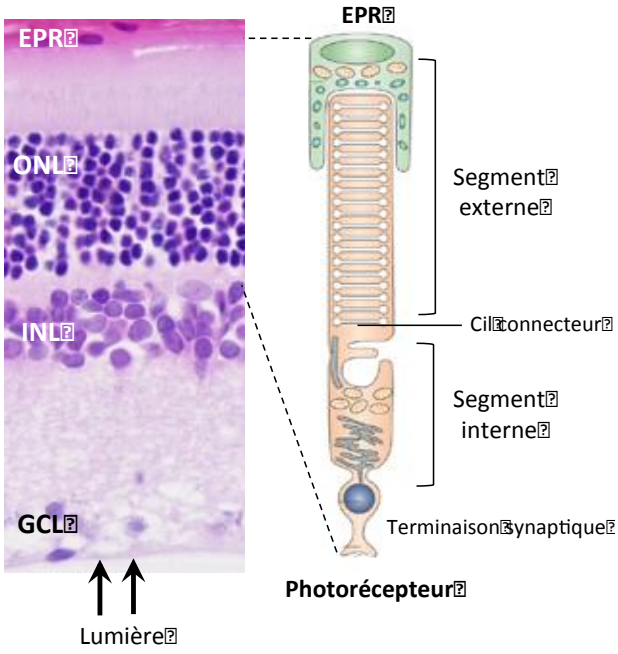

Figure 1. Organisation fonctionnelle de la rétine de mammifères et des photorécepteurs. EPR, epithelium pigmentaire rétinien, ONL, couche nucléaire externe, INL, couche nucléaire interne, GCL, couche de cellules ganglionnaires

Les photorécepteurs sont les cellules qui détectent la lumière et convertissent le stimulus lumineux en signaux chimiques. Ces signaux sont lus par les cellules bipolaires qui les transmettent aux cellules ganglionnaires. Au niveau des cellules ganglionnaires, les signaux sont codés en potentiels d'action, puis transmis via le nerf optique dans les centres visuels supérieurs où ils seront interprétés en images. A chaque relai synaptique, les réponses sont modifiées par les connexions latérales des cellules horizontales et amacrines.

Les photorécepteurs

La rétine des mammifères contient deux types majeurs de photorécepteurs: les bâtonnets (120-135 millions), pour la vision en condition de faible luminosité, et les cônes (5-7 millions) pour la vision des couleurs et en condition de forte intensité lumineuse. Les photorécepteurs ne sont pas distribués uniformément sur la rétine. Les bâtonnets dominent dans les régions périphériques. Les cônes sont en grande majorité concentrés dans la rétine centrale, appelée macula. L'acuité visuelle est formée dans le centre de la macula, au niveau de la fovéa, une région composée uniquement de photorécepteurs cônes.

En dépit de leurs nombreuses différences de forme, composition et fonction, les photorécepteurs cônes et bâtonnets ont une même architecture générale. Ils sont composés d'un segment externe (compartiment photosensible), d'un segment interne (lieu de biosynthèse), d'un corps cellulaire et d'une terminaison synaptique **(Figure 1**). Le segment externe est relié au segment interne par un cil connecteur (**Figure 1**). Le segment externe est entouré de cellules de l'EPR, qui supportent les fonctions de la rétine.

Trois mécanismes majeurs sont nécessaires à la fonction des photorécepteurs : (i) la cascade de phototransduction, (ii) le cycle visuel et (iii) le transport ciliaire. La cascade de phototransduction est le mécanisme par lequel les photorécepteurs convertissent l'énergie des photons absorbés en signaux chimiques. Le cycle visuel est un processus continu de recyclage du chromophore, le composant qui initie la cascade de phototransduction. Le transport ciliaire effectué par la machinerie du transport intra-flagellaire, permet le mouvement bidirectionnel des protéines et des lipides entre le segment interne du photorécepteur (zone de biosynthèse) et le segment externe du photorécepteur (partie photosensible).

La cascade de phototransduction

La cascade de phototransduction débute par l'absorption d'un photon par les photopigments ancrés dans la membrane des segments externes des photorécepteurs. Le photopigment est constitué d'un chromophore qui absorbe l'énergie des photons (le 11-*cis* rétinal) couplé à une opsine, qui affine le spectre de lumière absorbée. Les photorécepteurs bâtonnets contiennent une opsine sensible à la lumière bleue, la rhodopsine. Les cônes contiennent l'une des 3 opsines L, M ou S dont la sensibilité maximale se situe dans le rouge, le vert ou le bleu.

L'absorption de photons par le rétinal provoque son isomérisation de la forme 11-*cis* à une forme tout-*trans*. Ce changement de conformation active le photopigment et déclenche une cascade de signalisation via l'activation d'une protéine de la famille des protéines G, la transducine. La transducine active la phosphodiestérase 6 (PDE6). Cette enzyme contient deux sous-unités catalytiques, PDE6α et PDE6β dans les bâtonnets et deux sous-unités catalytiques PDE6α' dans les cônes. Elle hydrolyse le GMP cyclique (GMPc) situé dans le segment externe des photorécepteurs. La diminution de la concentration intracellulaire de GMPc provoque la fermeture de canaux cationiques GMPc-dépendants situés dans la membrane du segment externe des photorécepteurs. La réduction du flux entrant de cations entraîne l'hyperpolarisation du potentiel de membrane des photorécepteurs, qui bloque la libération du neurotransmetteur glutamate au niveau de la terminaison synaptique du photorécepteur. Ces changements en glutamate sont perçus par les cellules bipolaires et horizontales voisines.

Le cycle visuel

Pour permettre au photorécepteur de répondre à l'arrivée d'un nouveau photon, de nombreuses protéines sont impliquées dans l'arrêt de la cascade de phototransduction puis le recyclage du chromophore 11-*cis* rétinal. Les photorécepteurs ne possèdent pas l'activité *cis-trans* isomerase nécessaire au recyclage du all-*trans* rétinal en 11-*cis* rétinal. Ainsi, ce recyclage s'effectue en trois étapes: (i) la dissociation du all-*trans* rétinal de l'opsine activée et sa conversion en all-trans rétinol dans le cytoplasme du photorécepteur, (ii) le transport du all-*trans* rétinal dans les cellules EPR et sa ré-isomérisation en 11-*cis* rétinal, (iii) le transport du 11-*cis* rétinal dans les photorécepteurs et sa liaison aux opsines libres pour reformer un photopigment.

Le transport ciliaire

Le photorécepteur est une cellule polarisée. La majorité des protéines sont produites au niveau du segment interne du photorécepteur. Le segment externe, la partie photosensible du photorécepteur est reliée au segment interne par le cil connecteur. Ce cil connecteur et impliqué dans le transport bidirectionnel de très nombreuses protéines impliquées dans le processus visuel, comme les protéines de la cascade de phototransduction. Le transport ciliaire est effectué par la machinerie du transport intra-flagellaire. Des protéines cargo sont associées à de vastes complexes protéiques le long de l'axoneme du cil connecteur par des protéines motrices. Il s'agit d'un processus complexe, très régulé, et encore mal connu.

Les dystrophies rétiniennes héréditaires

Les dystrophies rétiniennes héréditaires forment un large groupe de pathologies caractérisées par la perte de fonction et la dégénérescence des photorécepteurs rétiniens en réponse à une mutation génétique. Elles conduisent à une perte irréversible de la vision et représentent la cause principale de cécité familiale en Europe, avec une prévalence de 1/2000. Les dystrophies rétiniennes héréditaires sont très hétérogènes, sur le plan clinique, génétique et moléculaire.

Caractéristiques cliniques

Historiquement, les dystrophies rétiniennes héréditaires sont classifiées en fonction de leur vitesse de progression ou du type de photorécepteur, cônes ou bâtonnets, dont la fonction est impactée en premier. On distingue ainsi:

- les achromatopsies, des pathologies majoritairement stationnaires caractérisées par la perte de la fonction des photorécepteurs cônes
- les dystrophies des cônes, des pathologies évolutives caractérisées par la perte progressive de la fonction des photorécepteurs cônes
- les dystrophies cônes-bâtonnets, caractérisées par la perte progressive de la fonction des photorécepteurs cônes puis des bâtonnets
- les cécités nocturnes congénitales, des pathologies stationnaires caractérisées par la perte de la fonction des photorécepteurs bâtonnets
- les dystrophies bâtonnets-cônes ou rétinites pigmentaires, caractérisées par la perte progressive de la fonction des photorécepteurs bâtonnets puis cônes.

Lorsque que la fonction des photorécepteurs bâtonnets et cônes est absente ou sévèrement atteinte depuis les premières années de la vie, le terme d'Amaurose congénitale de Leber (LCA) est généralement préféré.

Le diagnostic est réalisé à l'aide de l'électrorétinogramme (ERG), qui met en évidence l'état fonctionnel des photorécepteurs bâtonnets et/ou cônes dans des conditions de luminosité adaptées. Cet examen clinique est généralement couplé à l'étude du fond d'œil, qui évalue de manière non invasive les modifications morphologiques de la rétine. Enfin, la tomographie à cohérence optique (OCT) est un examen particulièrement utile pour mesurer *in vivo* l'épaisseur de la couche des photorécepteurs.

Caractéristiques génétiques

La dégénérescence des photorécepteurs dans les dystrophies rétiniennes héréditaires a une origine génétique. Ces pathologies sont causées par des mutations dans des gènes généralement exprimés dans les photorécepteurs eux-mêmes (cônes et/ou bâtonnets), mais également parfois dans les cellules de l'EPR. A ce jour, plus de 202 gènes et 242 loci ont été impliqués dans l'étiologie des dystrophies rétiniennes héréditaires chez l'homme (RetNet, dernier accès 28 Octobre 2013).

- Les mutations dans les gènes spécifiques des cônes altèrent généralement la fonction et/ou la survie des cônes uniquement (achromatopsies ou dystrophies des cônes).

- Les mutations dans les gènes spécifiques des bâtonnets altèrent la fonction et/ou la survie des photorécepteurs bâtonnets. Cependant, la perte physique des photorécepteurs bâtonnets provoque la mort des cônes « génétiquement sains » et la perte de la vision diurne et des couleurs (dystrophies bâtonnets-cônes).

  Différentes hypothèses ont été avancées pour expliquer la dégénérescence secondaire des cônes [1]. Premièrement, les bâtonnets pourraient libérer lors de leur dégénérescence un ou des facteurs toxiques responsable(s) de la mort des cônes [2], [3]; ou les bâtonnets pourraient sécréter des facteurs trophiques nécessaires à la survie des cônes [4], [5], [6]. Cependant, il est fréquent que les cônes survivent pendant plusieurs années après la perte totale des bâtonnets (et donc des facteurs libérés par les bâtonnets). Les effets paracrines semblent donc contribuer plutôt que gouverner la mort secondaire des cônes. Une autre explication pourrait être que la perte des bâtonnets, qui représentent 95% des photorécepteurs, endommage les cônes de façon indirecte, en perturbant l'homéostasie de la rétine via une chute de la consommation en oxygène [7], [8], [9], [10], [11] et/ou une perturbation du transport de glucose dans les cônes [12].

- Quand les mutations touchent les photorécepteurs cônes et bâtonnets, la perte de fonction cône peut précéder la perte de fonction bâtonnet (dystrophies cônes-bâtonnets) ou inversement (dystrophies bâtonnets-cônes). Le phénotype clinique dépendra alors du gène mis en cause, du type de mutation, de l'influence de facteurs environnementaux ou de modificateurs génétiques. De la même façon, les mutations dans les gènes de l'EPR, qui impactent aussi la fonction et/ou la survive des deux types de photorécepteurs peuvent être associés à des dystrophies cônes-bâtonnets ou bâtonnets-cônes.

Caractéristiques moléculaires

Les gènes associés aux dystrophies rétiniennes héréditaires peuvent coder pour des protéines impliquées dans la cascade de phototransduction, dans le cycle visuel, le transport ciliaire ou la structure des photorécepteurs. Les mutations peuvent également impacter des fonctions plus générales comme l'expression des gènes, la formation des protéines, la régulation du cytosquelette ou encore le métabolisme cellulaire. Dans de nombreux cas, la fonction des gènes associés à des rétinopathies héréditaires reste inconnue. Il en est de même pour les mécanismes qui entrainent la dégénérescence des photorécepteurs.

La thérapie génique pour le traitement des dégénérescences rétiniennes héréditaires

A ce jour, aucun traitement efficace n'est disponible pour prévenir ou stopper la progression des rétinopathies héréditaires. Une approche thérapeutique intéressante pourrait être la correction du défaut génétique par thérapie génique. Pour les dystrophies rétiniennes acquises par transmission autosomique récessive (65%) ou liées à l'X (6%), cette approche consisterait en l'apport d'une version sauvage du gène muté dans les cellules malades pour restaurer la fonction protéique et prolonger la survie des photorécepteurs. Il s'agit de la thérapie génique d'addition.

La rétine : une cible de choix pour la thérapie génique

La rétine est un tissu cible idéal pour la thérapie génique d'addition. En effet, l'œil est un organe de petite taille et compartimenté, ce qui permet d'utiliser de petites quantités de vecteurs et de limiter le risque d'effets secondaires liés à une dissémination systémique du vecteur thérapeutique. De plus, la barrière hémato-rétinienne protège les tissus traités des éventuelles réponses immunitaires dirigées contre le vecteur ou le produit du transgène; qui pourraient limiter l'efficacité du transfert de gène. Enfin, les structures transparentes de l'œil permettent de visualiser les tissus oculaires transduits par des techniques d'imagerie *in vivo* non invasives.
L'injection sous-rétinienne permet de placer le vecteur au contact des photorécepteurs et des cellules de l'EPR, tandis que l'injection intra-vitréenne place les vecteurs à proximité des cellules ganglionnaires.

Les vecteurs recombinants adéno-associés (AAV)

Plusieurs stratégies ont été développées pour transférer le gène thérapeutique dans les cellules de la rétine. Aujourd'hui, la technique la plus utilisée fait appel à des vecteurs dérivés des virus adéno-associés (AAV) car (i) les AAV sont capables de transduire efficacement les photorécepteurs et les cellules de l'EPR à la suite d'une injection sous-rétinienne chez la souris, le rat, le chien, le porc et le primate, (ii) les AAV sont peu immunogènes, (iii)les AAV sont bien tolérés, et (iv) leur génome persiste dans les cellules hôtes sous la forme d'épisomes, ce qui permet une expression du transgène stable à long terme dans les cellules post-mitotiques [13].

Le génome de l'AAV est composé d'une molécule d'ADN linéaire simple brin d'environ 4,7kb composée de deux cadres ouverts de lecture, les gènes REP et CAP, encadrés par deux séquences terminales inversées [14]. Ce génome est encapsulé dans une capside protéique icosaédrique
Les vecteurs AAV recombinants (rAAV) sont produits à partir du virus de l'AAV sauvage par délétion de la séquence codante (*REP* et *CAP*) et insertion de la cassette d'expression (promoteur-transgène-site de poly-adénylation) entre les ITR de l'AAV. Les fonctions *REP* et *CAP* sont apportées *en trans* pour permettre la réplication et l'encapsidation des virus recombinants

De façon très intéressante, il est possible de modifier le tropisme cellulaire des vecteurs AAV recombinants en utilisant (i) des promoteurs spécifiques et/ou (ii) des capsides virales différentes. En effet, les capsides interagissent avec des récepteurs spécifiques présents à la surface des cellules et il est possible de créer des vecteurs pseudotypes qui possèdent les ITR de l'AAV2 et une capside d'un autre sérotype d'AAV (**Figure 2b**). Ces vecteurs sont appelés rAAV2/n où le premier chiffre indique l'origine des ITR et le second l'origine de la capside. Il existe plus de 120 variantes naturelles de capside AAV ainsi qu'une centaine de variantes générées en laboratoire par mutagénèse dirigée ou évolution dirigée [13].

L'AAV2 est le sérotype le plus commun chez l'homme. Après une injection sous-rétinienne, il est capable de transduire efficacement les cellules de l'EPR et les photorécepteurs chez le rongeur [15], le chien [16], [17] et le primate [18]. Cependant, sa cinétique d'expression du transgène est lente [18]. Les vecteurs rAAV2/5, 2/7, 2/8 et 2/9 ont une efficacité de transduction des photorécepteurs plus importante et une cinétique d'expression du transgène plus rapide que l'AAV2/2 [19], [17], [20], [21], [22]. Un sérotype d'AAV8 contenant une mutation ponctuelle Y733F au niveau d'un résidu tyrosine exposé à la surface de la capside permets une expression du transgène plus forte et plus rapide dans les photorécepteurs que le vecteur AAV2/8 standard [23], [24].

Thérapie génique d'addition pour le traitement des dystrophies rétiniennes

Au cours des dix dernières années, la thérapie génique d'addition médiée par des vecteurs AAV a donné des résultats très encourageants chez une douzaine de modèles murins ou canins de dystrophies rétiniennes héréditaires. Chez ces modèles, l'introduction d'une copie saine du gène muté a permis d'améliorer la fonction et/ou de prévenir ou ralentir la dégénérescence des photorécepteurs chez les animaux traités, parfois à long terme [25], [26] [27], [28].
Traditionnellement, la thérapie génique d'addition médiée par des vecteurs AAV est considérée plus efficace dans les formes de dystrophies rétiniennes causées par des mutations dans les gènes exprimés dans l'EPR. Ce résultat peut s'expliquer par (i) la plus faible efficacité de transduction des photorécepteurs, et par (ii) le fait que les photorécepteurs dégénèrent parfois plus rapidement quand ils sont directement impactés par la mutation génétique.

Pathologies de l'EPR: Le transfert de gène *RPE65* (65-kDa RPE-specific isomerase) chez le chien RPE65-déficient est un très bon exemple d'étude préclinique de thérapie génique pour une pathologie de l'EPR [29], [30], [31], [32], [33], [34], [35]. Le gène *RPE65*, exprimé dans l'EPR, code pour une protéine impliquée dans la ré-isomérisation du all-*trans* rétinal and 11-*cis* rétinal. La perte de fonction ou l'absence d'activité RPE65, bloque le cycle visuel et entraîne la perte de fonction et la dégénérescence progressive des photorécepteurs cônes et bâtonnets. Chez le chien RPE65-déficient, la perte de fonction des photorécepteurs intervient au cours des premiers mois de la vie, tandis que la dégénérescence des cellules progresse lentement (-40% de photorécepteurs bâtonnets et -15% de photorécepteurs cônes à l'âge de 6 ans) [36], [37], [34].
Chez les chiens traités à l'âge de 2 à 6 ans avec de l'AAV2/2 ou de l'AAV2/4 codant pour le gène RPE65 humain, la fonction rétinienne et les capacités visuelles ont été restaurées de manière stables, pendant plus de 11 ans postinjection (dernier examen rapporté dans la littérature) [29], [30], [31], [32], [33], [34], [35]. Ces résultats ont ouvert la voie à plusieurs essais cliniques indépendants de phase I/II chez des patients atteints d'ACL liées à une mutation dans le gène *RPE65*, avec des résultats encourageants en terme d'efficacité et de biosécurité [38], [39], [40], [16], [41], [42], [43], [44], [34]. En effet, chez près de 30% des patients traités, les cliniciens ont démontré (i) une amélioration de la sensibilité rétinienne à la lumière, (ii) une réduction du nystagmus, (iii) une augmentation du champ visuel, (iv) une augmentation de l'acuité visuelle, (v) une réactivation du cortex visuel et (vi) une amélioration du déplacement des patients à travers un parcours d'obstacle [26], [28].

Cependant, contrairement à ce qui avait été montré lors des études précliniques, aucun patient n'a récupéré de fonction rétinienne mesurable par ERG. Cette différence entre les patients et les chiens peut être expliquée par la dégénérescence plus rapide des photorécepteurs chez l'homme. La plupart des patients ont été traités à des stades tardifs de la pathologie. La perte d'un nombre important de photorécepteurs et/ou l'accumulation de dommages dans les cellules restantes peut influencer le niveau global de restauration de fonction en :

- limitant le niveau d'expression de la protéine RPE65 (par diminution du nombre de cellules de l'EPR transduites et/ou diminution de l'efficacité de transduction de l'EPR)
- compromettant de façon irréversible la fonction des cellules de l'EPR ou des photorécepteurs encore présents au moment du traitement

Ainsi, le niveau de fonction rétinienne restaurée chez les patients RPE65-déficients traités pourrait être *globalement* trop faible pour être détectable par ERG.
Cette hypothèse a été renforcée par des travaux récents qui ont montré par OCT que la cinétique de dégénérescence rétinienne n'était pas modifiée dans la zone traitée des patients, et ce malgré

une amélioration *stable* des capacités visuelles [34]. Le nombre *global* de photorécepteurs préservés chez les patients est peut-être trop faible pour que leur survie puisse être détectée par OCT avant que l'ensemble des photorécepteurs « non-sauvés » ait disparu. Il est également possible que le transfert de gène n'est pas été suffisant pour stopper la dégénérescence des photorécepteurs et que les cellules fonctionnelles soient les cellules qui meurent en dernier. Dans ce cas, la fonction visuelle restaurée chez les patients ne sera impactée par la dégénérescence des photorécepteurs qu'à des stades plus tardifs de la pathologie [34].

Pathologies des photorécepteurs: Des résultats très encourageants de thérapie génique d'addition ont été obtenus chez plusieurs modèles murins et canins de dystrophies des photorécepteurs [25], [26] [27], [28].

Pour le traitement des pathologies peu évolutives, nous pouvons noter le traitement de plusieurs modèles animaux d'achromatopsie, dont la souris *Cngb3*$^{-/-}$ déficiente pour les canaux cGMP-dépendants exprimés dans les segments externes des cônes [45]. Chez ce modèle, la perte de fonction cône est quasi-totale dès la naissance mais 50% des cônes sont encore présents à l'âge de 12 mois. L'injection sous-rétinienne de vecteur AAV2/8 codant pour le gène CNGB3 chez des souris *Cngb3*$^{-/-}$ âgées de 2 semaines a permis de restaurer des réponses ERG cônes équivalent à 90% de celles enregistrées chez un animal sain. L'effet thérapeutique est resté stable pendant au moins 9 moins après l'injection (durée de l'étude). Cependant, malgré la dégénérescence lente des photorécepteurs chez la souris *Cngb3*$^{-/-}$ seulement 60% de la fonction rétinienne normale a pu être récupérée chez les souris traitées à l'âge de 6 mois [45]. Une altération précoce de la physiologie des photorécepteurs pourrait impacter l'efficacité de la thérapie génique d'addition.
Un phénomène similaire a été démontré chez deux modèles canins CNGB2-déficients [46], [47]. Chez ces chiens, l'injection d'AAV2/5 codant pour le gène Cngb3 canin permet de restaurer 5-10% de la fonction cône normale chez les animaux traités avant l'âge de 1 an (fonction stable jusqu'à 33 mois postinjection). Au contraire, chez les animaux traités après l'âge d'1 an, aucune restauration stable de la fonction cône n'est possible, et ce malgré le maintien de 75% des cônes dans la rétine des chiens traités au moment de l'injection [46], [47].

Chez des modèles animaux de formes sévères de dégénérescence rétiniennes, le développement de nouveaux vecteurs AAV recombinants qui permettent une expression du transgène plus efficace et plus rapide dans les photorécepteurs a permis d'améliorer significativement le phénotype de plusieurs modèles animaux de rétinopathies héréditaires. Par exemple, chez la souris *Aipl1*$^{-/-}$, déficiente pour une protéine nécessaire à l'assemblage des enzymes PDE6, l'injection d'un vecteur AAV2/8 codant pour le gène AIPL1 humain 10 jours après la naissance a

permis de restaurer 50% des réponses ERG bâtonnets mesurables chez une souris saine [48], [49], [50]. Cet effet thérapeutique a été évalué jusqu'à 4 semaines après injection. Le traitement a également prolongé de manière significative la survie des photorécepteurs. Néanmoins, aucun effet thérapeutique n'a pu être démontré chez ce modèle avec un vecteur AAV2/5 qui a une cinétique d'expression du transgène un peu plus lente que l'AAV2/8 chez la souris [49].

Conclusion:

L'ensemble de ces résultats indique que la thérapie génique d'addition pour le traitement des dystrophies rétiniennes héréditaires pourrait être une approche intéressante. Cependant, l'efficacité de transduction des photorécepteurs, l'altération physiologique précoce des cellules de la rétine et la perte rapide des photorécepteurs semblent être des facteurs limitant l'efficacité de la thérapie génique d'addition pour le traitement des formes sévères de dégénérescence des photorécepteurs. Pour permettre le transfert vers la clinique de ces approches thérapeutiques, la confirmation de ces résultats chez d'autres modèles animaux et une meilleure compréhension des mécanismes pathologiques de ces pathologies sont nécessaires.

Objectifs de la thèse

Les études précliniques de thérapie génique chez des modèles gros animaux de dystrophies rétiniennes héréditaires comme le chien, le chat ou le porc, peuvent jouer un rôle très important dans le développement et la validation d'approches de thérapie génique pour le traitement de ces pathologies. En effet, la taille et l'anatomie de l'œil des gros animaux, très proches de celle de l'homme, constituent un modèle très pertinent pour la détermination des doses de vecteur à administrer et des approches chirurgicales à mettre en place. La durée de vie des modèles gros animaux permet également de suivre les effets du traitement sur le long terme, un point important pour le traitement des dystrophies rétiniennes héréditaires qui évoluent chez l'homme sur plusieurs années ou décennies [51].

Enfin, la distribution, la densité et la proportion des photorécepteurs cônes et bâtonnets des modèles gros animaux sont plus proches de celles des primates. Bien que seuls les primates possèdent une fovéa, les grands mammifères ont une région riche en cônes, appelée « *visual streak* » qui s'étend de la rétine nasale à la rétine temporale au-dessus du nerf optique (**Figure 2a-c**). Dans ce « *visual streak* », il existe une zone temporale particulière de densité de photorécepteurs maximale et avec un ratio cônes : bâtonnets élevé. Cette région est appelée l'*area centralis* (**Figure 2d**) [52].

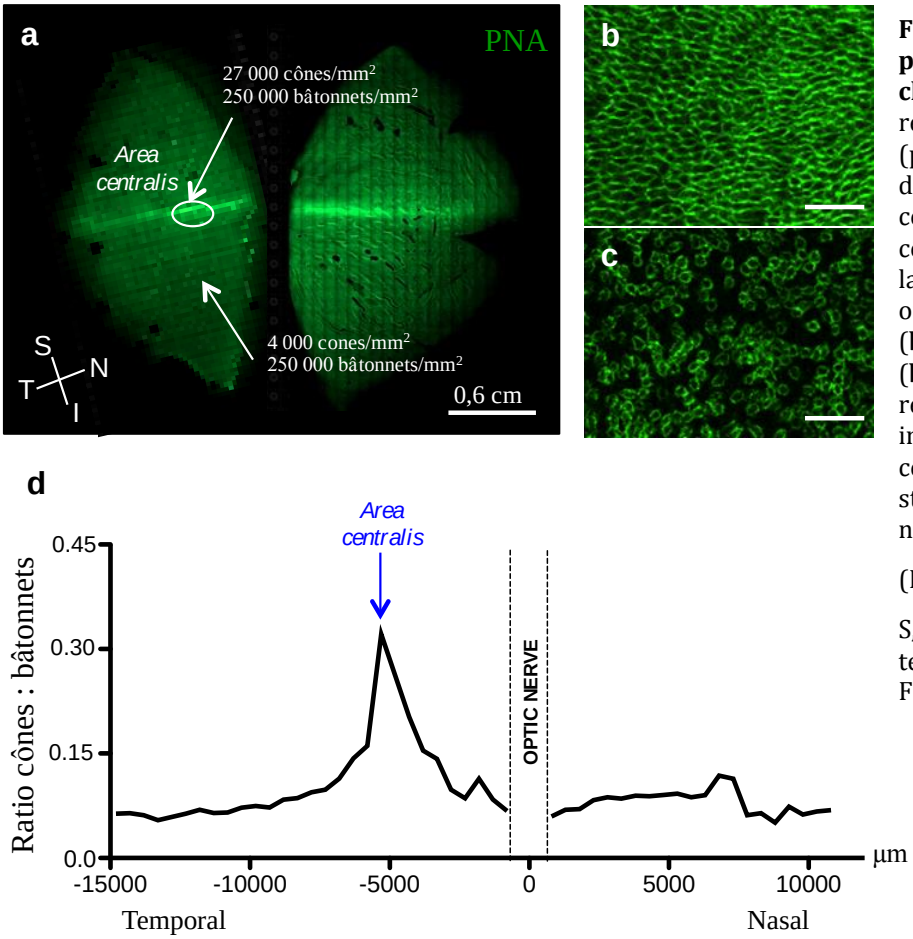

Figure 2. Distribution et densité des photorécepteurs cônes et bâtonnets chez le chien. (**a**) Montage à plat de rétine de chien marqué avec PNA (peanut agglutinin-FITC), un marqueur des segments internes et externes des cônes. Une bande horizontale riche en cônes s'étend de la rétine temporale à la rétine nasale, au-dessus du nerf optique. Il s'agit du « visual streak » (**b,c**) Images agrandies représentatives (**b**) du « visual streak » et (**c**) d'une région similaire dans la rétine inférieure mi-périphérique. (**d**) Ratio cônes : bâtonnets à travers le « visual streak ». Le ratio est plus élevé au niveau de l'area centralis.

(Petit L. *et al.* en préparation)

S, supérieur ; N, nasal ; I, inférieur, T, temporal ; PNA, peanut agglutinin - FITC

De façon importante, la répartition des photorécepteurs et le ratio cônes : bâtonnets sont des variables qui affectent le phénotype clinique des pathologies. Par exemple, la macula est la région principalement impliquée dans les dystrophies des cônes. Au contraire, dans les dystrophies bâtonnets-cônes, les cônes situés dans la fovéa sont souvent préservés jusqu'à des stades très tardifs de la pathologie, un mécanisme attribué à leur densité élevée dans cette région. L'altération précoce des photorécepteurs et leur dégénérescence rapide pouvant être des facteurs limitant l'efficacité des approches de thérapie génique, il est très intéressant d'évaluer le potentiel de ces stratégies thérapeutiques chez des modèles animaux qui miment les variations spatio-temporelles des rétinopathies.

Dans ce contexte, l'objectif principal de cette étude a été d'évaluer l'efficacité d'approches de thérapie génique d'addition chez deux modèles canins de formes sévères de dystrophies héréditaires des photorécepteurs, (i) le chien PDE6β-déficient, un modèle gros animal de dystrophies bâtonnets-cônes et (ii) le chien RPGRIP1-déficient, un modèle gros animal de dystrophies cônes-bâtonnets.

La dystrophie « bâtonnets-cônes » liée à une mutation dans le gène PDE6β

Les dystrophies « bâtonnets-cônes » sont les formes de dystrophies rétiniennes héréditaires les plus fréquentes, avec une prévalence de 1 : 4000. Les dystrophies « bâtonnets-cônes » sont caractérisées par la dégénérescence progressive des photorécepteurs bâtonnets puis cônes. Les premiers symptômes sont la perte de la vision nocturne et un rétrécissement du champ visuel à cause de la dégénérescence des bâtonnets. Cette phase est suivie par la mort des cônes et la perte concomitante de la vision diurne et centrale [53].

A ce jour, plus de 45 gènes ont été associés à l'étiologie des dystrophies « bâtonnets-cônes ». Parmi ces gènes, le gène codant pour la sous unité β de l'enzyme PDE6 des bâtonnets (PDE6β) est associée à une des formes les plus fréquentes de dystrophies « bâtonnets-cônes » autosomique récessive (4 à 6% des cas totaux, 36 000 patients à travers le monde) [54], [55], [56], [57], [58], [59], [60], [61], [62], [63].

PDE6 est une des enzymes clés de la cascade de phototransduction. Elle contrôle le niveau de GMPc et de calcium dans le segment externe des photorécepteurs bâtonnets. Les deux sous-unités catalytiques PDE6α et PDE6β sont nécessaires à l'activité d'hydrolyse du GMPc de l'enzyme PDE6 des bâtonnets. Ainsi, les mutations « perte-de-fonction » dans le gène PDE6β provoquent une perte ou une absente totale d'activité PDE6 dans les bâtonnets et l'accumulation massive de GMPc et de calcium dans les segments externes des photorécepteurs [64],[65].

Les niveaux élevés de GMPc et/ou de calcium provoquent, par des mécanismes encore mal définis [66], [67], [68], la mort des photorécepteurs bâtonnets, puis des cônes [1], [69].

Plusieurs modèles murins de dystrophies bâtonnets-cônes liées à une mutation dans le gène PDE6β ont été caractérisés, dont les modèles naturels « rodless » *rd1* et « rod degeneration » *rd10*. Le modèle *rd1* présente une dégénérescence rétinienne très rapide avec un début de dégénérescence dès la première semaine de vie et une dégénérescence complète à 20 jours [70], [71], [72], [73], [74]. Le modèle *rd10* présente une dégénérescence plus lente avec un début de dégénérescence 2 semaines après la naissance et une perte totale des photorécepteurs à l'âge de 5 semaines [75], [76], .

Les premiers essais de thérapie génique d'addition ont été réalisés chez la souris *rd1* avec des vecteurs dérivés des adénovirus [77], [78], des lentivirus [79] ou de l'AAV2 [80]. Ces vecteurs ne transduisent pas efficacement les photorécepteurs. Ainsi, dans la plupart de ces études, malgré une préservation partielle des photorécepteurs dans les rétines traitées, l'amélioration fonctionnelle n'a été que très limitée.

Un effet thérapeutique plus marqué a été obtenu chez la souris *rd10* traitée à l'âge de 15 jours avec un AAV2/5-smCBA-m*Pde6β* [81]. Trois semaines après l'injection, 37% des réponses

bâtonnets mesurées par ERG étaient maintenues dans les yeux traités, soit trois fois plus que les réponses enregistrées dans les yeux controlatéraux non-injectés. De plus, la survie des photorécepteurs a été prolongée jusqu'à 35 jours après la naissance, un âge auquel seules quelques cellules sont encore présentes dans les yeux non traités [81]. Ce résultat indique que les difficultés à traiter les modèles murins PDE6β-déficient ne sont pas liées à la voie de signalisation complexe à laquelle participe l'enzyme PDE6 mais au fait que (i) les modèles *rd1* et *rd10* présentent des dégénérescences rétiniennes très rapides, et que (ii) il est difficile d'obtenir des niveaux d'expression du transgène suffisamment tôt dans les photorécepteurs mutés pour prévenir leur dégénérescence. Cette hypothèse a été renforcée par le succès récent d'une approche de thérapie génique chez la souris *rd10* avec un vecteur AAV2/8 (Y733F)-smCBA-m*Pde6β* qui permet une expression plus rapide et plus intense du transgène dans les photorécepteurs [82]. Pour la première fois, la fonction des photorécepteurs bâtonnets a été préservée à la hauteur de 58% de celle observée chez des souris saines, et ce jusqu'à 6 mois postinjection [82].

Le chien Setter Irlandais *rcd1* (*rod-cone dysplasia 1*) est un modèle canin spontané de dégénérescence rétinienne. Il porte une mutation non-sens dans l'exon 21 du gène *Pde6β*, responsable de la formation d'une sous-unité PDE6β tronquée de 49 acides aminés à l'extrémité C-terminale et dépourvue de son domaine d'encrage à la membrane [83], [84]. Il n'y a pas d'activité PDE6 détectable chez le chien *rcd1*. Le phénotype du chien *rcd1* est très proche de celui observé chez l'homme, avec une dégénérescence rapide des photorécepteurs bâtonnets entre l'âge de 1 à 5 mois, suivis par la perte de fonction cône vers l'âge de 1 à 2 ans [85], [86]. De nombreux cônes sont encore présents dans l'*area centralis* des chiens *Rcd1* à l'âge de 8 ans (Petit L *et al*. manuscrit en préparation).

Cette progression rapide de la pathologie est très intéressante car elle permet d'évaluer rapidement les effets du traitement sur la fonction et la dégénérescence rétinienne. De plus, la corrélation importante entre la mort des photorécepteurs bâtonnets et cônes chez ce chien en font un très bon modèle pour évaluer l'effet du traitement sur la mort secondaire des cônes. Néanmoins, les caractéristiques cliniques du chien *rcd1* laissent penser que la fenêtre thérapeutique chez ce modèle pourrait être plus large que chez les souris *rd1* et *rd10*.

La dystrophie cône-bâtonnet liée à une mutation dans le gène RPGRIP1

Les mutations dans le gène RPGRIP1, qui code pour Retinitis Pigmentosa GTPase Regulator-interacting protein 1 sont associées à 2% des cas de dystrophies cônes-bâtonnets [87], [88] et 6% des cas d'ACL [89], [90], [91], [92], [93], [94], [95], [96]. RPGRIP1 est essentiellement exprimée dans les photorécepteurs. Il en existe de nombreuses isoformes avec des localisations cellulaires et des propriétés biochimiques variées [97], [98], [99].
RPGRIP1 a été tout d'abord identifiée comme un partenaire moléculaire de RPGR [100], [101], [102], une protéine qui lorsqu'elle est mutée est associée à la forme la plus fréquente de dystrophies rétiniennes héréditaires liées à l'X (70-80% des cas) [103], [104], [105]. RPGRIP1 jouerait un rôle dans l'ancrage de RPGR au niveau du cil connecteur des photorécepteurs cônes et bâtonnets [97], [102], [106]. Cependant, RPGRIP1 pourrait également avoir un rôle supplémentaire dans les photorécepteurs, car l'absence de RPGRIP1 chez la souris est associée à une pathologie plus sévère que la perte de RPGR [28]. En particulier, RPGRIP1 pourrait contrôler l'organisation des microtubules du cil connecteur [106] et/ou être nécessaire au développement et au maintien des segments externes des photorécepteurs [107], [108].

Chez la souris *Rpgrip1*$^{-/-}$, la structure des segments externes est très perturbée. Les opsines des photorécepteurs cônes et bâtonnets sont délocalisées au niveau du segment interne. La dégénérescence des photorécepteurs cônes et bâtonnets est visible dès 15 jours après la naissance. A 5 mois, la quasi-totalité des photorécepteurs ont disparus [107].
Les premières approches de thérapie génique d'addition chez la souris *Rpgrip1*$^{-/-}$ ont donné des résultats encourageants [109], [110]. Dans une première étude, les souris ont été traitées à l'âge de 20 jours avec un vecteur AAV2/2 codant pour le gène Rpgrip1 murin sous le contrôle d'un promoteur bâtonnet spécifique. La localisation de RPGRIP1 et RPGR au niveau du cil connecteur des photorécepteurs transduits a été restaurée. Les souris traitées ont montré une meilleure préservation des photorécepteurs et de la fonction rétinienne jusqu'à 5 mois postinjection [109]. Dans la seconde étude, l'utilisation d'un vecteur AAV2/8 codant pour le gène RPGRIP1 humain sous le contrôle d'un promoteur actif dans les cônes et les bâtonnets a permis de préserver un tiers de la fonction rétinienne initialement présente dans les yeux traités à 5 mois postinjection. A cet âge, aucune réponse ERG n'était encore détectable dans les yeux non traités [110]. Néanmoins, la fonction rétinienne a continué de décliner au cours du temps dans les yeux traités.

Le chien mini-teckel à poil long *Cord1* (*Cone-rod dystrophy 1*) est un modèle intéressant pour évaluer l'efficacité des vecteurs thérapeutiques avant leur application clinique. Il s'agit d'un modèle canin spontané de dystrophie cône-bâtonnet associée à une insertion de 44bp dans

l'exon 2 du gène *Rpgrip1* [111]. Chez le chien *Cord1*, la fonction cône est totalement absente dès l'âge de 1 mois [112, 113]. A cet âge, la fonction bâtonnet est normale, mais elle décroit ensuite rapidement jusqu'à l'âge de 12 mois [112, 113].. Cette perte de fonction est associée à une dégénérescence progressive des photorécepteurs entre l'âge de 3 et 24 mois [112, 113]. Ces caractéristiques cliniques sont très proches de celles observées chez certains patients RPGRIP1-déficients qui connaissent une perte de la vision centrale et des couleurs dès les premières années de la vie, et une rapide dégénérescence des photorécepteurs cônes et bâtonnets dans l'enfance. Ces caractéristiques cliniques font de ce modèle canin un très bon modèle préclinique pour l'évaluation d'un traitement par thérapie génique des dystrophies cônes-bâtonnets.

Résultats et discussion

Evaluation du tropisme du vecteur AAV2/5-RK-eGFP chez le chien

Le chien *Rcd1* et le chien *Cord1* sont des modèles gros animaux de dystrophies rétiniennes héréditaires liées à des mutations dans des gènes spécifiques des photorécepteurs. Pour cette raison, nous avons choisi d'utiliser des vecteurs dérivés des AAV car ce sont les seuls vecteurs capables de transduire efficacement les photorécepteurs rétiniens différenciés. Nous avons utilisé des vecteurs AAV2/5 et AAV2/8 qui sont capables de transduire efficacement les cellules de l'EPR et les photorécepteurs chez les rongeurs [19], [22], le chien [17], [114], [115], le porc [14], [22] et le primate [20], [21], [116] après une injection sous-rétinienne.

Le chien *Rcd1* est un modèle canin de dystrophie bâtonnets-cônes liée à une mutation dans le gène spécifique des photorécepteurs bâtonnets, *Pde6β*. A ce jour, aucun promoteur bâtonnet-spécifique efficace n'a été caractérisé. Nous avons donc choisi d'utiliser le promoteur humain rhodopsine kinase (RK) qui permet une expression du transgène forte dans les photorécepteurs bâtonnets, mais également dans les cônes, chez la souris [117], [22]et le singe [116]. Une étude précédente avait montré que le promoteur RK n'était pas actif dans les cônes de chien, sauf après injection d'un fort titre d'AAV (3.10^{12} copies injectées) [118].

Nous avons souhaité vérifier ce résultat en construisant un vecteur AAV2/5 contenant le gène rapporteur eGFP sous le contrôle du promoteur RK (vecteur AAV2/5-RK-eGFP). L'injection sous-rétinienne de 150µL de vecteur AAV2/5-RK-eGFP (1.10^{11} vg/mL) dans des yeux de chiens sains (n=2) a conduit à une expression d'eGFP localisée uniquement dans la zone directement exposée au vecteur viral (**Figure 3b, c**) [119]. Le niveau maximal de fluorescence eGFP a été obtenu 6 semaines après l'injection (résultat non montré). Il est ensuite resté stable jusqu'à 9 mois postinjection, au moment où les animaux ont été euthanasiés pour permettre l'analyse

histologique de leurs rétines (**Figure 3c**). Nous avons réalisé des coupes histologiques des rétines traitées dans la zone exposée au vecteur, et plus particulièrement dans la zone du « visual streak » riche en cônes (ratio cônes : bâtonnets = 1 : 10, versus 1 :41 en périphérie). Par microscopie à épifluorescence, nous avons confirmé que l'expression de la GFP était limitée aux photorécepteurs rétiniens (au niveau des corps cellulaires, des segments internes et externes) (**Figure 3d**). La transduction des bâtonnets dans cette région a été particulièrement efficace, avec presque 100% des photorécepteurs exprimant la GFP à proximité du site d'injection.

Une transduction des cônes, plus rare mais importante, a également été détectée. Les photorécepteurs cônes ont été identifiés sur la base de deux critères : leur forme très caractéristique, et l'immuno-marquage de leurs segments externes et internes avec un anticorps dirigé contre l'opsine de cônes L/M. Dans la zone du « visual streak », le vecteur AAV2/5-RK-eGFP a transduit en moyenne 49±21% des cônes LM marqués (n=2 yeux)[119]. **Ces résultats ont indiqué que le promoteur RK pouvait permettre une expression du transgène efficace et spécifique dans les photorécepteurs bâtonnets et cônes (au moins L/M) chez le chien sain (au moins dans la région riche en cônes)**.

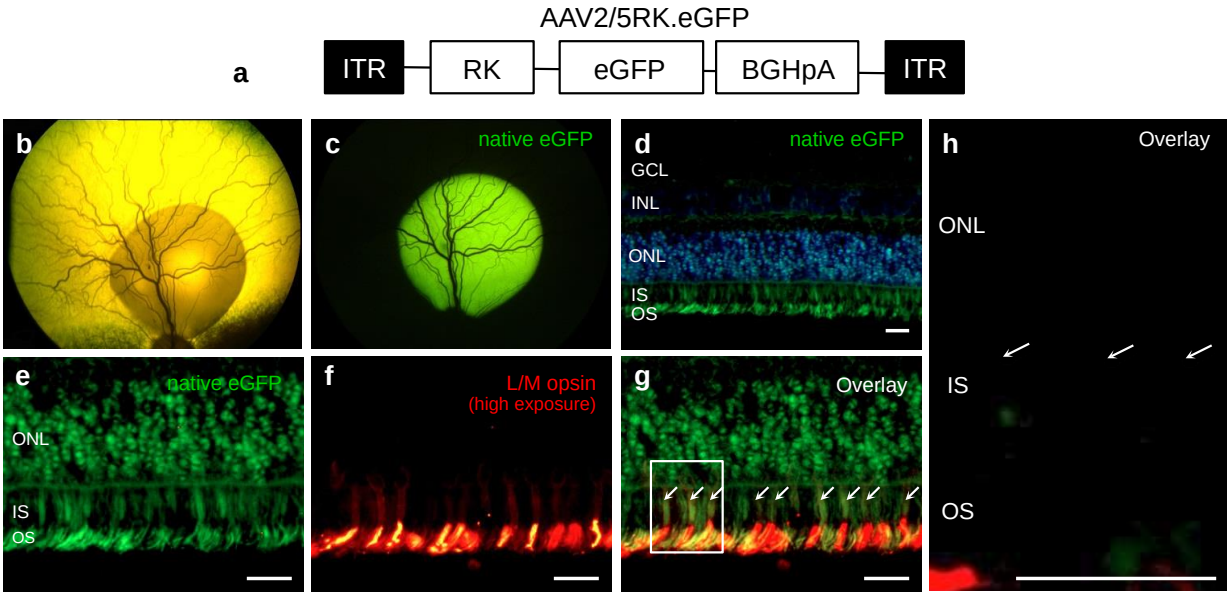

Figure 3. Expression de la GFP dans les photorécepteurs cônes et bâtonnets après injection sous-rétinienne d'un vecteur AAV2/5-RK-eGFP chez le chien sain. (a) Structure schématique du vecteur AAV2/5-RK-eGFP. (**b**) Décollement rétinien créé par l'injection sous-rétinienne de vecteur AAV2/5-RK-eGFP 20 minutes après l'injection chez le chien. (**c**) Photographie du fond d'œil montrant la fluorescence de la GFP au niveau de la zone directement exposée au vecteur

Ce promoteur est donc susceptible de conduire à une expression ectopique de PDE6β dans les cônes de chien *Rcd1*. Chez la souris, l'expression ectopique des sous-unités PDE6αβ dans les cônes peut remplacer l'enzyme PDE6α'α' des cônes et activer la voie de signalisation visuelle [120]. Inversement, l'enzyme PDE6α'α' des cônes peut activer la voie de signalisation des photorécepteurs bâtonnets [121]. La capacité de la sous-unité PDE6β de se lier à la sous-unité PDE6α' des cônes n'est pas connue.
Il n'a pas été possible d'évaluer l'expression ectopique de PDE6β dans les cônes car aucun des anticorps testés ne reconnait spécifiquement la sous-unité PDE6β canine [86]. Néanmoins, chez le chien *Rcd1*, la fonction cône est normale jusqu'à l'âge de 9-12 mois. Il était donc possible de suivre les effets délétères potentiels de l'expression ectopique du transgène dans les cônes par ERG (au moins pendant cette période, et selon la sensibilité de la technique d'analyse)[86]. Des études préliminaires n'ont pas montré de diminution apparente de la fonction cône chez les chiens *Pde6β*$^{-/-}$ après injection sous-rétinienne d'AAV-RK-c*Pde6β* (il était important ici de réaliser cette étude chez des chiens *Pde6β*$^{-/-}$ car les cônes peuvent être fragilisés par la dégénérescence des photorécepteurs bâtonnets).

Le chien *Cord1* est un modèle canin de dystrophie cônes-bâtonnets liée à une mutation dans le gène *Rpgrip1*, exprimé dans les photorécepteurs cônes et bâtonnets chez la souris, et dans les photorécepteurs et certains sous-types de cellules amacrines chez l'homme. Chez le chien, l'expression de la protéine RPGRIP1 dans la rétine n'a pas pu être caractérisée car aucun anticorps ne reconnait la protéine canine de manière spécifique, et ce, quelle que soit la technique d'analyse utilisée (immunohistochimie sur coupes congelées, paraffine ou montage à plat). Nous avons également choisi d'utiliser le promoteur RK chez le chien *Cord1* car celui-ci permet une expression du transgène dans les cônes et les bâtonnets. Ce promoteur, couplé à des vecteurs AAV2/5 ou AAV2/8 avait été utilisé avec succès chez plusieurs modèles animaux de dystrophies rétiniennes liées à des mutations dans des gènes exprimés dans les photorécepteurs bâtonnets et cônes [49], [110], [122], [123], [124], [22].

Production des vecteurs rAAV thérapeutiques et injection chez le chien *Rcd1* et *Cord1*

Afin d'évaluer l'efficacité de la thérapie génique d'addition chez le chien *Rcd1 et Cord1*, nous avons générés des vecteurs AAV2/5 et AAV2/8 contenant la séquence codante du gène *Pde6β* canin (c*Pde6β*) ou Rpgrip1 canin (c*Rpgrip1*) sous le contrôle du promoteur RK (**Figure 4a**).

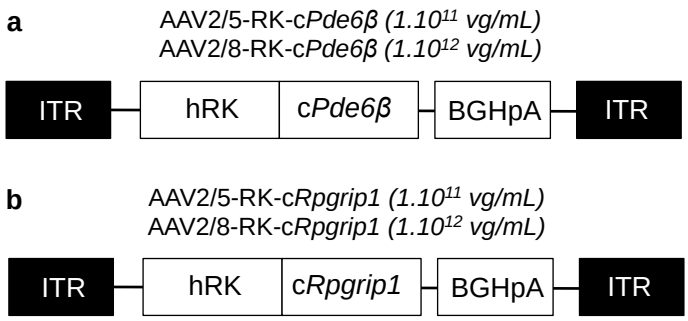

Figure 4. Schéma représentant la structure des vecteurs AAV thérapeutiques.
(**a**) Vecteurs AAV2/5-RK-c*Pde6β* et AAV2/8-RK-c*Pde6β*. Ils contiennent l'ADNc Pde6β canin sous le contrôle du promoteur RK humain (-112 bp à +87 bp).
(**b**) Vecteurs AAV2/5-RK-c*Rpgrip1* et AAV2/8-RK-c*Rpgrip1*. Ils contiennent l'ADNc Rpgrip1 canin sous le contrôle du promoteur RK humain (-112 bp à +87bp).
BGHpA, bovine growth hormone poly-adenylation signal, ITR, séquences terminales répétées de l'AAV2, RK, promoteur rhodopsine kinase humain.

Le gène c*Pde6β* a été amplifié par PCR à partir d'ARN messagers extraits de rétines de chiens sains et la séquence obtenue vérifiée par séquençage. La fonctionnalité de l'ADNc *Pde6β* canin a été vérifiée *in vitro* par transfection de cellules HEK293 avec un plasmide CMV-c*Pde6β* par RT-PCR et Western-Blot (résultats non montrés). Le gène *Rpgrip1* canin a été amplifié par RACE-PCR à l'aide d'amorces dirigées contre des séquences consensus *RPGRIP1* humaine, bovine et murine, et des séquences putatives canines (réalisé par Elsa Lhériteau). La fonctionnalité de l'ADNc *Rpgrip1* canin a été vérifiée *in vitro* par transfection de cellules HEK293 avec un plasmide CMV-c*Rpgrip1* par Western-Blot (résultats non montrés).

Les chiens *Rcd1* et les chiens *Cord1* ont été traités avant la phase de dégénérescence massive des photorécepteurs. Ils ont reçu des quantités équivalentes de vecteurs thérapeutiques (100-150µL de vecteur rAAV2/5 à 1.10^{11} vg/mL ou de vecteur rAAV2/8 à 1.10^{12} vg/mL) [86], [119]. Dans cette étude, l'objectif principal n'était pas de comparer l'efficacité des vecteurs rAAV2/5 et rAAV2/8 mais d'identifier une approche thérapeutique permettant une restauration prononcée du phénotype dystrophique. C'est pourquoi les vecteurs ont été injectés à leur titre maximum de production. Ces doses sont similaires ou inférieures à celles utilisées dans d'autres études précliniques chez des modèles murins ou canins de dystrophies rétiniennes héréditaires.

Au total, huit chiens *Rcd1* ont été traités à l'âge de 20 jours et sept chiens *Cord1* ont été traités à l'âge de 30 jours (**Tableau 1**)**:**

- les chiens ***Rcd1*-A2** à ***Rcd1*-A5** ont reçu de l'AAV2/5-RK-c*Pde6β* (n=4)
- les chiens ***Rcd1*-A6** à ***Rcd1*-A9** ont reçu de l'AAV2/8-RK-c*Pde6β* (n=4)
- les chiens ***Cord1*-A2** à ***Cord1*-A6** ont reçu de l'AAV2/5-RK- c*Rpgrip1* (n=5)
- les chiens ***Cord1*-A7** et ***Cord1*-A8** ont reçu de l'AAV2/8-RK- c*Rpgrip1* (n=2)

Les injections ont été unilatérales, à l'exception du chien *Rcd1*-A9 qui a été injecté dans les deux yeux après un reflux important du vecteur dans le vitré lors de l'injection du premier œil [86]. Les injections ont été majoritairement réalisées dans la partie nasale de la rétine, et couvraient 25-30% de la surface rétinienne totale [86], [119].

Table 1. Liste des chiens inclus dans l'étude et amplitudes ERG.

Chien	Vecteur	Suivi (mpi)	ERG bâtonnet (µV)				30Hz Flicker (µV)			
			1mpi (T/U)	9mpi (T/U)	12mpi (T/U)	24mpi (T/U)	1mpi (T/U)	9mpi (T/U)	12mpi (T/U)	24mpi (T/U)
Rcd1-NA1	None	30	169/166	215/182	150/204	194/162	45/46	67/65	46/49	47/45
Rcd1-A1		36	0/0	11/15	0/0	0/0	44/38	43/56	10/8	11/8
Rcd1-A2	AAV2/5RK-c*Pde6b*	36	47/0	43/10	59/0	44/0	45/53	54/53	27/14	25/9
Rcd1-A3		36	34/0	34/0	48/0	44/0	39/35	17/15	22/8	30/10
Rcd1-A4		30	40/0	52/0	48/0	52/0	51/27	41/39	33/19	32/11
Rcd1-A5		1	nd	†	†	†	nd	†	†	†
Rcd1-A6	AAV2/5RK-c*Pde6b*	30	37/0	87/0	36/0	30/0	21/46	38/15	36/0	30/0
Rcd1-A7		30	45/0	37/0	36/0	30/0	113/114	23/17	22/13	22/6
Rcd1-A8		24	41/0	41/0	52/0	49/0	197/118	62/44	31/13	32/10
Rcd1-A9		4	19/64	†	†	†	37/30	†	†	†

Chien	Vecteur	Suivi (mpi)	30Hz Flicker (µV)				ERG bâtonnet (µV)			
			1mpi (T/U)	9mpi (T/U)	12mpi (T/U)	24mpi (T/U)	1mpi (T/U)	9mpi (T/U)	12mpi (T/U)	24mpi (T/U)
Cord1-NA1	none	24	nd	nd	nd	69/77	nd	nd	nd	186/199
Cord1-A1		24	0/0	0/0	0/0	0/0	121/128	20/12	0/0	0/0
Cord1-A2	AAV2/5-RK-c*Rpgrip1*	24	18/0	21/0	29/0	33/0	185/197	27/16	32/0	41/0
Cord1-A3		18	20/0	15/0	16/0	nd	139/110	46/16	40/0	nd
Cord1-A4		18	26/0	13/0	15/0	16/0[b]	194/184	45/12	48/0	48/0[b]
Cord1-A5		6	19/0	20/0[a]	nd	nd	176/155	107/72[a]	nd	nd
Cord1-A6		0,8	nd	†	†	†	nd	†	†	†
Cord1-A7	AAV2/8-RK-c*Rpgrip1*	24	15/0	27/0	13/0	13/0	113/114	28/0	0/0	0/0
Cord1-A8		24	48/0	53/0	49/0	53/0	197/118	62/44	56/0	50/0

Abréviations : 30Hz Flicker, amplitude du 30Hz Flicker photopique ; A, affecté ; mpi, mois postinjection ; NA, non-affecté, nd , examen non réalisé, T, oeil traité, U, oeil non traité - [a] Examen à 6 mois postinjection - [b] Examen à 18 mois postinjection

Vérification de l'expression du transgène après injection sous-rétinienne

Dans les deux modèles canins, l'injection de vecteur rAAV-c*Pde6β* ou rAAV-c*Rpgrip1* a permis l'expression d'ARNm *Pde6β* ou *Rpgrip1* sains, détectables par RT-PCR allèle spécifique (**Figure 5**) [86], [119]. Au contraire, seuls les produits PCR dérivés des allèles mutés ont été détectés dans les yeux non traités. Ces résultats n'ont pas pu être confirmés au niveau protéique car aucun des anticorps anti-PDE6β murine et humaine et anti-RPGRIP1 murine et humaine ne reconnait spécifiquement les protéines canines en Western-Blot ou immunohistochimie sur coupes de rétines congelées, en paraffine ou montage à plat (résultats non montrés).

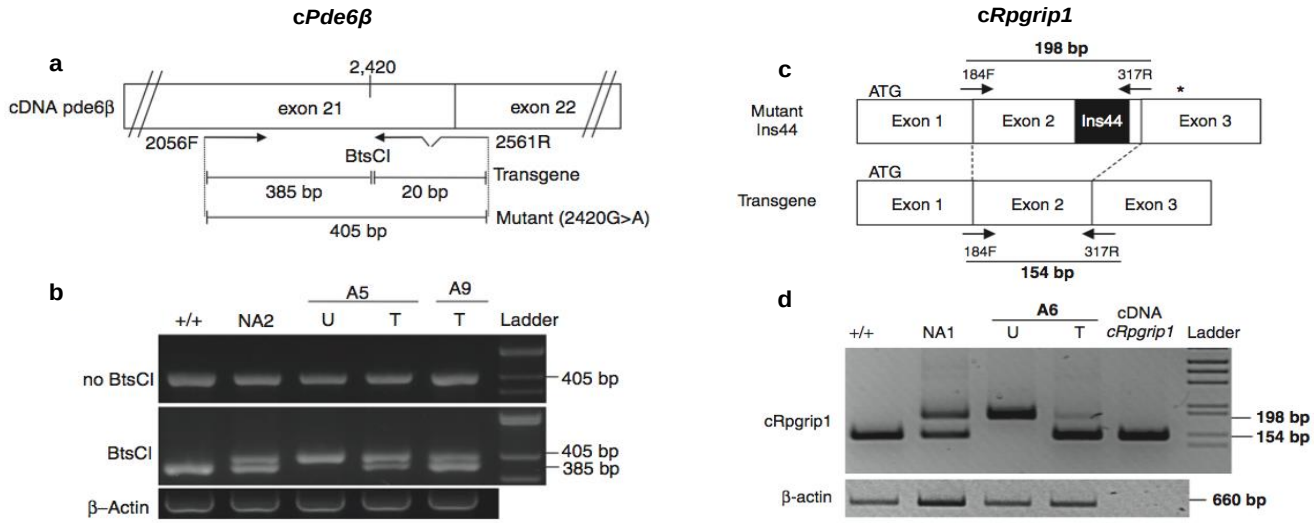

Figure 5. Détection des transcrits *Pde6β* ou *Rpgrip1* issus du transgène (sauvages) ou endogènes (mutés) dans les rétines de chiens *Rcd1*-A5 et *Rcd1*-A9 à 4mpi et *Cord*1-A6 à 1mpi.

(**a-b**) Détection des transcrits *Pde6β*. (**a**) L'amplification d'ADNc rétiniens avec les amorces 2056F et 2561R génère un produit PCR de 405bp comprenant une partie des exons 21 et 22 des transcrits *Pde6β* issus du transgène ou endogènes. L'amorce 2561R crée un site de restriction BtsCl unique dans les produits PCR issus des transcrits *Pde6β* du transgène. Après digestion enzymatique, on obtient alors deux fragments de 385bp et 20bp. Le site BtsCI n'est pas présent dans les produits PCR issus des transcrits *Pde6β* endogènes. (**b**) Gel d'électrophorèse des produits de RT-PCR après digestion complète par BtsCI.

(**c-d**) Détection des transcrits *Rpgrip1*. (**c**) L'amplification d'ADNc rétiniens avec les amorces 184F et 317R génère un produit PCR de 154bp comprenant l'exon 2 des transcrits *Rpgrip1* issus du transgène, et un produit PCR de 198bp comprenant l'exon 2 des *Rpgrip1* endogènes. (**d**) Gel d'électrophorèse des produits de RT-PCR.

+/+, rétine de chien homozygote sain, NA1 ou NA2, rétine de chien non-affecté hétérozygote, T, oeil traité, U, oeil non traité, Ladder, marqueur de taille.

Evaluation de l'effet thérapeutique du transfert de gène chez le chien *Rcd1* et *Cord1*

Après avoir vérifié l'expression du transgène dans les rétines de chiens traités, nous avons évalué l'effet thérapeutique du transfert de gène chez le chien *Rcd1* et *Cord1*. Les dystrophies rétiniennes héréditaires liées à une mutation dans le gène PDE6β ou RPGRIP1 sont caractérisées par une **perte de fonction** et une **dégénérescence** des photorécepteurs rétiniens. Ainsi, l'effet thérapeutique du transfert de gène a été évalué sur les deux composantes de ces pathologies.

➔ *La thérapie génique médiée par des vecteurs AAV a-t-elle amélioré la composante dysfonctionnelle chez les chiens Rcd1 et Cord1 traités?*

Le chien *Rcd1* n'a pas de fonction bâtonnet détectable par ERG dès l'âge de 1 mois (premier examen clinique réalisé). Chez ce chien, l'absence de fonction bâtonnet peut être directement corrélée à la perte de l'activité PDE6 dans les photorécepteurs bâtonnets. En effet, le chien *Rcd1* possède une mutation non-sens dans l'exon 21 du gène *Pde6β* qui tronque la sous-unité catalytique PDE6β de 49 résidus et élimine le domaine C-terminal nécessaire à l'encrage de la sous-unité PDE6β à la membrane (et peut-être également de l'holoenzyme PDE6) [83]. Aucune activité PDE6 des bâtonnets n'est détectée chez de jeunes chiots *Rcd1* [83].

Le chien *Cord1* n'a pas de fonction cône détectable par ERG dès l'âge de 1 mois (premier examen clinique réalisé). Chez le chien *Cord1*, la raison de l'absence totale de fonction cône n'est pas connue. Les analyses histologiques n'ont pas révélé de changement au niveau des segments externes des cônes à l'âge de 6 semaines, même si elles n'excluent pas la possibilité que certains cônes ne soient jamais formés normalement [113]. L'insertion de 44 bp dans le gène *Rpgrip1* canin doit conduire à la production d'une protéine RPGRIP1 dépourvue de son domaine d'interaction avec RPGR. L'absence d'interactions RPGRIP1-RPGR pourrait expliquer l'absence totale de fonction cône chez le chien *Cord1* [111]. Il est également possible qu'une activité supplémentaire de RPGRIP1 soit absente dans les cônes de chien *Cord1*, ou diminuée en dessous du seuil nécessaire au fonctionnement des cônes.

La thérapie génique d'addition médiée par des vecteurs AAV restaure la fonction bâtonnet chez les chiens PDE6β-déficients

Pour évaluer la fonction bâtonnet chez les chiens *Rcd1* après transfert de gène, nous avons réalisé des examens ERG à différents temps postinjection, jusqu'à 30 mois postinjection. Ces examens ont été réalisé en parallèle chez des chiens contrôles *Pde6β*$^{+/-}$ et *Pde6β*$^{-/-}$ non injectés [86].

Dès 1 mois postinjection, une restauration de fonction bâtonnet a été détectée dans les yeux traités. De façon très intéressante cette fonction est restée **stable pendant au moins 30 mois** (dernier examen réalisé) (**Figure 6a**). **Elle correspondait à 28-35% de la réponse détectée chez des animaux sains, en accord avec la surface de la rétine directement exposée au vecteur thérapeutique (25-30% de la surface totale).**
Les amplitudes des réponses ERG restaurées ont été identiques chez les chiens traités avec le vecteur rAAV2/5 ou rAAV2/8, et ce malgré le fait que le vecteur rAAV2/8 ait été injecté à un titre dix fois plus élevé que le vecteur rAAV2/5 [86]. **Il est possible que dans les deux cas, le seuil d'expression de PDE6β permettant d'obtenir une fonction PDE6 totale ait été atteint.** PDE6β est probablement titrée par la quantité de sous-unités PDE6α présente, et l'activité PDE6 fortement régulée.
Il n'a malheureusement pas été possible de vérifier cette hypothèse en quantifiant les niveaux relatifs d'expression de PDE6β dans les rétines traitées avec le vecteur rAAV2/5 ou rAAV2/8. Nous avons développé une RT-qPCR allèle spécifique pour quantifier les niveaux d'expression des ARNm PDE6β mutés et sauvages, mais l'efficacité et la reproductibilité de la méthode n'étaient pas suffisantes. La mise au point test enzymatique *in vitro* pourrait être intéressante pour comparer les niveaux d'activité PDE6 restaurés dans les yeux traités avec de l'AAV2/5 et de l'AAV2/8.

La thérapie génique d'addition médiée par des vecteurs AAV restaure la fonction cône chez les chiens RPGRIP1-déficients

Pour évaluer la fonction cônes chez les chiens *Cord1* après transfert de gène, nous avons réalisé des examens ERG à différents temps postinjection, jusqu'à 24 mois postinjection. Ces examens ont été réalisé en parallèle chez des chiens contrôles *Rpgrip1*$^{+/-}$ et *Rpgrip1*$^{-/-}$ non injectés .[119]

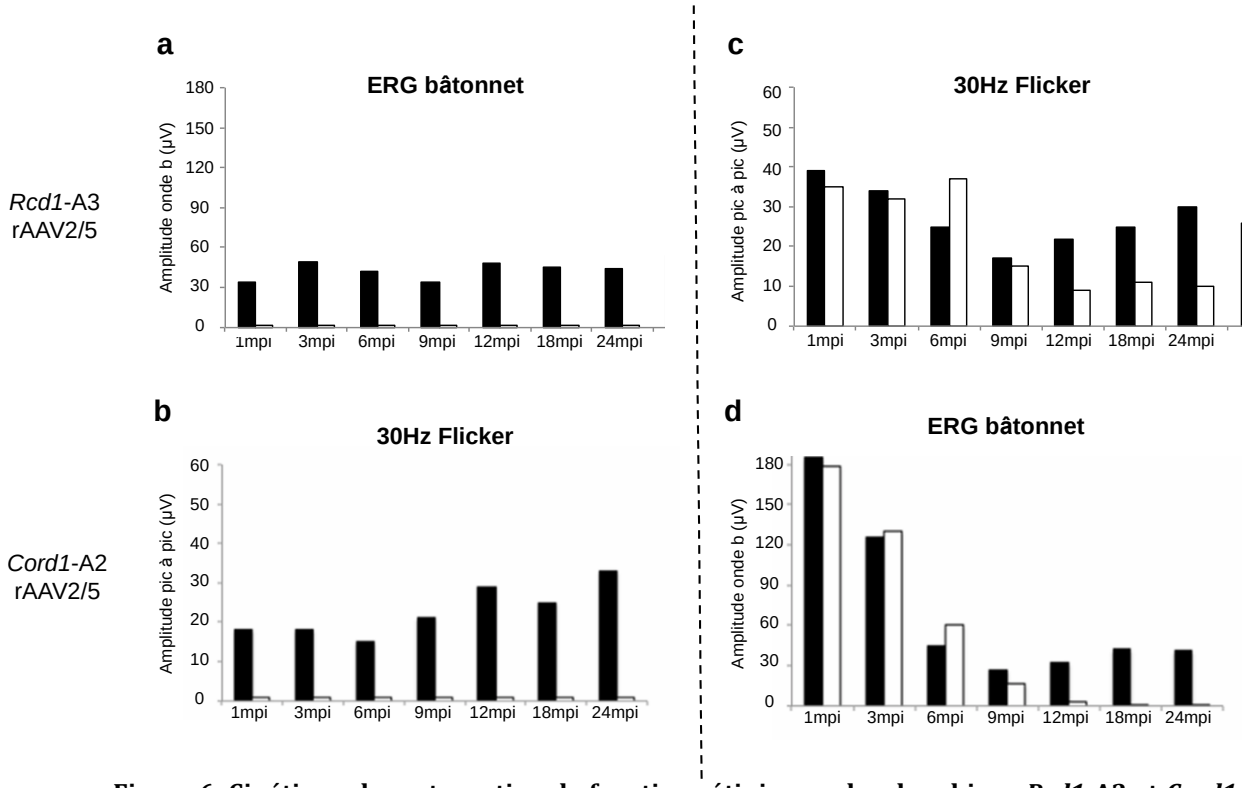

Figure 6. Cinétique de restauration de fonction rétinienne chez les chiens *Rcd1*-A3 et *Cord1*-A2. Amplitudes des réponses ERG obtenues chez le chien Rcd1-A3 de 1 à 24 mois après l'injection d'AAV2/5-RK-c*Pde6β*. (**c-d**) Amplitudes des réponses ERG obtenues chez le chien Cord1-A2 de 1 à 24 mois après l'injection d'AAV2/5-RK-c*Rpgrip1*. Les graphiques a et d représentent les amplitudes de l'onde b de l'ERG scotopique. Les graphiques b et c représentent les amplitudes pic à pic du flicker 30Hz photopique. Les yeux traités sont en noir. Les yeux non-traités sont en blanc. AAV, virus adéno-associé ; mpi, mois postinjection.

L'injection d'AAV2/5-RK-c*Rpgrip1* ou d'AAV2/8-RK-c*Rpgrip1* a restauré une fonction cône dans tous les yeux traités dès 1 mois postinjection. Cette fonction cône, est restée stable pendant au moins 24 mois (dernier examen réalisé) (Figure 6b). Elle représentait **18 à 72%** de la réponse détectée chez des animaux sains, et ce malgré le fait que les injections sous-rétiniennes couvraient toujours environ 30% de la surface totale de la rétine. Les différents niveaux de fonction cône restaurée ne semblent pas être corrélés au sérotype d'AAV utilisé [119]. Néanmoins, il est nécessaire d'injecter plus de chiens avec le sérotype 8 pour tirer une conclusion définitive.

Les différents niveaux de fonction cône obtenus pourraient refléter des variations interindividuelles au niveau de l'efficacité de transduction des cônes et/ou d'une éventuelle l'**altération physiologique des cellules au moment du traitement**. Ils pourraient également refléter une **corrélation entre le niveau de fonction cône restaurée et le lieu de l'injection**. En effet, la distribution des cônes au niveau de la rétine de chien est particulièrement hétérogène. Compte-tenu de la forte proportion de cônes dans le « visual streak » (ratio cônes : bâtonnets = 1 : 10), il est possible que l'inclusion ou non de cette région dans la zone traitée conduise à des variations importantes du nombre total de cônes transduits (et donc du niveau de fonction cône

restaurée). De plus, les cônes situés dans le « visual streak » pourraient être mieux préservés que les cônes situés dans la rétine périphérique riche en bâtonnets.
Chez les chiens RPE65-déficients, une récente étude a démontré une corrélation positive entre le niveau d'amplitude des réponses ERG restaurées et l'inclusion de l'*area centralis* dans la zone traitée. Chez le chien *Rpe65*$^{-/-}$, les photorécepteurs situés dans l'*area centralis* dégénèrent plus lentement que les photorécepteurs situés dans la rétine périphérique [35].

➔*La thérapie génique médiée par des vecteurs AAV a-t-elle amélioré la composante dégénérescence chez les chiens Rcd1 et Cord1?*

Pour être efficace, la thérapie génique d'addition doit permettre de restaurer la fonction des photorécepteurs déficients, mais également prévenir leur dégénérescence. En effet, pour obtenir un effet au long-terme du transfert de gène, il faut que la dégénérescence rétinienne s'arrête.

La thérapie génique d'addition médiée par des vecteurs AAV permet aux bâtonnets *Rcd1* transduits de retrouver un équilibre physiologique.

Chez le chien *Rcd1*, la mort des bâtonnets est supposée être directement corrélée à l'absence de fonction PDE6 et l'accumulation de GMPc et de calcium dans les segments externes des photorécepteurs. Pour déterminer si la thérapie génique pouvait prévenir la mort des photorécepteurs bâtonnets chez le chien *Rcd1*, nous avons (i) évalué la morphologie et l'épaisseur des rétines des chiens traités par fond d'oeil et OCT de 4 à 30 mois postinjection et (ii) compté le nombre de noyaux de photorécepteurs restants dans la couche externe de noyaux à 4 et 30 mois postinjection à partir de coupes congelées de rétine contenant la zone exposée au vecteur thérapeutique, et la zone non-exposée au vecteur thérapeutique [86].
Ces examens ont tous montré un maintien significatif de la structure de la rétine dans les zones exposées aux vecteurs thérapeutiques chez les chiens traités avec de l'AAV2/5-RK-c*Pde6β* ou de l'AAV2/8-RK-c*Pde6β*. **Plus de 90% des photorécepteurs ont été préservés dans les zones exposées aux vecteurs pendant au moins 24 mois postinjection (Figure 7a, droite et gauche)**. A cet âge, dans les zones non-exposées aux vecteurs thérapeutiques, tous les photorécepteurs avaient disparus, à l'exception d'une ou deux rangées de noyaux de cônes encore présents au niveau du « visual streak » (**Figure 7a, milieu**). **Il semble donc que le transfert de gène Pde6β chez le chien *Rcd1* ait permis aux photorécepteurs bâtonnets transduits de retrouver leur équilibre**

physiologique. Il s'agit du traitement le plus durable d'une pathologie liée à une mutation dans un gène spécifique des photorécepteurs.

Une préservation presque complète des photorécepteurs a précédemment été observée chez des chiens *Rpe65*$^{-/-}$ (modèles de dystrophies rétiniennes liées un défaut dans l'EPR) traités avec de l'AAV2/2-CBA-h*RPE65* avant le début de la dégénérescence des photorécepteurs. Dans les rétines des chiens *Rpe65*$^{-/-}$ traités, l'épaisseur de la couche externe de noyaux dans la zone exposée au vecteur était proche de la normale 9 ans postinjection, alors que cette couche externe de noyaux avait complètement disparu dans les zones non-exposées au vecteur [34].

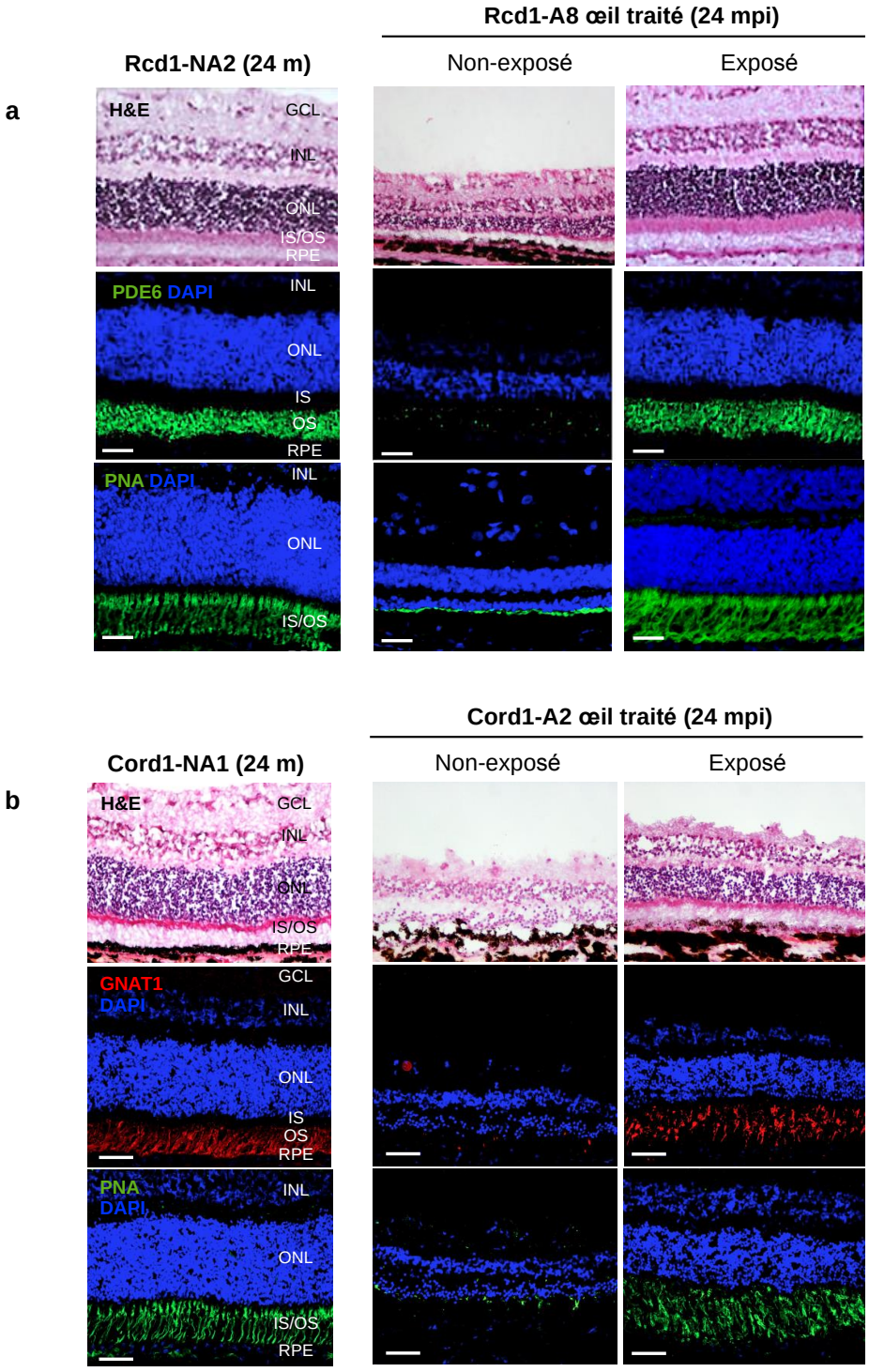

Figure 7. Evaluation post-mortem de la morphologie rétinienne chez les chiens *Rcd1*-A8 et *Cord1*-A2 à 24 mois postinjection.

(**a**) Images microscopiques de coupes de rétine de l'oeil traité du chien *Rcd1*-A8 à 24 mois postinjection et du chien contrôle *Rcd1*-NA2 à 24 mois. Les coupes de rétine, ont été colorées à l'hématoxyline-et éosine ou immunomarquées avec un anticorps dirigé contre l'holoenzyme PDE6 ou peanut agglutinin (PNA)-FITC.

(**b**) Images microscopiques de coupes de rétine de l'oeil traité du chien Cord1-A1 à 24 mois postinjection et du chien contrôle *Cord1*-NA1 à 24 mois. Les coupes de rétine ont été colorées à l'hématoxyline et éosine ou immunmarquées avec un anticorps dirigé contre la protéine GNAT1 (transducine) ou peanut agglutinin (PNA)-FITC.

GCL, couche de cellule ganglionnaires; INL, couche nucléaire interne ; ONL, couche nucléaire externe, IS, segments internes ; OS, segments externes.

`De façon très intéressante, la mort des deux tiers des photorécepteurs qui n'avaient pas été exposés au vecteur thérapeutique n'a pas eu d'impact négatif majeur sur la survie des photorécepteurs *Rcd1* dans la région traitée, comme cela avait été précédemment montré chez le chien *Rpe65*$^{-/-}$ [34]. Ce phénomène de mort non-autonome des photorécepteurs avait pourtant été mis en évidence dans des rétines de souris chimères qui contiennent des photorécepteurs bâtonnets génétiquement sains et des photorécepteurs bâtonnets mutés dans le gène de la rhodopsine [2]. Chez ces souris, la mort des photorécepteurs mutés provoquait la mort des photorécepteurs sains, et ce, même lorsque 42% de la rétine était composée de photorécepteurs sains [2]. La mort des bâtonnets chez le chien *Rcd1* ou *Rpe65*$^{-/-}$ pourrait faire intervenir un mécanisme différent de celui impliqué dans la mort des bâtonnets déficients en rhodopsine. Il est également possible que la survie au long-terme des photorécepteurs traités chez les modèles canins reflète **la forte densité des cellules sauvées dans les zones exposées au vecteur**. En effet, chez les souris chimères, les bâtonnets sains et mutants formaient une mosaïque, et la vitesse de dégénérescence des bâtonnets sains ralentissait quand le nombre de photorécepteurs sains dans la rétine augmentait [2]. Chez le chien *Rcd1,* une démarcation nette entre la zone traitée et les zones non traitées a été observée (**Figure 8**).

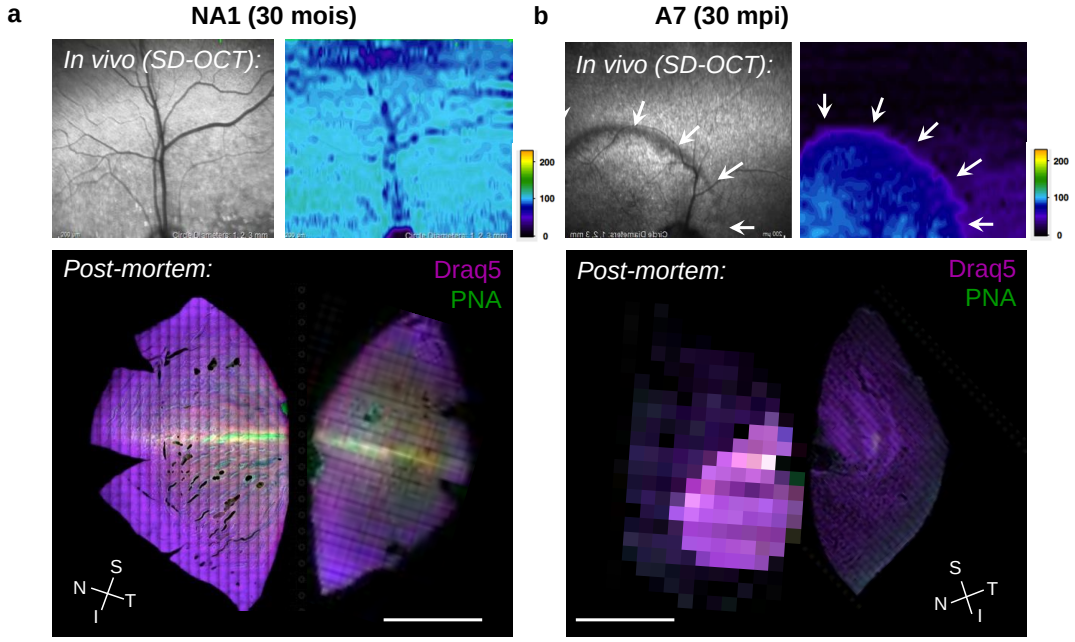

Figure 8. Evaluation in vivo et post-mortem de l'épaisseur de la couche des photorécepteurs chez le chien *Rcd1*-NA1 et *Rcd1*-A7 à 30 mois postinjection. Haut : photographies du fond d'œil et cartographie de l'épaisseur de la couche nucléaire externe. Les flèches blanches représentent la zone directement exposée au vecteur thérapeutique. Bas : images de microscopie confocale de rétines en montage à plat marquées avec Draq5 (marqueur de noyaux) et PNA-FITC. Dans la rétine du chien A7, l'épaisseur de la couche nucléaire externe est uniquement préservée dans la zone traitée. S, supérieur, T, temporal, I, inférieur, N, nasal. (Petit L et al. manuscrit en préparation).

Cette hypothèse est cohérente avec les études précédemment menées chez le poisson zèbre qui ont démontré qu'il existait **un seuil critique de photorécepteurs en dessous duquel les photorécepteurs sains sont impactés et meurent.** Ceci pourrait avoir une importance pour le futur traitement des patients PDE6β-déficients qui ont une dégénérescence rétinienne très avancée en périphérie au moment de leur diagnostic.

La thérapie génique d'addition médiée par des vecteurs AAV préserve les photorécepteurs cônes chez le chien *Rcd1*.

Chez le chien *Rcd1*, comme chez la plupart des modèles animaux de dystrophies bâtonnets-cônes, la mort de photorécepteurs bâtonnets provoque la dégénérescence des photorécepteurs cônes [1]. Ainsi, si le nombre de photorécepteurs bâtonnets préservés est trop faible, il est possible que les photorécepteurs cônes ne survivent pas à long-terme. Les photorécepteurs cônes sont les cellules les plus importantes pour la vue humaine car ils sont responsables de la vision diurne, chromatique et de l'acuité visuelle. La dégénérescence et la perte de fonction cône constituent de ce fait un handicap majeur pour les patients.

En accord avec la préservation de 90% des photorécepteurs bâtonnets dans la zone traitée des chiens *Rcd1*, nous avons observé une perte de fonction cône retardée dans les yeux *Rcd1* traités (**Figure 6c**). A 24 mois postinjection, 67% de la fonction cône initiale était préservée dans les yeux traités, soit 3 fois plus que les réponses enregistrées dans les yeux non-traitées (23%) (Petit L, *et al*., manuscrit en préparation). **Ce résultat indique que la préservation des photorécepteurs bâtonnets chez le chien *Rcd1* a été suffisante pour repousser et/ou ralentir la mort secondaire des cônes dans les rétines de chiens traités. Il s'agit de l'effet le plus marqué sur la survie des cônes observé jusqu'à présent chez un modèle animal de dystrophies bâtonnets-cônes.** Les études précédentes, réalisées chez la souris, n'ont pas poursuivi leur suivi si longtemps.

Un projet de recherche est actuellement en cours pour caractériser et comprendre la survie des cônes chez le chien *Rcd1* traité. Les résultats préliminaires indiquent que le délai d'initiation de la perte de fonction cône correspond à la préservation des cônes dans la zone traitée. Chez des chiens non-traités, ces cônes sont les premiers à mourir entre l'âge de 12 et 18 mois (Petit L, *et al*., manuscrit en préparation). Les cônes situés dans la zone traitée sont complètement préservés jusqu'à 24 mois postinjection (**Figure 7a**). Au contraire, dans le reste de la rétine, la cinétique de dégénérescence des cônes reste globalement inchangée. Une chute drastique du nombre de cônes survivants est observée

à la frontière de la zone traitée, ce qui indique que les cônes pourraient dépendre de la présence physique des bâtonnets pour leur survie au long-terme (Petit L, *et al*., manuscrit en préparation) (**Figure 8**).

Chez le chien *Cord1*, la dégénérescence rétinienne continue malgré le transfert de gène.

Chez le chien *Cord1*, les raisons de la mort des photorécepteurs cônes et bâtonnets ne sont pas connues. Pour déterminer si la thérapie génique pouvait prévenir la mort des photorécepteurs bâtonnets chez le chien *Cord1*, nous avons (i) évalué la morphologie et l'épaisseur des rétines des chiens traités par fond d'œil et OCT de 3 à 24 mois postinjection, (ii) cartographié la distribution des photorécepteurs dans la rétine des chiens traités et (iii) compté le nombre de noyaux de photorécepteurs restants dans la couche externe de noyaux à 24 mois postinjection à partir de coupes congelées de rétine contenant une zone exposée au vecteur et une zone non-exposée au vecteur [119].
Ces examens ont tous montré un maintien significatif de la structure de la rétine dans les zones exposées aux vecteurs thérapeutiques chez les chiens traités avec de l'AAV2/5-RK-c*Rpgrip1* ou de l'AAV2/8-RK-c*Rpgrip1* (**Figure 7b**). **Cependant, contrairement à ce qui avait été observé chez le chien *Rcd1*, le nombre de photorécepteurs dans la zone traité a continué de diminuer entre 3 à 24 mois après le traitement (Figure 9)**.

Ainsi, à 24 mois postinjection, seulement 50 à 60% des photorécepteurs étaient encore présents dans la zone traitée des rétines de chiens *Cord1* (**Figure 7b**). Une diminution de l'épaisseur de la rétine traitée au cours du temps avait déjà été observée (i) chez le chien XLPRA2, un modèle gros animal de dystrophie « bâtonnets-cônes » liée à une mutation dans le gène RPGR [118] et chez (ii) des patients atteints l'ACL liée à des mutations dans le gène RPE65, traités à des stades tardifs de la dégénérescence rétinienne [34].
Plusieurs raisons peuvent expliquer pourquoi la dégénérescence des photorécepteurs continue malgré le traitement : (i) certains photorécepteurs n'ont pas été transduits, (ii) la dégénérescence des photorécepteurs avait déjà débutée au moment de l'expression maximale du transgène et l'introduction du gène sauvage n'a pas permis d'empêcher l'apoptose (iii) le niveau d'expression du transgène dans certains photorécepteurs n'était pas suffisant pour prévenir leur dégénérescence.

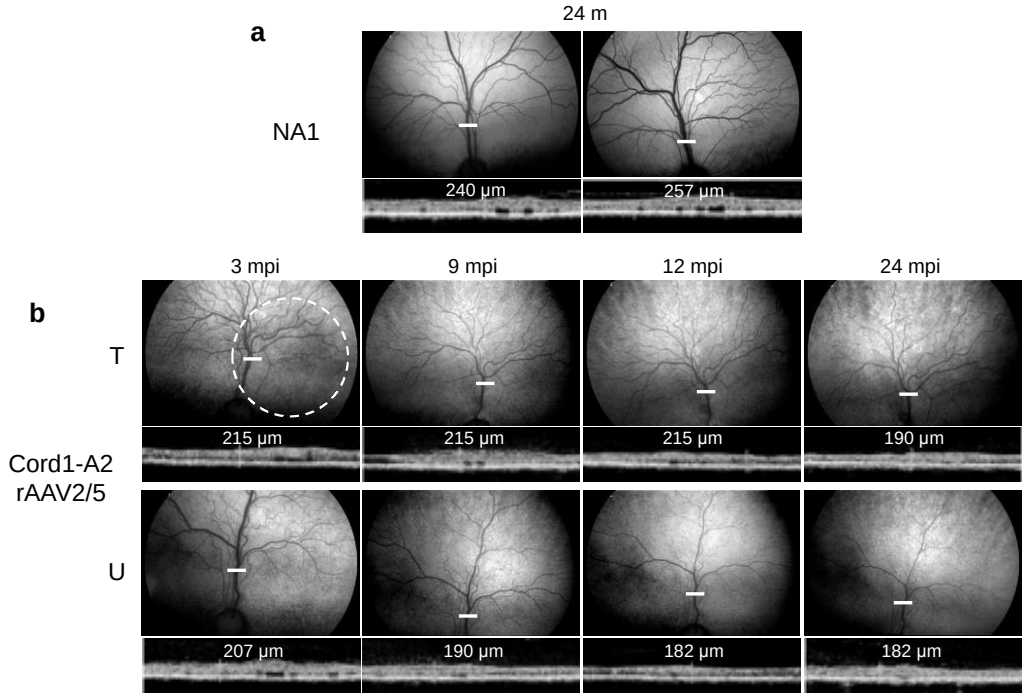

Figure 9. Evaluation *in vivo* de la morphologie rétinienne chez le chien Cord1-A2 à 3, 9, 12 et 24 mois postinjection. (**a**) Photographies du fond d'œil et images OCT obtenues à partir des yeux droite et gauche du chien contrôle *Cord1*-NA1. (**b**) Photographies du fond d'œil et images OCT obtenues à partir de la rétine traitée (T) et non-traitée (U) du chien Cord1-A2 traité avec de l'AAV2/5-RK-cRpgrip1. Le cercle blanc indique la zone directement exposée au vecteur thérapeutique. Les OCT ont été réalisés selon une ligne horizontale représentée en blanc sur les photographies du fond d'œil. L'épaisseur rétinienne a été mesurée à des endroits similaires (13mm au dessus du nerf optique). m, mois, mpi, mois postinjection.

Chez le chien *Cord1*, la fonction visuelle reste stable malgré la dégénérescence des photorécepteurs

De façon très intéressante, la dégénérescence des photorécepteurs dans la zone traitée du chien *Cord1*, visible par OCT de 3 à 24 mois postinjection, n'est pas associée à une perte de la fonction cône restaurée (qui reste stable de 1 à 24 mois postinjection) ou de la fonction bâtonnet (qui se stabilise de 12 à 24 mois postinjection) (**Figure 6b,d**) [119]. Un résultat similaire a été récemment obtenu chez des patients RPE65-déficients traités à des stades tardifs de la pathologie. Chez ces patients, la cinétique de dégénérescence rétinienne n'est pas modifiée 3 ans après traitement, et ce malgré une amélioration stable des capacités visuelles [34].

Pour expliquer le résultat obtenu chez les patients RPE65-déficients, Cideciyan et al. ont proposé que le transfert de gène n'était pas suffisant pour stopper la dégénérescence des photorécepteurs et que les cellules fonctionnelles étaient les cellules qui allaient mourir en dernier [34]. Selon ce modèle, la perte de fonction est lente au départ (lors de la mort de cellules non-traitées), puis la fonction visuelle restaurée est de plus en plus impactée au

fur et à mesure que les dernières cellules survivantes (traitées) commencent à mourir [34]. Cette hypothèse est cohérente avec l'observation que la dégénérescence des photorécepteurs n'est pas homogène chez la plupart des patients atteints de dystrophies rétiniennes héréditaires. Cependant, comme la dégénérescence des photorécepteurs progresse lentement chez les patients RPE65-déficients, plusieurs années de suivi seront encore nécessaires pour valider ou réfuter cette hypothèse.

Chez les chiens *Cord1*, la dégénérescence rétinienne est beaucoup plus rapide. Une perte quasi totale des photorécepteurs rétiniens est observée à l'âge de 24 mois. De plus, la perte de fonction bâtonnet, qui précède la dégénérescence des photorécepteurs, est totale à l'âge de 12 mois [113], [112]. Nos analyses de la fonction bâtonnet chez les chiens *Cord1* ont indiqué que pendant les 6-9 premiers mois après le traitement, la perte de fonction bâtonnet progressait de manière identique dans les yeux traités et non-traités. Cependant, un suivi des animaux traités à plus long terme a montré que la fonction bâtonnet se stabilisait ensuite de 12 à 24 mois postinjection (**Figure 6d**). **Ce résultat semble indiquer que certains photorécepteurs fonctionnels survivent à des stades tardifs de la dégénérescence rétinienne** [119].

Un suivi à plus long terme de l'épaisseur de la couche des photorécepteurs par OCT sera essentiel pour déterminer s'il y aura ou non une stabilisation du nombre de photorécepteurs dans la zone traitée à un stade plus tardif de la maladie**. Néanmoins, ces résultats préliminaires indiquent déjà qu'il pourrait y avoir une population mixte de photorécepteurs dans la zone traitée au moment de l'intervention thérapeutique:**

- **des photorécepteurs qui ne répondent pas du tout au traitement : les photorécepteurs ne sont pas sauvés fonctionnellement <u>et</u> dégénèrent physiquement (appelés cellules « OFF »)**
- **des photorécepteurs qui répondent entièrement au traitement : ils sont sauvés fonctionnellement <u>et</u> ils sont physiquement stables (appelés cellules « ON »).**

Il est alors très intéressant de noter ici que trois modèles murins de dystrophies des photorécepteurs, la souris *Rpgrip1*$^{-/-}$ [109], la souris *Aipl1*$^{h/h}$ [48] et la souris *Bbs4*$^{-/-}$ [126] partagent la même cinétique de dégénérescence des bâtonnets après un traitement par thérapie génique, c'est à dire, une diminution initiale de la fonction bâtonnet (cellules OFF) suivie par une stabilisation (cellules ON). En particulier, chez la souris *Aipl1*$^{h/h}$, **la stabilisation de la fonction bâtonnet dans les yeux traités apparait plus tôt lorsque**

la vitesse de dégénérescence rétinienne est augmentée par l'exposition constante des souris à la lumière (stabilisation à 9 semaines contre 12 semaines après l'injection) [48]. **Ce résultat suggère que la population de bâtonnets sauvés (cellules ON) est présente très rapidement après l'injection, mais que cette population est faible et ne peut pas être détectée par ERG avant que la plupart des photorécepteurs non sauvés perdent leur fonction (cellules OFF).**

L'état physiologique des photorécepteurs au moment du traitement pourrait déterminer leurs caractéristiques « ON » ou « OFF ». De plus, lors de la progression de la pathologie, la proportion de cellules « ON » ou « OFF » présentes dans la rétine pourrait changer, avec une diminution rapide du nombre de cellules « ON ».

Ce modèle « OFF/ON » peut être considéré, à juste titre, comme un facteur limitant pour l'application de ces thérapies chez des patients à des stades avancés de la pathologie.

Néanmoins, il est très important de mentionner ici, que si certains patients RPE65-déficients, conservent une amélioration fonctionnelle alors que la dégénérescence des photorécepteurs continue de progresser dans la zone traitée, certaines cellules « ON » pourraient être toujours présentes à des stades tardifs de la pathologie [34]. De plus, malgré la présence de très peu de cellules « ON », certains patients RPE65 ont connu une amélioration très significative de leur qualité de vie après traitement. Il pourrait donc toujours y avoir un réel potentiel de la thérapie génique d'addition pour le traitement des dystrophies rétiniennes héréditaires, en particulier si le traitement des cellules « ON » est un gage de stabilité de l'effet thérapeutique dans le temps.

Conclusion

L'objectif de cette thèse était d'évaluer l'efficacité de la thérapie génique d'addition chez deux modèles canins de formes sévères de dégénérescence des photorécepteurs : (i) le chien *Pde6β*$^{-/-}$, un modèle de dystrophie bâtonnets-cônes et (ii) le chien *Rpgrip1*$^{-/-}$, un modèle canin de dystrophie cônes-bâtonnets. A l'aide de vecteurs AAV2/5 et AA2/8, nous avons montré pour la première fois qu'il était possible restaurer la fonction rétinienne, de préserver la structure des photorécepteurs et le comportement visuel de modèles gros animaux de dystrophies des photorécepteurs. Les caractéristiques physiopathologiques de ces modèles canins étant très proches de celles rencontrées chez l'homme, ces résultats précliniques représentent une étape importante pour le traitement futur des patients atteints de dégénérescence des photorécepteurs.

References

1. Punzo, C., W. Xiong, and C.L. Cepko, *Loss of daylight vision in retinal degeneration: are oxidative stress and metabolic dysregulation to blame?* J Biol Chem, 2012. **287**(3): p. 1642-8.

2. Huang, P.C., et al., *Cellular interactions implicated in the mechanism of photoreceptor degeneration in transgenic mice expressing a mutant rhodopsin gene.* Proc Natl Acad Sci U S A, 1993. **90**(18): p. 8484-8.

3. Kedzierski, W., D. Bok, and G.H. Travis, *Non-cell-autonomous photoreceptor degeneration in rds mutant mice mosaic for expression of a rescue transgene.* J Neurosci, 1998. **18**(11): p. 4076-82.

4. Mohand-Said, S., et al., *Normal retina releases a diffusible factor stimulating cone survival in the retinal degeneration mouse.* Proc Natl Acad Sci U S A, 1998. **95**(14): p. 8357-62.

5. Mohand-Said, S., et al., *Selective transplantation of rods delays cone loss in a retinitis pigmentosa model.* Arch Ophthalmol, 2000. **118**(6): p. 807-11.

6. Leveillard, T. and J.A. Sahel, *Rod-derived cone viability factor for treating blinding diseases: from clinic to redox signaling.* Sci Transl Med, 2010. **2**(26): p. 26ps16.

7. Shen, J., et al., *Oxidative damage is a potential cause of cone cell death in retinitis pigmentosa.* J Cell Physiol, 2005. **203**(3): p. 457-64.

8. Komeima, K., et al., *Antioxidants reduce cone cell death in a model of retinitis pigmentosa.* Proc Natl Acad Sci U S A, 2006. **103**(30): p. 11300-5.

9. Usui, S., et al., *Increased expression of catalase and superoxide dismutase 2 reduces cone cell death in retinitis pigmentosa.* Mol Ther, 2009. **17**(5): p. 778-86.

10. Usui, S., et al., *NADPH oxidase plays a central role in cone cell death in retinitis pigmentosa.* J Neurochem, 2009. **110**(3): p. 1028-37.

11. Usui, S., et al., *Overexpression of SOD in retina: need for increase in H2O2-detoxifying enzyme in same cellular compartment.* Free Radic Biol Med, 2011. **51**(7): p. 1347-54.

12. Punzo, C., K. Kornacker, and C.L. Cepko, *Stimulation of the insulin/mTOR pathway delays cone death in a mouse model of retinitis pigmentosa.* Nat Neurosci, 2009. **12**(1): p. 44-52.

13. Vandenberghe, L.H. and A. Auricchio, *Novel adeno-associated viral vectors for retinal gene therapy.* Gene Ther, 2012. **19**(2): p. 162-8.

14. Mussolino, C., et al., *AAV-mediated photoreceptor transduction of the pig cone-enriched retina.* Gene Ther, 2011. **18**(7): p. 637-45.

15. Ali, R.R., et al., *Adeno-associated virus gene transfer to mouse retina.* Hum Gene Ther, 1998. **9**(1): p. 81-6.

16. Bainbridge, J.W., et al., *Stable rAAV-mediated transduction of rod and cone photoreceptors in the canine retina.* Gene Ther, 2003. **10**(16): p. 1336-44.

17. Le Meur, G., et al., *Postsurgical assessment and long-term safety of recombinant adeno-associated virus-mediated gene transfer into the retinas of dogs and primates.* Arch Ophthalmol, 2005. **123**(4): p. 500-6.

18. Bennett, J., et al., *Cross-species comparison of in vivo reporter gene expression after recombinant adeno-associated virus-mediated retinal transduction.* Methods Enzymol, 2000. **316**: p. 777-89.

19. Allocca, M., et al., *Novel adeno-associated virus serotypes efficiently transduce murine photoreceptors.* J Virol, 2007. **81**(20): p. 11372-80.

20. Vandenberghe, L.H., et al., *Dosage thresholds for AAV2 and AAV8 photoreceptor gene therapy in monkey.* Sci Transl Med, 2011. **3**(88): p. 88ra54.

21. Vandenberghe, L.H., et al., *AAV9 targets cone photoreceptors in the nonhuman primate retina.* PLoS One, 2013. **8**(1): p. e53463.

22. Manfredi, A., et al., *Combined Rod and Cone Transduction by Adeno-Associated Virus 2/8.* Hum Gene Ther, 2013.

23. Petrs-Silva, H., et al., *Novel properties of tyrosine-mutant AAV2 vectors in the mouse retina.* Mol Ther, 2011. **19**(2): p. 293-301.

24. Mowat, F.M., et al., *Tyrosine capsid-mutant AAV vectors for gene delivery to the canine retina from a subretinal or intravitreal approach.* Gene Ther, 2013.

25. Smith, A.J., J.W. Bainbridge, and R.R. Ali, *Gene supplementation therapy for recessive forms of inherited retinal dystrophies.* Gene Ther, 2012. **19**(2): p. 154-61.

26. Colella, P. and A. Auricchio, *Gene therapy of inherited retinopathies: a long and successful road from viral vectors to patients.* Hum Gene Ther, 2012. **23**(8): p. 796-807.

27. Pang, J.J., et al., *AAV-mediated gene therapy in mouse models of recessive retinal degeneration.* Curr Mol Med, 2012. **12**(3): p. 316-30.

28. Boye, S.E., et al., *A comprehensive review of retinal gene therapy.* Mol Ther, 2013. **21**(3): p. 509-19.

29. Acland, G.M., et al., *Gene therapy restores vision in a canine model of childhood blindness.* Nat Genet, 2001. **28**(1): p. 92-5.

30. Narfstrom, K., et al., *Functional and structural recovery of the retina after gene therapy in the RPE65 null mutation dog.* Invest Ophthalmol Vis Sci, 2003. **44**(4): p. 1663-72.

31. Narfstrom, K., et al., *Assessment of structure and function over a 3-year period after gene transfer in RPE65-/- dogs.* Doc Ophthalmol, 2005. **111**(1): p. 39-48.

32. Acland, G.M., et al., *Long-term restoration of rod and cone vision by single dose rAAV-mediated gene transfer to the retina in a canine model of childhood blindness.* Mol Ther, 2005. **12**(6): p. 1072-82.

33. Le Meur, G., et al., *Restoration of vision in RPE65-deficient Briard dogs using an AAV serotype 4 vector that specifically targets the retinal pigmented epithelium.* Gene Ther, 2007. **14**(4): p. 292-303.

34. Cideciyan, A.V., et al., *Human retinal gene therapy for Leber congenital amaurosis shows advancing retinal degeneration despite enduring visual improvement.* Proc Natl Acad Sci U S A, 2013. **110**(6): p. E517-25.

35. Annear, M.J., et al., *Successful gene therapy in older Rpe65-deficient dogs following subretinal injection of an adeno-associated vector expressing RPE65.* Hum Gene Ther, 2013. **24**(10): p. 883-93.

36. Hernandez, M., et al., *Altered expression of retinal molecular markers in the canine RPE65 model of Leber congenital amaurosis.* Invest Ophthalmol Vis Sci, 2010. **51**(12): p. 6793-802.

37. Mowat, F.M., et al., *RPE65 gene therapy slows cone loss in Rpe65-deficient dogs.* Gene Ther, 2013. **20**(5): p. 545-55.

38. Maguire, A.M., et al., *Safety and efficacy of gene transfer for Leber's congenital amaurosis.* N Engl J Med, 2008. **358**(21): p. 2240-8.

39. Maguire, A.M., et al., *Age-dependent effects of RPE65 gene therapy for Leber's congenital amaurosis: a phase 1 dose-escalation trial.* Lancet, 2009. **374**(9701): p. 1597-605.

40. Simonelli, F., et al., *Gene therapy for Leber's congenital amaurosis is safe and effective through 1.5 years after vector administration.* Mol Ther, 2010. **18**(3): p. 643-50.

41. Bainbridge, J.W., et al., *Effect of gene therapy on visual function in Leber's congenital amaurosis.* N Engl J Med, 2008. **358**(21): p. 2231-9.

42. Jacobson, S.G., et al., *Gene therapy for leber congenital amaurosis caused by RPE65 mutations: safety and efficacy in 15 children and adults followed up to 3 years.* Arch Ophthalmol, 2012. **130**(1): p. 9-24.

43. Hauswirth, W.W., et al., *Treatment of leber congenital amaurosis due to RPE65 mutations by ocular subretinal injection of adeno-associated virus gene vector: short-term results of a phase I trial.* Hum Gene Ther, 2008. **19**(10): p. 979-90.

44. Cideciyan, A.V., et al., *Human RPE65 gene therapy for Leber congenital amaurosis: persistence of early visual improvements and safety at 1 year.* Hum Gene Ther, 2009. **20**(9): p. 999-1004.

45. Carvalho, L.S., et al., *Long-term and age-dependent restoration of visual function in a mouse model of CNGB3-associated achromatopsia following gene therapy.* Hum Mol Genet, 2011. **20**(16): p. 3161-75.

46. Komaromy, A.M., et al., *Gene therapy rescues cone function in congenital achromatopsia.* Hum Mol Genet, 2010. **19**(13): p. 2581-93.

47. Komaromy, A.M., et al., *Transient photoreceptor deconstruction by CNTF enhances rAAV-mediated cone functional rescue in late stage CNGB3-achromatopsia.* Mol Ther, 2013. **21**(6): p. 1131-41.

48. Tan, M.H., et al., *Gene therapy for retinitis pigmentosa and Leber congenital amaurosis caused by defects in AIPL1: effective rescue of mouse models of partial and complete Aipl1 deficiency using AAV2/2 and AAV2/8 vectors.* Hum Mol Genet, 2009. **18**(12): p. 2099-114.

49. Sun, X., et al., *Gene therapy with a promoter targeting both rods and cones rescues retinal degeneration caused by AIPL1 mutations.* Gene Ther, 2010. **17**(1): p. 117-31.

50. Ku, C.A., et al., *Gene therapy using self-complementary Y733F capsid mutant AAV2/8 restores vision in a model of early onset Leber congenital amaurosis.* Hum Mol Genet, 2011. **20**(23): p. 4569-81.

51. Stieger, K., et al., *AAV-mediated gene therapy for retinal disorders in large animal models.* ILAR J, 2009. **50**(2): p. 206-24.

52. Mowat, F.M., et al., *Topographical characterization of cone photoreceptors and the area centralis of the canine retina.* Mol Vis, 2008. **14**: p. 2518-27.

53. Hartong, D.T., E.L. Berson, and T.P. Dryja, *Retinitis pigmentosa.* Lancet, 2006. **368**(9549): p. 1795-809.

54. McLaughlin, M.E., et al., *Recessive mutations in the gene encoding the beta-subunit of rod phosphodiesterase in patients with retinitis pigmentosa.* Nat Genet, 1993. **4**(2): p. 130-4.

55. McLaughlin, M.E., et al., *Mutation spectrum of the gene encoding the beta subunit of rod phosphodiesterase among patients with autosomal recessive retinitis pigmentosa.* Proc Natl Acad Sci U S A, 1995. **92**(8): p. 3249-53.

56. Danciger, M., et al., *Mutations in the PDE6B gene in autosomal recessive retinitis pigmentosa.* Genomics, 1995. **30**(1): p. 1-7.

57. Danciger, M., et al., *A homozygous PDE6B mutation in a family with autosomal recessive retinitis pigmentosa.* Mol Vis, 1996. **2**: p. 10.

58. Bayes, M., et al., *Homozygous tandem duplication within the gene encoding the beta-subunit of rod phosphodiesterase as a cause for autosomal recessive retinitis pigmentosa.* Hum Mutat, 1995. **5**(3): p. 228-34.

59. Saga, M., et al., *A novel homozygous Ile535Asn mutation in the rod cGMP phosphodiesterase beta-subunit gene in two brothers of a Japanese family with autosomal recessive retinitis pigmentosa.* Curr Eye Res, 1998. **17**(3): p. 332-5.

60. Hmani-Aifa, M., et al., *Identification of two new mutations in the GPR98 and the PDE6B genes segregating in a Tunisian family.* Eur J Hum Genet, 2009. **17**(4): p. 474-82.

61. Clark, G.R., et al., *Development of a diagnostic genetic test for simplex and autosomal recessive retinitis pigmentosa.* Ophthalmology, 2010. **117**(11): p. 2169-77 e3.

62. Simpson, D.A., et al., *Molecular diagnosis for heterogeneous genetic diseases with targeted high-throughput DNA sequencing applied to retinitis pigmentosa.* J Med Genet, 2011. **48**(3): p. 145-51.

63. Kim, C., et al., *Microarray-based mutation detection and phenotypic characterization in Korean patients with retinitis pigmentosa.* Mol Vis, 2012. **18**: p. 2398-410.

64. Farber, D.B. and R.N. Lolley, *Enzymic basis for cyclic GMP accumulation in degenerative photoreceptor cells of mouse retina.* J Cyclic Nucleotide Res, 1976. **2**(3): p. 139-48.

65. Farber, D.B., S. Park, and C. Yamashita, *Cyclic GMP-phosphodiesterase of rd retina: biosynthesis and content.* Exp Eye Res, 1988. **46**(3): p. 363-74.

66. Paquet-Durand, F., et al., *PKG activity causes photoreceptor cell death in two retinitis pigmentosa models.* J Neurochem, 2009. **108**(3): p. 796-810.

67. Paquet-Durand, F., et al., *A key role for cyclic nucleotide gated (CNG) channels in cGMP-related retinitis pigmentosa.* Hum Mol Genet, 2011. **20**(5): p. 941-7.

68. Xu, J., et al., *cGMP Accumulation Causes Photoreceptor Degeneration in CNG Channel Deficiency: Evidence of cGMP Cytotoxicity Independently of Enhanced CNG Channel Function.* J Neurosci, 2013. **33**(37): p. 14939-48.

69. Murakami, Y., et al., *Receptor interacting protein kinase mediates necrotic cone but not rod cell death in a mouse model of inherited degeneration.* Proc Natl Acad Sci U S A, 2012. **109**(36): p. 14598-603.

70. Blanks, J.C., A.M. Adinolfi, and R.N. Lolley, *Photoreceptor degeneration and synaptogenesis in retinal-degenerative (rd) mice.* J Comp Neurol, 1974. **156**(1): p. 95-106.

71. LaVail, M.M., *Kinetics of rod outer segment renewal in the developing mouse retina.* J Cell Biol, 1973. **58**(3): p. 650-61.

72. Tansley, K., *Hereditary degeneration of the mouse retina.* Br J Ophthalmol, 1951. **35**(10): p. 573-82.

73. Carter-Dawson, L.D., M.M. LaVail, and R.L. Sidman, *Differential effect of the rd mutation on rods and cones in the mouse retina.* Invest Ophthalmol Vis Sci, 1978. **17**(6): p. 489-98.

74. Jimenez, A.J., et al., *The spatio-temporal pattern of photoreceptor degeneration in the aged rd/rd mouse retina.* Cell Tissue Res, 1996. **284**(2): p. 193-202.

75. Chang, B., et al., *Two mouse retinal degenerations caused by missense mutations in the beta-subunit of rod cGMP phosphodiesterase gene.* Vision Res, 2007. **47**(5): p. 624-33.

76. Gargini, C., et al., *Retinal organization in the retinal degeneration 10 (rd10) mutant mouse: a morphological and ERG study.* J Comp Neurol, 2007. **500**(2): p. 222-38.

77. Bennett, J., et al., *Photoreceptor cell rescue in retinal degeneration (rd) mice by in vivo gene therapy.* Nat Med, 1996. **2**(6): p. 649-54.

78. Kumar-Singh, R. and D.B. Farber, *Encapsidated adenovirus mini-chromosome-mediated delivery of genes to the retina: application to the rescue of photoreceptor degeneration.* Hum Mol Genet, 1998. **7**(12): p. 1893-900.

79. Takahashi, M., et al., *Rescue from photoreceptor degeneration in the rd mouse by human immunodeficiency virus vector-mediated gene transfer.* J Virol, 1999. **73**(9): p. 7812-6.

80. Jomary, C., et al., *Rescue of photoreceptor function by AAV-mediated gene transfer in a mouse model of inherited retinal degeneration.* Gene Ther, 1997. **4**(7): p. 683-90.

81. Pang, J.J., et al., *AAV-mediated gene therapy for retinal degeneration in the rd10 mouse containing a recessive PDEbeta mutation.* Invest Ophthalmol Vis Sci, 2008. **49**(10): p. 4278-83.

82. Pang, J.J., et al., *Long-term retinal function and structure rescue using capsid mutant AAV8 vector in the rd10 mouse, a model of recessive retinitis pigmentosa.* Mol Ther, 2011. **19**(2): p. 234-42.

83. Suber, M.L., et al., *Irish setter dogs affected with rod/cone dysplasia contain a nonsense mutation in the rod cGMP phosphodiesterase beta-subunit gene.* Proc Natl Acad Sci U S A, 1993. **90**(9): p. 3968-72.

84. Clements, P.J., et al., *Confirmation of the rod cGMP phosphodiesterase beta subunit (PDE beta) nonsense mutation in affected rcd-1 Irish setters in the UK and development of a diagnostic test.* Curr Eye Res, 1993. **12**(9): p. 861-6.

85. Parry, H.B., *Degenerations of the dog retina. II. Generalized progressive atrophy of hereditary origin.* Br J Ophthalmol, 1953. **37**(8): p. 487-502.

86. Petit, L., et al., *Restoration of vision in the pde6beta-deficient dog, a large animal model of rod-cone dystrophy.* Mol Ther, 2012. **20**(11): p. 2019-30.

87. Hameed, A., et al., *Evidence of RPGRIP1 gene mutations associated with recessive cone-rod dystrophy.* J Med Genet, 2003. **40**(8): p. 616-9.

88. Huang, L., et al., *Exome sequencing of 47 chinese families with cone-rod dystrophy: mutations in 25 known causative genes.* PLoS One, 2013. **8**(6): p. e65546.

89. Dryja, T.P., et al., *Null RPGRIP1 alleles in patients with Leber congenital amaurosis.* Am J Hum Genet, 2001. **68**(5): p. 1295-8.

90. Gerber, S., et al., *Complete exon-intron structure of the RPGR-interacting protein (RPGRIP1) gene allows the identification of mutations underlying Leber congenital amaurosis.* Eur J Hum Genet, 2001. **9**(8): p. 561-71.

91. Roepman, R., et al., *The retinitis pigmentosa GTPase regulator (RPGR) interacts with novel transport-like proteins in the outer segments of rod photoreceptors.* Hum Mol Genet, 2000. **9**(14): p. 2095-105.

92. Jacobson, S.G., et al., *Leber congenital amaurosis caused by an RPGRIP1 mutation shows treatment potential.* Ophthalmology, 2007. **114**(5): p. 895-8.

93. Seong, M.W., et al., *LCA5, a rare genetic cause of leber congenital amaurosis in Koreans.* Ophthalmic Genet, 2009. **30**(1): p. 54-5.

94. Fakhratova, M., *Identification of a Novel LCA6 Mutation in an Emirati Family.* Ophthalmic Genet, 2013. **34**(4): p. 234-7.

95. Khan, A.O., et al., *The RPGRIP1-related retinal phenotype in children.* Br J Ophthalmol, 2013. **97**(6): p. 760-4.

96. Chen, Y., et al., *Comprehensive mutation analysis by whole-exome sequencing in 41 Chinese families with Leber congenital amaurosis.* Invest Ophthalmol Vis Sci, 2013. **54**(6): p. 4351-7.

97. Mavlyutov, T.A., H. Zhao, and P.A. Ferreira, *Species-specific subcellular localization of RPGR and RPGRIP isoforms: implications for the phenotypic variability of congenital retinopathies among species.* Hum Mol Genet, 2002. **11**(16): p. 1899-907.

98. Lu, X. and P.A. Ferreira, *Identification of novel murine- and human-specific RPGRIP1 splice variants with distinct expression profiles and subcellular localization.* Invest Ophthalmol Vis Sci, 2005. **46**(6): p. 1882-90.

99. Lu, X., et al., *Limited proteolysis differentially modulates the stability and subcellular localization of domains of RPGRIP1 that are distinctly affected by mutations in Leber's congenital amaurosis.* Hum Mol Genet, 2005. **14**(10): p. 1327-40.

100. Roesch, K., M.B. Stadler, and C.L. Cepko, *Gene expression changes within Muller glial cells in retinitis pigmentosa.* Mol Vis, 2012. **18**: p. 1197-214.

101. Boylan, J.P. and A.F. Wright, *Identification of a novel protein interacting with RPGR.* Hum Mol Genet, 2000. **9**(14): p. 2085-93.

102. Hong, D.H., et al., *Retinitis pigmentosa GTPase regulator (RPGRr)-interacting protein is stably associated with the photoreceptor ciliary axoneme and anchors RPGR to the connecting cilium.* J Biol Chem, 2001. **276**(15): p. 12091-9.

103. Demirci, F.Y., et al., *X-linked cone-rod dystrophy (locus COD1): identification of mutations in RPGR exon ORF15.* Am J Hum Genet, 2002. **70**(4): p. 1049-53.

104. Ayyagari, R., et al., *X-linked recessive atrophic macular degeneration from RPGR mutation.* Genomics, 2002. **80**(2): p. 166-71.

105. Vervoort, R., et al., *Mutational hot spot within a new RPGR exon in X-linked retinitis pigmentosa.* Nat Genet, 2000. **25**(4): p. 462-6.

106. Patil, H., et al., *Selective loss of RPGRIP1-dependent ciliary targeting of NPHP4, RPGR and SDCCAG8 underlies the degeneration of photoreceptor neurons.* Cell Death Dis, 2012. **3**: p. e355.

107. Zhao, Y., et al., *The retinitis pigmentosa GTPase regulator (RPGR)- interacting protein: subserving RPGR function and participating in disk morphogenesis.* Proc Natl Acad Sci U S A, 2003. **100**(7): p. 3965-70.

108. Won, J., et al., *RPGRIP1 is essential for normal rod photoreceptor outer segment elaboration and morphogenesis.* Hum Mol Genet, 2009. **18**(22): p. 4329-39.

109. Pawlyk, B.S., et al., *Gene replacement therapy rescues photoreceptor degeneration in a murine model of Leber congenital amaurosis lacking RPGRIP.* Invest Ophthalmol Vis Sci, 2005. **46**(9): p. 3039-45.

110. Pawlyk, B.S., et al., *Replacement gene therapy with a human RPGRIP1 sequence slows photoreceptor degeneration in a murine model of Leber congenital amaurosis.* Hum Gene Ther, 2010. **21**(8): p. 993-1004.

111. Mellersh, C.S., et al., *Canine RPGRIP1 mutation establishes cone-rod dystrophy in miniature longhaired dachshunds as a homologue of human Leber congenital amaurosis.* Genomics, 2006. **88**(3): p. 293-301.

112. Lheriteau, E., et al., *The RPGRIP1-deficient dog, a promising canine model for gene therapy.* Mol Vis, 2009. **15**: p. 349-61.

113. Turney, C., et al., *Pathological and electrophysiological features of a canine cone-rod dystrophy in the miniature longhaired dachshund.* Invest Ophthalmol Vis Sci, 2007. **48**(9): p. 4240-9.

114. Beltran, W.A., et al., *rAAV2/5 gene-targeting to rods:dose-dependent efficiency and complications associated with different promoters.* Gene Ther, 2010. **17**(9): p. 1162-74.

115. Stieger, K., et al., *Subretinal delivery of recombinant AAV serotype 8 vector in dogs results in gene transfer to neurons in the brain.* Mol Ther, 2008. **16**(5): p. 916-23.

116. Boye, S.E., et al., *The human rhodopsin kinase promoter in an AAV5 vector confers rod- and cone-specific expression in the primate retina.* Hum Gene Ther, 2012. **23**(10): p. 1101-15.

117. Khani, S.C., et al., *AAV-mediated expression targeting of rod and cone photoreceptors with a human rhodopsin kinase promoter.* Invest Ophthalmol Vis Sci, 2007. **48**(9): p. 3954-61.

118. Beltran, W.A., et al., *Gene therapy rescues photoreceptor blindness in dogs and paves the way for treating human X-linked retinitis pigmentosa.* Proc Natl Acad Sci U S A, 2012. **109**(6): p. 2132-7.

119. Lheriteau, E., et al., *Successful Gene Therapy in the RPGRIP1-deficient Dog: a Large Model of Cone-Rod Dystrophy.* Mol Ther, 2013.

120. Kolandaivelu, S., B. Chang, and V. Ramamurthy, *Rod phosphodiesterase-6 (PDE6) catalytic subunits restore cone function in a mouse model lacking cone PDE6 catalytic subunit.* J Biol Chem, 2011. **286**(38): p. 33252-9.

121. Deng, W.T., et al., *Cone Phosphodiesterase-6alpha' Restores Rod Function and Confers Distinct Physiological Properties in the Rod Phosphodiesterase-6beta-Deficient rd10 Mouse.* J Neurosci, 2013. **33**(29): p. 11745-53.

122. Boye, S.L., et al., *Long-term preservation of cone photoreceptors and restoration of cone function by gene therapy in the guanylate cyclase-1 knockout (GC1KO) mouse.* Invest Ophthalmol Vis Sci, 2011. **52**(10): p. 7098-108.

123. Mihelec, M., et al., *Long-term preservation of cones and improvement in visual function following gene therapy in a mouse model of leber congenital amaurosis caused by guanylate cyclase-1 deficiency.* Hum Gene Ther, 2011. **22**(10): p. 1179-90.

124. Boye, S.L., et al., *AAV-mediated gene therapy in the guanylate cyclase (RetGC1/RetGC2) double knockout mouse model of Leber congenital amaurosis.* Hum Gene Ther, 2013. **24**(2): p. 189-202.

125. Goc, A., et al., *Structural characterization of the rod cGMP phosphodiesterase 6.* J Mol Biol, 2010. **401**(3): p. 363-73.

126. Portera-Cailliau, C., et al., *Apoptotic photoreceptor cell death in mouse models of retinitis pigmentosa.* Proc Natl Acad Sci U S A, 1994. **91**(3): p. 974-8.

127. Simons, D.L., et al., *Gene therapy prevents photoreceptor death and preserves retinal function in a Bardet-Biedl syndrome mouse model.* Proc Natl Acad Sci U S A, 2011. **108**(15): p. 6276-81.

Development of AAV-mediated gene addition therapies in canine models of severe inherited photoreceptor dystrophies

Inherited retinal dystrophies are untreatable blinding disorders caused by mutations in genes expressed in photoreceptors or in retinal pigment epithelium (RPE).

Over the last decade, gene addition therapy has been used successfully in different animal models of recessive inherited retinopathies. These studies have paved the way to several clinical trials for RPE diseases with encouraging results. The next level of challenge is to initiate treatment of the majority of disorders that primarily involve photoreceptor cells.

For the development of new therapies, proof-of-concept studies in large animal models that share clinical features with their human counterparts represent a pivotal step. It is particularly true for primary photoreceptor dystrophies because the distribution, density and proportion of photoreceptors in large models more closely match those of primates.

Here, we evaluated the efficacy of gene addition therapy in two canine models of severe photoreceptor dystrophies: (i) the *Pde6β*$^{-/-}$ dog, a model of rod-cone dystrophy caused by a defect in rods and (ii) the *Rpgrip1*$^{-/-}$ dog, a model of cone-rod dystrophy caused by a defect in both rods and cones

Using vectors derived from adeno-associated virus, we showed that it is possible to restore retinal function, preserve photoreceptor structure and visually guided behavior in the two canine models, for at least 24 months postinjection. The efficacy of gene addition therapy in these large animal models of photoreceptor dystrophies provides great promise for human treatment.

Key words
Inherited retinal dystrophies, photoreceptors, gene therapy, AAV, canine models

Développement d'approches de thérapie génique d'addition médiées par des vecteurs AAV chez des modèles canins de dégénérescence héréditaires des photorécepteurs

Les dystrophies rétiniennes héréditaires sont des maladies cécitantes causées par des mutations dans des gènes exprimés par les photorécepteurs ou l'épithélium pigmentaire rétinien (EPR).

Récemment, la thérapie génique d'addition a été utilisée avec succès chez des modèles animaux de rétinopathies héréditaires récessives. Ces études ont ouvert la voie à plusieurs essais cliniques pour des maladies de l'EPR, avec des résultats encourageants. L'étape suivante est de développer un traitement pour les pathologies qui touchent directement les photorécepteurs.

Pour le développement de ces nouvelles thérapies, les preuves de concept chez des modèles gros animaux qui miment les symptômes des patients sont une étape importante. En effet, la distribution, la densité et la proportion des photorécepteurs chez les modèles gros animaux sont très proches de celles des primates.

Ici, nous avons évalué l'efficacité de la thérapie génique d'addition chez deux modèles canins de formes sévères de dégénérescence des photorécepteurs: (i) le chien *Pde6β*$^{-/-}$, un modèle de dystrophie bâtonnet-cone et (ii) le chien *Rpgrip1*$^{-/-}$, un modèle de dystrophie cône-bâtonnet.

A l'aide de vecteurs dérivés du virus adeno-associé, nous avons montré qu'il était possible de restaurer la fonction rétinienne, de préserver la structure des photorécepteurs et le comportement visuel des deux modèles canins, pendant au moins 24 mois après l'injection. Ces résultats sont prometteurs pour le traitement des patients atteints de dégénérescence des photorécepteurs.

Mots clés
Dystrophies rétiniennes héréditaires, photorecepteurs, thérapie génique, AAV, modèles canins

PETIT Lolita
4 rue Francis Merlant
44000 Nantes, France

Visa du directeur de thèse